Connection of Simple-Span Precast Concrete Girders for Continuity

DETAILS

191 pages | | PAPERBACK

ISBN 978-0-309-08793-3 | DOI 10.17226/13746

AUTHORS

R A Miller; M Hastak; A Mirmiran; R Castrodale; Transportation Research Board

NATIONAL COOPERATIVE HIGHWAY RESEARCH PROGRAM

NCHRP REPORT 519

Connection of Simple-Span Precast Concrete Girders for Continuity

RICHARD A. MILLER
University of Cincinnati
Cincinnati, OH

REID CASTRODALE
Ralph Whitehead Associates
Charlotte, NC

AMIR MIRMIRAN
North Carolina State University
Raleigh, NC

AND

MAKARAND HASTAK
Purdue University
West Lafayette, IN

SUBJECT AREAS
Bridges, Other Structures, and Hydraulics and Hydrology

Research Sponsored by the American Association of State Highway and Transportation Officials
in Cooperation with the Federal Highway Administration

TRANSPORTATION RESEARCH BOARD

WASHINGTON, D.C.
2004
www.TRB.org

NATIONAL COOPERATIVE HIGHWAY RESEARCH PROGRAM

Systematic, well-designed research provides the most effective approach to the solution of many problems facing highway administrators and engineers. Often, highway problems are of local interest and can best be studied by highway departments individually or in cooperation with their state universities and others. However, the accelerating growth of highway transportation develops increasingly complex problems of wide interest to highway authorities. These problems are best studied through a coordinated program of cooperative research.

In recognition of these needs, the highway administrators of the American Association of State Highway and Transportation Officials initiated in 1962 an objective national highway research program employing modern scientific techniques. This program is supported on a continuing basis by funds from participating member states of the Association and it receives the full cooperation and support of the Federal Highway Administration, United States Department of Transportation.

The Transportation Research Board of the National Academies was requested by the Association to administer the research program because of the Board's recognized objectivity and understanding of modern research practices. The Board is uniquely suited for this purpose as it maintains an extensive committee structure from which authorities on any highway transportation subject may be drawn; it possesses avenues of communications and cooperation with federal, state and local governmental agencies, universities, and industry; its relationship to the National Research Council is an insurance of objectivity; it maintains a full-time research correlation staff of specialists in highway transportation matters to bring the findings of research directly to those who are in a position to use them.

The program is developed on the basis of research needs identified by chief administrators of the highway and transportation departments and by committees of AASHTO. Each year, specific areas of research needs to be included in the program are proposed to the National Research Council and the Board by the American Association of State Highway and Transportation Officials. Research projects to fulfill these needs are defined by the Board, and qualified research agencies are selected from those that have submitted proposals. Administration and surveillance of research contracts are the responsibilities of the National Research Council and the Transportation Research Board.

The needs for highway research are many, and the National Cooperative Highway Research Program can make significant contributions to the solution of highway transportation problems of mutual concern to many responsible groups. The program, however, is intended to complement rather than to substitute for or duplicate other highway research programs.

Note: The Transportation Research Board of the National Academies, the National Research Council, the Federal Highway Administration, the American Association of State Highway and Transportation Officials, and the individual states participating in the National Cooperative Highway Research Program do not endorse products or manufacturers. Trade or manufacturers' names appear herein solely because they are considered essential to the object of this report.

NCHRP REPORT 519

Project 12-53 FY '99

ISSN 0077-5614

ISBN 0-309-08793-7

Library of Congress Control Number 2004105765

Price $27.00

NOTICE

The project that is the subject of this report was a part of the National Cooperative Highway Research Program conducted by the Transportation Research Board with the approval of the Governing Board of the National Research Council. Such approval reflects the Governing Board's judgment that the program concerned is of national importance and appropriate with respect to both the purposes and resources of the National Research Council.

The members of the technical committee selected to monitor this project and to review this report were chosen for recognized scholarly competence and with due consideration for the balance of disciplines appropriate to the project. The opinions and conclusions expressed or implied are those of the research agency that performed the research, and, while they have been accepted as appropriate by the technical committee, they are not necessarily those of the Transportation Research Board, the National Research Council, the American Association of State Highway and Transportation Officials, or the Federal Highway Administration, U.S. Department of Transportation.

Each report is reviewed and accepted for publication by the technical committee according to procedures established and monitored by the Transportation Research Board Executive Committee and the Governing Board of the National Research Council.

Published reports of the

NATIONAL COOPERATIVE HIGHWAY RESEARCH PROGRAM

are available from:

Transportation Research Board
Business Office
500 Fifth Street, NW
Washington, DC 20001

and can be ordered through the Internet at:

http://www.national-academies.org/trb/bookstore

Printed in the United States of America

THE NATIONAL ACADEMIES

Advisers to the Nation on Science, Engineering, and Medicine

The **National Academy of Sciences** is a private, nonprofit, self-perpetuating society of distinguished scholars engaged in scientific and engineering research, dedicated to the furtherance of science and technology and to their use for the general welfare. On the authority of the charter granted to it by the Congress in 1863, the Academy has a mandate that requires it to advise the federal government on scientific and technical matters. Dr. Bruce M. Alberts is president of the National Academy of Sciences.

The **National Academy of Engineering** was established in 1964, under the charter of the National Academy of Sciences, as a parallel organization of outstanding engineers. It is autonomous in its administration and in the selection of its members, sharing with the National Academy of Sciences the responsibility for advising the federal government. The National Academy of Engineering also sponsors engineering programs aimed at meeting national needs, encourages education and research, and recognizes the superior achievements of engineers. Dr. William A. Wulf is president of the National Academy of Engineering.

The **Institute of Medicine** was established in 1970 by the National Academy of Sciences to secure the services of eminent members of appropriate professions in the examination of policy matters pertaining to the health of the public. The Institute acts under the responsibility given to the National Academy of Sciences by its congressional charter to be an adviser to the federal government and, on its own initiative, to identify issues of medical care, research, and education. Dr. Harvey V. Fineberg is president of the Institute of Medicine.

The **National Research Council** was organized by the National Academy of Sciences in 1916 to associate the broad community of science and technology with the Academy's purposes of furthering knowledge and advising the federal government. Functioning in accordance with general policies determined by the Academy, the Council has become the principal operating agency of both the National Academy of Sciences and the National Academy of Engineering in providing services to the government, the public, and the scientific and engineering communities. The Council is administered jointly by both the Academies and the Institute of Medicine. Dr. Bruce M. Alberts and Dr. William A. Wulf are chair and vice chair, respectively, of the National Research Council.

The **Transportation Research Board** is a division of the National Research Council, which serves the National Academy of Sciences and the National Academy of Engineering. The Board's mission is to promote innovation and progress in transportation through research. In an objective and interdisciplinary setting, the Board facilitates the sharing of information on transportation practice and policy by researchers and practitioners; stimulates research and offers research management services that promote technical excellence; provides expert advice on transportation policy and programs; and disseminates research results broadly and encourages their implementation. The Board's varied activities annually engage more than 5,000 engineers, scientists, and other transportation researchers and practitioners from the public and private sectors and academia, all of whom contribute their expertise in the public interest. The program is supported by state transportation departments, federal agencies including the component administrations of the U.S. Department of Transportation, and other organizations and individuals interested in the development of transportation. **www.TRB.org**

www.national-academies.org

AUTHOR ACKNOWLEDGMENTS

This research was performed under NCHRP Project 12-53 by the Department of Civil and Environmental Engineering at the University of Cincinnati. Dr. Richard Miller was the principal investigator. Co-investigators were Dr. Reid Castrodale of Ralph Whitehead Associates, Dr. Amir Mirmiran of North Carolina State University, and Dr. Makarand Hastak of Purdue University. The research team included University of Cincinnati faculty member Michael Baseheart; technicians Robert Muench, Art Case, and Dave Kruezeman; and graduate research assistants Amy Dimmerling, Michael Slack, Angela Mueller, Ronak Shah, Siddharth Kulkarni, R. Ramachandran, and A. Deshini.

The research team is indebted to Prestressed Services of Melbourne, KY, for allowing the use of its facilities for the experimental work. The research team would like to thank Don Bosse, Joe Roche, Chris Fuchs, Gene Johnson, and all the workers at PSM for their help and cooperation.

Finally, the research team would like to thank NCHRP Program Officer David Beal and the members of the NCHRP 12-53 Panel: Raymond Shaefer (Chair), Yassin Askar, Richard Elliott, Steven Ernst, Mark Holloran, Alan Matejowsky, David Sanders, Brian Thompson, and Joey Hartmann.

FOREWORD

By David B. Beal
Staff Officer
Transportation Research Board

This report contains the findings of research to develop recommended details and specifications for the design of continuity connections for precast concrete girders. Examples illustrating the design of four precast girder types made continuous for live load were also developed. The material in this report will be of immediate interest to bridge designers.

Many states make precast/prestressed girder bridges continuous using a cast-in-place connection between girders over the piers. Compared with simple-span bridges, continuous bridges require less expansion joint maintenance, have improved seismic performance, and have reduced bending moments. Although bridges constructed in this fashion have been in service for many years in a number of states, there had been limited verification of the ability of the connection to provide predicted continuity. As a result, some states design the girders as simple spans for both dead load and live load, neglecting any moment resistance of the connection.

The objective of this project was to recommend details and specifications for the design of durable and constructible connections that achieve structural continuity between simple-span precast/prestressed concrete girders. The report's recommendations are based on experimental verification of the effectiveness of the continuity connection, considering significant variables such as concrete placement sequence, reinforcement details, concrete properties, diaphragm cracking, and beam depth. Specifications and connection details to achieve the full benefits of continuity are recommended based on physical testing and analysis.

The research was performed by the University of Cincinnati, with the assistance of Ralph Whitehead Associates, Amir Mirmiran, and Makarand Hastak. The report fully documents the research leading to the recommended details and specifications. Detailed design examples are included as appendixes.

CONTENTS

CONNECTION OF SIMPLE-SPAN PRECAST CONCRETE GIRDERS FOR CONTINUITY

SUMMARY

Precast/prestressed concrete girders can be made continuous for live load by connecting the girders at the support. The purpose of NCHRP Project 12-53 was to investigate the strength, serviceability, and continuity of connections between precast/prestressed concrete girders made continuous. For live-load continuity, a negative moment connection is usually made through a composite, cast-in-place, reinforced concrete deck. A diaphragm is usually cast between girder ends. However, once the girders are connected, they may camber upward due to the effects of creep, shrinkage, and temperature. These effects cause the formation of a positive moment at the diaphragm. If no positive moment connection is supplied, the joint cracks and continuity may be lost. Positive moment connections are usually made either by extending the prestressing strand from the girder into the diaphragm or by embedding reinforcing bar from the end of the girder into the diaphragm.

In the first phase of the research, surveys were conducted to establish the frequency of use of positive and negative moment connections and how they were constructed. The survey examined the type of negative moment connection; the use and type of positive moment connection (extended bar or extended strand); connection details; construction sequence; the age at which continuity is established; constructability issues; and design methodologies. A spreadsheet program called RESTRAINT was developed to conduct parametric studies of the continuous system.

Using the results of the surveys and the parametric studies, six positive moment connection details were developed: extended strand, extended bar, extended strand with the girder ends embedded into the diaphragm 6 in. into the diaphragm, extended bar with the girder ends embedded into the diaphragm 6 in. into the diaphragm, extended bar with the girder ends embedded into the diaphragm 6 in. into the diaphragm and additional stirrups in the diaphragm, and extended bar with the girder ends embedded into the diaphragm 6 in. into the diaphragm and horizontal bars placed through the web of the girder. All details had a strength of 1.2 M_{cr}, where M_{cr} is the positive cracking moment of the composite cross section. The details were tested using short (16-ft.) Type II AASHTO girders, with a composite slab, attached to a diaphragm. The test results showed that both the extended strand and the extended bar connections developed sufficient strength. Embedding the girders into the diaphragm seemed to improve

the connection performance, but the improvement was difficult to quantify. Adding additional stirrups in the diaphragm area did not improve strength, but did improve ductility and may be beneficial in seismic applications. Placing horizontal bars through the webs of the girders improved strength, stiffness, and ductility, but the failure mode was cracking of the girders.

In a second experimental phase, 50-ft-long Type III AASHTO I girders were assembled into two-span, 100-ft-long, continuous-for-live-load specimens. The first specimen used a reinforced concrete deck for the negative moment connection and an extended bar for the positive moment connection. The positive moment connection had a strength of 1.2 $M_{cr.}$ Part of the diaphragm was cast 28 days before the slab was cast. It was thought that weight of the slab would cause the girder ends to rotate into the partial diaphragm, precompress the diaphragm, and prevent cracking if positive moments formed due to creep and shrinkage. However, very little precompression was found.

When the slab was cast, the concrete temperature increased due to heat of hydration. Later, the slab cooled and contracted. This contraction caused negative moment to form at the diaphragm.

The specimen was monitored for 120 days. It was expected that additional negative moment would form due to differential shrinkage of the deck, but this did not occur. Instead, positive moment from creep and shrinkage developed. Thermal effects were found to be significant. Temperature effects caused daily variations of the moments at the diaphragm of ±250 k-ft. This was approximately 50% of the capacity of the connection. During the monitoring period, positive moment cracking occurred at the connection.

After monitoring, the specimen was loaded to test for continuity. Initial loading showed the system remained continuous even though the connection had cracked. A post-tensioning system was used to create additional positive moment at the connection and to open the cracks. Subsequent loading showed the system maintained continuity even though positive moment cracks as large as 0.01 in. had formed.

A second 100-ft.-long, continuous-for-live-load specimen was created. This specimen used an extended strand connection. As with the first specimen, a post-tensioning system was used to create positive moment at the connection, and additional positive moment was created by jacking up the ends of the specimen. The combination of the post-tensioning and jacking up the ends of the specimen caused positive moment cracks as large 0.07 in. to form. There were also signs that the connection was about to fail. However, subsequent loading showed that the connection maintained 70% continuity.

The second specimen was tested for negative moment connection capacity. The negative moment connection was shown to have sufficient strength. The negative cracking moment was lower than predicted, but this was due to pre-existing cracks in the slab that occurred during positive moment testing.

The results of the survey, the parametric study and the experimental work have been incorporated in proposed changes to the AASHTO Load Resistance Factor Design Specifications. The results have also been used to create four design examples.

CHAPTER **1**

INTRODUCTION AND RESEARCH APPROACH

PROBLEM STATEMENT AND RESEARCH OBJECTIVES

Many states use continuous-for-live-load prestressed/precast concrete bridges. These bridges are built by first placing the precast/prestressed girders on the abutments and then casting a composite deck. Diaphragms are usually placed between the girder ends. Since the girders are not connected until the deck and diaphragms harden, the girders behave as simple spans for girder and slab dead load. After the concrete deck and diaphragms harden, they connect the girders together and make the entire structure continuous for any additional dead load and all live loads. Reinforcing bar placed in the deck over the connection between the girders provides the negative moment continuity.

Early studies on this type of construction by the Portland Cement Association (PCA) showed that using a reinforced deck was an adequate connection for resisting negative moments over the piers and for shear (*1–7*). However, these studies also showed that cracking occurred in the diaphragm. The cause of this cracking was positive moment, which developed from time-dependent deformations of the prestressed girders. It was recommended that a positive moment connection be made between the bottom of the girders and the diaphragms.

Two basic types of positive moment connections were developed. The first was a bent bar connection, which was based on the PCA studies (*1–7*). In this connection, hooked, mild reinforcing bars are embedded in the end of the precast girder (see Figure 1). The hooks are then embedded in the diaphragm. The second type of connection is the bent-strand connection. In this type of connection, a predetermined length of prestressing strand is left protruding from the end of the girder when the girder is detensioned. This strand is then bent into a 90° hook, and the hook is embedded in the diaphragm (see Figure 2). The Missouri DOT published an investigation of this type of connection in the 1970s (*8, 9, 10*), the results of which are discussed in Chapter 2.

In 1989, the National Cooperative Highway Research Program (NCHRP) published *NCHRP Report 322* (*11*), which studied the forces that were likely to occur on positive moment connections. As part of this study, the authors developed two computer programs to evaluate the positive moments caused by time-dependent effects and the moments caused by live loads. The authors of *NCHRP Report 322* concluded that positive moment connections were costly and provided no structural benefit. The later conclusion is based on the fact that the positive moment connection restrains the girder ends. The designer must account for the effects of these restraint moments by adding them to the effects of the live-load moments. It was concluded that the maximum positive moment in a span was virtually the same whether it was designed as a simple span or as a continuous span with both live-load and restraint moments.

However, these conclusions were not universally accepted. Many engineers thought that there was still an advantage to making the bridge continuous and that positive moment connections were needed for continuity. These connections were assumed to control cracking at the diaphragms.

There were also lingering questions about overall connection. For the bent-strand connection, there was no accepted design method for determining the length of the bent strand and the number of strands needed. For both the bent-strand and bent-bar connections, there was concern over congestion in the diaphragm area. Many details called for several bars or strands extending from the ends of the girders and for the bars or strands of longitudinally adjacent girders to be meshed in the diaphragm area. This placed a large number of bars in a small area, often without adequate clearance between the bars or strands. There were concerns that this congestion would limit the capacity of the connections due to bar interactions and a possible inability to properly consolidate the concrete in the diaphragm.

Some questioned whether cracking at the girder-diaphragm interface affected the continuity of the system. Some assumed that if the girder-diaphragm interface cracked, the joint would act like a hinge or a rotational spring. This would limit the system's ability to transfer load across the joint and to reduce or eliminate continuity.

The goals of this research are (1) to determine how continuous-for-live-load connections are used in the various states; (2) to experimentally determine capacities and behaviors of some typical connection details through testing; (3) to develop design methods and suggested changes to the AASHTO Load Resistance Factor Design (LRFD) Specification (*12*) for making simple-span bridges continuous for live load.

Figure 1. Bent-bar positive moment connection.

Figure 2. Bent-strand positive moment connection.

OBJECTIVE OF THE STUDY

The objective of the study, as stated by the project panel, was to recommend details and specifications for the design of durable and constructable connections that achieve structural continuity between simple-span precast/prestressed concrete girders. The specifications developed should be suitable for consideration by the AASHTO Highway Subcommittee on Bridges and Structures (HSCOBS).

RESEARCH APPROACH

This project was divided into eight tasks.

Task 1: Review of Existing Data

Task 1 consisted of reviewing the existing data on precast/prestressed bridges made continuous for live load. Part of this task was accomplished with a literature search. The remainder was done using surveys of state DOTs, designers, fabricators, and contractors. The surveys focused on connection details, materials used, constructability issues, and reported problems.

Task 2: Propose Connections To Be Tested

Using the results of Task 1, it was determined that the typical connection details could be divided into four broad categories: (1) bent strand with the ends of the girders not embedded in the diaphragm, (2) bent bar with the ends of the girders not embedded in the diaphragm, (3) bent strand with the ends of the girders embedded into the diaphragm, and (4) bent bar with the ends of the girders embedded into the diaphragm. Some states used horizontal bars through the girder web for additional strength. There was also a suggestion that additional stirrups in the diaphragm, but outside of the girder bottom flange, would strengthen the connection. These data were used to propose six types of connection details for testing.

Task 3: Prepare a Work Plan

A work plan was developed which centered on testing six connection details for capacity and two full-size specimens. The capacity specimens consisted of two short (or stub) AASHTO Type II girders with a slab, connected to a diaphragm. The connections were loaded to the anticipated design load and then subjected to fatigue. The full-size specimens simulated a single beam line in a two-span bridge. This specimen used Type III girders. In preparing this work plan, an analysis program, RESTRAINT, was developed.

Task 4: Prepare an Interim Report

Task 4 was a report summarizing Tasks 1–3.

Task 5: Experimentally Validate the Connection Details

In Task 5, the connection details were tested in accordance with the work plan.

Task 6: Develop Connection Details, Recommended Specifications, Commentary, and Design Examples

For Task 6, the pertinent sections of the AASHTO LRFD Specifications were reviewed and changes were recommended based on the results of Tasks 1–5.

Task 7: Seismic Issues

Using available literature and some limited data from the experiments, a discussion of seismic issues was prepared.

Task 8: Prepare the Final Report

The findings of Tasks 1–7 are summarized in this report. The results of the survey done under Task 1 are found in Chapter 2. Chapter 2 also contains the proposed connection details that were tested, details of the experimental work plan, and the experimental results (Tasks 2, 3, and 5). Chapter 3 discusses the results and interpretation of data and addressed the seismic issues (Task 7). Chapter 4 contains conclusions and recommendations for future research. The RESTRAINT spreadsheet program, developed under Task 3, is Appendix A and is available upon request from NCHRP. Appendix B provides details of the experimental program (Task 5). The proposed changes to the AASHTO LRFD Specifications and Design Examples (Task 6) are contained in Appendixes C and D, respectively. Appendix E is the summary data from the project (in electronic form) and is also available (as a diskette) upon request from NCHRP.

CHAPTER 2

FINDINGS

This chapter summarizes the results of the surveys, the literature search, the analytical work, and the experimental program.

SUMMARY OF THE SURVEYS

Task 1 required the authors to assess the current state of the practice for continuous-for-live-load bridges. As part of this task, two surveys were conducted of state DOTs, contractors, fabricators, and designers. The first survey assessed the general use of continuous-for-live-load bridges and the use of various connection details. The second survey addressed constructability issues.

The purpose of the first survey was to determine typical parameters for the connections between precast girders that are made continuous for live load. This survey was sent to all 50 state DOTs and to selected designers and fabricators. Answering the survey were 39 state DOTs, 4 designers, and 8 fabricators for a total of 51 responses. Of the 51 respondents, 35 indicated that they used, designed, or fabricated continuous-for-live-load precast/prestressed bridges. The following assessments apply only to those respondents who indicated that they used continuous-for-live-load bridges.

In all but one case, negative moment continuity was established by using a reinforced deck over the diaphragm. One respondent used a mechanical splice between the top flanges of the girders. All those who designed for continuous live load used a positive moment connection.

It was clear from the outset of the project that the positive moment connection was of greater concern than was the negative moment connection, so most of the questions focused on the positive moment connection. The significant findings were as follows.

Type of Connection

When asked to identify the type of positive moment connection used, 17 respondents used a bent-bar connection, 4 used straight bars, 24 used bent strands, 3 used a welded-bar detail, and 3 used mechanical strand connectors (the responses add up to more than 35 as some respondents used more than one type of connection). It appears the bent-bar and bent-strand connections are the favored connections, with approximately equal usage. Of the respondents, 75% (26 total) overlap (mesh) the bar or strand in the diaphragm area. Seventeen respondents (50%) indicated that they provided transverse reinforcing through the beam into the diaphragm.

Type of Girder Used

The positive moment connection is used most frequently with I girders and bulb-T girders, although a number of respondents also used it for box girders and shapes specific to a given state.

Embedment

Seven respondents indicated that they did not embed the girder ends in the diaphragm. The remainder embedded the girder ends in the diaphragm anywhere from 2 to 12 in. There was no clear preference for embedment depth: 10 respondents indicated embeddings less than 2 in., 4 respondents embedded 2 to 4 in., 3 embedded 4 to 6 in., 6 embedded 6 to 8 in., 6 embedded 8 to 10 in., 11 embedded 10 to 12 in., and 12 embedded the girder ends more than 12 in. (responses total more than 35 as multiple responses were allowed).

Concrete Strength

Girder concrete compressive strength ranged from 3,500 to 7,000 psi at release and 4,000 to 9,000 psi at 28 days for normal mixes. Normal strength deck/diaphragm concrete was 3,000 to 5,000 psi at 28 days. Some respondents (19) indicated that high-performance mixes were occasionally used. For girders, these mixes ranged from 4,000 to 9,000 psi at release and 6,500 to 10,000 psi at 28 days, while the deck/diaphragm concrete ranged from 3,000 to 7,000 psi.

Support Conditions

More than 80% of the respondents indicated that the bearings were placed under the girder ends. Approximately 10% used no bearings, leaving the girder and diaphragm to sit directly on the bearing surface. The remaining 10% either placed the bearings under the diaphragm or under both the girder and diaphragm.

Construction Sequence

Twenty-eight respondents (80%) indicated that the diaphragm and deck were cast at the same time. Fourteen respondents (40%) cast the diaphragm, or some part of the diaphragm, first. Again, the total responses exceed 100% because some respondents did both. Only 12 respondents indicated specifying a minimum age for the girders before the diaphragm and deck are cast. The minimum ages varied from 28 to 90 days with no two respondents having the same age requirement. Some respondents indicated multiple age requirements. The initial survey also asked questions about constructability and connection performance. More detailed questions were asked in a second survey. The results of this second survey showed that the most common concerns were congestion in the diaphragm area and the possibility that the concrete could not be adequately consolidated in this area.

Fabrication problems included a difficulty in installing bars pre-bent (due to form interference), difficulties in bending bars or strands after the girders were fabricated, and that an extended bar or strand were sometimes cut off or broken off during fabrication or while being transported. If a bar or strand was accidentally cut or broken, the solution was to drill and epoxy a new bar or strand in place.

The respondents were asked to rate the significance of identified problems in terms of increased cost, increased construction time, decreased quality, or a combination thereof. In the overwhelming majority of responses, the problems were rated as being of only minor significance.

The respondents were also asked to provide costs for providing the connections. Many did not respond, and the responses that were received were difficult to interpret. In some cases, the respondents indicated that the cost of the connection could not be easily separated. In other cases, the cost depended largely on the detail used and the fabricator's methods. However, it appeared that the maximum cost of providing the positive moment connection was $200 per girder. This was insignificant compared with the overall girder cost.

LITERATURE REVIEW

A search was made for literature that had been published since the publication of *NCHRP Report 322* in 1989 (*11*) or that had not been included in that report. The most significant findings were a series of reports done for the Missouri Highway and Transportation Department (now the Missouri DOT) (*8–10*). These reports cover experimental work done on bent-strand types of connections.

In the early 1970s, the Missouri Cooperative Highway Research Program commissioned a study on the feasibility of using extensions of the prestressing strand to develop positive moment continuity of prestressed I-beam members. The first phase of the research dealt with an investigation of the bonding characteristics of untensioned prestressing strand (*8*), which could be used in the continuity connection. A relationship between the maximum force and embedment length of the untensioned prestressing strand in a stress field similar to that in the diaphragm of a highway bridge was developed. In all, 69 pull-out specimens were tested with three strand configurations: straight, frayed, and a 90° bent. From the investigation, the modulus of slip for each of the strand configurations was determined, and equations relating steel stress to the embedment length were developed. It was found that bent strand provided the best anchorage, having half the slip of the straight or frayed strand. Straight strand was found to perform marginally better than frayed strand. The other variables included in the testing program were strand diameter, concrete strength, and containment reinforcing, but they were found to be of little consequence.

The second phase was to verify and apply the expressions developed in the first phase to an actual I-beam end connection (*9*). Six full-scale bent-strand connections were tested: three specimens consisting of two short, 6-ft 3-in. stub beams, a 30-in. diaphragm, and a 6.5-in. slab; and three specimens made only of the beams and diaphragms (no slab). As with the PCA tests (*4,6*), the specimens were tested for positive moment as simple spans, but only monotonic static loads were applied. The stub girders were embedded 17.5 in. into the diaphragm and ¾-in.-diameter coil tie rods were used to transmit the force from the end of the beams to the diaphragm.

From the results of Phases I and II, a design method was proposed for positive moment connections using bent strand. The required area of extended, 90° bent strand (A_{ps} req'd) is given by:

$$A_{ps}(\text{req'd}) = \frac{M - A_s f_y \left(jd_{ps} + d - d_{ps} \right)}{f_{ps} jd_{ps}}$$

where

M = positive moment;
$A_s f_y$ = area and yield stress of the diaphragm coil tie rod;
d = depth from extreme compression fiber to centroid of diaphragm coil tie;
d_{ps} = depth from extreme compression fiber to centroid of strand;
jd_{ps} = internal moment arm;
$f_{ps} = (L_e - 8.25 \text{ in.})/0.228 \leq 150$ ksi; and
L_e = embedment length (in.).

After determining the required area of steel and embedment length, the section is checked for ultimate strength by:

$$f_{pu} = (L_e - 8.25 \text{ in.})/0.163;$$

$$a = (A_{ps} f_{pu} - A_s f_y)/0.85 f'_c b;$$

$$M_u = N[A_{ps} f_{pu}(d_{ps} - a/2) + A_s f_y (d - a/2)];$$

b = width of compression face (rectangular section assumed);

f'_c = compressive strength of concrete; and

N = understrength factor.

The results of the two phases are given in two interim reports (*8, 9*) and a summary appears in the final report (*10*).

Another study was conducted in 1980 (*13*). In this study, the fatigue resistance of the untensioned, bonded prestressing strand, consistent with the bent-strand configuration for a precast I-beam bridge, was examined. Eighteen single-type specimens, consisting of overlapping, opposing bent strand cast into a single block of concrete, and twenty-three double-type specimens, consisting of U-shaped strand with a concrete block cast on each end, were tested in cyclic tension. This study recommended that the stress in the strand be limited to 15% of the ultimate strength of the strand to prevent fatigue failure. It was further recommended that the diaphragm be cast before the slab.

In addition to the Missouri studies, five other studies on continuous span bridges were found. Abdalla, Ramirez, and Lee (*14*) tested three continuous Type I girders and a 27-in. box girder, all with debonded strands. In each case, the girders were assembled into a single beam line of a two-span bridge with 24-ft 4-in. spans and an 18-in. diaphragm (except for the first I girder specimen, which had 24-ft spans and a 30-in. diaphragm). The ends of the girders were embedded 6-in. into the diaphragm (except for the first Type I specimen, which had an 8.5-in. embedment). A total of 12 strands were used in each I girder, while the box girders had 20 strands. The number of debonded strands was 0%, 50%, 67%, or 83% for the I girders and was 50% for the boxes. Note that the *AASHTO Standard Specifications for Highway Bridges* (*15*) does not limit the number of debonded strands, but this level of debonding would not be permitted under the AASHTO LRFD Specifications (*12*). Continuity for negative moment was achieved by using eight No. 6 bars in the 4-ft × 4-in. deck slab. For positive moment continuity, four strands were bent at 90° angles and embedded in the diaphragm.

The significant conclusions of these studies were as follows.

1. **Time-dependent moments were measured at the connection by evaluating the change in center support reactions.** These moments were compared with the predictions from the PCA method (*7*) and the method suggested in *NCHRP Report 322* (*11*) (called the "CTL method" [Construction Technology Laboratories method] in Reference 14). When using the CTL method, the time-dependent moments were evaluated both with and without the effect of restraint from the deck reinforcing steel. It was found that the method given in *NCHRP Report 322* did a better job of predicting time-dependent moments if the effect of the deck steel was accounted for; however, there were still some significant differences between measured and predicted values.
2. **The girders were loaded to produce negative moment over the support: the debonded girders exhibited flexural shear cracking where the fully bonded girders did not.** Deflection behavior was the same for both bonded and debonded girders until the flexural shear cracks occurred, at which point the debonded girders showed more deflection.
3. **The negative moment behavior was evaluated by two models: the PCA model and the CTL model.** The PCA model considers center supports to be a single support and the connection to be zero width and infinitely rigid (i.e., the beam is modeled as two spans). In the CTL model, the center support is modeled as two supports and the connection is considered to be of finite width and flexible (i.e., the beam is modeled as three spans with the center span being the finite length connection/diaphragm). The results show the CTL method provides reasonable and conservative estimates of continuity moments and negative moment capacity and that the PCA method was not conservative.
4. **Flexural shear cracks in the I girder specimens occurred earlier than predicted by the PCA and CTL methods.** For the CTL method, analysis was done using both uncracked and cracked transformed sections. The PCA method and the CTL method using the uncracked sections overpredicted the flexural shear cracking load by 35% for the specimens with 50% debonding, by 52% for specimens with 67% debonding, and by 82% percent for specimens with 83% debonding. When evaluated with the CTL method, but using the cracked section, the overprediction dropped to 19%, 33%, and 49%, respectively. The cracks opened prematurely in the debonded regions, and moment redistribution was noted.
5. **The equations for web shear cracking given in the *AASHTO Standard Specifications for Bridge Design* (*15*), coupled with the PCA and CTL methods, provided conservative estimates of shear strength for the I girders.** For the debonded girders, the measured load was 25 to 60% greater than predicted. The measured load was 10 to 30% greater than predicted for the fully bonded girders. The web shear cracking for the box girders was slightly underpredicted, with the measured load being 80% of the predicted load for the debonded girders and 93% of the predicted load for the fully bonded girders.

In another series of studies, Ramirez and Peterman (*16, 17*) studied continuous, topped deck panels. However, since these studies were on panels, not girder and deck bridges, they were not seen as germane to this research.

Tadros et al. (*18*) and Ma et al. (*19*) explored continuity in Nebraska NU-type girders. The first phase of the research was a parametric study to examine the effect of construction sequence on the development of time-dependent moments. It

was concluded that the construction sequence greatly affects the development of positive moments. It was recommended that if the diaphragm is cast first (without the slab), the slab should be cast within 230 days to prevent cracking. It was also recommended that if the diaphragm is cast first, negative moment connections be supplied between the beams to prevent cracking and spalling at the joint between the diaphragm and deck. The study further recommends that when the diaphragm and deck are cast together, an unbonded joint be used between the diaphragm and beam to allow the beam to rotate under the deck weight.

Tadros et al. (*18*) and Ma et al. (*19*) also explored the use of negative moment connections between the tops of the precast beams. Providing this connection has two advantages. This connection allows the beams to take some of the negative moment rather than relying on the deck to take all of the negative moment. The other advantage occurs when the diaphragm is cast before the slab. When the slab weight is added, the end of the beam will attempt to rotate and this will put tension into the negative moment connection. This tension is balanced by compressing the bottom of the diaphragm, and this precompression will mitigate the tensile force caused by time-dependent positive moments.

Two negative moment connections were tested. The first used threaded rods embedded in the top of an NU 1100 girder. The rods were passed through a connection plate and held with nuts. The second connection used strand that projected from the top flange of the beams. The strands of adjacent beams were connected by a strand connector. Both connection types were tested and found to perform well.

GIRDER CRACKING IN ALABAMA

A number of bridges constructed in Alabama with prestressed concrete girders made continuous have experienced significant cracking at interior supports. This experience has been widely discussed and was even reported in the national media (*20*). As a result, the authors were asked to investigate and discuss this experience.

The focus of the Alabama experience of bridges with prestressed concrete girders made continuous is the I-565 viaduct in Huntsville, where cracking was observed in the continuity diaphragms and in girders near the continuity diaphragms. A summary of information on the viaduct and the cracking observed in the prestressed girders and continuity diaphragms follows. The data were gathered from several sources, including a report on the cracked girder investigations prepared by the Alabama DOT for these bridges (*21*).

Details of the Viaduct

The viaduct is composed of dual 12,200-ft-long bridges with a combination of steel and prestressed concrete spans. The majority of the prestressed concrete girders in the bridge were PCI BT-54 or BT-63 girders. A limited number of other AASHTO girders were also used. The girders were composite with a 6.5-in. composite deck, and the decks were formed using steel stay-in-place forms or removable plywood formwork.

The ends of the prestressed girders were embedded 3 in. into continuity diaphragms. Mild reinforcement was extended from the ends of the girders into the continuity diaphragms to provide a positive moment connection. The positive moment connection reinforcement was hooked in the continuity diaphragm and was embedded into the end of the girder. The total thickness of the continuity diaphragm was 16 in.; this is significantly greater than the typical continuity diaphragm used in Alabama at that time, which was 8 or 10 in. thick. The bridge was opened to traffic in 1991.

Details of the Observed Cracks

Limited cracking in girders as described below was observed during the first inspections in Spring 1992. Cracks had opened significantly by the next inspection in March 1994, which prompted the thorough inspection of all girders on the bridge. Three types of cracks were observed:

1. Spalling in the face of the continuity diaphragm was caused as the embedded girders pulled out of the diaphragm.
2. Vertical or inclined cracks in the girders near continuity diaphragms at interior supports were observed. In some cases, the girder cracking initiated at or near the ends of the embedment of the positive moment reinforcement, which were all terminated at one location. The positive moment reinforcement terminated within the debonded length of some of the strands.
3. Vertical cracks in the end faces of the continuity diaphragms were also observed.

All three types of cracking can be attributed to the effects of positive moment at the interior support. In no cases were all girders in the bridge cross section cracked. Girders exhibiting cracking tended to be grouped in the cross section. Cracked girders were reported in 2-, 3-, and 4-span units. Cracking beyond the end region was not reported for any girders where cracking of any type was reported near an interior support.

Cracks large enough to be repaired were injected with epoxy in September 1994. In some cases, new cracks reappeared after repair although it was reported that repair specifications were not closely followed. In 1995, inspections of the approximately 2,000 girders in the project indicated that 74 girders were cracked and the continuity diaphragm was cracked from girder pull-out at the ends of 200 to 250 girders.

Girder Characteristics and Testing

Detailed monitoring and load tests were conducted on two continuous units where a number of girders were cracked.

One of the units was instrumented and subjected to load tests. Characteristics of the girders and results from the unit tested are summarized below:

- The girders in the subject span on the main line structure were PCI BT-54 girders. There were nine girders in the cross section, spaced at 8 ft. The pier-to-pier distance was 100 ft, with a design span of 98.5 ft between bearings.
- The girders were manufactured in December 1988 and January 1989. The deck was cast in late April and early May 1989.
- Cracks in the girders were monitored during load testing of the bridge. The maximum crack opening reported from the effect of two load-testing vehicles was reported to be about 0.0055 in. A maximum crack opening of about 0.030 in. was reported during the course of a day as the sun heated the deck slab.
- The camber at midspan was observed to be about 0.41 in. due to the solar effect.
- ALDOT concluded that the cracking was caused by positive moments that developed as a result of the thermal gradient across the section.
- Measured deflections from two load-testing vehicles placed on the bridge were only about 75% of the deflection computed using a finite element model; therefore, it was concluded that the presence of the cracks did not significantly affect the structural behavior of the bridge.

As a result of the experience of cracking with this and other bridges, ALDOT no longer allows the use of prestressed concrete girders made continuous.

Subsequent to the investigation of the I-565 bridge in Huntsville, another bridge was found with cracking in the girders near the continuity diaphragms. This bridge was located on US 280 in Lee County, Alabama. The bridge was constructed using AASHTO Type II girders with mild reinforcement extending into the continuity diaphragms to make a positive moment connection. The girders were also embedded several inches into the continuity diaphragm. The behavior of this bridge was investigated by monitoring crack widths and performing a load test. The investigation produced the same results regarding the cause of cracking and the remaining capacity of the bridge as for the previous bridge.

Conclusions Drawn from ALDOT Bridge Cracking

The cracking observed in the girders and continuity diaphragms of the Alabama bridges was significant and definitely a matter of concern. However, similar situations with widespread cracking of this type have not been reported in the United States for bridges with prestressed concrete girders made continuous. In fact, similar bridges constructed at about the same time in Alabama have not exhibited the extent and type of cracking observed on the I-565 bridge.

In conclusion, several points can be made:

1. The effects of the thermal gradient across the depth of the superstructure may be significant in the design of bridges with precast concrete girders made continuous.
2. The Alabama bridges continued to perform as designed even with significant cracking at the ends of some girders in the cross section.
3. Very few bridges with precast concrete girders made continuous have experienced significant cracking of the type observed on the I-565 and US 280 bridges in Alabama. In general, performance of this type of bridge has been very satisfactory.
4. The thickness of the continuity diaphragm and the embedment of the girders into the diaphragms may have been a significant factor in causing the observed cracking in the girders.

INITIAL ANALYTICAL STUDIES

Using the information gained in the literature search and from the survey, the next task was to propose specimen configurations for the experimental work. To accomplish this task, an analytical model was created. This model, a modernized version of BRIDGERM (*11*), was named RESTRAINT and works within a standard spreadsheet program (see Appendix A).

The program models a two-span continuous structure. The support conditions assume that there is a support at each end of the girder (see Figure 3) because this was the most common support condition identified in the survey. This is also consistent with the support condition used in analysis program BRIDGERM given in *NCHRP Report 322* (*11*). RESTRAINT used flexibility-based analysis by discretizing the span and the diaphragm into several elements. Prior to using the restraint program, moment curvature relationships are developed for the cross section. Any convenient method of determining the moment-curvature relationship (e.g., hand calculations, computer program, finite element analysis, or experimental data) can be used. For this study, the RESPONSE Program (*22*) was used to find the moment-curvature relationship. These data are then input into the spreadsheet.

The time the diaphragm and deck are cast as input into RESTRAINT, assuming that release of the pretensioning force is time = 0 (this can be a different time based on the age of girder; however, the reference is made to the time after the release of post-tensioning). Because some states cast the diaphragm first, the program allows the time the diaphragm and deck are cast to be different. Basic material properties are also input.

With the basic information available, the program calculates the internal moments that would result from creep of the prestressed girder and shrinkage of the girder and deck. Creep and shrinkage strains are found from the relationships given

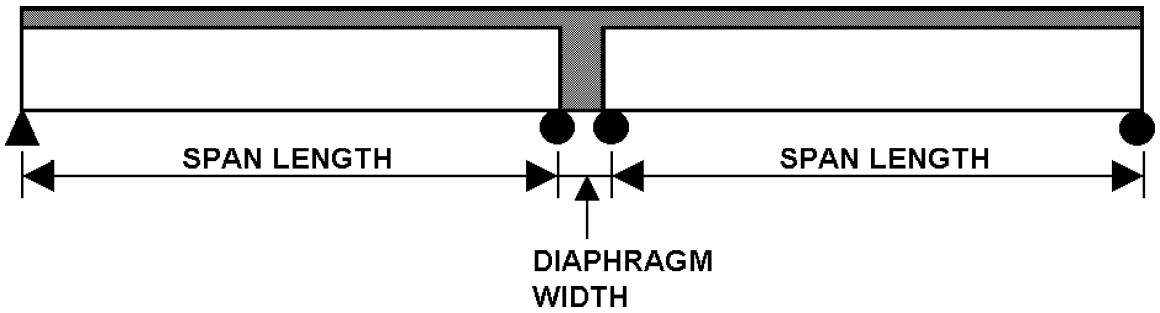

Figure 3. RESTRAINT Model.

in the American Concrete Institute Report 209 (*23*). The program also accounts for loss of prestressing force using the method given in the Precast/Prestressed Concrete Institute Handbook (*24*). In the span, shrinkage of the deck and girder is assumed to be uniform, while creep caused by dead load plus prestressing force is assumed to be parabolic. At the diaphragm there is no prestressing, so the creep is 0. Since the slab and diaphragm are usually cast together, the differential shrinkage between them is assumed to be 0.

Once the internal moments are known, the program adds the dead-load moments. If desired, a live load, consisting of a point load at midspan, can be included and the moment from this force is also added. The program then divides each span into 10 or more elements (defined by the user). A single element is used for the diaphragm. With the moments known, the program can determine the curvature of each element from the moment-curvature relationship. The program then performs a consistent deflection analysis. The center reactions are removed to make the system statically determinate. Using the curvatures, the deflection at the center supports can be found. The required reactions needed to restore the center support deflection to 0 are found. The other reactions are found from equilibrium and are used to calculate the continuity moments. The continuity moments are then added to the other moments, and the entire analysis is repeated until the answer converges.

To verify this program, the ½-scale I girders used in the original PCA tests were modeled (*6*). The results showed a reasonable agreement with the experiment (see Figure 4), although the effect of differential shrinkage (the first peak in the curve) was overestimated.

A parametric study was conducted on a two-span bridge consisting of AASHTO Type III girders. The spans were 65 ft, and the girder spacing was 8 ft. A 2-ft-wide diaphragm was

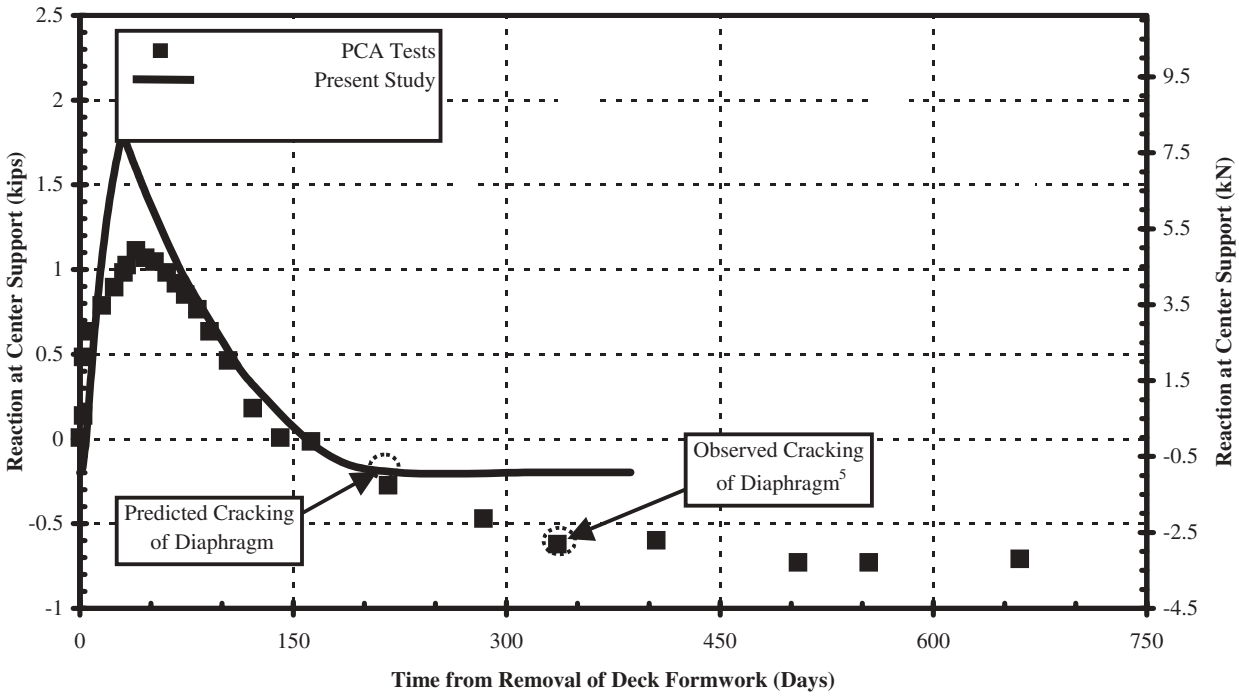

Figure 4. Comparison of RESTRAINT (Present Study) with PCA data.

used and the deck thickness was taken as 8 in. Complete details of this study can be found in the literature (*25*).

The conclusions of the parametric study were as follows:

1. **The age of the girders at the time continuity is established was the single most important factor in behavior,** as expected. If continuity is established when the girders are young, creep of the girders dominates the behavior leading to the formation of large positive restraint moments. If the girders are older, the dominant effect is differential shrinkage between the girder and the deck. This causes the formation of an initial negative moment. Depending on the relative age and properties of the girder and deck, this initial negative moment may be larger than the positive restraint moments cause by girder creep, leading to a net negative moment at the connection.
2. **The amount of positive moment reinforcement at the diaphragm had a significant effect on performance.** If no positive moment connection was used, the system cracked and the system behaved as simple rather the continuous spans. As the amount of positive moment reinforcement at the connection was increased, there was an increase in continuity—that is, the midspan positive moment due to live load decreased and the negative moment over the pier due to live load increased. Greater amounts of positive moment reinforcement also reduced the cracking at the connections; however, greater amounts of positive moment reinforcing increased the positive restraint moment. The effect of the positive restraint moment must be added to the positive moments caused by dead and live loads. For the limited number of cases studied, the net positive moment at the midspan is essentially independent of amount of reinforcement used in the positive moment connection at the diaphragm. This conclusion was similar to that drawn by *NCHRP Report 322* (*11*).
3. **Some designers and owners recommend that the positive moment connection at the diaphragm have a capacity of no greater than 1.2 M_{cr},**where M_{cr} is the positive cracking moment calculated using the nontransformed composite cross section and the concrete strength of the diaphragm (it assumes that failure will occur in the diaphragm, but in the shape of the composite cross section). The results of the parametric study showed that using connection details with capacities above 1.2 M_{cr} did not significantly improve the behavior of the structure. Thus, limiting the positive moment reinforcement such that the capacity does not exceed 1.2 M_{cr} seems reasonable from a practical standpoint because additional reinforcement is not beneficial and it increases diaphragm congestion.
4. **Using RESTRAINT, a continuity index was defined as the ratio of the calculated live-load moment divided by the live-load moment that would occur if the system were linear elastic and continuous.** A continuity index of 1 indicates full continuity. For the midspan, the continuity index will be 1 or greater and the continuity will be 1 or less at the supports. The parametric study indicated that, due to cracking, the system will never be 100% continuous and the maximum continuity will be about 80%.
5. **The program did not show any significant effect of diaphragm width.** In this study, diaphragm width is perpendicular to the span. The diaphragm dimension parallel to the span is referred to as the thickness. Initially, the diaphragm was modeled as a rectangular section with a width equal to the effective width of the composite girder flange. The diaphragm was also modeled as a T beam with a flange width equal to the effective width of the composite girder flange and a web width equal to the bottom flange of the girder. There was no significant difference in the results.

An additional parametric study was performed on a two-span bridge using AASHTO Type V girders with 100-ft spans to see whether girder size and span altered results; however, the results showed that the conclusions of the original study remained valid.

EXPERIMENTAL STUDIES

Positive Moment Connection Capacities—Stub Specimens

The survey results showed a wide variety in positive moment connection details used by the various states. One of the issues the experimental program attempted to address was the capacity of different details for the positive moment connections. To test positive moment connection capacities, a series of six short, or stub, specimens were tested. The specimens consisted of two 16-ft-long Type II AASHTO I girders joined by a diaphragm (see Figure 5). They were intended to represent the length between live-load inflection points at a connection in a multispan bridge consisting of equal 50-ft spans. The distance between the ends of the girders in the connection was always 10 in., but the dimension of the diaphragm varied with the connection being tested.

The six connections consisted of different combinations of connection type (bent bar or bent strand) and diaphragm widths. Table 1 details the connections and Figure 6 shows typical details. Specimens 1 and 2 tested basic bent-strand or bent-bar connections. Since some states embed the girder ends into the diaphragm, Specimens 3 and 4 had the stub girders embedded into the diaphragm. Specimen 5 examined whether adding stirrups in the diaphragm just outside of girders would strengthen the connection. Some states place horizontal bars through the webs, flanges, or both of the girder to strengthen the connection. This was tested in Specimen 6.

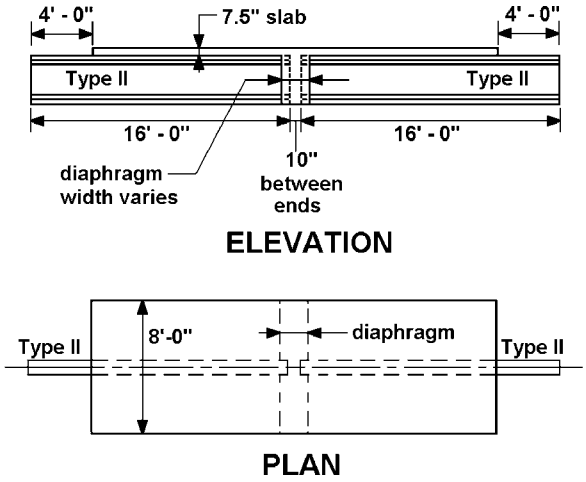

Figure 5. Connection capacity (stub girder) specimen.

The analytical study had suggested that, to counteract the time-dependent effects, it was not efficient to have a connection where the capacity exceeded 1.2 times the cracking moment (1.2 M_{cr}), so the bent-strand or bent-bar connections were detailed to have a capacity of 1.2 M_{cr}. The usual design assumption is that cracking will occur at the interface of the beam and the diaphragm, but that the failure will occur in the diaphragm concrete. Therefore, the cracking moment, M_{cr} is usually based on the composite cross section, but assuming the entire section is made of diaphragm concrete.

All bent bar connections were detailed using hooked No. 5 bars meeting the provisions for hooked bars in the AASHTO LRFD Specifications (see Figure 6). It was necessary to offset bars so that they would mesh without interference, resulting in an asymmetrical connection. As will be discussed later, this asymmetry seems to have affected the connection behavior.

For the bent strand, the number of strand and the length of the strand to be embedded in the diaphragm were determined based on the equations suggested by Salmons and others (*8–10, 13*), which are given in the previous section on the literature search. The number of strands was chosen arbitrarily as six because this number used the entire bottom row of strands. The equations are then used to determine the required length of strand to be embedded in the diaphragm. Salmons and his coauthors suggest that the length of strand be determined based both on a working stress and an ultimate strength and on the largest of the two chosen. For these details, the connection was assumed to have a working strength of M_{cr} and an ultimate strength of 1.2 M_{cr}. The length of strand embedded into the diaphragm was calculated to be 26 in., consisting of an 8-in. projection into the diaphragm before the bend and an 18-in. tail after the bend. Detailed calculations are given in Appendix B.

The specimens were tested as cantilever beams (see Figure 7). The specimen sat on a center support and was temporarily supported at both ends. Loading mechanisms were placed at each end (see Figure 8). During testing, one end was lifted off its support and the support was removed, creating a cantilever beam. The free end was then subjected to the required loading regime. Complete details of the experimental set-up are in Appendix B. On Specimens 1 and 2, the deck was not cast all the way to the end. This was done so that the stub girders could be reused. After testing the first connection, the diaphragm was cut out and the girders were turned end-for-end, placing the previously unused end of the stub at the diaphragm. The diaphragm and a portion of the slab could then be cast and new specimens created (Specimens 3 and 4). For consistency and to allow attachment of the loading mechanism, the ends of the slabs were cut off of the previously used girders when they were turned end-for-end (Specimens 3 and 4). Specimens 5 and 6 each used new girders, but the slabs were not cast all the way to the end. Again, this was for consistency and to allow attachment of the loading mechanism.

To understand the loading regime, it is necessary to consider a multispan bridge. As the truck traverses the first two spans, the connection between the first two spans is subjected to the maximum negative live-load moment. As the truck enters the third span, this same connection is now subjected to the maximum positive live-load moment. The value of the maximum negative live-load moment was determined by analyzing two-, three-, and four-span bridges, with each span being 50 ft. The maximum negative live-load moment was almost the same for all three bridges and was found to be approximately 365 k-ft. Analysis of three- and four-span bridges yielded the maximum positive live-load moment, which was determined to be

TABLE 1 Details of positive moment connections in the stub specimens

Specimen Number	Type of Specimen	Diaphragm Width (in.)	Girder End Embedment (in.)	Special Feature	Cycles to Failure
1	Bent strand	10	0	None	16,000
2	Bent bar	10	0	None	25,000
3	Bent strand	22	6	None	55,000
4	Bent bar	22	6	None	11,600
5	Bent bar	22	6	Extra stirrups in diaphragm	56,000
6	Bent bar	26	8	Web bars	13,3000

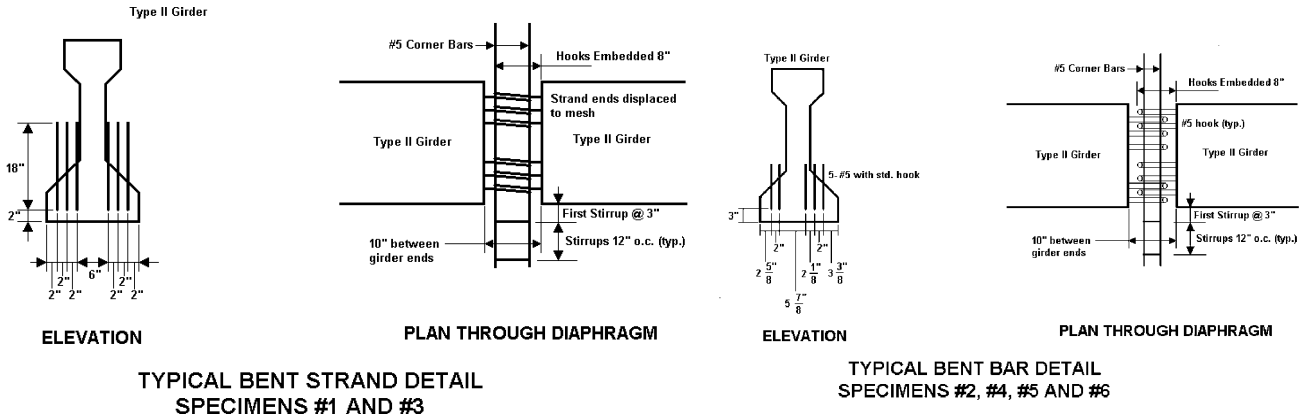

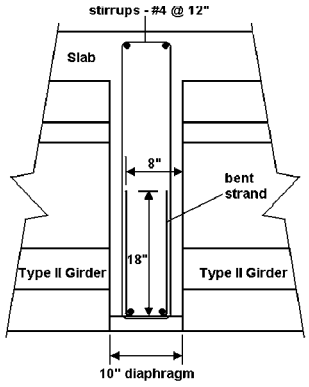

Specimen #1 - Bent Strand

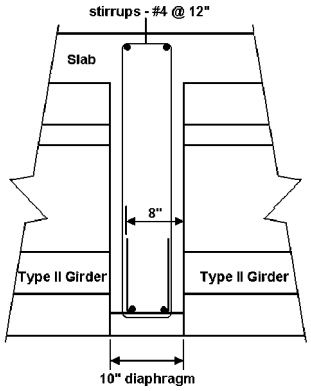

Specimen #2 - Bent Bar

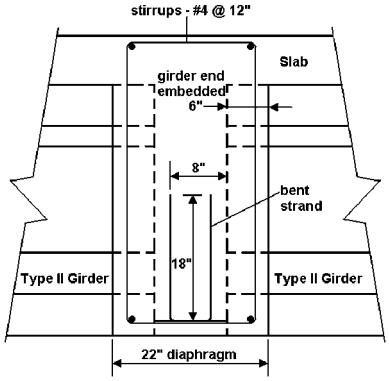

Specimen #3 - Bent Strand - Girder Ends Embedded

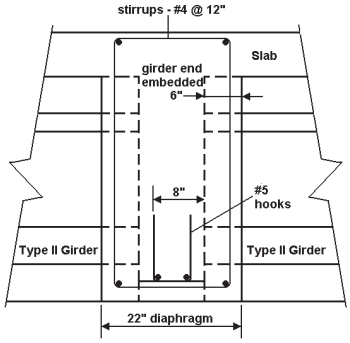

Specimen #4 - Bent Bar - Girder Ends Embedded

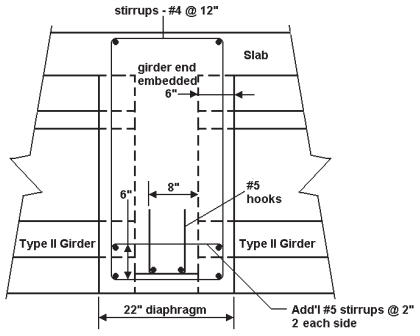

Specimen #5 - Bent Bar - Girder Ends Embedded - Additional Stirrups

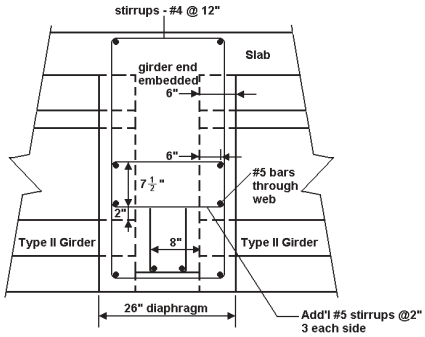

Specimen #6 - Bent Bar - Girder Ends Embedded - Web Bars

Figure 6. Details of the connections.

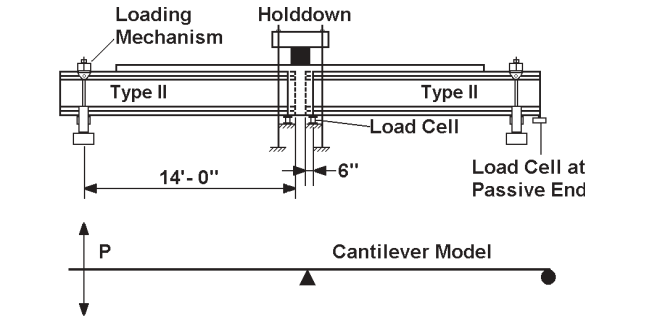

Figure 7. Test set-up for the stub girder specimens.

approximately 90 k-ft. All moment values were at the face of the diaphragm.

The loading regime was designed to represent the worst case loading. In this case, it was assumed that creep, shrinkage, and/or temperature strains in the deck and girders would produce a positive moment equal to the nominal cracking moment, M_{cr}. It was also assumed that the cracking would occur at the beam-diaphragm interface and that the limiting factor would be properties of the diaphragm concrete. Therefore, the nominal cracking moment was calculated using the geometry of the composite beam, but the properties of diaphragm concrete. The section is considered as reinforced but not prestressed. This is consistent with normal design practice. The deck and diaphragm were assumed to have a nominal strength of 4,000 psi, and the nominal cracking moment is calculated as 245 k-ft. Since the connection was assumed to be loaded to M_{cr} by time-dependent and temperature effects, the live load would cycle the moment about M_{cr}.

The loading regime is shown in Figure 9. The first three cycles are between the positive and negative live-load moments. This simulates loading the bridge without any time-dependent moments and provides initial stiffness data for the connection. Next, the connection is loaded three cycles to the cracking moment to simulate the assumed effect of the time dependent and temperature moments.

The connection was then loaded to the combination of the live-load moments and the assumed time-dependent and temperature moments: $M_{cr} \pm M_{LL}$. This is a very severe loading sequence, which is thought to represent a worst-case scenario. The first load cycle exceeded the nominal capacity of 1.2 M_{cr}, so there was a possibility that the connection would fail on the first load cycle. The connection would be cycled at $M_{cr} \pm M_{LL}$ for 1,000,000 cycles or until the connection failed.

General Observations on the Stub Specimens

While each connection had its own unique characteristics, there were some characteristics that were common to all the specimens. Figures 10 and 11 show the actual load versus the end deflection of Specimen 5 and a set of best-fit linear curves. The linear curve fitting was done automatically in a standard spreadsheet program. These results are representative of all specimens. The initial stiffness of the system is consistent with theoretical results (see following section on finite element modeling analysis). The section retains this stiffness until it is loaded to the cracking moment, M_{cr}. After this, the specimen shows a bilinear response. This is the result of the loading system (see Appendix B), which loads the specimen as a cantilevered beam. When the applied load is 0, the connection is being compressed by the dead-load moment, which is approximately 100 k-ft. At an applied load of 7 kips, the dead load is relieved and the crack begins to open. Until the compressive stress from the dead load is relieved, the connection maintains a stiffness equal to the initial stiffness. After the compressive stress is relieved, the connection stiffness drops markedly. There is a slight reduction in stiffness with additional cycles, but the change is small. However, during the cyclic loading, there is still load transfer across the joint. Eventually the positive moment connection fails, either by pull out of the strand or fracture of the bars. The resulting load versus deflection graph shows the resistance, and eventual failure, of the slab alone (see Figure 10). At this point, the connection behaves like a hinge.

It was noted that the cracking behavior is quite different than that assumed in theoretical models. These models assume the concrete is monolithic and when cracking occurs, the resulting cracked section shows the cracks going all the way into the slab (see Figure 12). In reality, there are cold (construction) joints at the beam-diaphragm interface and at the beam-slab interface. Because the joint at the beam-diaphragm interface is based on a weak chemical bond, which is not as strong as the tensile strength of monolithic concrete, cracks may form before the calculated cracking moment is reached. However, at the top of the crack, the joint at the beam-slab interface tends to act as a crack arrestor. It was noted that the crack would form at the bottom of the joint, propagate to the top of the beam, and stop. The cracks did not propagate into the slab until just before the connection failed (see Figure 13). In fact, it was found that formation of cracks in slab was usually a sign of impending failure.

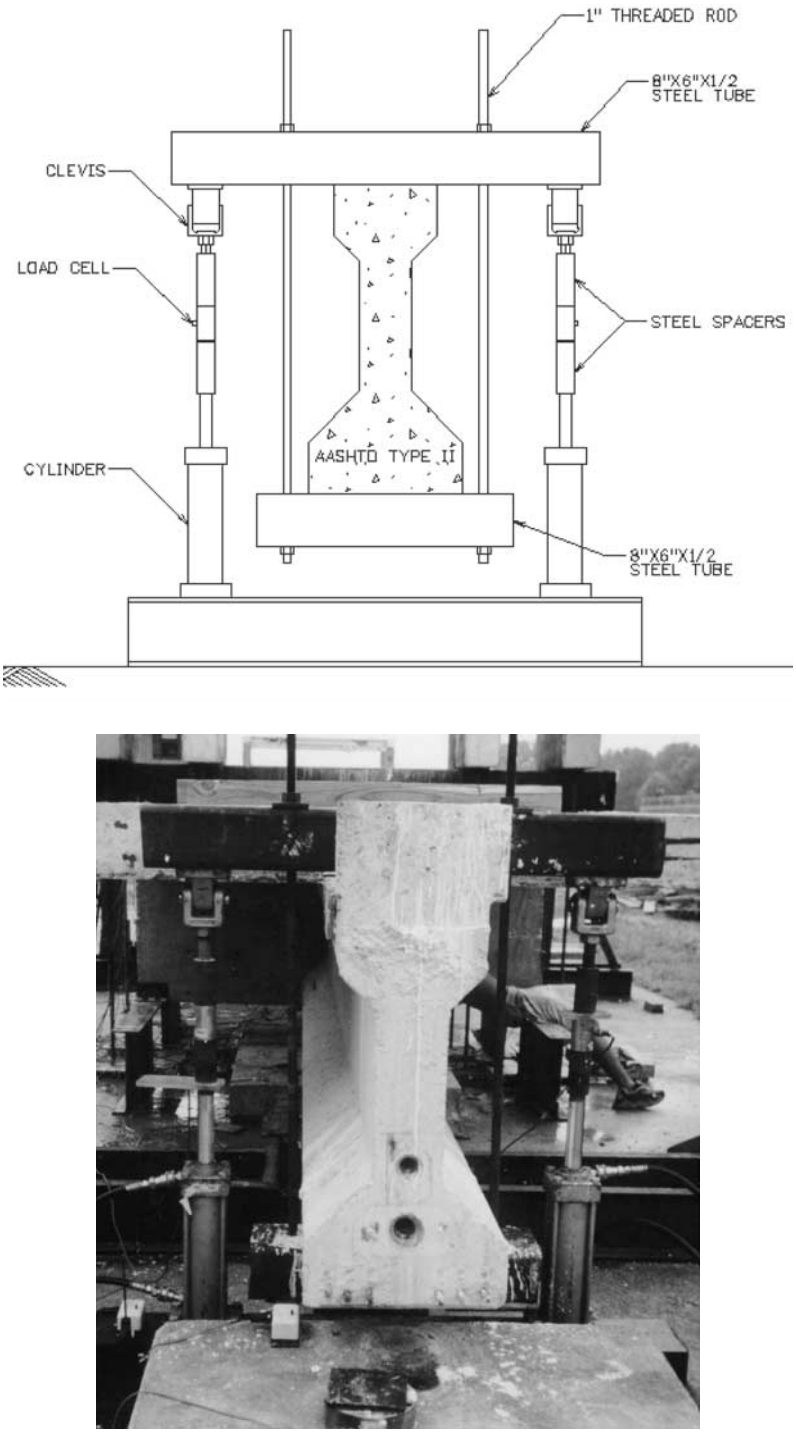

Figure 8. Loading device.

Stub Specimen 1: Bent Strand

Specimen 1 was a bent-strand connection where the girder ends were not embedded in the diaphragm (see Figure 14). This specimen proved rather easy to construct. The strand was bent by the fabricator using a small hand-pumped hydraulic device, which had been designed by one of the maintenance workers. This device provided sharp, clean, 90° bends. However, it was noted that this device kinks the strand with a bend radius of about 0.5 in. and did break individual wires on some of the bent strands.

It was not difficult to place the girders end-to-end because the strand is very flexible and could be easily moved. However, the strands touched each other on the sides (see Fig-

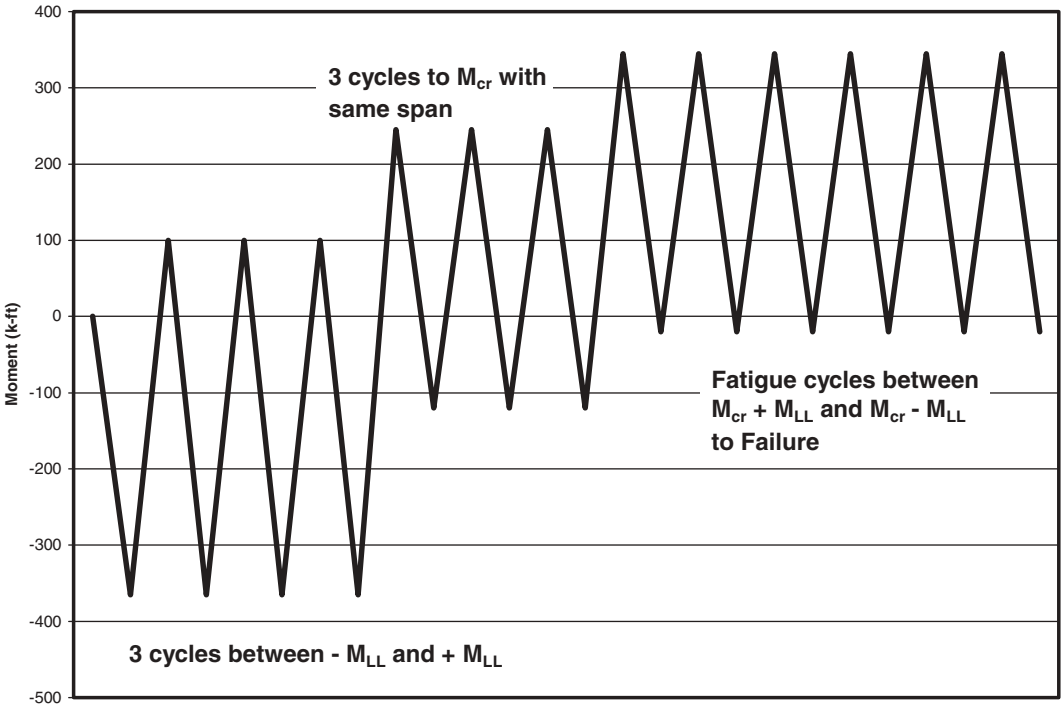

Figure 9. Loading of the stub girder specimens.

ure 14), so concrete could not completely surround the strand. This would lead to interaction effects. It was also found that when the concrete was placed and vibrated, the strand ends moved from side to side with the placement and vibration, so the actual final position of the strand tails was not known.

Unfortunately, there were a few problems with testing this first specimen. After the assembly of the specimen, the hydraulic system suffered a break down and was not operational for about 4 months. During this time, the specimen was subjected to thermal deformations. By the time the test had started, it was noted that hairline cracks had formed at the girder-diaphragm interface.

A second problem occurred when the specimen was loaded to M_{cr}. Using the loading system described in Appendix B,

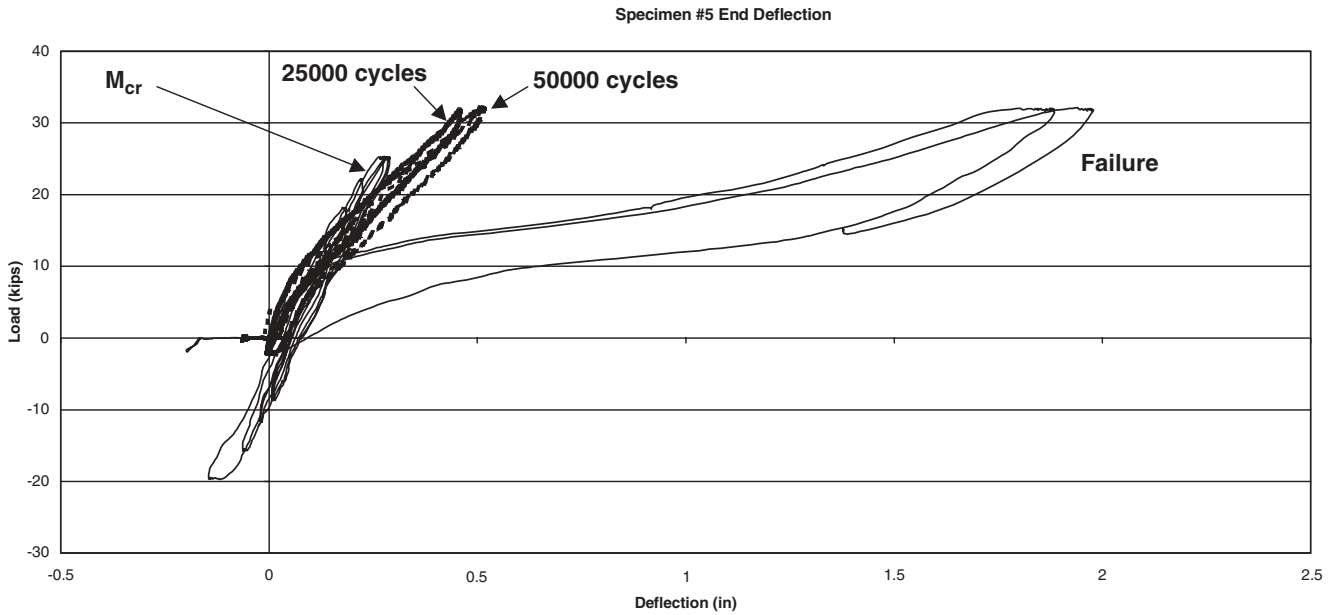

Figure 10. Load versus end deflection for Specimen 5.

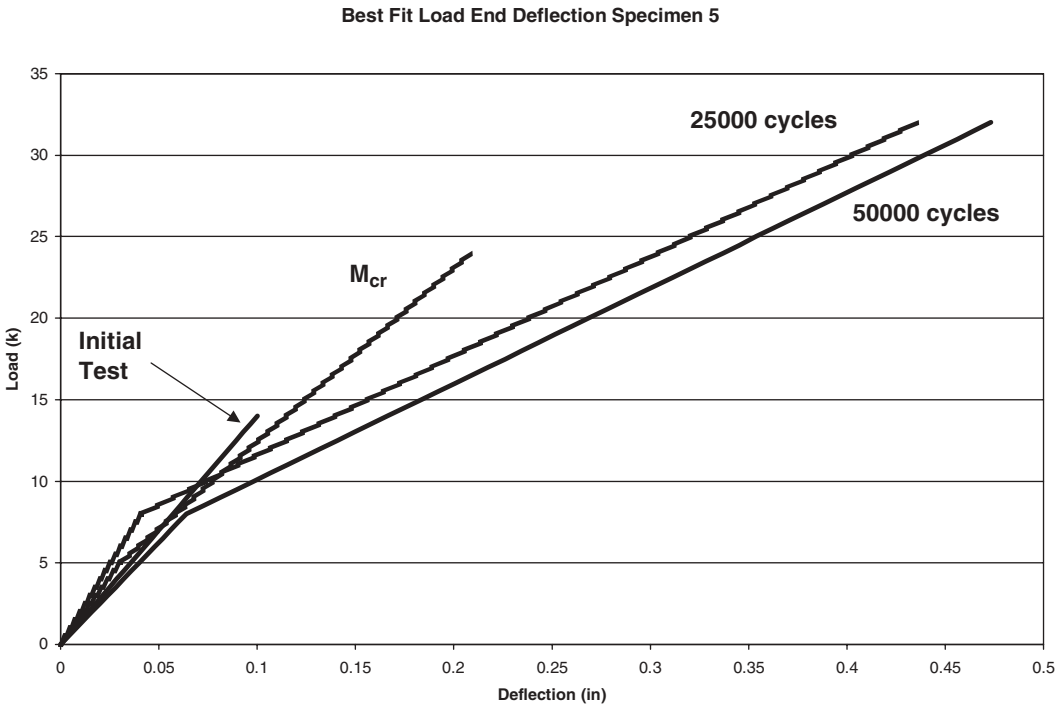

Figure 11. Best-fit load versus end deflection for Specimen 5.

the load applied to the system had to be calculated taking dead-load effects into account. The load at the end supports was read from the load cells. It was assumed that all the load was dead load; however, subsequent calculations revealed that thermal effects had caused the specimen to camber up and the end reactions had increased. This thermal effect was inadvertently added to the applied load, and the specimen was overloaded in the positive moment direction by approximately 35% on the first few load cycles. After the error was discovered, the specimen was loaded correctly for subsequent load cycles. However, it is possible that the overload may have damaged the connection and shortened the cyclic load life span.

The specimen survived for 16,000 cycles before failing. Failure occurred when the concrete on the bottom of the diaphragm split and popped off (see Figure 15). Usually a splitting type of failure is a sign of slipping and pull-out of the strand. There was noticeable spread, or "bird-caging," of the strand. The strands were not broken, although some individual wires were broken.

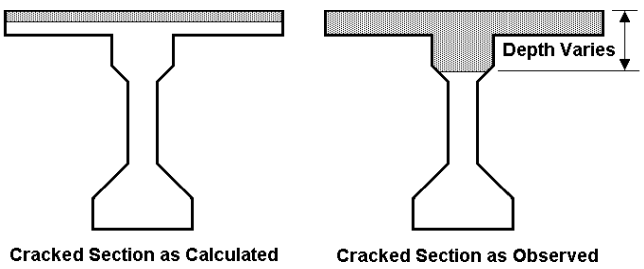

Figure 12. Theoretical and observed cracked sections.

Stub Specimen 2: Bent Bar

Specimen 2 used a bent-bar configuration (see Figures 1 and 16). The girder ends were not embedded in the diaphragm. This specimen was more difficult to construct. An unsymmetrical bar pattern must be used to avoid interference when the connection is assembled. It was also found that the bars cannot be installed pre-bent. As shown in Figure 6, the bent bars extend above the top of the bottom flange of the specimen. If the bars are installed pre-bent, the metal beam forms cannot be closed. As a result, straight bars were cast into the

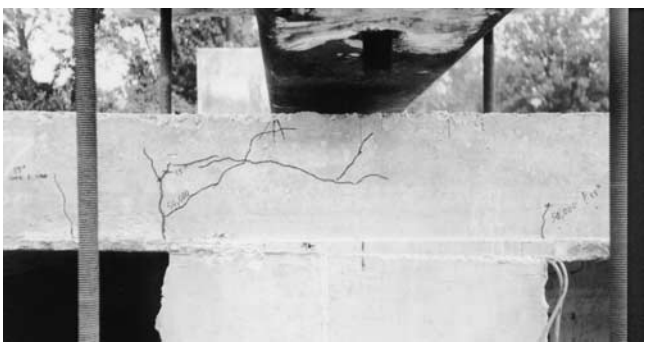

Figure 13. Typical slab cracking.

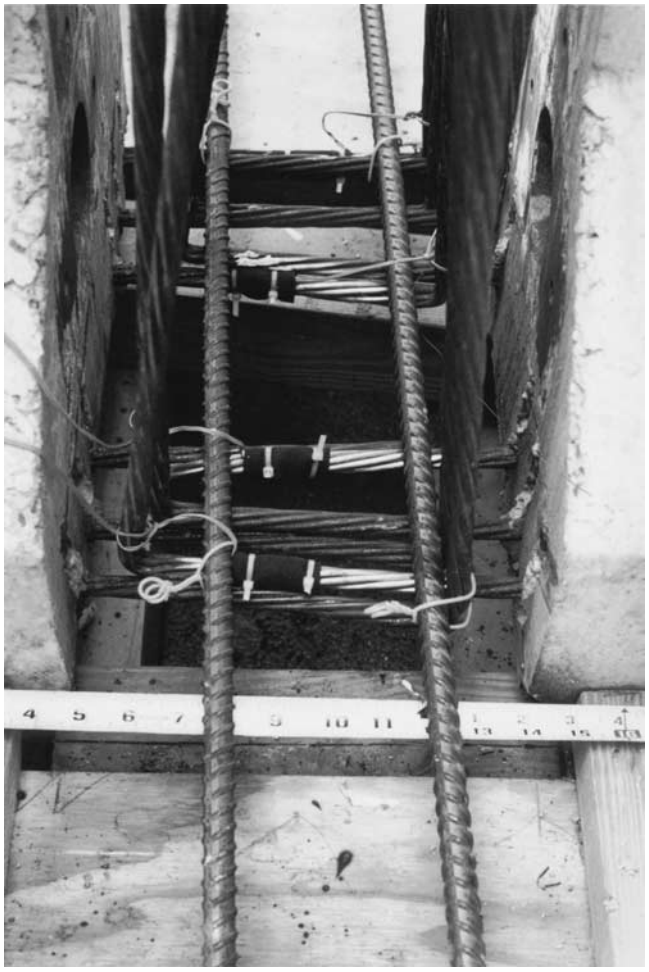

Figure 14. Bent strand, Specimen 1.

end of the girder and the bars were field bent. In the field-bending operation, it was difficult to bend the bars consistently to the same length and radius. The lack of consistency in the bends made it hard to install the corner bar in the bends (see Figure 16).

Once assembled, the specimen was tested in the same manner as Specimen 1 (see Appendix B for details). This specimen lasted for 25,000 cycles before failure. At failure, there were diagonal cracks that formed in the faces of the diaphragm and part of the diaphragm spalled off (see Figures 17 and 18). These cracks are similar to those found in actual bridges (see Figure 19). The bars were found to have fractured (see Figure 20). A visual examination of the bars by a metallurgist showed the bars had failed in fatigue.

An observation was made with respect to crack opening: in Specimen 1, crack openings on either side of the stub beam were the same, but this was not true of Specimen 2. As shown in Figures 6 and 16, the bars in the stub beam are closer to one side of the bottom flange than to the other. The crack openings on the side of the flange where the bar was closer were smaller than those on the opposite side.

Figure 15. Failure of Specimen 1, bent strand.

Stub Specimen 3: Bent Strand, Beam Ends Embedded

Specimen 3 was identical to Specimen 1 except that the diaphragm width was increased to 22 in. (560 mm) and the stub girder ends were embedded 6 in. into the diaphragm. This specimen lasted for 55,000 cycles before failing. The mode of failure was quite different from the nonembedded specimen: while both specimens showed extensive spalling of the concrete on the bottom of the diaphragm, the embedded specimen also exhibited cracking and spalling on the face of the diaphragm (see Figure 21).

Stub Specimen 4: Bent Bar, Beam Ends Embedded

Specimen 4 was identical to Specimen 2 except that the girders were embedded 6 in. into the diaphragm. This specimen

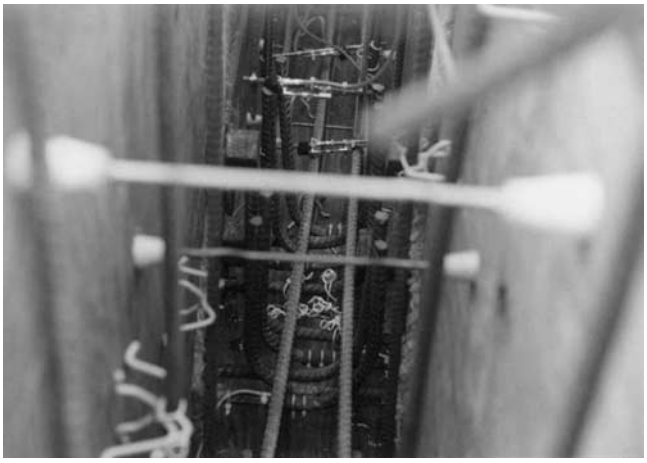

Figure 16. Bent bar, Specimen 2.

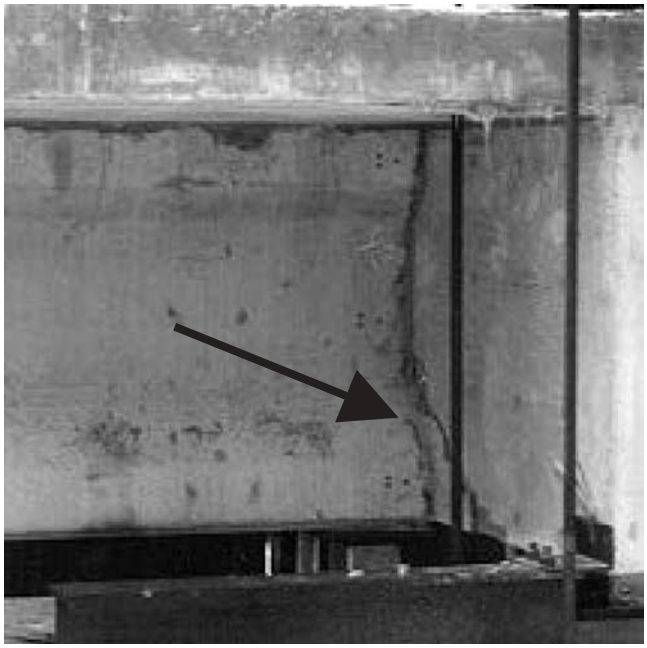

Figure 17. Diaphragm diagonal cracking.

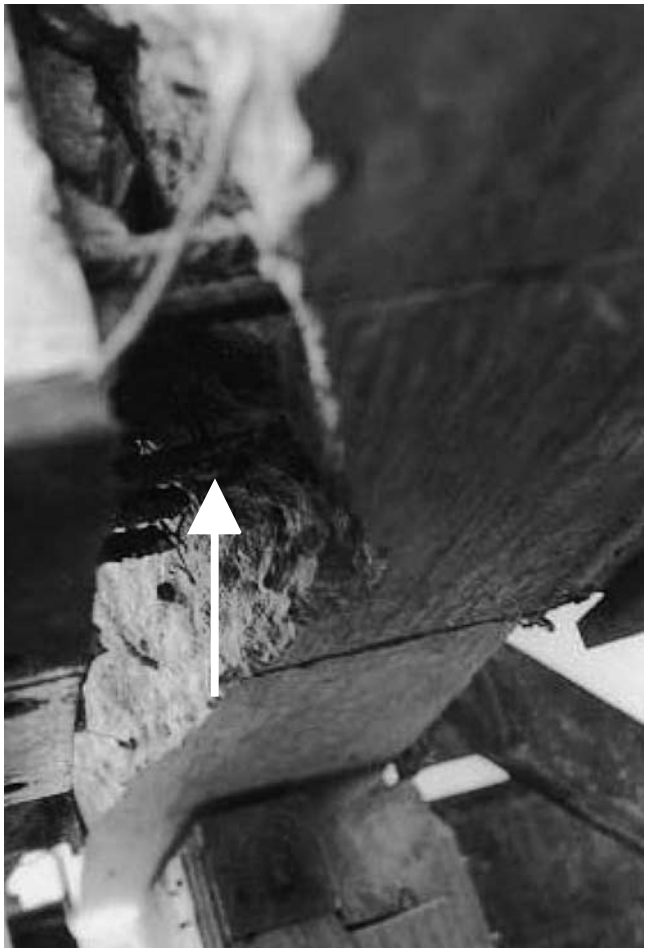

Figure 18. Spalling of the diaphragm.

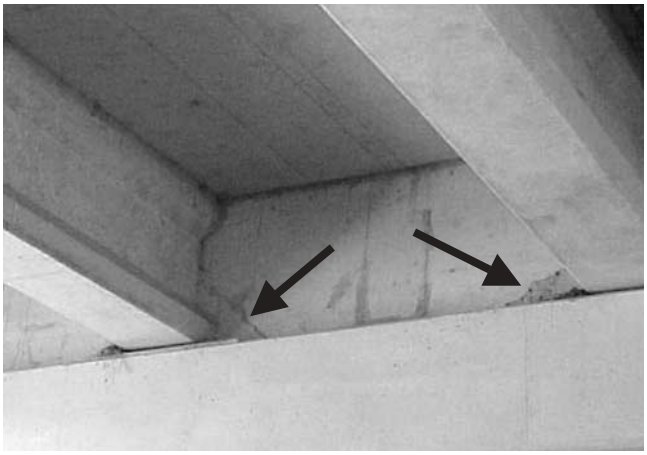

Figure 19. Diagonal cracking and spalling in a bridge in Tennessee.

Figure 20. Fractured bars.

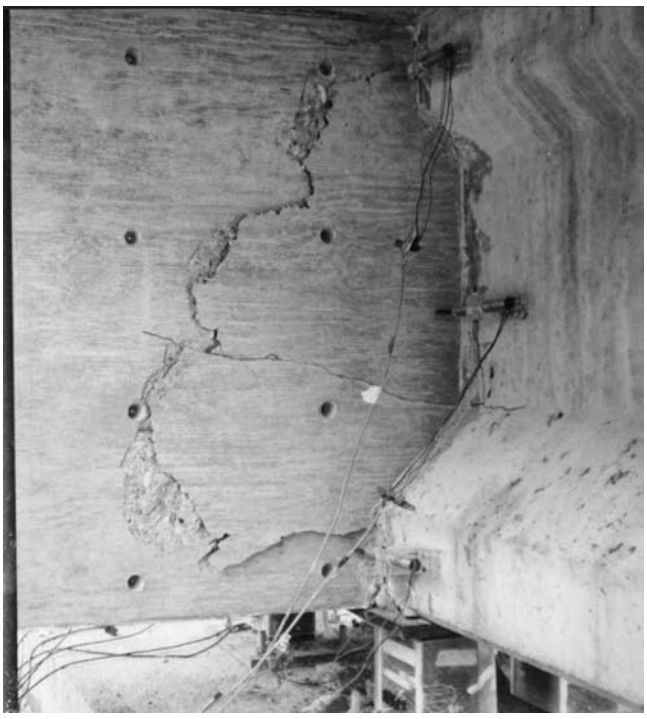

Figure 21. Diaphragm spalling, Specimen 3.

only lasted for 11,600 cycles. Examination of the data showed no particular or peculiar behavior that might account for this unexpected failure. As explained in Appendix B, the cyclic loading was stopped at certain intervals and static load tests were performed. The static load test at 10,000 cycles showed that the cracks on one side of the diaphragm were opening much wider than those on the other side (0.05 in. on one side, 0.025 in. on the other). These crack openings were not unusually large compared with those for other specimens. Approximately 1,000 cycles later, the specimen failed. The bars fractured and diagonal cracks occurred in the diaphragm.

The cause of this early failure is uncertain, but the most probable explanation is uneven stresses in the bars. Bent-bar connections are difficult to construct because the bars must be installed straight and then field bent. As a result, the bar bends are inconsistent (see Figure 16). This inconsistency in the bends may have caused some bars to take more load than others, leading to a premature failure. Bonded strain gages had been installed on some of the bars; but only one survived beyond 5,000 cycles, so comparisons of bar strains are not possible.

Stub Specimen 5: Bent Bar, Beam Ends Embedded, Additional Stirrups in Diaphragm

Specimen 5 was identical to Specimen 4 except that additional stirrups were placed in the diaphragm, close to the outside edge of the bottom flange (see Figures 6 and 22). This test was to see if these additional stirrups would strengthen the connection. If these stirrups strengthen the connection, they could be used in place of some of the bars extended from the end of the girder, lessening the congestion in the diaphragm area.

This specimen took 56,400 cycles before failure, and the failure was similar to that of Specimen 4. It did not appear that the additional stirrups added any strength to the connection. However, the stirrups did preserve the strength after the main bars had fractured. After fracture of the bars in Specimen 4, the largest load that could be applied was 26 kips and the end deflection was 4 in. Specimen 5 was able to hold the test load of 32 kips with an end deflection of 2 inches. Visual observation of the failure area showed that the additional stirrups were spanning the crack and preventing failure (see Figure 23). This detail may be useful in seismic zones to provide additional ductility.

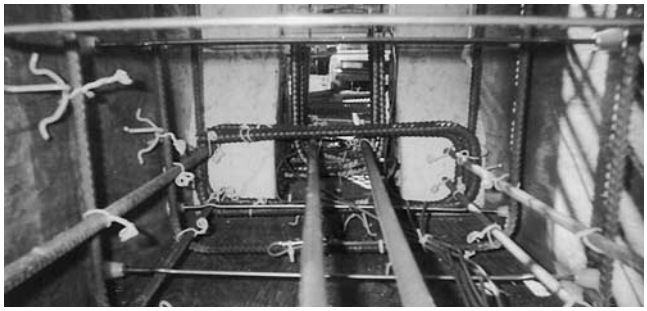

Figure 22. Additional diaphragm stirrups, Specimen 5.

Stub Specimen 6: Bent Bar, Beam Ends Embedded, Web Bars Added

Specimen 6 used the same bent-bar configuration as Specimens 2, 4, and 5, but this connection used horizontal bars passed through the web of the beam (see Figures 6 and 24). The survey results showed details similar to this are used by some states. Since the stub beams were fabricated before it was decided to use this type of specimen, no holes were cast in the web for these bars. As a result, the holes had to be drilled. The vertical beam stirrups were located with a magnetometer, and a hammer drill was used to make the holes. No. 5 reinforcing bars were then passed through the holes and encased in stirrups (see Figures 6 and 24). In order to accommodate these web bars, the diaphragm had to be enlarged to 26 in.

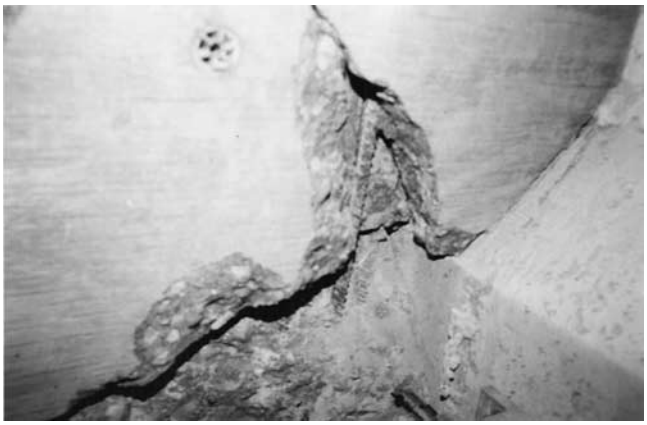

Figure 23. Failure of Specimen 5, stirrups span the crack.

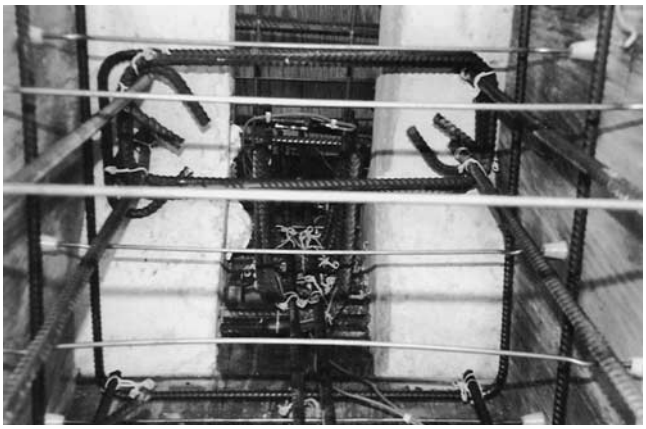

Figure 24. Web bars, Specimen 6.

This detail significantly improved the behavior of the connection. The connection lasted for 133,000 cycles before failing. This connection was also stiffer than the others tested (see the finite element modeling analysis section, this chapter). After the bars in the positive moment area fractured, the specimen was still able to hold the applied load of 32 kips with an end deflection of 1.2 in.

Failure was due to fracture of the bars in the positive moment connection and by the girders pulling out of the diaphragm. At failure, there was significant spalling of the diaphragm concrete. After the test was complete, the spalled diaphragm concrete was broken out so the beams could be inspected. Cracking was found in the webs (see Figure 25), so while this connection performed better than any other, the cracking in the beams at failure might be an undesirable result.

The Effect of Embedment

Four of the six specimens had the girder end embedded into the diaphragm. For the bent-strand connection, embedment seemed beneficial. The number of cycles to failure increased by a factor of three. A change in failure mode was observed. In the nonembedded bent-strand specimen, the girders separated from the face of the diaphragm, but there was no damage to the face of the diaphragm. In the embedded specimen, diagonal cracks indicating a pull-out type of failure were observed.

For the bent-bar specimens, the results were less conclusive. The embedded bent-bar specimen (Specimen 4) failed at less than half the cycles of the nonembedded specimen (Specimen 2), but another embedded bent-bar specimen (Specimen 5) failed at twice the number of cycles as the nonembedded specimen. Bonded strain gages were placed on four of the bent bars in each specimen, but the survival rate of these gages was low. Often, only one or two gages survived to failure. However, the gages that did survive suggest that bar strains were lower in the embedded specimens than in the nonembedded specimen.

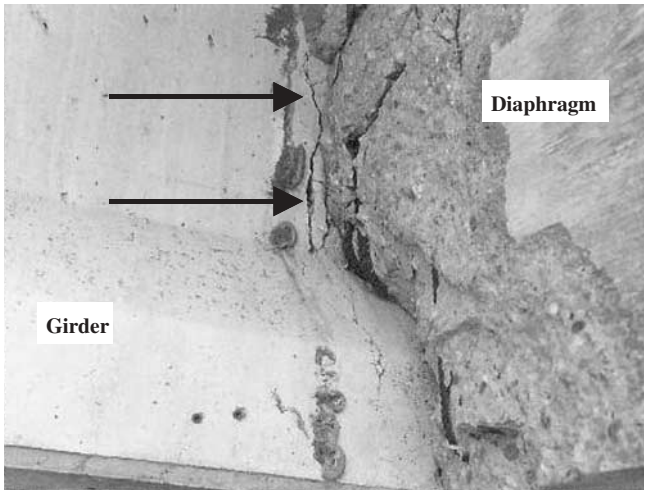

Figure 25. Cracking of the girder in Specimen 6.

FULL-SIZE SPECIMENS

Description of the Specimens

The full-size specimens were constructed of two 50-ft Type III AASHTO I girders joined with a 10-in. diaphragm. An 8-ft-wide × 7.5-in. thick composite concrete deck slab was cast on top (see Figures 26 and 27). As with the stub specimens, the slab was not cast all the way to the end (see Figure 26). The girders were to be reused by turning them end-for-end and creating a new specimen. The last 12 ft of the deck slab was not cast to create the second specimen without having to remove any of the deck slab. For reference, the cardinal compass directions are shown in Figure 26. The girders are designated as "east" and "west." The girder faces are "north" and "south." A discussion of the experimental set up and instrumentation is included in Appendix B.

Each end of the girder specimens was cast with both bent bar and extended strands so that either end could be used for either type of connection (see Figure 28). Unlike the Type II girders used for the stub specimens, it was possible to install some of the bars pre-bent and still close the forms; however, some of the bars had to be installed straight and then field bent later.

A constructability issue arose during the fabrication of the girders. When the strands were detensioned, some or all of the wires in some strands unwrapped and deformed, creating a "bird cage" effect, as is visible on most strands shown in Figure 28. The strands were rewrapped, but some of the bird-caging remained. This occurred approximately 6 to 8 inches from the face of the girders, just about at the point where the strand would be bent. Since there is a possibility that this situation might occur in real field applications, it was decided to proceed with using these strands to see whether there was an effect on connection strength.

Figure 26. Full-size specimen.

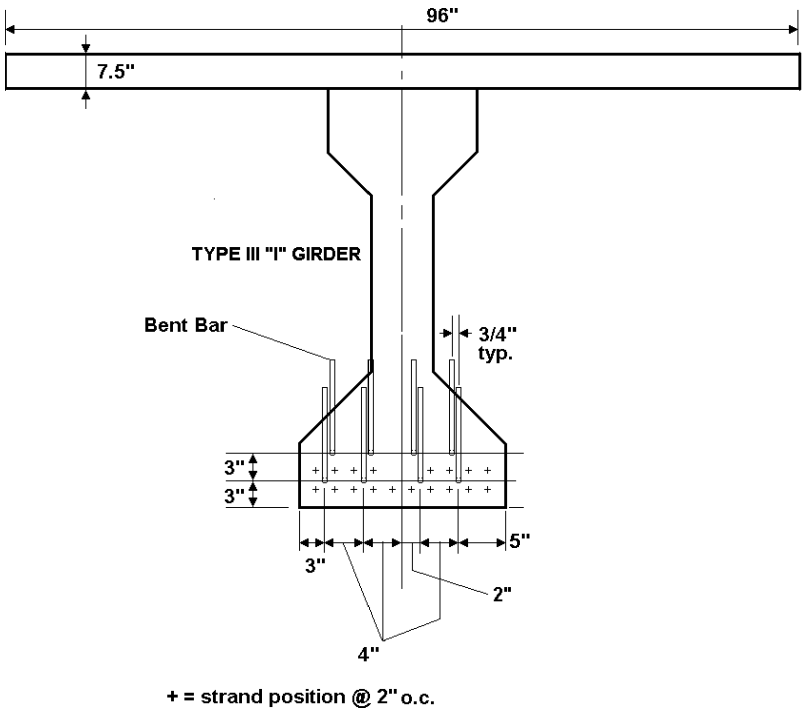

Figure 27. Cross section of full-size specimen.

Full-Size Specimen 1

Behavior During Construction

The first specimen used a bent-bar configuration in the positive moment connection. As with the stubs, the connection was designed to provide a capacity of 1.2 M_{cr}. This required eight No. 5 hooked bars (see Figures 27 and 29). Since the stub specimen tests indicated that asymmetrical connections were undesirable, the bars in the connection were placed as symmetrically as possible, but still allowed for meshing of the bars. This configuration was still slightly asymmetrical and resulted in a very congested diaphragm area. Tolerances in bending rebar result in bends that do not line up (see Figure 30). This creates problems in inserting corner bars as detailed in Figure 29. A similar problem occurred with the bent-bar stub specimens as shown in Figure 16.

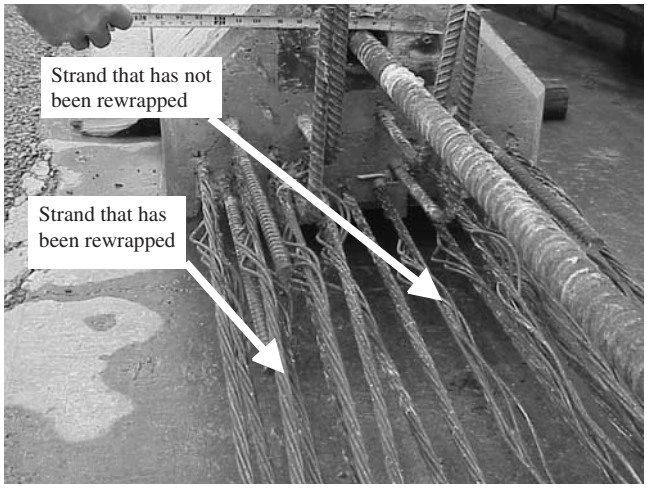

Figure 28. End of the girders for the full-size specimens.

The first specimen used a partial diaphragm pour (see Figure 29). This configuration is used by several states. In this connection, the bottom of the diaphragm is poured well before the deck slab is added. The idea of the partial diaphragm is that the weight of the deck slab concrete will rotate the end of the girder into the partial diaphragm and compress the concrete. Then, any tension caused by positive moments will simply reduce the compression rather than cause tensile cracking. The partial diaphragm was poured when the girders were 28 days old. According to the survey, the depth of the diaphragm pour is usually one-third to one-half of the diaphragm depth. In this case, the diaphragm was poured to depth of 19 in. This was determined as the minimum depth that would allow the tails of the bent bars to be completely covered with the initial pour.

Figure 31 shows the variation of the east-end reaction with time. The west-end reaction data are almost identical. From the time the partial diaphragm is cast to the time the slab is added 28 days later, the end reactions increase approximately 3 kips, creating a positive moment at the diaphragm of 150 k-ft. This positive moment is caused by a combination

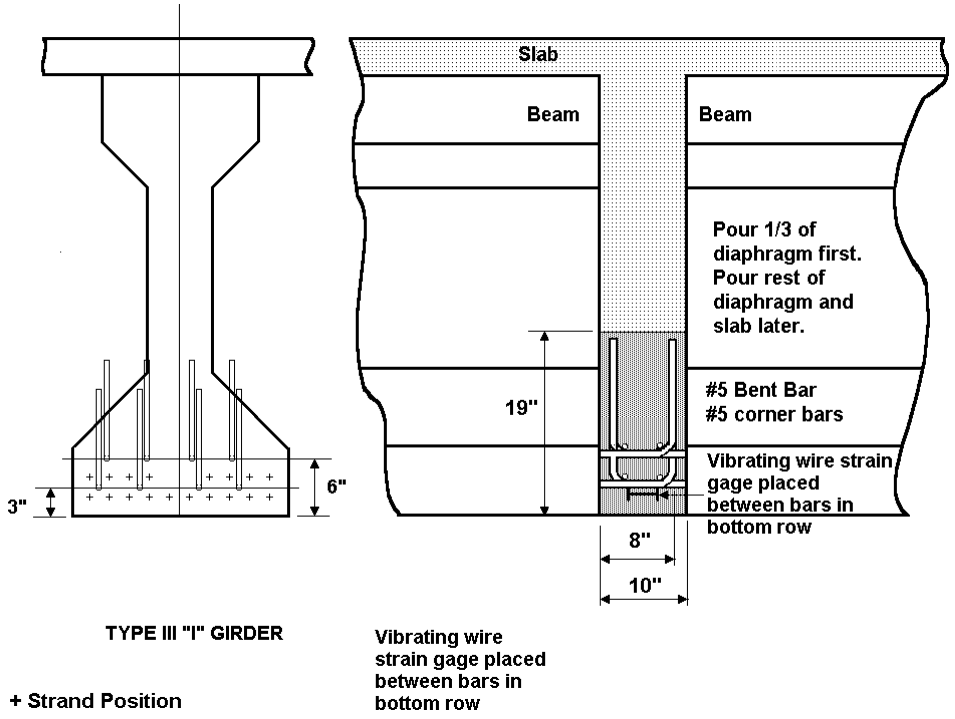

Figure 29. Bent bar specimen with partial diaphragm.

of creep, shrinkage, and average temperature effects in the girders. The effect of daily temperature variation is seen as the waves in the graph. Prior to adding the slab, this effect of daily temperature variation is approximately ±1k.

The deck slab was added 28 days later. Figure 32 shows the results of a vibrating wire strain gage placed at the level of the positive moment connection bar, in the middle of the diaphragm (see Figure 29). The graph shows the time period when the deck slab was cast to a few days after. During the time from casting the partial diaphragm to adding the deck slab, tensile strains ranging from 60 to 90 microstrain develop in the diaphragm. The variation seen is due to temperature.

Figure 30. Misaligned bars due to field bending.

After the deck slab is added, this strain gage at the bottom of the diaphragm shows an immediate increase in compressive strain of 40 microstrain, which would correspond to a stress of approximately 160 psi. Vibrating wire strain gages placed 6 in. from ends of the girders (at the level of the bottom row of strand) show an increased compressive strain of 50 microstrain, which corresponds to a stress of approximately 250 psi. Therefore, some compressive stress develops at the joint. It is important to remember that the stresses cited are the instantaneous stressed caused by pouring the deck slab. At the time the deck slab was cast, the diaphragm was in tension because of creep, shrinkage, and temperature effects in the girders. The compressive stresses created when the deck slab was poured were not enough to overcome this tension, and the diaphragm still shows a net tension even after the deck slab is added.

After the deck slab is poured, the instruments show an unexpected response. A few hours after the pour, the strain in the diaphragm increases (becomes more tensile) then decreases (becomes more compressive) over the next 2 days. After 2 days, the net strain is compressive. This is caused by thermal effects. In Figure 32, the second curve shows the temperature in the deck slab. The strains in the diaphragm are constant for a few hours, and then they follow the deck slab temperature curve.

A similar response is seen in the reactions. Figure 33 shows the east-end reaction at the time the deck slab is cast until

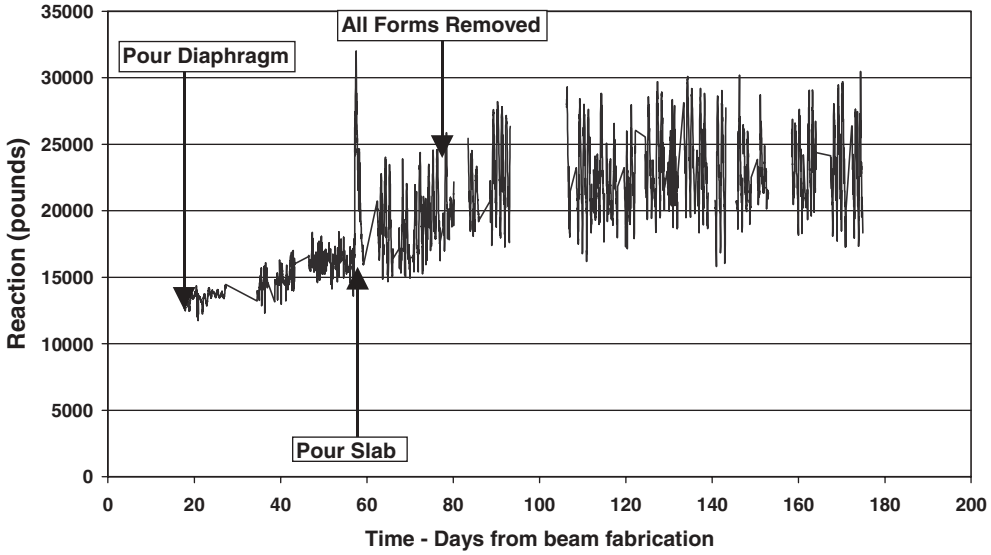

Figure 31. Variation of east end reaction with time.

2 days after. There is an immediate increase in load of about 10 kips when the deck slab is poured. This is consistent with the girders still behaving as simple spans, so the partial diaphragm does not provide continuity. Over the next 8 h, the end loads increase an additional 4 kips. The peak load corresponds to peak concrete temperature in the deck slab. During the next 2 days, the end supports lose almost all the load gained during the deck slab pour. The loss of load mimics the deck slab temperature graph.

These responses are caused by the heat of hydration in the deck slab. After the concrete is poured, the deck slab concrete begins to heat up as the chemical reaction progresses. This will also heat up the top flange of the girder, causing an expansion. The data show the girders camber upward 0.01 in. Since the partial diaphragm provides some connectivity, the entire system appears to deflect upward with the girders. This causes the tension at the diaphragm and the increase in the end reactions.

The final set of the concrete—the point at which there are measurable mechanical properties in the concrete—is usually taken as just before the point at which the heat of hydration graph peaks. At this point, the hardened deck slab begins to influence the system. When the deck slab begins to cool, it will contract. Since the concrete and the reinforcing steel have almost the same coefficient of thermal expansion, the reinforcing steel expands and contracts with the concrete and

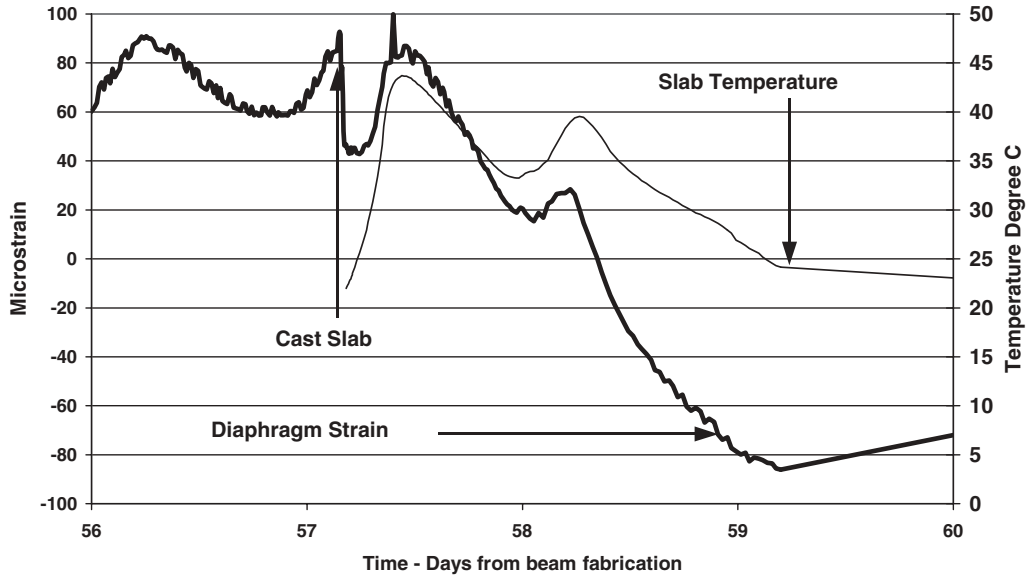

Figure 32. Variation of strain at bottom of diaphragm with time.

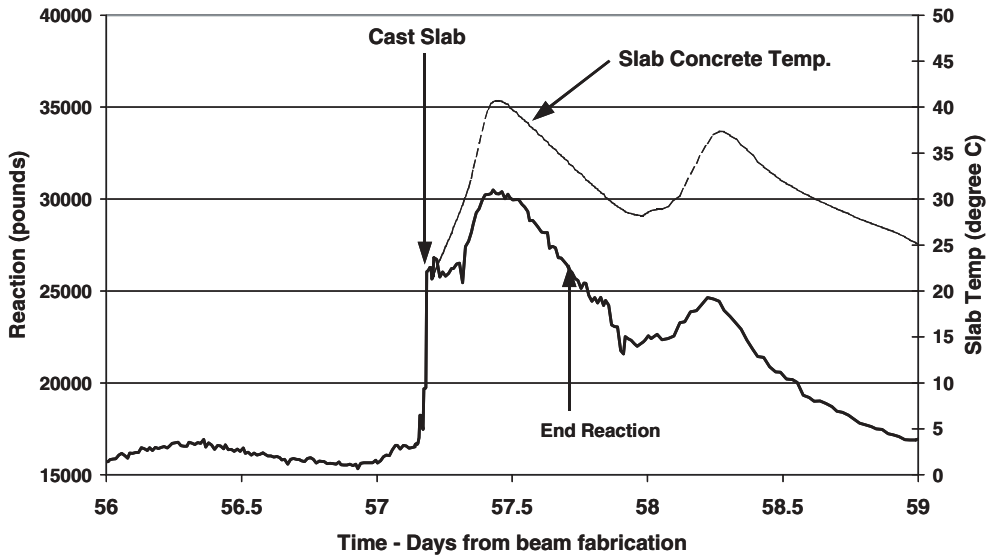

Figure 33. East end reaction after deck slab pour.

offers little resistance to the thermal movements. Thus, the cooling of the deck slab results in a contraction of the deck slab, which mimics the effect of deck slab shrinkage. The models predict that contraction of the deck slab will cause a decrease in the end reactions, compression at the bottom of the diaphragm, and a downward deflection of the girders. All of these responses are seen in the data.

Figure 34 shows the placement of vibrating wire strain gages in the cross section. All gages shown in Figure 34 are placed at midspan of the girders. Figures 35 and 36 show the strains in the top and bottom flanges of one of the girders. The initial values are the compressive strains due to prestressing and any creep or shrinkage that has occurred. The graph also shows the temperature measured in the deck slab and in the top or bottom flange of the girder. When the deck slab weight is added, there is a positive (i.e., tensile) change in the strain in the bottom flange and a negative (i.e., compressive) strain in the top flange, as expected. Both the top and bottom flange strains stay reasonably constant until just before the peak in the deck slab temperature, which is approximately the time of the final set for the concrete. The strains then approximately follow the temperature curve. It therefore appears that at this point, the deck slab has hardened sufficiently to begin affecting the girder behavior. The peak strains in the flanges occur slightly before either the peak deck slab temperatures or the peak girder temperature. There is slightly better agreement with the gradient (slab temperature – bottom flange temperature), but the strain still peaks earlier. The reason for this is not apparent. Clearly, the girder is subject to a complex series of interactions involving the thermal contraction of the slab and thermal strains in the girder. Completely understanding this behavior would require complex computer analysis beyond the scope of this project.

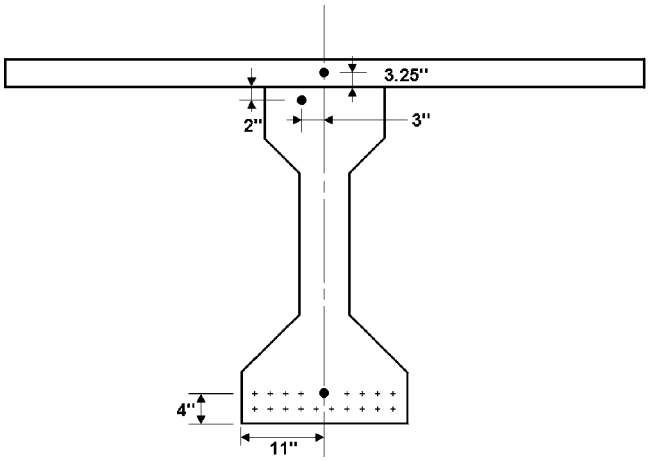

Figure 34. Placement of vibrating wire strain gages in cross section at midspan.

Figure 37 shows the strain in the slab. The strain is taken as 0 at the point of final set, as determined from Figures 35 and 36. The deck slab strain follows the slab temperature. Temperature decreases cause tension as the deck slab attempts to contract but is restrained by the girder. Increases in temperature cause compression as the deck slab expands but is restrained by the girder. Again, this is the expected behavior.

Monitoring after Construction

The deck slab was wet cured for 7 days, and the forms were removed during the next 14 days. Form removal took some time because of the specimen geometry. In order to duplicate field conditions as clearly as possible, the specimen was supported by three load cells placed under each girder (see Appendix B). Thus, all the support was near the centerline of the specimen and there was a possibility that the spec-

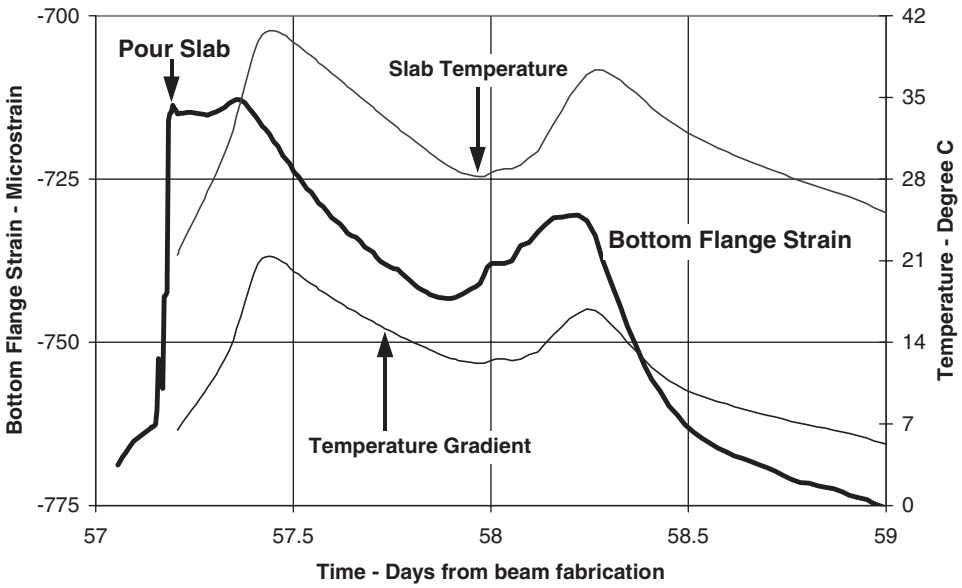

Figure 35. Bottom flange strain after deck slab pour.

imen might tip over unless stabilizers were installed (see Figure 26) as the forms were removed. Until the stabilizers were installed, the specimen was kept stable by formwork under the diaphragm. As a result, it was not possible to accurately monitor the center reaction while the formwork was under the diaphragm. However, since the only formwork support was at the center, changes in the center reaction should result in changes to the end reactions—for example, if the center reaction increases, the end reactions should decrease by the same amount. Thus, during the form removal period, development of moments due to time-dependent effects can be determined from the end reactions.

During the form removal period, the end reactions showed daily variation due to temperature, but the average reaction did not change. This was unexpected because it was thought that these reactions would continue to decrease due to shrinkage of the deck slab. A shrinkage specimen was made when the deck slab was cast. It was water cured for 7 days (the same as the deck slab) and then allowed to shrink. The specimen was kept in a trailer near the beam. Shrinkage was measured through an embedded vibrating wire gage. During the period of form removal, a shrinkage of approximately 350 microstrain was measured. A similar shrinkage specimen had been made for the girder; and, during the same period, the girder

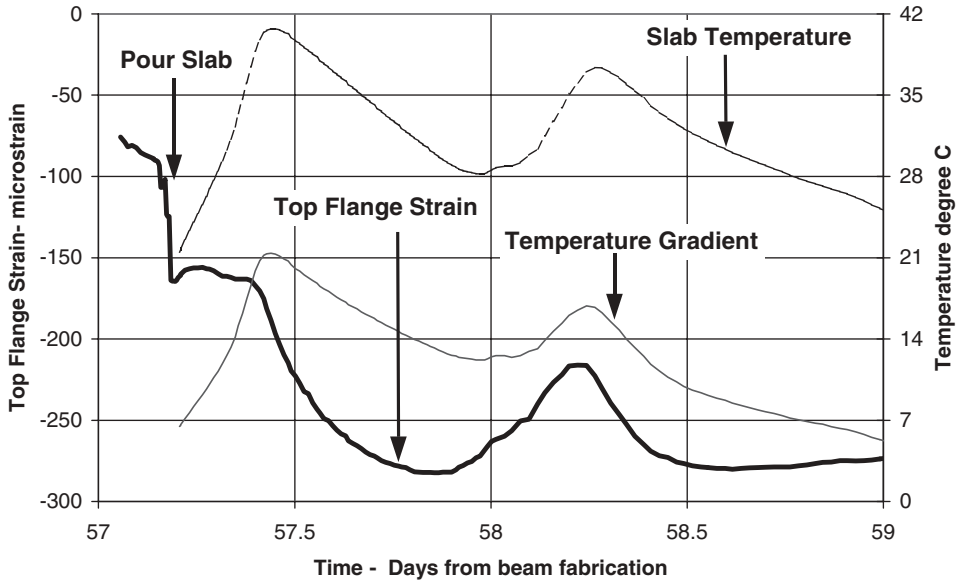

Figure 36. Top flange strain after deck slab pour.

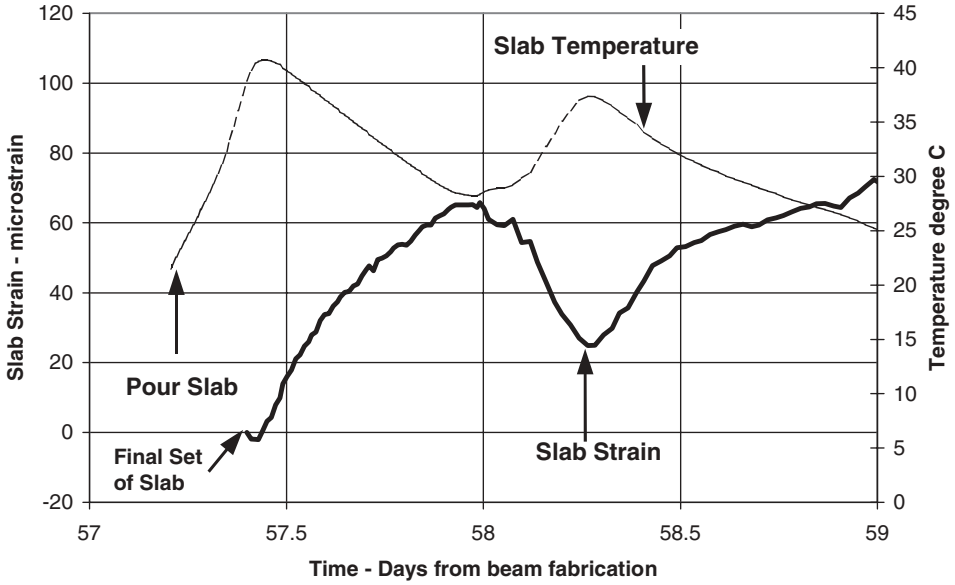

Figure 37. Deck slab strain after deck slab pour.

concrete shrank only 45 microstrain. With a differential shrinkage of almost 300 microstrain, some development of negative moment should have been seen through a decrease in the end reactions.

After all the forms were removed, the system was monitored for 4 months. The most striking observation was the daily change in the reactions due to temperature (see Figure 31). The end reactions vary by approximately ±5 kips per day. This is a daily variation equal to approximately 20% of the reaction. For this variation in reaction, the moment at the diaphragm would vary ±250 k-ft per day. Given that the nominal cracking moment at the diaphragm was calculated as 420 k-ft and the positive moment connection capacity was 504 k-ft, this daily variation is significant.

During the monitoring period, the average end reaction increases about 5 kips while the center reaction drops by 10 kips, and there are not large differences in the girder-slab strains. Figure 38 shows that after the slab is cast, the deck slab and top flange strains decrease the same amount (200 microstrain) while the bottom flange strain decreases slightly more

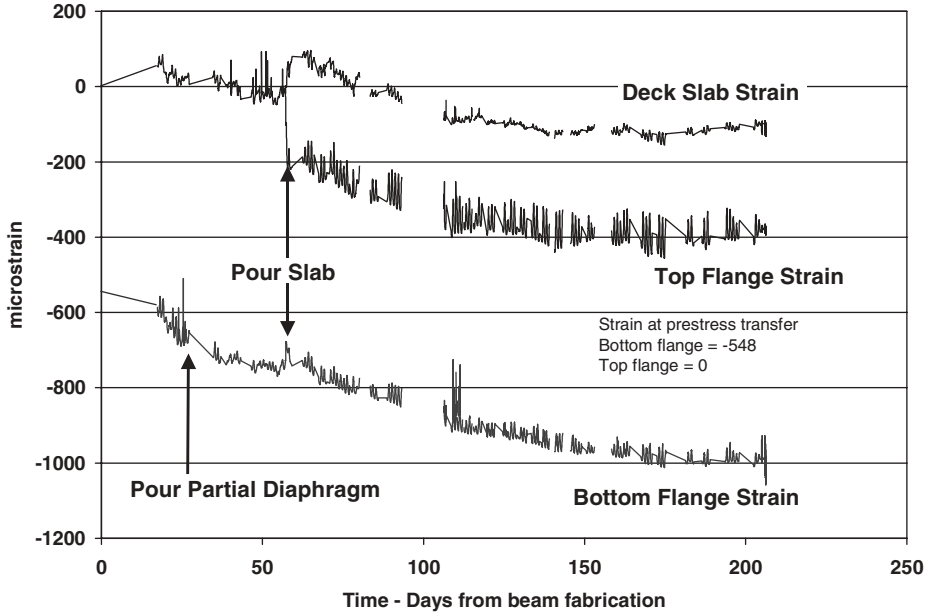

Figure 38. Change in girder/deck slab strain with time.

(250 microstrain). It was expected that the center reaction would increase and that there would be large differences between the strains due to differential shrinkage of the deck slab. Most analyses of this type of system show that if the girders are older than 60 days when the deck slabs are placed, a large increase in the center reaction and development of large negative moment occurs. The PCA tests (*7*) found an increase in center reaction with time.

The results of the current study are consistent with recent field studies of bridges. FHWA sponsored a program to build high-performance concrete highway bridges in several states. The results are compiled on CD-ROM (*26*). Strain gages were placed in girders in three states: Louisiana, South Dakota, and Washington. In these projects, the girders were rather old when the deck slabs were placed (approximately 60 days for Louisiana, 200 days for Washington, and 300 days for South Dakota), so the effects of the differential shrinkage should have been noticeable through large strain changes and downward cambers of the girders. However, the strains in the girders remained almost constant (except for daily temperature variation), and there was little change in the cambers. Thus, it does not appear that large negative moments develop. This is also consistent with anecdotal field evidence that negative moment distress has not been observed in these bridges.

The results found in the present study seem to agree with the studies by Ramirez et al. (*14*), which showed that the models overpredict formation of negative moment due to differential shrinkage. The reasons why bridges do not show the predicted negative moment development is not entirely clear; however, some possibilities can be offered.

The actual deck shrinkage potential may be overestimated. Analytical shrinkage values are usually based an assumed relative humidity. Real decks may be exposed to much higher humidity, especially at early ages when shrinkage potentials are greatest. In the case of the specimen reported here, the specimen was monitored over the summer at a facility near the Ohio River. The daily relative humidity frequently exceeded 90%. Decks are also subject to frequent rewetting from rain and snow.

The models base negative moment development on differential shrinkage, but usually use the free shrinkage values. These are usually obtained from equations given in the AASHTO Codes or ACI 209 (*12, 23*). In reality, the deck is not free to shrink. Decks are usually heavily reinforced, and this reinforcement will restrain the shrinkage.

Because the deck shrinkage is restrained by the steel, the shrinkage strain in the deck will not be the unrestrained shrinkage, but rather an effective shrinkage strain. The effective shrinkage strain in the deck can be found from

$$\varepsilon_{\text{effective}} = \varepsilon_{sh}(A_c / A_{tr})$$

where

ε_{sh} = unrestrained shrinkage strain for deck concrete;
A_c = gross area of concrete deck slab;
A_{tr} = area of concrete deck slab with transformed longitudinal deck reinforcement, $A_c + A_s(n - 1)$;
A_s = total area of longitudinal deck reinforcement;
n = modular ratio = E_s/E_c;
E_s = modulus of elasticity of the steel; and
E_c = modulus of elasticity of the concrete.

If the concrete modulus is low (as at early ages), the modular ratio increases and the effective shrinkage decreases. Thus, at early ages when the incremental shrinkage is high, the effect of bar restraint is also high. At later ages, the concrete modulus increases and the effect of bar restraint is less pronounced, but the incremental shrinkages are also lower.

BRIDGERM and RESTRAINT (the program developed for this study) both incorporate an equation developed by Dischinger (*11*). According to *NCHRP Report 322*, this equation is used to account for the restraining effect of the bar in the slab; what the equation actually does is attempt to correct for the fact that the modular ratio of the slab changes with time because the concrete modulus changes with time. However, even with corrections for relative humidity and reinforcement, RESTRAINT still predicts that a negative moment due to differential shrinkage should form. Clearly, more work is needed on this aspect of the model.

As previously noted, the end reactions did not decrease due to differential shrinkage as was expected, but rather increased. The cause of increase in end reaction is due to two effects. One was a slight settlement at the center support. In order to duplicate field conditions, bearing pads had been placed under the load cells. These pads seemed to have creeped slightly, and the center support showed a settlement of 0.06 in. An analysis was run and it was determined that this settlement would cause an increase in the end reactions of 1.8 k, about one-third of the observed change.

The remaining change is a combination of temperature effects and creep/shrinkage effects; however, it is very difficult to separate the individual contributions. What is clear is that over the monitoring period, the girder bottom flanges at midspan showed an average of 80 microstrain more compression than did the top flanges (see Figure 38). This strain gradient would have caused the girders to camber up and increase the end reactions. During the monitoring period, the center deflection decreased by 0.02 in.; but, when the effect of the center support movement is removed, the girder actually cambered up 0.02 in.

During the monitoring period, cracks were observed at the girder-diaphragm interface. During the monitoring period, these cracks opened an average of 0.015 in. when measured 3 in. from the bottom of the specimens, but there was variation. The average crack openings were 0.007 in. on the southwest joint, 0.015 in. on the northeast and northwest joints, and 0.020 in. on the southeast joints (see Figure 26 for direction). Note that cracks on the east side of the diaphragm

opened more than did those on the west side of the diaphragm and that the cracks on opposite sides of the same girder did not open the same amount. The reason the cracks on opposite sides of the girder do not open the same is because of the bar placement (see Figure 27). Although it was desirable to place the bars in a symmetric pattern, this cannot be done and still allow for the bars to mesh. As a result, the bars had to be offset about 3/4 in. This places the bars closest to the northeast and southwest faces, which had less crack opening than did those on the opposite faces where the bars were further from girder faces.

Figures 39 and 40 show the variation of crack opening with time for cracks at the bottom of west girder. The crack openings appear to show some softening of the connection during the monitoring period as the crack opening amplitude increases with subsequent cycles. No similar trend is seen with the reactions as the amplitude of the daily change remains fairly constant over the monitoring period (see Figure 31).

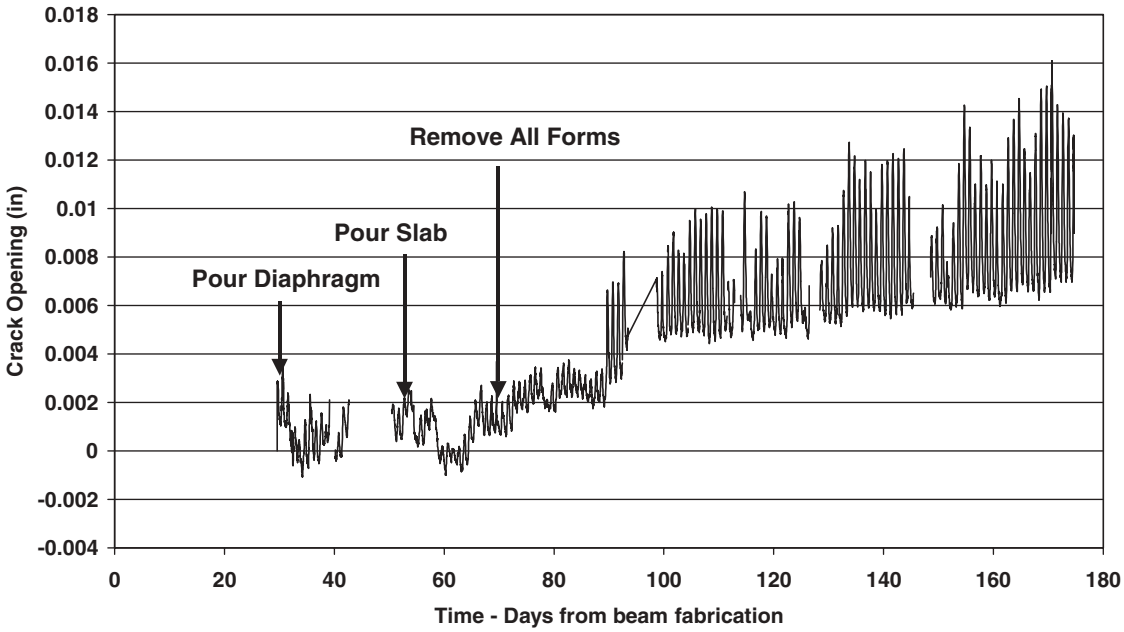

Figure 39. Opening of the crack at the bottom flange of the girder, northwest joint.

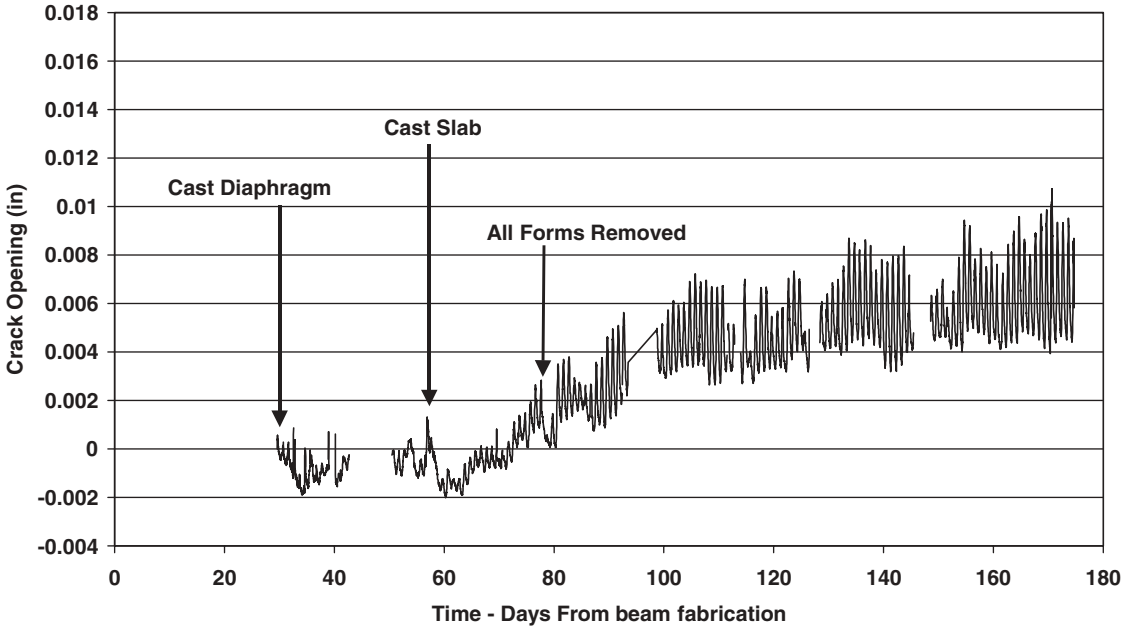

Figure 40. Opening of the crack at the bottom flange of the girder, southwest joint.

During the monitoring period, there was virtually no opening at the top of the joint.

Testing after Monitoring

After the monitoring period was over, the girders were tested to determine continuity. It is thought that cracking at the diaphragm will result in a partial or complete loss of continuity. By loading the specimen one span at a time, the continuity of the structure could be determined. Load was applied to the specimens with a pair of hydraulic cylinders (see Figure 41) placed in each span at 22 ft from the face of the diaphragm. Analysis showed that this was the most efficient positioning of the loads.

The specimen was loaded as follows to create a negative moment at the center support:

1. Span 1 was loaded with a downward load,
2. Span 2 was loaded with a downward load,
3. Span 1 was unloaded, and
4. Span 2 was unloaded.

The loads were such that when both spans were loaded, the applied moment was equal to the negative live-load moment. This is consistent with design procedures where the maximum negative moment occurs when the design truck has at least one axle on either side of the support. This loading also allowed for checking the requirements of the current AASHTO LRFD Specifications Art. 5.14.1.2.7c (*12*), which states:

> If the calculated stress at the bottom of the joint for the combination of superimposed permanent loads, settlement, creep, shrinkage, 50% live load and temperature gradient, if applicable, is compressive, the joint may be considered fully effective.

When one span is loaded, the applied negative moment is 50% of the negative live-load moment.

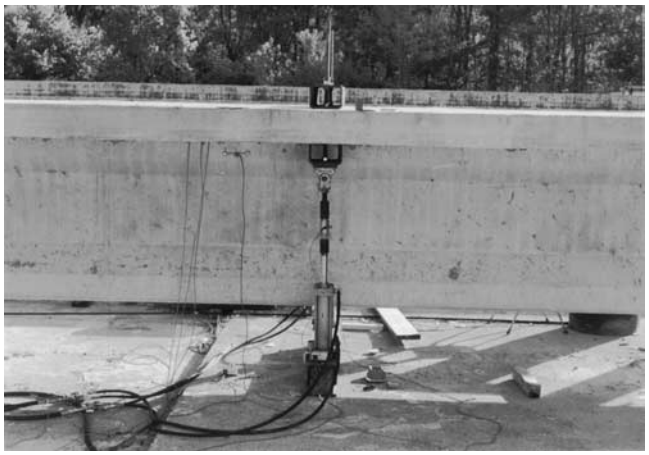

Figure 41. Loading device.

Continuity was determined by the change in reactions and the changes in girder strains. If the girder is continuous, loading one span will have a known effect on the reactions and strains in the other span. In a simple-span case, loading one span will have no effect on the other. If there is partial continuity, the strains and reactions will be between the simple and continuous cases.

Figures 42 and 43 show the results of loading the specimen after the monitoring was complete. The test consisted of one load cycle to establish a baseline. The east girder was loaded first, and then the west girder was loaded. The *x* axis is time, and horizontal lines on the graphs show the anticipated reactions and strains for both the continuous and simple spans cases. The reactions and strains are consistent with continuity, even though cracking exists at the connection.

After the initial testing, the cracks at the diaphragm were opened by simulating the positive moment that would develop from creep and shrinkage of the girders if continuity was established at an early age. To do this, a post-tensioning bar was placed through the bottom flange of the girder, and a post-tensioning force was applied (see Figures 44 and 45). This would cause the girders to camber up—simulating the formation of additional positive moment. Note that the post-tensioning (called "PT" in the figures) bars only went through the girders and did not go through the diaphragm (i.e., the bar was dead-headed at the end of the girder where the girder was attached to the diaphragm). The bar was a 1.375-in.-diameter Dywidag bar. It was tensioned to the maximum allowable force of 160 kips. This increased each end reaction by 8 kips, resulting in an additional positive moment of 400 k-ft or 0.96 M_{cr}. The cracks at the bottom of the joint opened as follows: southeast—0.01 in., northwest—0.008 in., and southwest—0.004 in. The instrument on the northeast joint malfunctioned, so no data are available.

The post-tensioning load was applied in four stages. After each stage of post-tensioning, vertical loads were applied to the specimen. Downward loads were applied to the specimen as mentioned above to obtain the negative live-load moment. After the negative moment was applied and removed, positive (upward) loads of 10 kips were applied in sequence in each span. This upward load placed the maximum positive live-load moment on the connection when both spans were loaded. Figures 46 and 47 show the crack opening at the bottom of the specimen for two cracks: northwest and southeast. The northwest crack appears to close under the initial load, even though the crack opening does not return to zero. This is not unusual with cracks in concrete—the surfaces tend to be rough and the rough cracks will often not close all the way back. The southwest crack does not appear to close under initial load. By the time all the post-tensioning is applied, both cracks are opening and staying open on loading. However, the data from subsequent loading still show that the connection remains effective because the girders act as if continuous (see Figure 48).

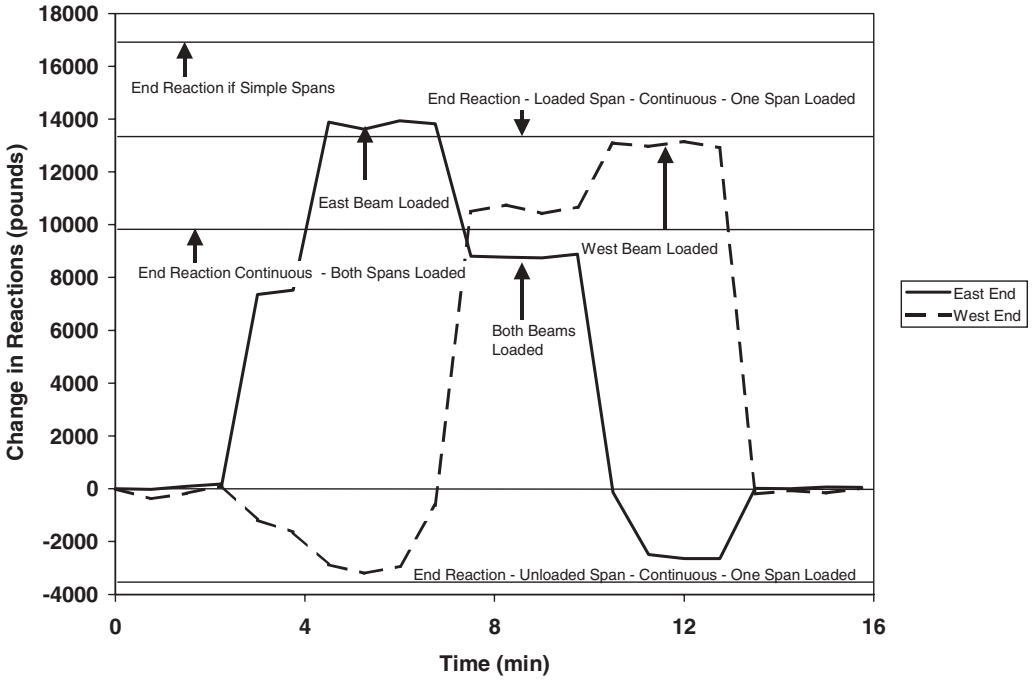

Figure 42. Change in end reactions: loading to negative LL *moment before post-tensioning.*

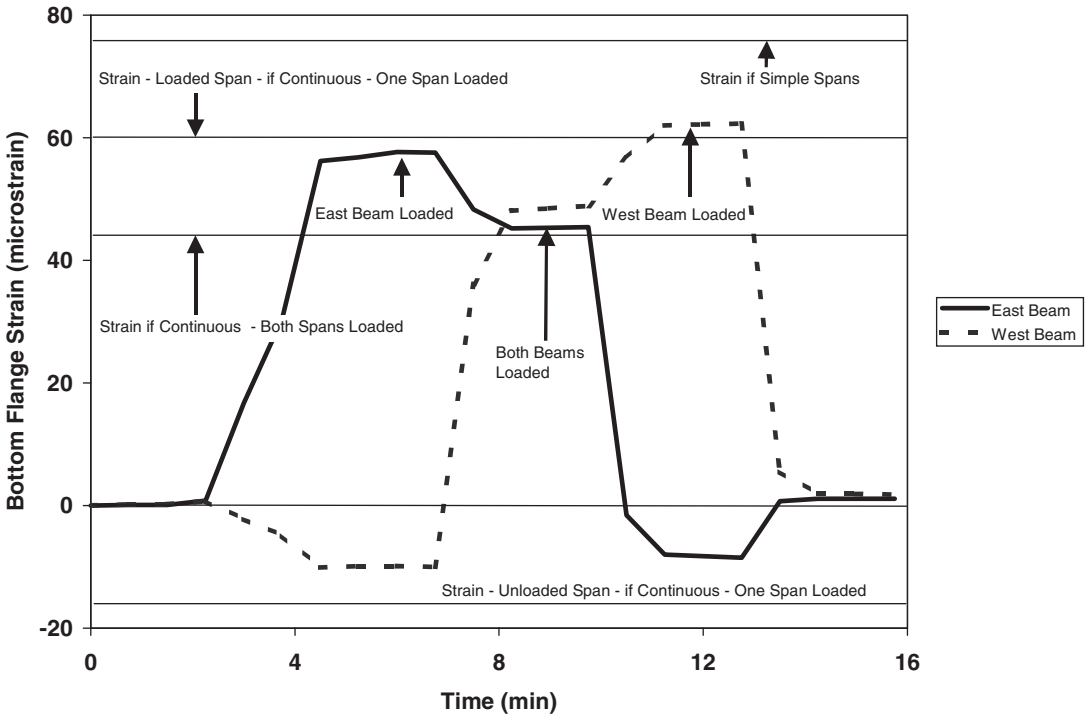

Figure 43. Change in bottom flange strain: loading to negative LL *moment before post-tensioning.*

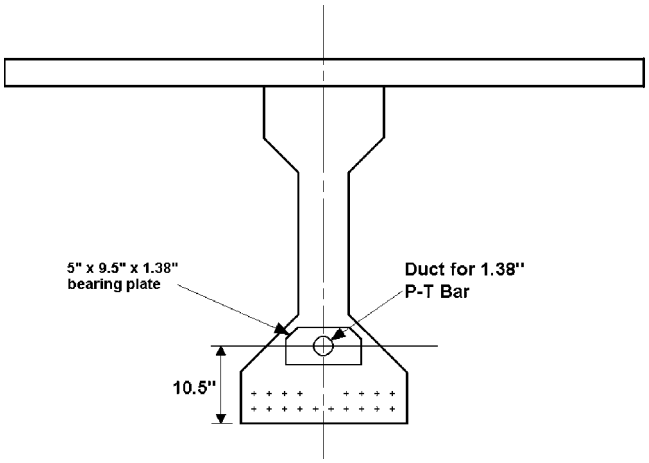

Figure 44. Position of post-tensioning duct.

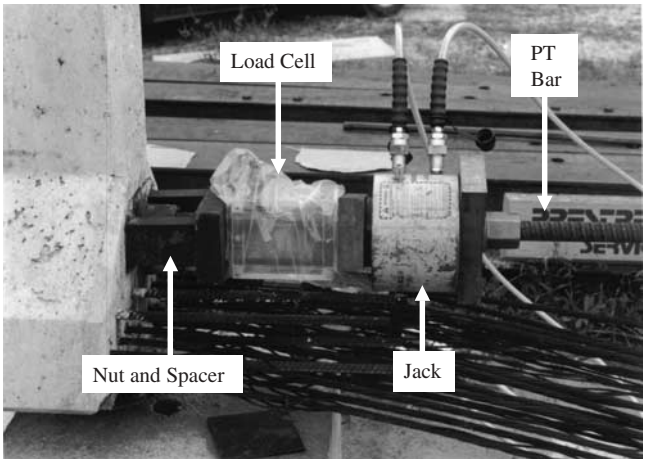

Figure 45. Post-tensioning device.

Since the girders remained continuous after the post-tensioning, the girders were loaded by increasing the positive load (creating positive moment) to determine the load at which, if any, the continuity was lost. Figures 49 and 50 show the end reactions and bottom flange strains for a loading to the maximum negative moment (−38 kips at each point) followed by loading up to +40 kips at the east point and +42 kips at the west point. This positive load would cause an additional positive moment of 395 k-ft. Added to the 400 k-ft caused by the post-tensioning, the total positive moment was 795 k-ft or 1.90 M_{cr}. This exceeded the nominal design capacity of 1.2 M_{cr}, but that capacity was calculated using nominal properties. The nominal bar yield was 60 ksi, but the actual bar yield was 83 ksi. The nominal concrete strength was 4 ksi, but the actual strength was 6.7 ksi. Using the actual properties, the capacity becomes 828 k-ft or 2.0 M_{cr}. There was no indication that the bars had yielded, nor was cracking observed in the diaphragm.

It appears from Figures 49 and 50 that the girders maintained continuity as the values of the reactions and strains at each load increment are those expected for a continuous system. It should be noted that when the west load was increased to 42 kips, the structure began to lift off the center supports, so the test was stopped at this point. Crack openings at the maximum load were as follows: southeast—0.035 in., northwest—0.029 in., northeast—0.025 in., and southwest—0.015 in.

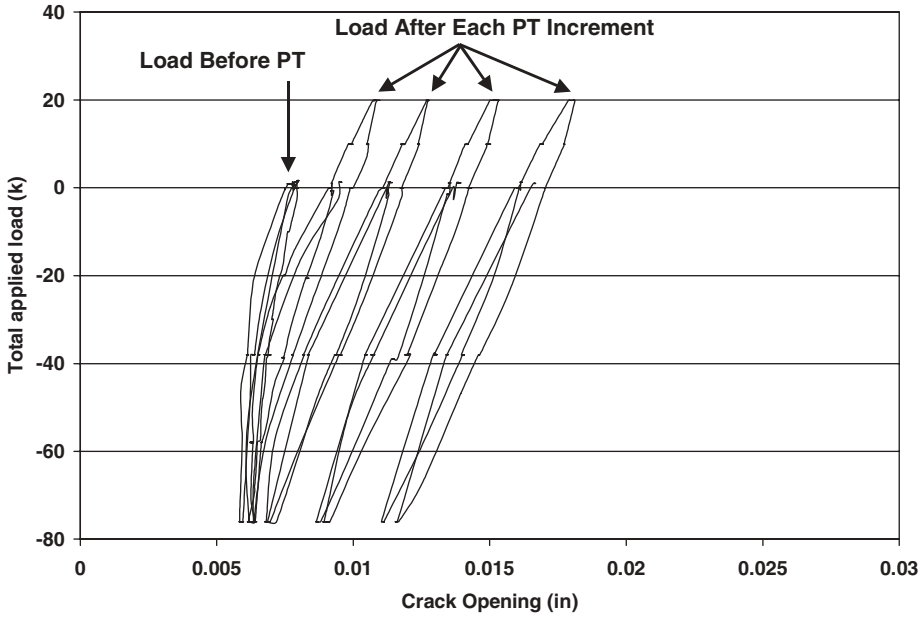

Figure 46. Crack opening at bottom of girder load during post-tensioning, northwest joint.

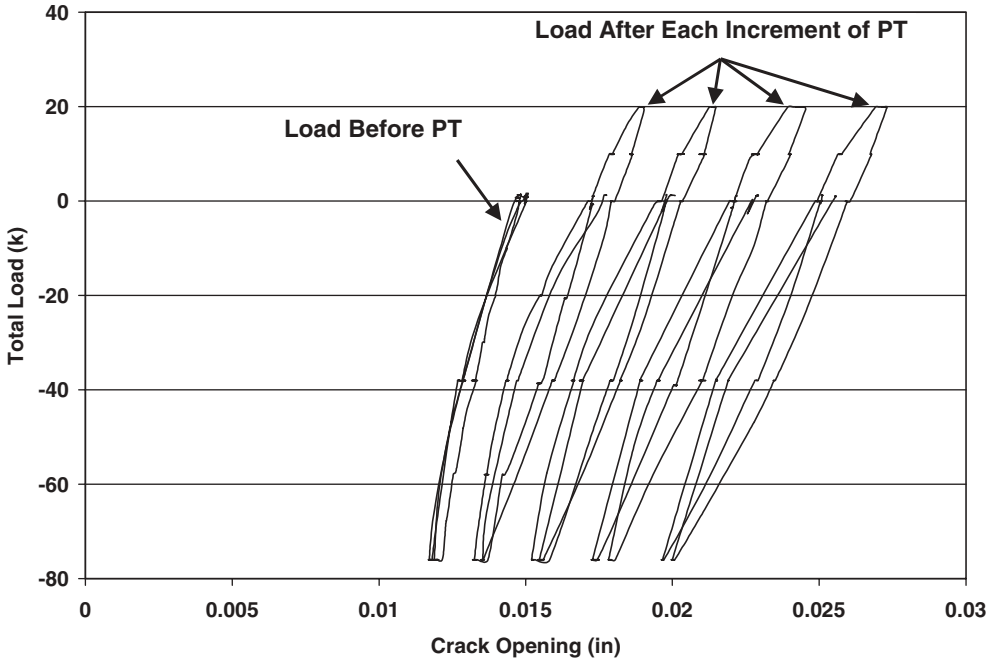

Figure 47. Crack opening at bottom of girder load during post-tensioning, southeast joint.

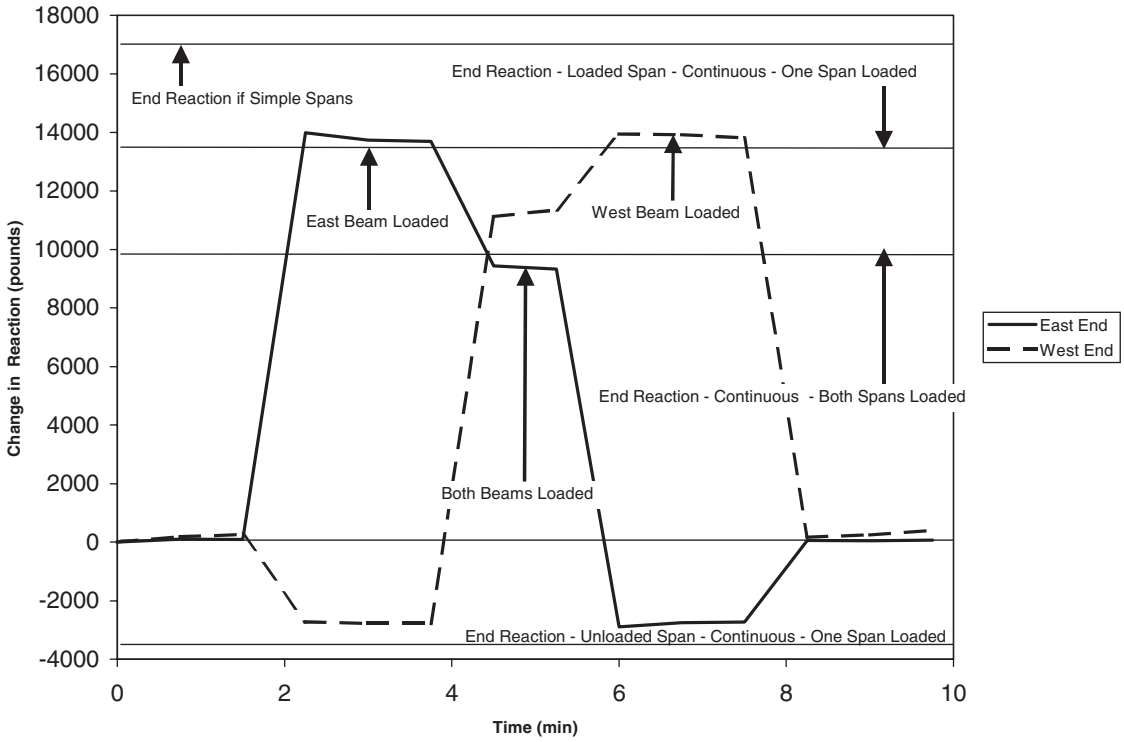

Figure 48. Change in end reactions: Loading to negative LL *moment after post-tensioning.*

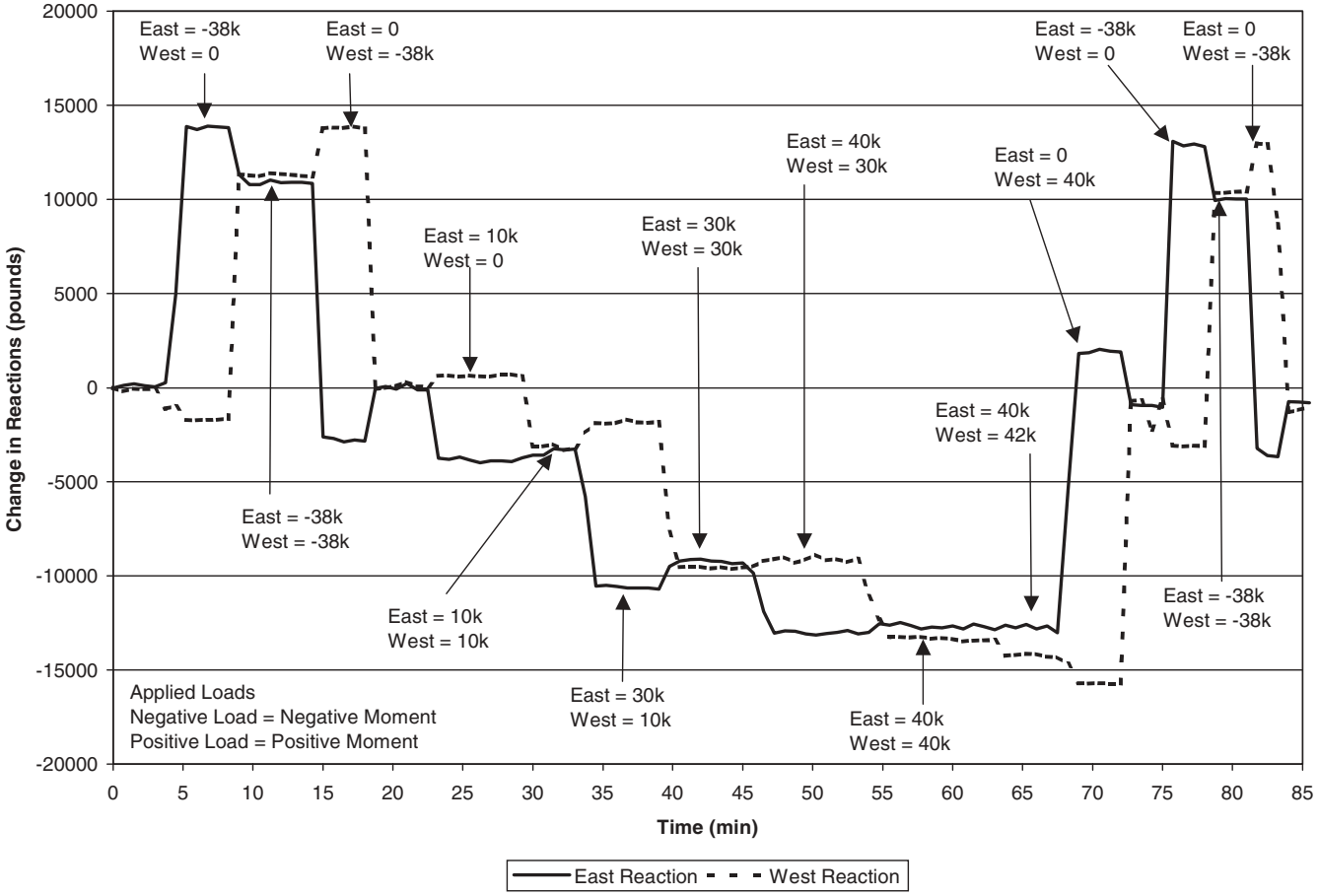

Figure 49. Change in end reactions: application of additional positive moment.

Figures 49 and 50 also show that continuity is maintained for negative moment after unloading.

Full-Size Specimen 2

After completion of the first full-size test, the diaphragm and girders were cut apart. The second specimen was formed by turning the same girders end-for-end and forming a new diaphragm. When the slab was cast for the first specimen, the last 12 ft (3.7 m) of the slab was left off (see Figure 26). When the girders were turned around, there was room to cast 12 ft of slab on either side of the new diaphragm so that a complete joint was formed. The new slab was connected to the existing slab by bars extending from the existing slab. The slab section and diaphragm were poured as a single monolithic pour.

The connection for the second full-size specimen was a bent-strand connection (see Figure 51). This connection was designed to a capacity of 1.2 M_{cr}, the same as full-size Specimen 1. The strand length was kept at 26 in., the same as Specimens 1 and 3. To get the proper capacity, a total of 10 bent strands were needed. The girder had a total of 20 strands, so only half of the strands were needed. The pattern for the extended strands (see Figure 51) was chosen so that the strands were symmetrical and there was as much space as possible between adjacent strands. This minimizes interaction between the strands and maximizes bond strength.

This specimen was tested at 21 days, after ensuring that deck slab-diaphragm concrete strength exceeded 4,000 psi. As with the first specimen, the loading mechanisms were placed 22.5 ft from the face of the diaphragm. The second full-size specimen was loaded as follows:

1. The east span was loaded to –38 kips.
2. The west span was loaded to –38 kips; at this point, the negative live-load moment was applied at the connection.
3. The east span was unloaded.
4. The west span was unloaded.
5. The east span was loaded to +20 kips; at this point, the positive live-load moment was applied at the connection.
6. The west span was loaded to +20 kips; at this point, twice the positive live-load moment was applied at the connection.
7. The east span was unloaded; at this point, the positive live-load moment was applied at the connection.
8. The west span was unloaded.

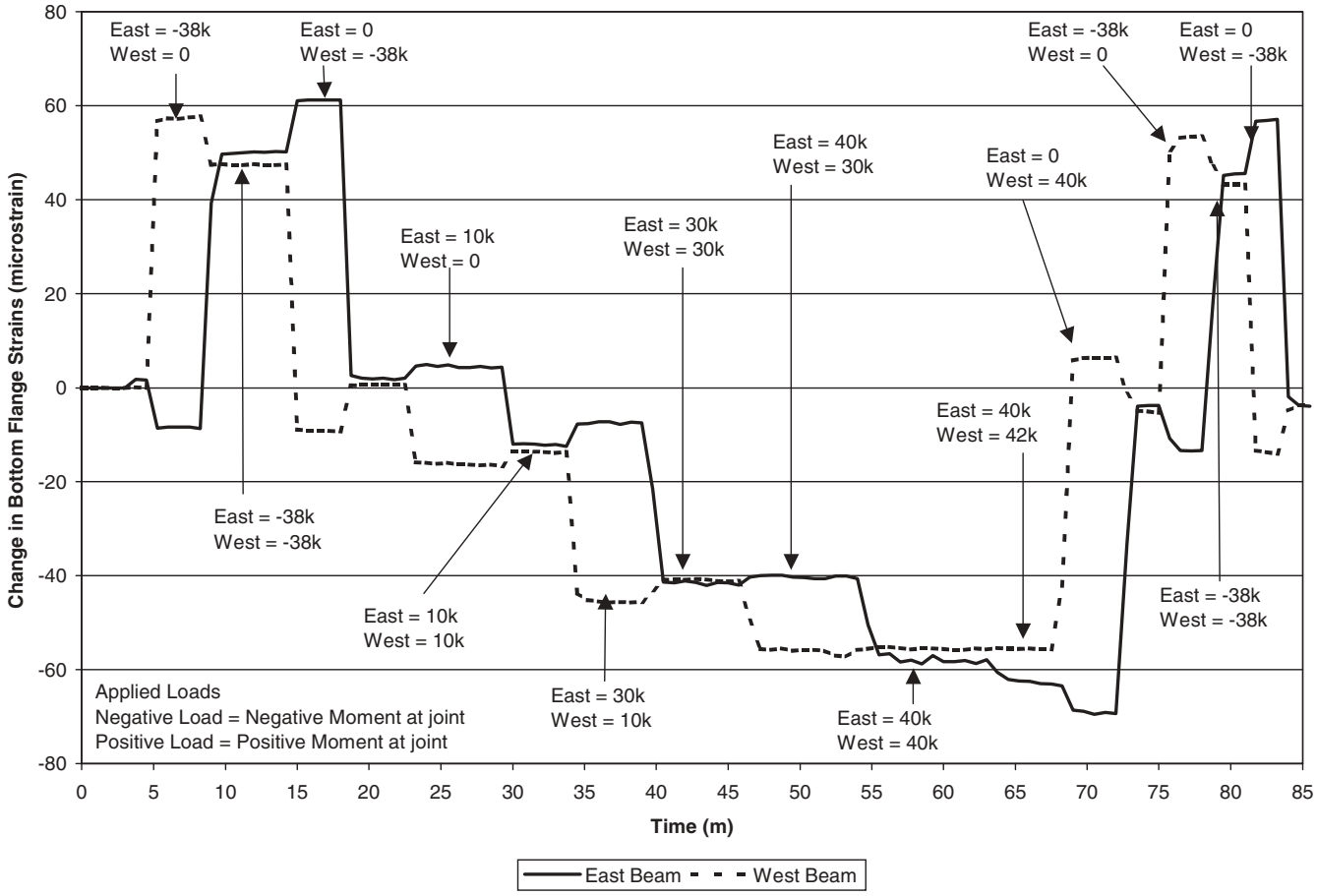

Figure 50. Change in bottom flange strain: application of additional positive moment.

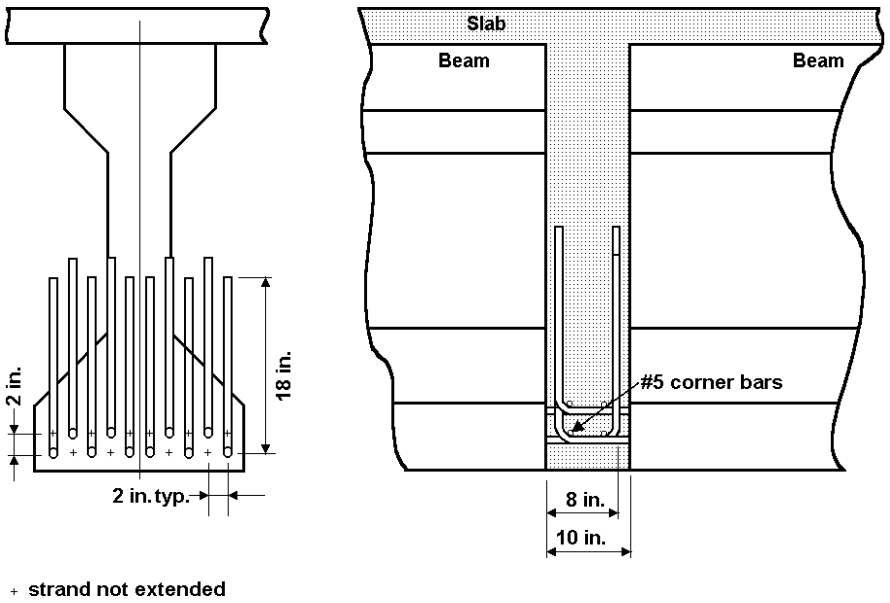

Figure 51. Full-size Specimen 2, bent strand.

Figures 52, 53, 54, and 55 show the results of the first loading. The load and bottom flange strains generally exceed those predicted by elastic analysis, especially when positive moment is applied and both spans are loaded. However, since there was no cracking observed at the diaphragm, the system should be continuous, so results of the load distribution and the strains will be used as a baseline for comparison with other results.

As with the first full-size specimen, the girders were post-tensioned in four increments to simulate creep and shrinkage. At the start of post-tensioning, the end reactions were 33 kips. The post-tensioning should have increased the end reactions by 8 kips. The first increment of post-tensioning increased the end reactions to 35 kips as expected; but, after the first increment of post-tensioning was applied, the pump for the post-tensioning ram broke and repairs took several days. When it was time to apply the last three increments of post-tensioning, it was found that the end reactions had dropped 3 kips. This drop was mostly due to temperature changes, although there was also a slight movement of the west-end support (this support was monitored for the remainder of the test, and no further movement was found). As a result of this drop in the end reaction, the post-tensioning, when complete, increased the end reactions by 5 kips to a total of 38 kips rather than to the expected 41 kips. At this point, the applied positive moment was approximately 250 k-ft or 0.6 M_{cr}. As expected, no cracking was detected at the diaphragm.

In an effort to crack the joint, the specimen was loaded with a positive load in order to create additional positive moment at the joint. When a positive load of 20 k was applied at both points, the first cracks appeared at the diaphragm. The total applied positive moment at the joint was approximately 445 k-ft or 1.07 M_{cr}.

Additional positive load up to 40 kips/point was applied. The moment at the diaphragm reached 640 k-ft or 1.54 M_{cr}. The average crack opening at the diaphragm was 0.011 in. As with the initial load, the data showed that the responses generally exceeded that expected from elastic analysis. However, when compared with the base line (see Figures 54 and 55), the responses indicated that continuity was maintained. Table 2 compares the end reactions and midspan bottom flange strains for both the uncracked section under a load of +20 kips/point and the cracked section under a load +40 kips/point. Since the positive load is doubled, the ratio of the responses should be 2. As seen in Table 2, the average ratio of the end reactions is 1.97. This is a reasonable agreement. The average ratio of the strains is 2.13, higher than 2, but reasonable considering that in some cases small numbers are being compared.

When additional positive load was applied, the specimen began to lift off the center supports, so it was no longer possible to apply positive moment to the connection through load. The research team had two choices: wait for the weather to warm up (which would increase the end reaction) or artificially increase the end reaction. It was decided to increase the end reactions by jacking and shimming the end supports.

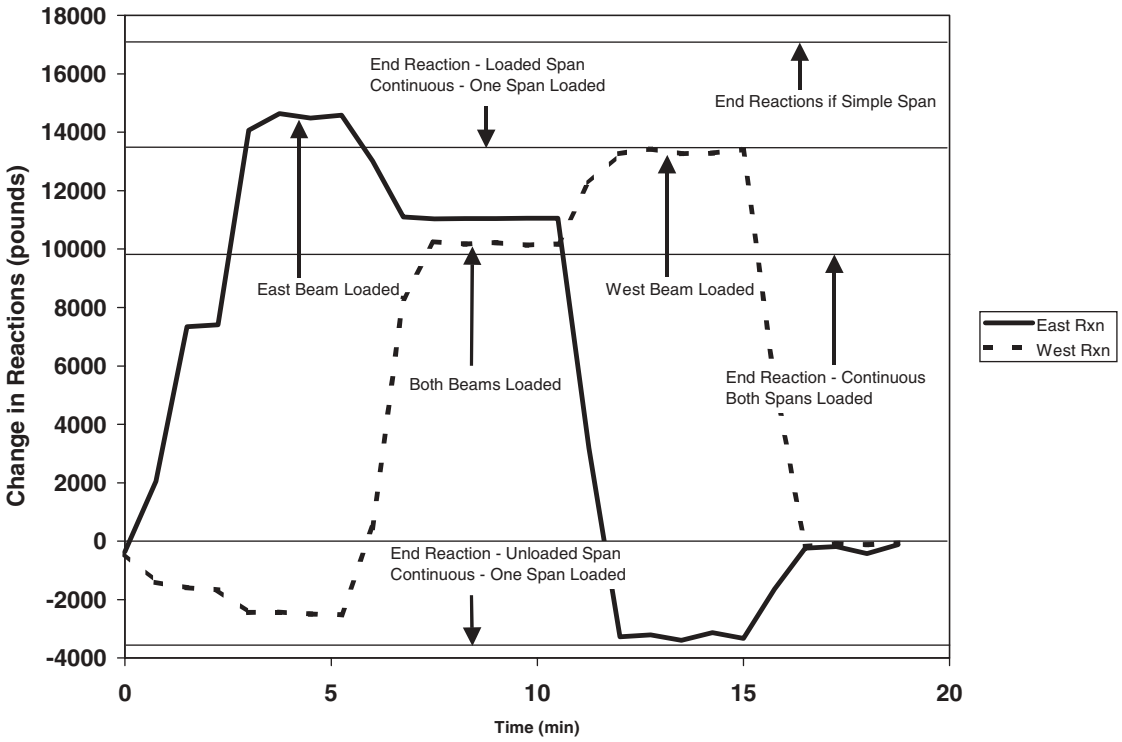

Figure 52. Change in end reactions: load to negative LL *moment.*

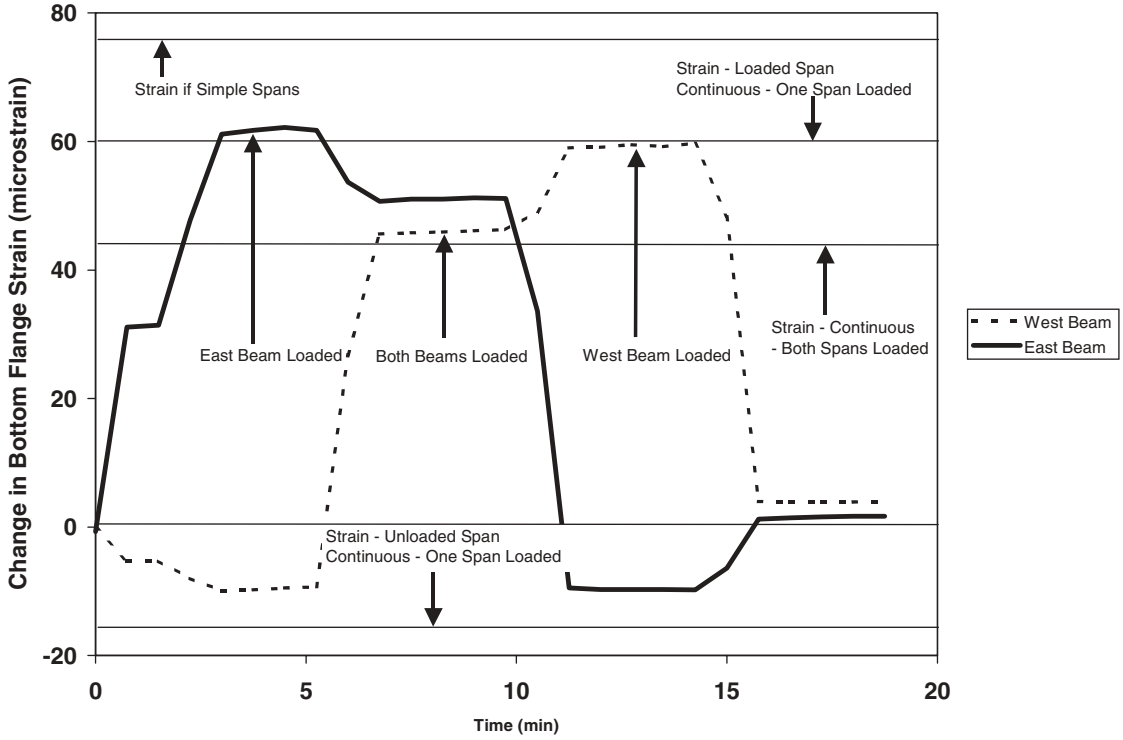

Figure 53. Change in bottom flange strains: load to negative LL *moment.*

The west end was jacked and shimmed approximately 2.5 in., and then the east end was shimmed by a similar amount. With the combination of post-tensioning and shimming, the end reactions increased to 58 kips or 25 kips above the original reaction value, providing a total positive moment of 1,250 k-ft, which equals 3.0 M_{cr} or 2.5 times the nominal capacity of 1.2 M_{cr}. The cracks at the bottom flange of the girder had opened to an average of 0.07 in. (see Figure 56). Unlike the bent-bar specimen, the crack openings were reasonably consistent on all four faces. Figure 57 shows the opening of one crack as a function of applied moment. There were cracks in the slab (see Figure 58) and at the bottom of

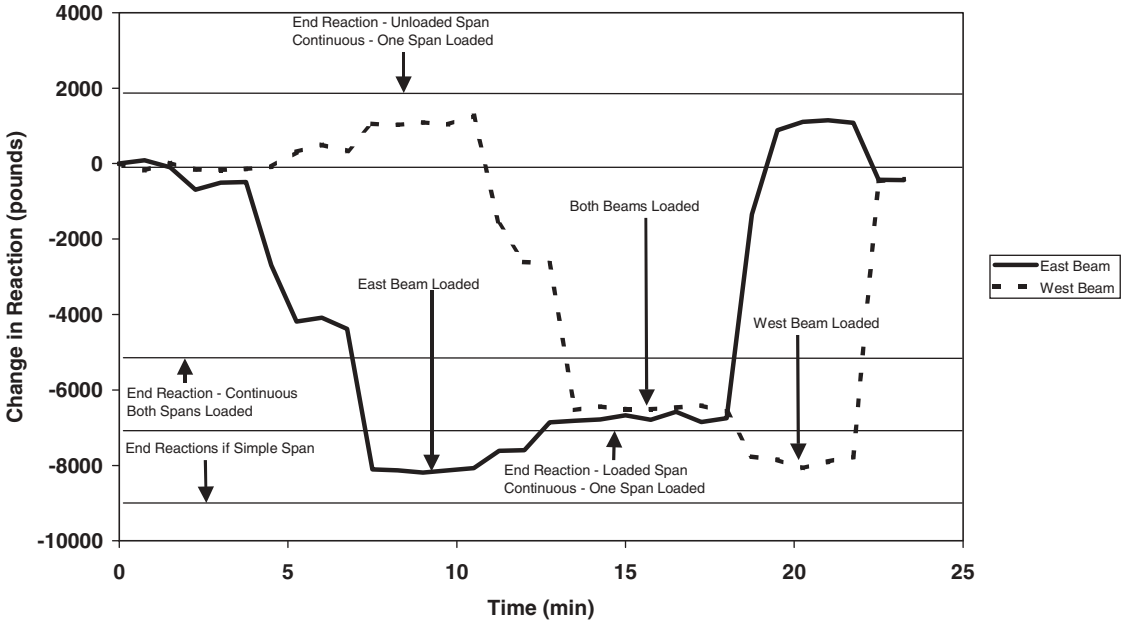

Figure 54. Change in end reactions: load to positive LL *moment.*

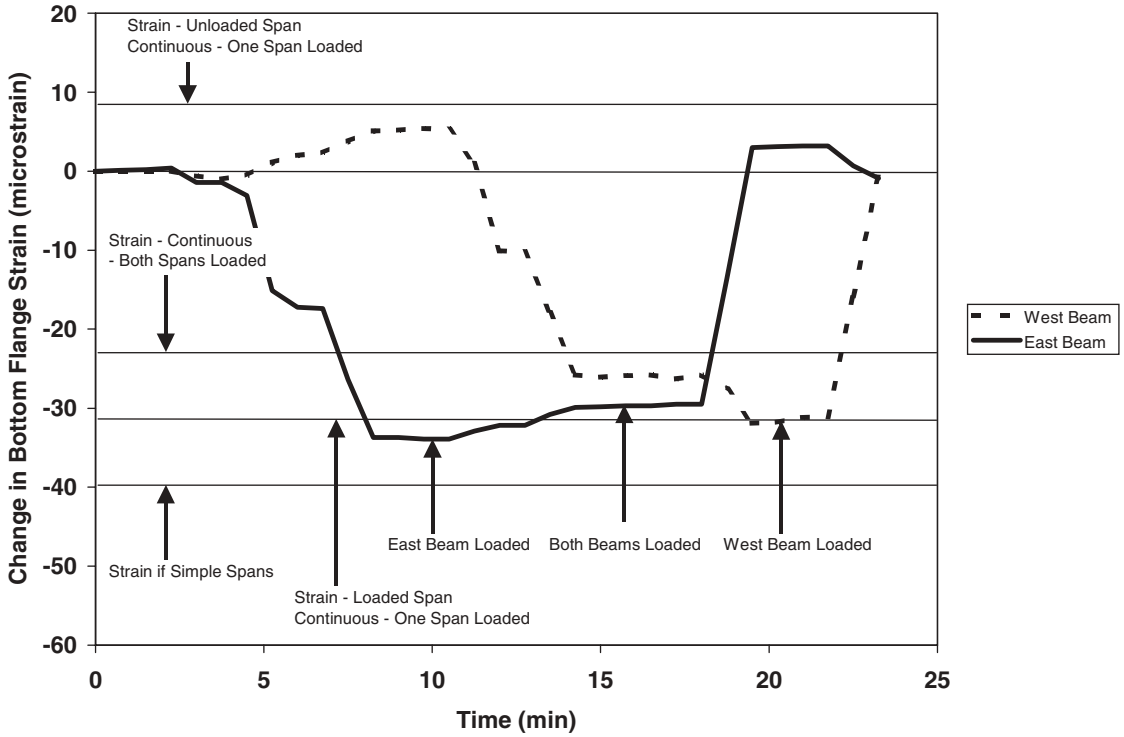

Figure 55. Change in bottom flange strains: load to positive LL *moment.*

the diaphragm, and a small diagonal crack formed in the face of the diaphragm. This type of cracking was seen in the stub specimens and was usually a sign of impending failure.

The jacking and shimming was done in increments, and the system was loaded to the negative live-load moment at various points during this process. Continuity, as measured by changes in the end reactions and strains in the girders, was maintained until the last load cycle. In the last load cycle, the end reactions increased and strains increased significantly over the fully continuous case. Table 3 compares the end reactions and bottom flange strains of the baseline case for negative moment at the support (see Figures 52 and 53). The important ratio is the case in which both spans are loaded because this case represents the full live-load moment at the

TABLE 2 Comparison of responses for positive moment: full-size Specimen 2

	Baseline Load = +20k	Load = +40k	Ratio
End Reaction East/Load East (lb)	–8,200	–16,500	2.01
End Reaction East/Load Both (lb)	–6,800	–13,500	1.99
End Reaction East/Load West (lb)	1,150	2,700	2.35
End Reaction West/Load East (lb)	1,040	1,550	1.49
End Reaction West/Load Both (lb)	–6,500	–13,500	2.08
End Reaction West/Load West (lb)	–8,075	–15,250	1.89
		Average	*1.97*
Strain East/Load East (microstrain)	–34	–73	2.15
Strain East/Load Both (microstrain)	–30	–63	2.10
Strain East/Load West (microstrain)	3	9	3.00
Strain West/Load East (microstrain)	5	7	1.40
Strain West/Load Both (microstrain)	–26	–56	2.15
Strain West/Load West (microstrain)	–32	–63	1.97
		Average	*2.13*

Figure 56. Crack at bottom of girder after post-tensioning and shimming.

support. The ratio here is about 1.3, indicating a 30% drop in continuity. The system still shows some continuity, but it is clearly reduced.

In the section on the analytical studies, it was found that after cracking, continuity was predicted to drop by 20% or more. This was not found in the experimental study until now, the point at which the connection was about to fail and the crack had propagated into the slab. Actually, this is the point where the experiment became consistent with the model. As noted previously, the models predict that when positive moment cracks occur in the joint, the crack immediately propagates into the slab (see Figure 12). The experiments show this does not happen. The cracks start at the bottom of the joint and propagate upward under increasing load or under cyclic loading. When the crack finally penetrates the slab (as it did in this last case), the cracked section is now reasonably close to the cracked section used in the models and the expected drop in continuity is seen.

Since the system was also to be tested for negative moment capacity, the positive moment testing was stopped at this point so that connection would not become excessively damaged. The ends of the girders were jacked up, and the shims were removed. The post-tensioning was also removed. The cracks closed back to openings of 0.005 in. Due to the tortuous nature of cracks in concrete, it is rare that the cracks close all the way back when load is removed. The end reactions also dropped to 25 kips because of the permanent deformations at the joint and in the diaphragm (recall that the diaphragm had also cracked). The system was subsequently reloaded with the negative live-load moment. Figures 59 and 60 show the end reactions and strains measured from the initial loading sequence (before post-tensioning and jacking the ends) compared with this final loading sequence. The results show full continuity was restored.

The tests show that the system maintains continuity even if positive moment cracking occurs at the joint. Loss of continuity does not occur until the slab and diaphragm crack and the connection is near failure.

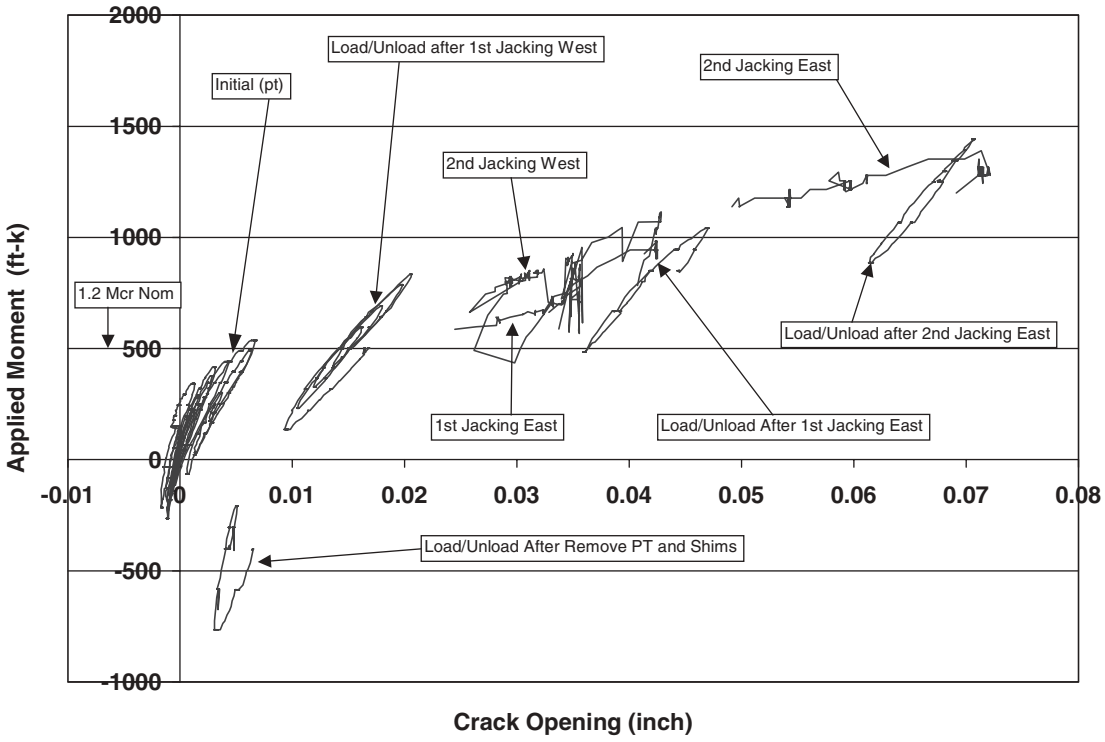

Figure 57. Crack opening at northwest joint as a function of applied moment.

Figure 58. Slab cracking in full-size Specimen 2.

NEGATIVE MOMENT CAPACITY

After the positive moment/continuity testing was complete, the specimen was tested for negative moment capacity. The deck was reinforced for negative load as required by the provision of the AASHTO LRFD Specifications (*12*). Figure 61 shows the deck reinforcing. Using the design concrete strength of 6,000 psi and assuming 60 ksi yield for the steel, the nominal moment capacity was calculated at 1,630 k-ft. This capacity increased to 2,200 k-ft when recalculated using actual material properties of 11 ksi for the concrete compressive strength and 80 ksi for yield of the steel. With the two-span configuration shown in Figure 26, the required applied load would have exceeded 200 kips/point. This would have required building a massive frame, and there were concerns that this much load would cause local failures.

The solution was to test the girder as a cantilever and to allow the dead load to apply some of the negative moment. The negative moment caused by the dead load can be calculated accurately since the weight of the specimen is known from the measured reactions. Referring to Figure 26 for directions, a downward load of 50 kips was applied to the east span to keep the system stable. Then, an upward load of 80 kips was applied in the west span. The combination of the two loads reduced the west-end reaction to about 7 kips. The west end was jacked up, and the west support was removed. The jack was released. At this point a negative moment of 545 k-ft was being applied. The west cylinder load was then reduced in increments of 5 kips.

Cracking occurred at a moment of 880 k-ft. This was less than the cracking moment of 930 k-ft calculated using the design concrete compressive strength for the deck slab, which was 4 ksi. Using the measured material properties, the expected cracking moment increased to 1,580 k-ft. The reduction in strength was probably caused by the cracking that occurred in the deck slab during the positive moment testing. When the deck cracked, the cracks were always full depth (see Figure 62).

As the negative moment increased, the deck continued to crack and the cracks propagated down into the girders (see Figure 63). The joint began to open from the top (see Figure 64). Finally, the bottom of the girder crushed (see Figure 65) at an applied moment of 2,250 k-ft, just 2% above the failure moment capacity predicted using actual material strengths. The cracking that occurred during the positive moment testing did not affect the negative moment capacity, although it did reduce the negative cracking moment.

FINITE ELEMENT MODELING

To evaluate the behavior of positive moment connections, a three-dimensional finite element model (FEM) was developed, which included nonlinear effects of cracking and crushing of concrete as well as yielding of steel bars and strands.

TABLE 3 Comparison of responses: cracked versus uncracked diaphragm

	Baseline, Uncracked	Baseline, Cracked	Ratio Highest/Lowest
End Reaction East/Load East (lb)	14,500	16,000	1.10
End Reaction East/Load Both (lb)	11,000	14,500	1.32
End Reaction East/Load West (lb)	–3,300	–900	3.67
End Reaction West/Load East (lb)	–2,500	–2,200	1.14
End Reaction West/Load Both (lb)	10,200	12,900	1.26
End Reaction West/Load West (lb)	13,300	14,900	1.12
Strain East/Load East (microstrain)	62	71	1.15
Strain East/Load Both (microstrain)	51	66	1.29
Strain East/Load West (microstrain)	–10	–3	3.33
Strain West/Load East (microstrain)	–10	–9	1.11
Strain West/Load Both (microstrain)	46	53	1.15
Strain West/Load West (microstrain)	60	62	1.03

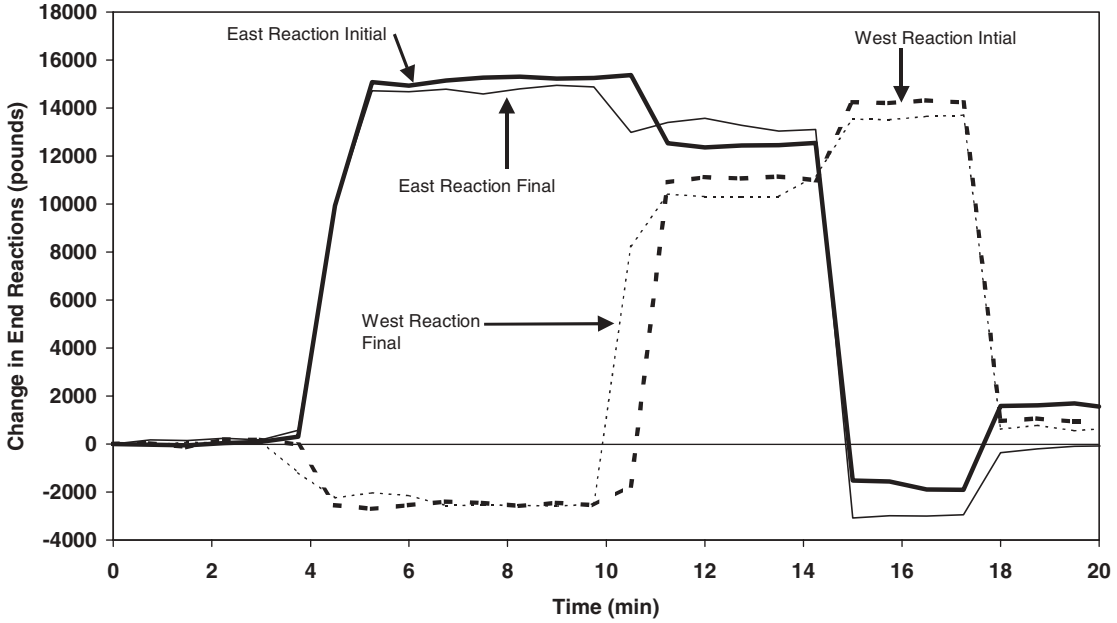

Figure 59. Comparison of change in end reactions: initial and final loading.

Among the available finite element programs, ANSYS was chosen owing to its efficient element library and material models for the analysis of reinforced and prestressed concrete members (*27*). The choice of three-dimensional modeling was due to the fact that concrete element in ANSYS is three-dimensional and accurate analysis of the variable width cross section of the composite section required three-dimensional analysis.

Concrete is modeled using eight-noded SOLID65 elements with three degrees of freedoms at each node. The element is capable of simulating smeared cracking in three orthogonal directions, crushing, and plastic deformations. Steel reinforce-

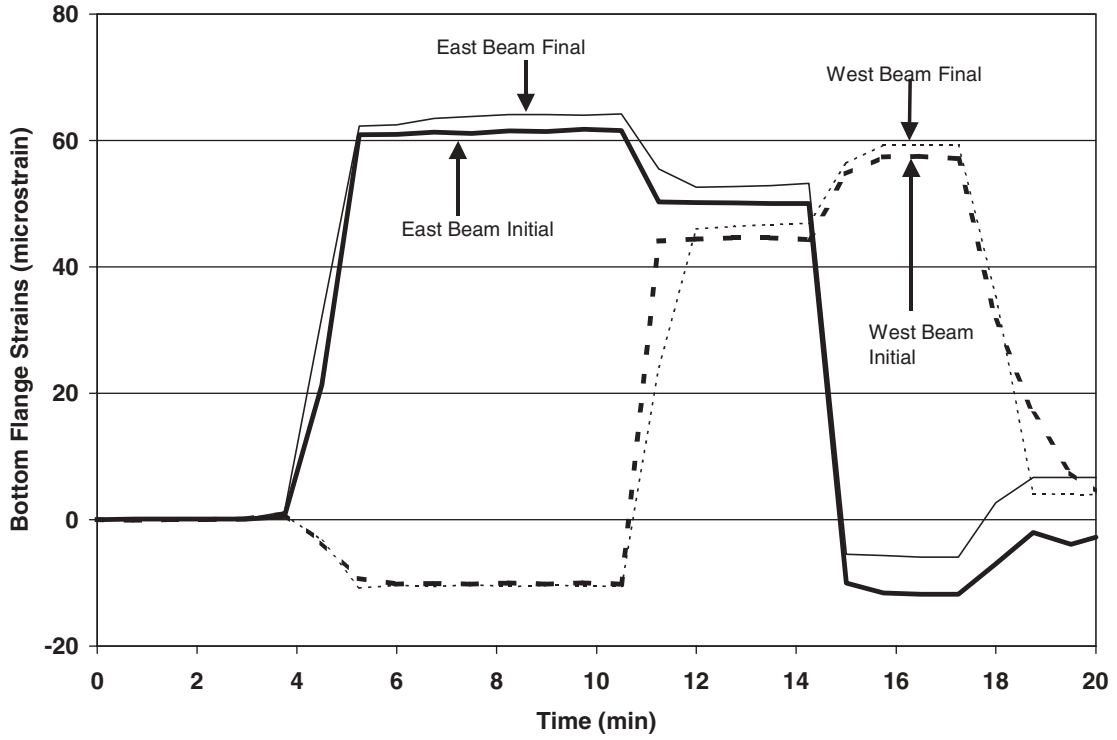

Figure 60. Comparison of change in bottom flange strains: initial and final loading.

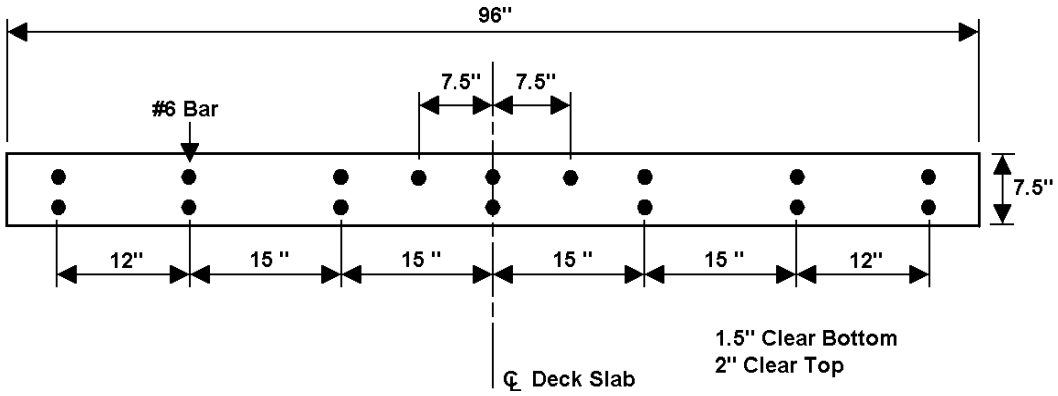

Figure 61. Deck slab reinforcement.

ment and prestressing strands are both modeled using the two-noded LINK-8 truss elements with three degrees of freedom at each node. The element is capable of simulating plasticity, stress stiffening, and large deflections. The equilibrium equations are solved using the Adaptive Descent method; this method switches to a stiffer matrix if convergence difficulties are encountered and to the full tangent matrix as the solution converges. Due to the softening behavior of concrete, a displacement control strategy is adopted. Information about the elements, convergence and solution methods can be found in the cited reference.

One of the challenges in modeling this type of bridge is the construction sequence, in which the girders are first prestressed and then assembled together with the deck and diaphragm concrete. Several methods were tried, but the approach adopted was to model the continuous bridge system. Since the main concern is on the behavior of the diaphragm and since the stiffness of the prestressed girder is considerably higher than that of the diaphragm, it was decided to model the prestressed girder as an equivalent reinforced concrete girder with equal stiffness and cracking moment. This method was verified by comparing the behavior of a prestressed concrete girder modeled as an equivalent reinforced concrete girder with the experiments of Elzanaty et al. (*28*) and fine element mesh (FEM) reported by Kotsovos and Pavlovic for the same experiment (*29*).

A FEM was created of the stub specimen (see Figure 66). Because of the large size of the model, only one-quarter of the specimen was modeled. This model would simulate the original experimental plan of lifting both ends simultaneously. However, the actual experimental procedure was to fix one end and lift the other. It can be shown by simple structural analysis that this FEM will still provide accurate stresses, but the deformation of the free end will be half that measured. Therefore, when comparing FEM deflections with the experiments, the FEM deflections are doubled. Three FEMs were created: no connection, bent strand, and bent bar. In all cases, the girder ends were not embedded in the diaphragm.

Figure 67 shows the predicted load versus deflection graphs compared with all six stub specimens (although the models do not account for embedment or web bars). The experimental

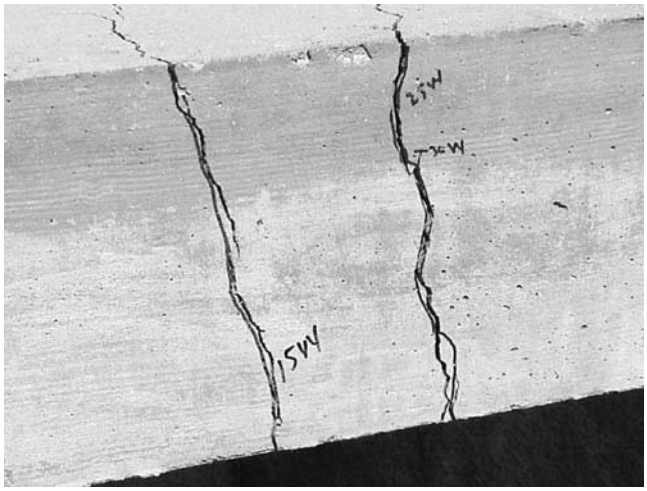

Figure 62. Full-depth slab cracks negative moment capacity testing.

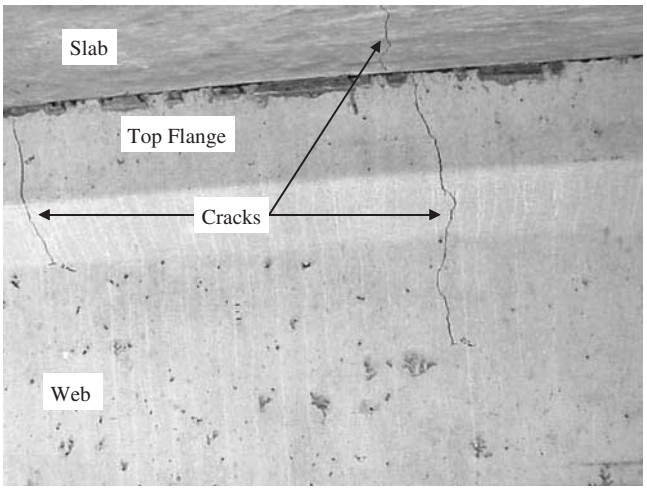

Figure 63. Negative moment cracks in girder.

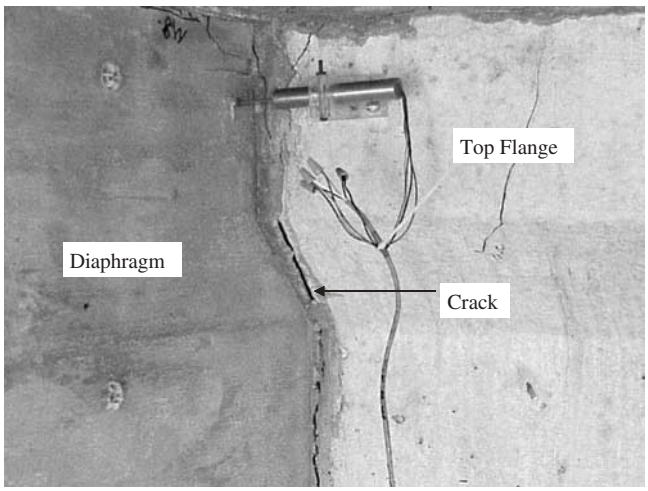

Figure 64. Separation at top of joint under negative moment.

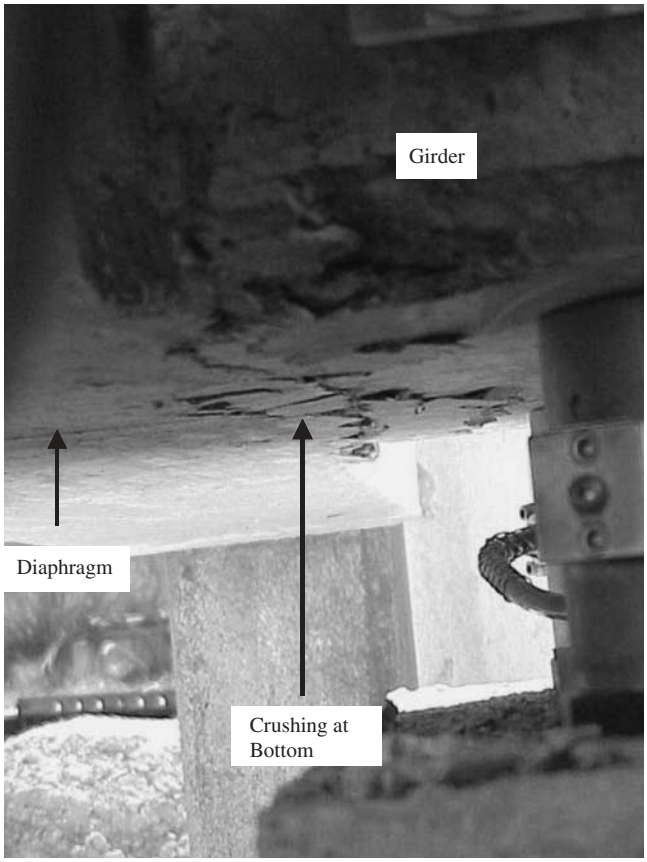

Figure 65. Crushing at bottom of joint under negative moment.

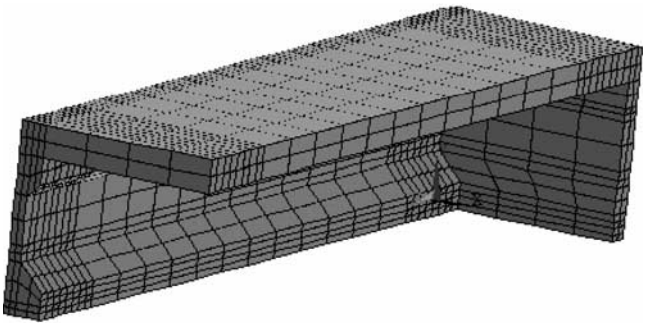

Figure 66. Finite element mesh for the stub specimens.

data shown are after 5,000 cycles. All of the specimen load vs. deflection lines are lower (less stiff) than the model, except for Specimen 6 (bent bar, embedded, web bars). All of the curves fall above the curve for no connection and below the curves for the bent bar and bent strand. The most probable reason for this is that the FEM did not account for the cold or construction joint at the beam-diaphragm interface. Such joints are much weaker than monolithic concrete. The experimental data end below the FEM data because failure in the FEM is based on rupture of the steel in monotonic loading while the experimental specimens failed by pull-out or fatigue. The FEM was not capable of simulating these failure modes.

Figure 68 shows the moment versus curvature relationship for the bent-strand model and the two bent-strand specimens, Specimens 1 and 3. The moment-curvature relationship obtained from the RESPONSE program (*22*), which was used to obtain the moment versus curvature response for the RESTRAINT program, is also shown. Note that a similar behavior to the load-deflection graphs is observed. Specimen 1 exhibits some odd behavior, but recall that this specimen may have sustained some damage because of thermal load before testing (see previous section). The moment-curvature relationship for the bent-bar Specimen 2 is shown in Figure 69 and confirms the behavior shown in Figures 67 and 68.

The FEMs show promise in predicting the behavior of the connections, but some improvements are needed. First, the joint between the girder and diaphragm should be modeled as a cold or construction joint. Second, the interface between the strands and the diaphragm concrete should be modeled appropriately to account for the slip observed in the experiments. Finally, the model must be able to account for pull-out and fatigue failures. Time and budget consideration prevented further FEM studies.

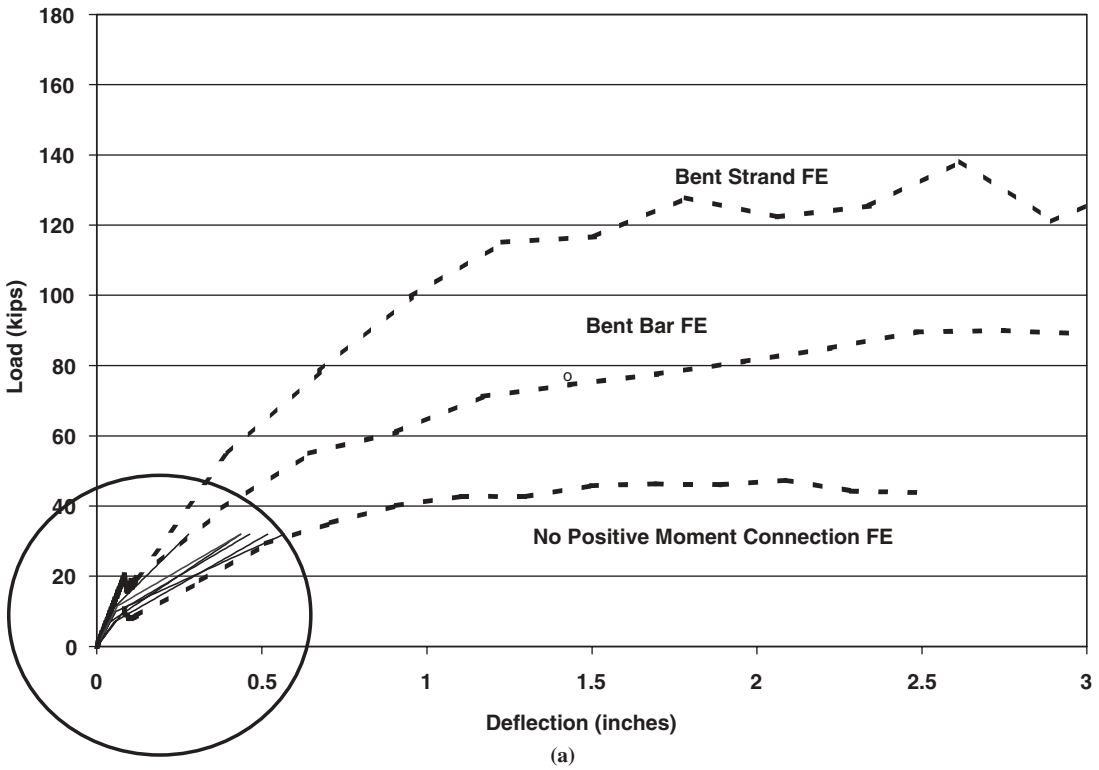

(a)

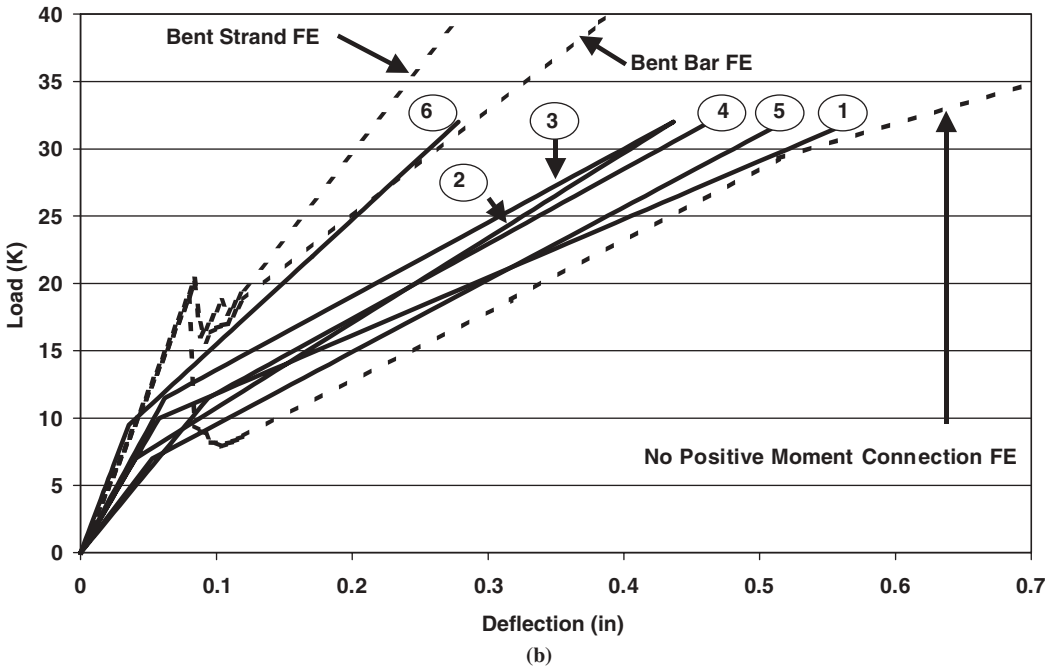

(b)

Figure 67. Stub specimen load versus deflection compared with FEM results.

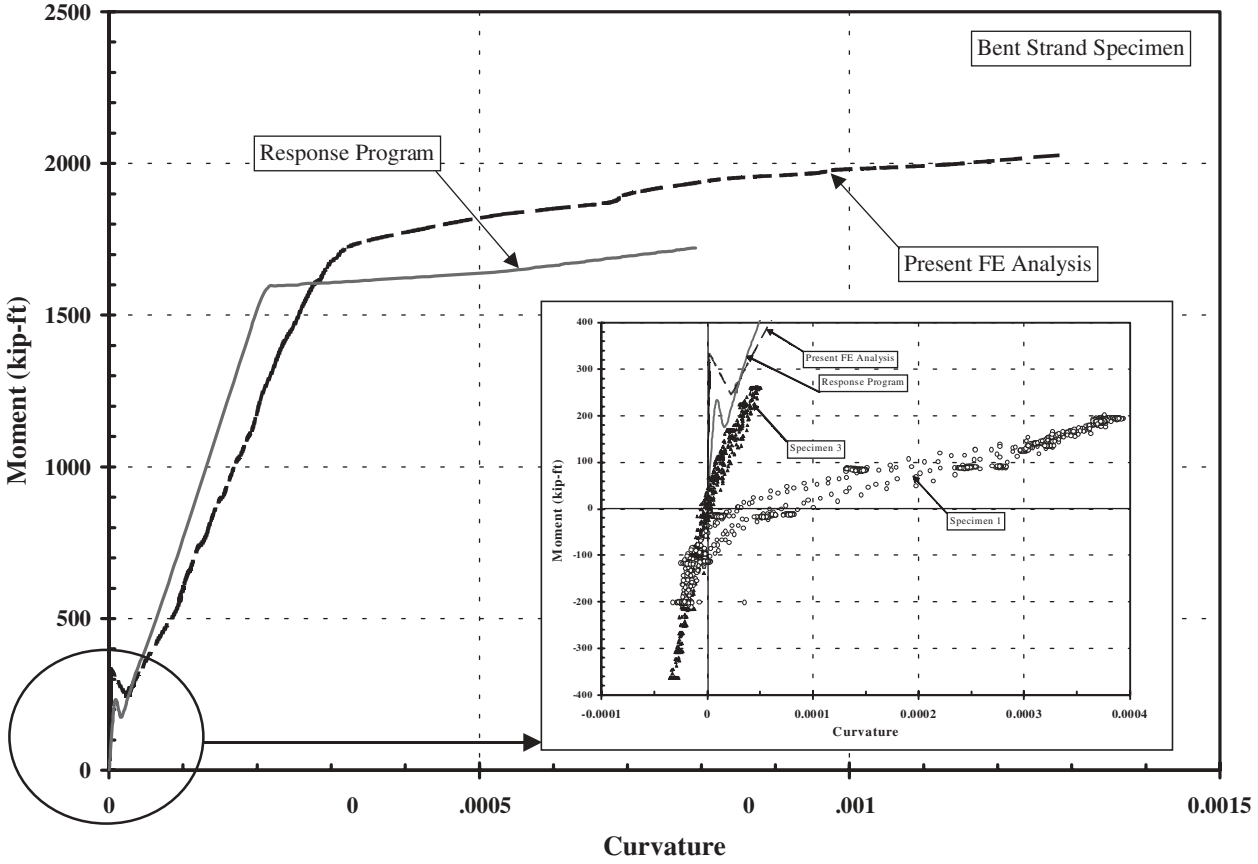

Figure 68. Stub specimen moment versus curvature compared with FEM results bent strand.

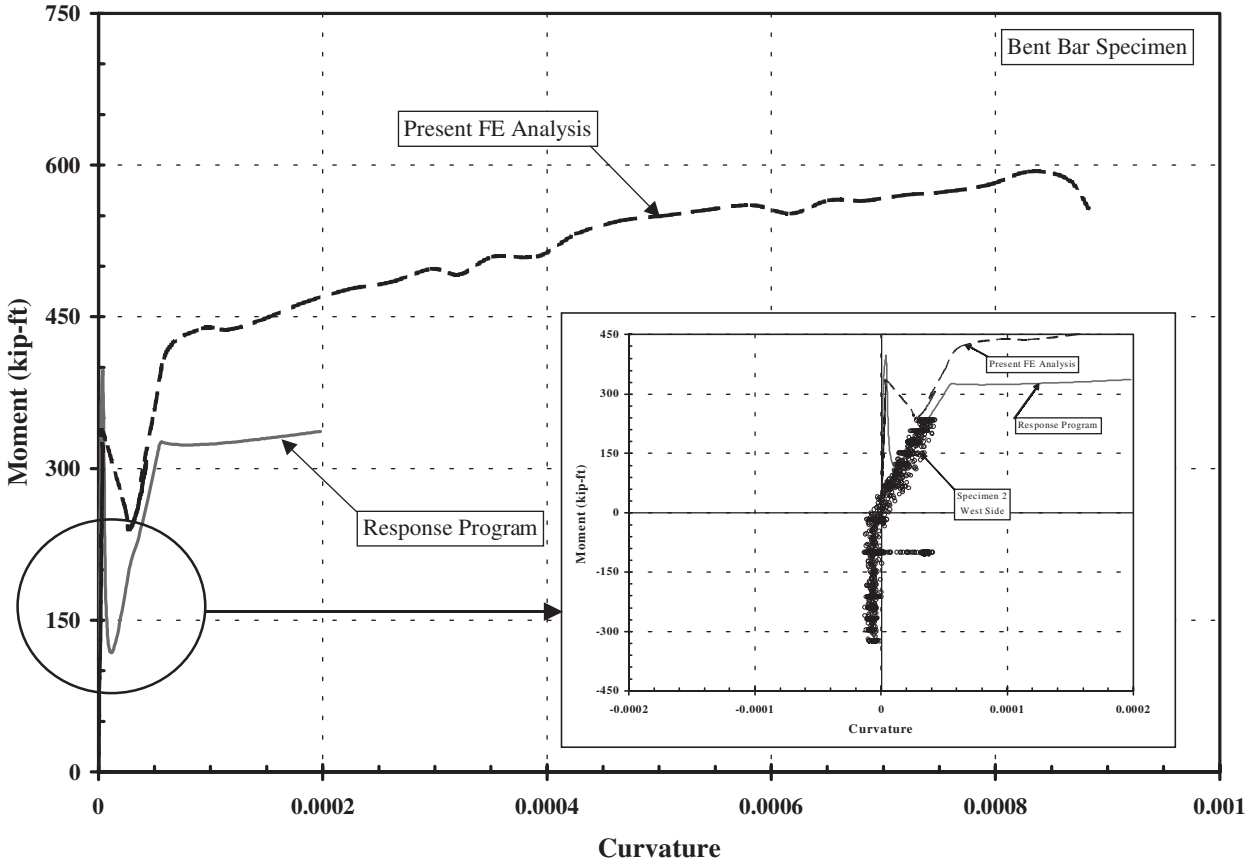

Figure 69. Stub specimen moment versus curvature compared with FEM results bent bar.

CHAPTER 3

INTERPRETATION, APPRAISAL, AND APPLICATION

CAPACITY OF CONNECTION DETAILS

The results of the experimental work answered several questions about details for positive moment connections. This work examined both bent-strand and bent-bar type connections. Connections using embedded girder ends, additional stirrups, and horizontal web bars were also examined.

The survey results showed that a bent-strand type of connection was used in many states, but the AASHTO LRFD Specifications and Standard Specifications do not provide a means of determining the strand length needed for this connection (*12, 15*). A set of equations from research done for the Missouri DOT was found (*8–10, 13*) and was used to detail the bent-strand connections in this study. The bent-strand connection, designed using the proposed equations, had adequate capacity to resist positive moment. The connections were easy to fabricate and to erect.

Using the bent strand connection may also help to reduce congestion at the end of the girder. The AASHTO LRFD Specifications require a check on the amount of longitudinal reinforcement at the end of concrete beams (*12*). The contribution of the prestressing strand is reduced if there is an inadequate development length. As a result, there is often a need for additional steel in the already congested end region of the girder. The extended bent strand clearly provides anchorage into the diaphragm. For the extended bent strand, the pull-out stress should be the sum of the pull-out stress from the development length at the end of the girder plus the pull-out stress from the bent strand as calculated by the given equations.

The bent-bar connections were designed using the provisions of the AASHTO Standard Specifications for hooked bars (*15*). These provisions are nearly identical to the AASHTO LRFD Specification provisions for hooked bars (*12*), so the results are applicable to either specification. The connections were capable of developing the nominal moment capacity. In the case of the bent bars, there was some concern that congestion in the diaphragm region might reduce the capacity since it is well known that there are interaction effects when bars are in proximity to each other; however, this was not found to be the case.

The bent-bar connections were found to be more difficult to construct. In flanged members such as bulb-T or I sections, the tails of the hooked bars extend beyond the top of the bottom flange. Pre-bent bars cannot be used because they interfere with the formwork. The bars are installed straight and then bent later. This is a labor-intensive operation, and the resulting hooks are usually not uniform, making it difficult to install anchor bars in the corners of the hooks. The uneven hooks may also cause uneven stresses in the bars. One possible solution is to make 180° bends in the bars (see Figure 70).

Another concern with bent-bar connections is that the bar pattern must usually be asymmetrical to allow for the meshing of the bars. This results in asymmetrical behavior of the connection, asymmetrical stresses in the bars, and asymmetrical crack openings. Some states avoid this problem by using a wide diaphragm and not meshing the bars.

Assembly of the bent-bar connection was slightly more difficult than for bent-strand connection. The strands are flexible and can be easily moved by hand from side to side during assembly. This is not true of the bars. However, neither type of connection required extraordinary effort to assemble.

Embedment of the end of the girders into the diaphragm did seem to reduce the stress in the connection and, in general, the embedded connections had a higher number of cycles to failure. However, this effect may be difficult to quantify. The reduction in stress is due to the weak chemical bond between the girder and diaphragm concrete and/or frictional effects as the girder tries to pull out. The magnitudes of these types of stresses vary widely and may be difficult to assess. It is probably best to ignore any embedment effects in design and to allow the embedment to provide an additional, although variable, factor of safety.

The placement of additional stirrups in the diaphragm just outside of the girder bottom flange (see Figure 22) does not increase strength. In fact, prior to pull-out of the connection, a vibrating wire strain gage placed in the diaphragm but outside of the area between the girder ends (see Figure 22) showed almost no response. This indicates that there is no stress in the diaphragm outside of the cross section of the girder; therefore, it is not surprising that steel placed in the diaphragm outside of the area between the girder ends does not affect behavior before pull-out. However, after the connection pulls out, the additional stirrups arrest the diagonal cracks that form in the diaphragm and provide additional ductility (see Figure 23). The specimen using the additional stirrups had the girder ends embedded in the diaphragm, and the experimental evidence suggests that embedded ends are needed for the additional stirrups to provide the ductility. The large diagonal cracks the

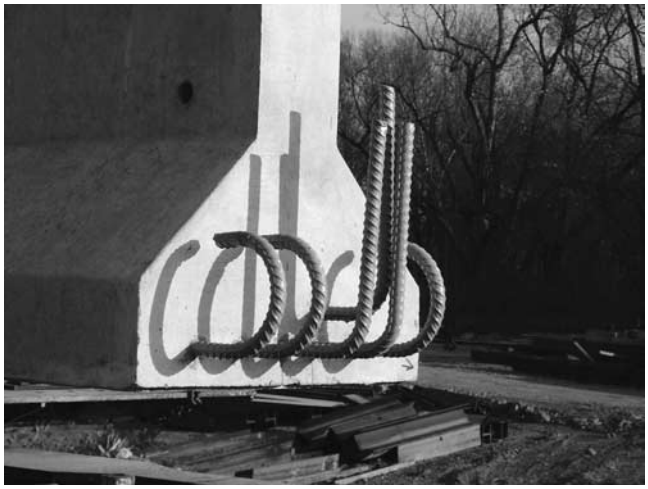

Figure 70. Positive moment connection with 180° hooks.

stirrups arrest form in the embedded specimens, but are less pronounced or nonexistent in the nonembedded specimens. This type of detail may be useful in providing additional ductility in seismic zones.

The use of horizontal bars through the web enhanced the performance of the connection. This type of connection was stiffer and more resistant to fatigue. However, when the connection failed, there was considerable cracking in the beam. This may not be desirable. The decision to test a connection with horizontal web bars was made after the girder sections were cast. Holes for bars were drilled into the webs between the shear stirrups. There was no additional reinforcement in the web around the holes. Had the holes been cast into webs and additional reinforcing added, the cracking in the girders might have been less severe.

The test results showed that all of the connection details performed adequately, and each had advantages and disadvantages. There was no detail that performed markedly better or worse than any other. Thus, the selection of a specific detail should be left to the preference of the engineer, state DOT, or both.

BRIDGE BEHAVIOR

Temperature Effects

The most striking result in the full-size tests was the influence of temperature in the system. During a single 24-h period, the end reactions often changed as much as ±5 kips, 20% of the average value of 25 kips. This change generated diaphragm moments of ±250 k-ft, approximately 60% of the positive cracking moment for the section or 2.5 times the live-load positive moment. The AASHTO LRFD Specifications require that temperature effects be considered (*12*), but these effects are often ignored in design. The experimental results show that temperature effects can be significant. Alabama attributes cracking in bridges to temperature effects (*20*, *21*).

Partial Diaphragm and Slab Casting Effects

In the first full-size specimen, a partial diaphragm was used. Initially, the bottom one-third of the height of the diaphragm was cast. After 28 days, the remaining part of the diaphragm was cast along with the slab. The idea was that the weight of the slab would cause the ends of the girder to rotate into the partial pour, compressing the diaphragm and the girder ends. This would then prevent positive moment cracking due to creep shrinkage. It is not clear how well this actually worked. During the process of casting the slab, about 50 microstrain of compression was seen at the diaphragm or at the girder ends. This would translate to a stress of 200 psi. However, the system was already in tension from positive moments, which had occurred since the partial diaphragm was cast. Even with the compressive stresses generated when the slab was cast, the system was still in a net state of tension.

After a few hours, the slab concrete began to heat up from hydration. The top of the specimen expanded, the system cambered up, the center reaction decreased, and the end reactions increased. This caused a positive moment on the connection, which relieved all compression caused by casting the slab. Later, the slab cooled and contracted. This caused the system to deflect downward, increasing the center reactions and decreasing the end reactions. It appears that a net negative moment on the order of 500 k-ft was created and that the girder ends were compressed into the diaphragm. A net negative strain of 100 microstrain was observed in the girder ends and in the diaphragm. This would correspond to a stress of approximately 400 psi. Thus, it appears that the partial diaphragm worked, but not by the mechanism assumed.

A tension tie at the top of the girders should improve performance because it seems that much higher compressive stresses were generated at the bottom of the diaphragm once continuity was established. This tension tie either can be a mechanical tie between the girder tops or it can be made by pouring the entire diaphragm and a portion of the slab in the negative moment region.

Effects of Creep and Shrinkage

The first full-size specimen was constructed and then monitored for a period of 4 months after the deck was cast. According to the model of the system, the girders should camber upward due to creep and shrinkage. Before the deck was cast, a partial diaphragm was cast. A total of 28 days elapsed between the time the partial diaphragm was cast and the time the deck was added. During this time, the girders cambered upward. This increased the end reactions, causing positive moment at the connection. Tensile strains were seen in the girder end and in the diaphragm.

When the deck is added, the models predict that the deck will shrink and the differential shrinkage between the slab and

girders will cause the formation of negative moment at the connection. This was not observed. In fact, over the monitoring period, the end reactions increased and the center reaction decreased, indicating the formation of positive moment.

Similar results were seen in three projects using high-performance concrete (*26*). The girders in these projects ranged from 60 to 300 days old. The data did not show the expected downward camber or formation of negative moment. The data presented by Ramirez et al. (*14*), show that the effect of differential shrinkage is overestimated by the models. This is also consistent with anecdotal evidence as there have been no reports of severe negative moment distress occurring in continuous-for-live-load bridges.

The problem does not appear to be the structural model. As noted in the previous section, there was a clear differential contraction of the deck due to temperature after casting, and the behavior was consistent with the model predictions for a contraction of the deck. The girders deflected downward, the end reactions increased, the bottom of the connection showed compressive strain, and there were tensile strains at the top of the connection. The problem appears to be that values used for deck shrinkage are not correct. In most models, the values for deck shrinkage are based on unrestrained shrinkage values. These values either are obtained experimentally or are from empirical equations based on the results of experimental studies. These values of shrinkage do not seem to duplicate the actual field conditions. Many models do not correctly account for the restraining effects of the reinforcing bar or the girder, actual field relative humidity, and rewetting of the deck by rain or snow.

This difficulty in assessing the effects of differential shrinkage has an impact on the assumed stresses in the connection. The models generally show that negative moment caused by differential shrinkage will mitigate positive moments cause by creep and shrinkage of the girders. However, if these negative moments do not form, the actual positive moments on the connection will be much greater. This issue needs further study.

Some states attempt to solve the creep and shrinkage issues by specifying maximum ages, minimum ages, or both for the girders at the time continuity is established. The maximum age limit is to prevent the formation of the large negative moments caused by differential shrinkage of the deck slab. Since the data suggest the models overestimate this effect, there does not appear to be a reason to limit the age of the girder at the time continuity is created. However, a minimum age does seem advisable. If continuity is formed when the girders are young, creep and shrinkage in the girders cause large positive moments to form. Since the data suggest that these positive moments are not mitigated by the deck slab shrinkage as much as the models predict, the actual positive moments that develop may be worse than predicted. If the girders are allowed to age, much of the creep and shrinkage will occur before continuity is established. This will lower the magnitude of the positive moments that form.

Continuity

In the first full-size specimen, cracks formed at interface of the girders and the diaphragm. These cracks varied in width (due to the asymmetrical bar pattern), but some were as wide as 0.02 in. The crack did not extend into the slab. Continuity was assessed by loading the specimen such that the moment at the diaphragm was either the positive or negative live-load moment and observing changes in reactions and strains in the cross section. This specimen showed continuity under all loads. This is consistent with observation from Alabama (*20*, *21*).

The second full-size specimen had cracks between the diaphragm and the girders of 0.07 in. These large cracks were induced by increasing the positive moment by raising the end supports. This specimen maintained continuity until the connection appeared near failure. This determination that the connection was near failure was based on the observations that the interface crack had propagated into the slab, the bottom of the diaphragm was cracked, and a diagonal crack had formed on the face of the diaphragm. The tests of the stub specimens indicated that these cracks were signs of the impending failure of the connection. At the point were the connection seemed near failure, the system still maintained approximately 70% continuity.

It therefore appears the cracking at the diaphragm does not affect continuity unless the cracking is severe. One reason for this is probably the condition of the center support. In most models, the system is modeled as having a single center support. In reality, the center support consists of two supports, one under each girder end. The girder ends and the diaphragm then form a "member" between the two center supports. The presence of a crack on either side of the diaphragm does not appear to alter the stiffness of this intermediate member enough to cause a complete loss of continuity. However, as the diaphragm cracks and the cracks propagate into the slab, this center section softens enough to cause some loss of continuity. From the results of the stub specimen tests, it appears that continuity will only be completely lost when the connection fails and a hinge forms.

The models predict some loss of continuity as soon as the section cracks; however, this is a limitation of the models. In theory, as soon as the section cracks, the crack propagates into the slab (see Figure 12). In reality, the crack starts at the bottom of the joint and propagates upward to the deck slab. Since the joint between the girder and the diaphragm is a cold (or construction) joint, the crack can follow this joint easily, but seems to be arrested when it hits the deck slab. Only when the connection is about to fail does the crack propagate into the slab. At this point, the cracked section at the joint matches that predicted by the model, and only then does the predicted loss of continuity occur.

This experimental program tested a single system using I girders. This certainly does not cover the entire range of bridge types, so only limited recommendations can be made.

The 2nd edition of the AASHTO LRFD Specifications (*12*) states:

> 5.14.1.2.7c: If the calculated stress at the bottom of the joint for the combination of superimposed permanent loads, settlement, creep, shrinkage, 50% live load and temperature gradient, if applicable, is compressive, the joint may be considered fully effective.

Given the experimental evidence, this specification seems both reasonable and justified. In cases in which the calculated stress at the bottom of the joint for the combination of superimposed permanent loads, settlement, creep, shrinkage, 50% live load, and temperature gradient is tensile, it might be justifiable to treat the joint as partially effective—that is, some portion of the live load would be carried as a continuous load and some portion as a simple-span load. However, the data from the experiments reported herein are insufficient to make a strong recommendation concerning degree of continuity as only a single structural system is considered.

EFFECT OF DIFFERENT CONFIGURATIONS ON THE CONNECTION

This experimental program tested six types of connections, but the number of possible variations on these types of connections is large, as was seen in the survey. From the experimental results, it is possible to comment on some of these other configurations.

Connecting Different Depth Girders

One of the concerns with the positive moment connections is congestion in the diaphragm area. The bars or strands used to create the positive moment connections tend to be meshed, leaving little or no clearance between adjacent bars. The interaction between the bars might limit the connection strength, but this was not found to be the case. The tests showed that the connections had adequate strength even though the diaphragm area was congested. Anything that relieves the congestion will improve the connection. When girders of different depths are connected into opposite sides of the diaphragm, the positive moment connection steel from each girder will not lie in the same plane, leaving more clearance between the bars and reducing interaction effects.

However, when the girders are the same depth, the forces in the positive moment connections are at the same level and will act in opposition to each other. When the girders are of different depths, the forces in the positive moment connections are now offset by the difference in the depths of the girders. This may lead to additional cracking in the diaphragm. The forces in the diaphragm area should be analyzed using an appropriate model, such as the strut-and-tie model, and additional reinforcing should be provided as needed.

Skewed Connections

Skewed connections present a particular difficulty. The skewed connection, by nature, has asymmetries, and the experimental evidence suggests that asymmetry affects connection performance. Unfortunately, no skewed connections were tested in this program, so it is difficult to make recommendations. More research is required on skewed connections.

DISCUSSION ON IMPLICATIONS OF SEISMIC EVENTS ON CONTINUITY CONNECTIONS

As outlined in the research problem statement of this project, the ability of these types of connections to maintain continuity during and after seismic events has been questioned and, therefore, needs to be evaluated. The authors were charged to prepare a discussion on the subject and to identify future research needs in this area.

Connection failures are the most common type of damage in bridge structures. Seismic events tend to overstress the entire bridge and, particularly, the connections. For the sake of this discussion on the seismic implications, three types of continuity connections are identified:

- **Type I: Continuity diaphragms with positive moment connections made of bent bars or bent strands and negative moment reinforcement in the composite deck or even in the continuity diaphragm.** The girders and/or continuity diaphragms are placed on bearing pads, which act as pin or roller supports. Therefore, the superstructure is basically isolated from the substructure in that no horizontal force is transferred from ground motions in the longitudinal or transverse direction. Variations of this type of connection has been used in many states, particularly in Tennessee and Missouri.
- **Type II: Integral continuity connections, in which the continuity diaphragm, the composite deck, and the columns are cast monolithically.** This type of connection provides fully rigid continuity and, therefore, the superstructure must be designed for a portion of the plastic hinge moment of the columns. This type of connection is primarily used in California.
- **Type III: Similar to Type I, but the diaphragm is connected to the pier cap and, therefore, limited shear and moment would be transferred during ground motion.** This type of connection is primarily used in the state of Washington, where the bottom 2 ft of the diaphragm is cast before the composite deck and the rest of the diaphragm.

Previous studies on the subject are very few and not directly relevant. Ductility of continuity diaphragm-deck connections is an important issue. Failure at the interior supports could be brittle and catastrophic because of the smaller compression area at the bottom of the girder-diaphragm. *NCHRP Report*

322 (*11*) carried out a parametric study of the negative moment strength of composite sections and found the typical sections to have adequate rotational ductility to allow formation of a failure mechanism. The static analysis indicated that an upper limit on deck reinforcement equal to 50% of its balanced reinforcement ratio would ensure sufficient ductility (of about 3.4) to develop the full-failure mechanism as well as to provide enough deformation to give adequate warning of failure.

Most recently, Holombo et al. (*30*) studied the continuity of precast/prestressed spliced-girder bridges under seismic loads for a typical construction in California. Since the girders were spliced, continuity was present for both self-weight and live load. Two 40% scale-model continuous bridge structures, one with bulb-T and the other with bath-tub girders, were tested under longitudinal seismic loads with up to eight and six times the first-yield displacement in the bulb-T and bathtub girder systems, respectively. Continuity was established by post-tensioning the girders together with strand. This is a common detail in spliced girders and a possible, but not common, detail for continuous-for-live-load systems. Although this system is not necessarily representative of continuous-for-live-load systems, it is presented here to give some indication of the performance of a continuous system under seismic load.

In the tests, significant ductility with only minor strength degradation was observed. An essentially elastic performance of the bent cap and superstructure was observed during the simulated seismic displacement cycles. Holombo et al. suggested approximating the superstructure seismic moments by giving two-thirds of the column plastic hinge moment to the girders adjacent to the column and the remaining one-third to the nonadjacent girders (*30*).

Since seismic events predominantly develop horizontal in-plane loads, the continuity connection may be subjected to longitudinal or transverse movements. If the superstructure is isolated from the substructure through pin or roller supports, the only implication of seismic event may be the unseating of the girders in the longitudinal or transverse direction. Piers may experience a significant level of damage or be "lost" after a major earthquake. At this stage, the connection is also expected to have cracked and damaged. From a life safety performance point of view, it would be important that the girders still be able to resist their self weight plus other superimposed gravity loads. Continuity connections do provide enhanced structural integrity and redundancy for the entire system. However, the positive moment connection is not designed for carrying, nor should it be expected to carry, such moments for the two adjacent spans. Previous experiences with continuity connections have demonstrated the benefits of such redundancy. For example, in the late 1970s, in a bridge on State Route 1 over the Wolf River in Memphis, Tennessee, a bent supporting two spans failed completely due to scour, but the simple spans—widened with continuous-for-live-and-composite-dead-load box beams—only sagged. Failure was averted by the alternate load path created by the continuous widened portion and the New Jersey parapet.

To avoid catastrophic failures due to unseating of the girders during seismic events, appropriate detailing must be developed based on the expected longitudinal and transverse movements of the support columns and the pier cap. In Type II connections, the superstructure is actually designed for the proper transfer of moments. In Type III connections, as discussed earlier, the dowel bars transfer some horizontal forces to the superstructure. However, rigidity of the girders in the longitudinal direction and that of the continuity diaphragm in the transverse direction should be more than adequate to resist such loads.

Another important implication of seismic events is that vertical ground accelerations may induce a significant level of inertia force for near-fault bridges. However, such forces have to first overcome the gravity accelerations before developing an uplift force at the continuity connections.

Based on the above discussion, future research on the subject should be focused on the analysis and testing of Type III connections, where some limited force transfer occurs, but perhaps is not designed for. Proper detailing must be developed to avoid unseating of the girders. Use of shear keys or dowel bars may be considered. Effect of vertical ground motion on the vibration of the superstructure and the continuity diaphragm also need to be studied.

Finally, in this study, no experimental work was done that was specifically related to seismic behavior, but the experimental work that was done does provide some relevant information that may be applicable to seismic design. The results of the connection capacity tests showed that the bent-strand connections tend to slip under cyclic loads. This type of behavior might not be desirable in a seismic area. Tests on the fifth stub specimen demonstrated that if the girder ends are embedded in the diaphragm and the additional stirrups are placed in the diaphragm just outside of the girders, the connection will be more ductile after the pull-out failure occurs. This additional ductility would be useful in seismic designs.

CHAPTER **4**

CONCLUSIONS AND SUGGESTED RESEARCH

CONCLUSIONS

This research detailed studies on connections for precast/prestressed concrete bridge girders made continuous for live load. From the research, the following conclusions can be drawn.

A survey was conducted of state DOTs, fabricators, and designers concerning connections for precast/prestressed concrete bridge girders made continuous for live load. The results of the survey show the following:

- Of 51 respondents, 35 had used, fabricated, or designed continuous-for-live-load bridges.
- In all but one case, negative moment continuity was established by the use of a reinforced concrete deck slab.
- Positive moment connections are used with the continuous-for-live-load bridges to control positive moments caused by creep and shrinkage of the precast girders. In almost all cases, the positive moment connection is made by using bent-strand or bent-bar connections. Of those who used positive moment connections, 80% also embedded the ends of the girders into the diaphragm.
- While the respondents reported some problems with constructability, all indicated that the problems were minor.
- Limited cost data was obtained, and it showed that the costs of providing continuous-for-live-load connections were insignificant. The highest cost was $200 per girder.

Positive moment connections should be proportioned to resist the moments caused by creep and shrinkage of the girders and deck slab, live load, and temperature effects. However, the results of an analytical study show that providing positive moment connections with a capacity above 1.2 M_{cr} (where M_{cr} is the positive cracking moment of the composite cross section) is not efficient. It is suggested that if analysis shows the positive moment connection needs a capacity above 1.2 M_{cr}, steps be taken to reduce the formation of positive moments. The easiest way to do this is to specify a minimum age of the girders at the formation of continuity to allow some of the girder creep and shrinkage to occur before continuity is created.

At present, there is no accepted method for designing the bent-strand connection. In this study, the number of strands and the extended length of strand needed were found from equations developed by Salmons and others (*8–10, 13*). Connections designed using these equations were found to have adequate strength. The connections fail by the strands pulling out of the concrete. In embedded connections, there is also a pull-out failure when the girder pulls out of the diaphragm. Since the equations developed by Salmons and his coauthors appear to be adequate for design of the bent-strand connection, they have been placed in the commentary of the proposed revisions to the *AASHTO LRFD Bridge Design Specifications*, which is found in Appendix C.

Bent-bar connections designed such that the embedment of the bar into the girder and the embedment of the hooks into the diaphragm meet the provisions of the AASHTO LRFD Specifications (*12*) have adequate strength. There was a concern that congestion in the diaphragm area might reduce the capacity because of bar interactions, difficulty in consolidating the concrete, or both. It was noted in the experiments that bent-bar-type connections must have the bars placed asymmetrically with respect to the cross section to allow meshing of the bars. This asymmetry causes asymmetrical responses in the connection. The connection fails by yield of the steel followed by a pull-out failure in the diaphragm. The pull-out failure occurred in both embedded and nonembedded specimens.

Embedding the girder ends in the diaphragm appears to reduce the stresses in the positive moment area; but, because this effect relies on the bond of a cold (or construction) joint, the effect is difficult to quantify.

Additional stirrups placed in the diaphragm, just outside of the girders, do not increase the strength of the connection. However, these stirrups cross the diagonal cracks that form in the diaphragm when the final pull-out failure occurs, and the stirrups increase the ductility of the connection after the connection fails.

Bars placed horizontally through the webs of the girders increase both the strength and the ductility of the connection. However, there is significant cracking in the girders at failure, and this may be undesirable.

To limit tensile stresses in the diaphragm, some state DOTs pour part of the diaphragm before the deck slab is cast. It is thought that the weight of the deck slab will cause the girder ends to rotate into the diaphragm and compress it. This method was found to be only marginally effective. However, it could possibly be improved if a tension tie was provided at the top of the girders.

When the deck slab is cast, it heats up while still plastic because of the heat of hydration. After the deck slab sets, it cools and contracts. This contraction causes the formation of negative moments at the connection. At present, analytical models do not account for this negative moment formation. Because this negative moment causes compression of the connection, it helps to mitigate later positive moment formation.

Temperature effects on the system are significant. Daily temperature changes caused end reactions to vary ±20% per day. Seasonal temperature variations also affect the behavior of the bridge. At present, few design methods account for temperature effects, but they can be as significant as the live-load effects.

Current analytical models predict that differential shrinkage between the deck slab and the girders should cause negative moment formation at the connection in some systems. For a particular bridge, the predicted development of this negative moment depends on a number of factors, such as the creep and shrinkage properties of the girder and slab, the amount of prestressing force, the dead load, and the span length. In this project, the analytical models predicted that a negative moment should have formed for full-size Specimen 1 and that there should have been a gradual downward deflection of the girders and a decrease in the end reactions. This was not observed. The data showed that the end reactions gradually increased, which indicates positive moment formation. An examination of data from other projects (*26*) confirms that differential shrinkage of the deck does not seem to cause a negative moment formation. In the other projects, the girders were anywhere from 60 to 300 days old when continuity was established. With girders at these ages when continuity is established, the analytical models predict that differential shrinkage should cause negative moments, which would be accompanied by a downward deflection of the girders. However, since the observed deflections remained almost constant (except for daily temperature-induced changes), negative moments do not appear to have developed. This finding has a potentially significant impact on the girder and connection design. The negative moment predicted by the models reduces the predicted maximum positive moment. If the negative moment does not form, the models may underpredict the positive moment formation. However, if the negative moment formation is ignored (by choosing a very low value of deck shrinkage), the models may predict unrealistically high values for the positive moment.

The presence of positive moment cracking at the diaphragm does not necessarily reduce continuity as predicted by analytical models. The analytical models treat the joint between the girder and the diaphragm as monolithic when it is really a cold joint. As a result, the analytical models tend to overpredict the load at which the cracks form. However, the models also predict that when the joint cracks, the crack will immediately propagate into the slab and continuity will be reduced. This does not happen. The crack propagates slowly along the joint, and as long as the connection remains elastic, continuity is maintained. When the positive moment connection approaches failure—which is signified by large crack openings at the diaphragm, cracking on the bottom of the diaphragm, diagonal (pull-out) cracking in the diaphragm, and propagation of the joint crack into the slab—there is an observed loss of continuity of 20% to 30%. This is consistent with models because, at this point, the cracking in the specimen matched that predicted by the models.

The presence of positive moment cracking does not affect negative moment capacity of the connection. However, if the positive moment cracking extends into the slab, the negative cracking moment is reduced.

COMPARISONS WITH PREVIOUS RESEARCH

Previous research done on the continuous moment connections was published as *NCHRP Report 322* (*11*). This report concluded that positive moment connections were of no structural benefit. If a positive moment connection is not used, the formation of time-dependent positive moments at the diaphragm due to creep and shrinkage will crack the joint. This cracking will release the positive moments, but will cause the joint to behave as a hinge. Continuity will be lost, and the girders will behave as simple spans for both dead and live loads. If a positive moment connection is used, the connection will resist cracking at the diaphragm and preserve continuity, and the midspan positive live-load moment in the girders will be lower than in the simple-span case. However, because the connection resists rather than releases the time-dependent positive moments, it causes time-dependent positive moments to form throughout the girder. The total midspan positive moment is then the sum of the dead-load moment (assumed simple span), the live-load moment (assumed continuous), and the time-dependent positive moments. *NCHRP Report 322* concluded that this total midspan positive moment was virtually identical to the midspan positive moment obtained by assuming simple spans for all loads. Thus, the conclusion is that positive moment connections provided no benefit.

NCHRP Report 322 was an analytical study and, as with any research study, considered only a limited set of parameters, mostly related to the creep and shrinkage characteristics of the concrete girders and deck (*11*). The conclusions of the *NCHRP Report 322* study are valid, within the limits of that study; however, the actual continuous system is more complex. Positive moment formation at the diaphragm is influenced by many factors including girder size and length, the amount of prestressing force, the age of the girders at the formation of continuity, the construction sequence, the use of partial diaphragms, contraction of the deck because of cooling after casting, deck reinforcement, and thermal effects. In some cases, it is possible to have a system in which there is little or no time-dependent positive moment formation at the diaphragm. In other cases, the time-dependent moments formed at the diaphragm are negative. Therefore, a blanket

statement that positive moment connections are not structurally beneficial may not be justified in all cases. As with any design, the decision on the use of positive moment connections should be based on a rational engineering analysis of the moments formed in the entire system.

However, even in cases in which analysis shows that the use of positive moment connections does not reduce the midspan positive moments, the positive moment connection may still be useful. The results of this research show these connections, when properly designed, are robust. These connections will contribute to the overall structural integrity of the system, especially in cases in which supports are damaged.

PROPOSED REVISIONS TO THE AASHTO LRFD BRIDGE DESIGN SPECIFICATIONS

Precast/prestressed concrete bridges made continuous are addressed in Section 5.14.1.2.7 of the *AASHTO LRFD Bridge Design Specifications* (*12*). Appendix C contains proposed revisions to this section. The proposed revisions are as follows:

1. A more complete definition of precast/prestressed concrete bridges made continuous is proposed.
2. A significant feature of precast/prestressed concrete bridges made continuous is the development of time-dependent moments. The existing specifications do not address methods of analysis for determining these time-dependent moments or suggested values for time-dependent material properties. Based on the information gained in the literature search and the analytical studies done as part of this project, suggested time-dependent material properties and analysis methods are presented.
3. The current specifications do not address the effect of the age of the girder(s) when continuity is established. Information obtained in this study from literature, surveys, and analytical work shows the girder age is of great importance in determining the time-dependent moments that form in the system. The literature search, surveys, and analytical work also shows that if the girders are more than 90 days old when continuity is formed, it is unlikely that positive time-dependent moments (called "restraint moment" in the proposed specifications) will form. The proposed specifications discuss the effect of girder age on the analysis and on the formation of positive time-dependent moments.
4. When cracking occurs at the connection between precast/prestressed concrete girders made continuous, it is possible that the continuity between adjacent spans will be lost. The current specifications require that this effect be considered, but provide no guidance. Based on the experimental work in this study, the connections between the precast/prestressed concrete girders can tolerate some cracking and still maintain continuity. In fact, loss of continuity is not seen until the connection is near failure, and then the loss is about 30%. The current specifications state that the connection can be considered fully effective if ". . . the calculated stress at the bottom of the continuity diaphragm for the combination of superimposed permanent loads, settlement, creep, shrinkage, 50% live load and temperature gradient, if applicable, is compressive." The research team could not determine the origin of this statement, but the experimental evidence confirms that this is a reasonable assumption.

   As stated in the previous conclusion, if the girders are at least 90 days old when continuity is established, there is a low probability that time-dependent positive moments will form. If these moments do not form, the connection will not crack and continuity will not be affected. This point is added to the proposed specifications. Finally, guidance on dealing with partially effective connections is provided.
5. Design limits for service and strength limit states are added. This is material found elsewhere in the LRFD Specifications, but it is added here for completeness.
6. The section in the current LRFD Specifications on negative moment connections has been expanded. The proposed changes do not add new information, but clarify the existing section.
7. The current LRFD Specifications do not contain a method for designing the positive moment connection. The proposed changes to the specifications suggest that the two possible ways to make the positive moment connection are as follows:
   a. Extending the prestressing strand from the end of the girder, bending it at 90°, and then embedding the bent strand into the continuity diaphragm. The length of the strand extension can be found from the equations proposed by Salmons and others (*8–10, 13*).
   b. Embedding mild reinforcing bar in the end of the girder. The protruding end of the bar should have a standard hook, which is embedded into the diaphragm. The connection will develop sufficient strength as long as both ends of the bar are embedded by the required development length (given in Article 5.11 of the LRFD Specifications).

   The experimental results from this study show that positive moment connections designed as stated above develop sufficient strength. Analytical studies done as part of this project show that the positive moment connection should be proportioned to provide a minimum strength of 0.6 M_{cr}, where M_{cr} is the cracking moment of the connection. This point is added to the body of the suggested changes. The analytical studies also show that proportioning the connection to provide more than 1.2 M_{cr} is not effective. This point is added as a suggested change to the commentary.
8. From information obtained in the surveys conducted in this study and from the experience of assembling

the experimental specimens, detailing requirements are proposed.

SUGGESTED FUTURE RESEARCH

This experimental program tested only AASHTO I shapes. Limited testing to verify positive moment connection capacity for other shapes may be advisable.

This experimental program tested only a single beam line as a full-size specimen. The result should be verified by monitoring the response of a complete bridge.

The analytical models do not accurately assess the effects of differential shrinkage between the deck slab and the girders. Work needs to be done to create more accurate models.

The effects of skew and seismic effects were not tested in this program. Additional experimental work on seismic and skew effects is advised.

REFERENCES

1. Kaar, P.H., Kriz, L.B., and Hognestad, E. "Precast-Prestressed Concrete Bridges 1: Pilot Tests of Continuous Girders," *Journal of the PCA Research and Development Laboratories*, Vol. 2, No. 2, May 1960; pp. 21–37. Also reprinted as *PCA Bulletin D-34*.
2. Hanson, N. W. "Precast-Prestressed Concrete Bridges 2: Horizontal Shear Connections," *Journal of the PCA Research and Development Laboratories,* Vol. 2, No. 2, May 1960; pp. 38–58. Also reprinted as *PCA Bulletin D-35.*
3. Mattock, A.H., and Kaar, P.H. "Precast-Prestressed Concrete Bridges 3: Further Tests of Continuous Girders," *Journal of the PCA Research and Development Laboratories,* Vol. 2, No. 3, Sept 1960; pp. 51–78. Also reprinted as *PCA Bulletin D-43*.
4. Mattock, A.H., and Kaar, P.H. "Precast-Prestressed Concrete Bridges 4: Shear Tests of Continuous Girders," *Journal of the PCA Research and Development Laboratories,* Vol. 3, No. 1, Jan 1961; pp. 19–46. Also reprinted as *PCA Bulletin D-45.*
5. Mattock, A.H. "Precast-Prestressed Concrete Bridges 5: Creep and Shrinkage Studies," *Journal of the PCA Research and Development Laboratories*, Vol. 3, No. 2, May 1961; pp. 32–66. Also reprinted as *PCA Bulletin D-46*.
6. Mattock, A.H., and Kaar, P.H. "Precast-Prestressed Concrete Bridges 6: Test of Half-Scale Highway Bridge Continuous over Two Spans," *Journal of the PCA Research and Development Laboratories*, Vol. 3, No. 3, Sept 1961; pp. 30–70. Also reprinted as *PCA Bulletin D-51*.
7. Freyermuth, C.L. "Design of Continuous Highway Bridges with Precast, Prestressed Concrete Girders," *Journal of the Prestressed Concrete Institute,* Vol. 14, No. 2, April 1969; pp. 14–39. Also reprinted as *PCA Engineering Bulletin EB014.01E,* August 1969.
8. Salmons, J.R., and McCrate, T.E. *Bond of Untensioned Prestress Strand.* Interim Report 73-5A, Missouri Cooperative Highway Research Program, Missouri State Highway Department, August 1973.
9. Salmons, J.R., and May, G.W. *Strand Reinforcing for End Connections of Pretensioned I-Beam Bridges.* Interim Report 73-5B, Missouri Cooperative Highway Research Program, Missouri State Highway Department, May 1974.
10. Salmons, J.R. *End Connections of Pretensioned I-Beam Bridges.* Final Report 73-5C, Missouri Cooperative Highway Research Program, Missouri State Highway Department, Nov 1974.
11. Oesterle, R.G., Glikin, J.D., and Larson, S.C. *NCHRP Report 322: Design of Precast Prestressed Bridge Girders Made Continuous*. Transportation Research Board, National Research Council; Washington, DC; November 1989.
12. *AASHTO LRFD Bridge Design Specifications, 2nd Edition.* American Assoc. of State Highway and Transportation Officials; Washington, DC; 1998.
13. Salmons, J.R. *Behavior of Untensioned-Bonded Prestressing Strand.* Final Report 77-1, Missouri Cooperative Highway Research Program, Missouri State Highway Department, June 1980.
14. Ramirez, J.A., Abdalla, O.A., and Lee, R.H. *Strand Debonding in Pretensioned Beams: Precast Prestressed Concrete Bridge Girders with Debonded Strands, Continuity Issues*, Joint Highway Research Project, Indiana DOT/Purdue University, FHWA/INDOT/JHRP-92-24, June 1993.
15. *AASHTO Standard Specifications for Bridge Design, 16th Edition.* American Assoc. of State Highway and Transportation Officials; Washington DC; 1996.
16. Peterman, R.J., and Ramirez, J.A. "Restraint Moments in Bridges with Full-Span Prestressed Concrete Form Panels," *PCI Journal*, Vol. 43, No. 1, January-February 1998; pp. 54–73.
17. Peterman, R.J., and Ramirez, J.A. "Behavior and Strength of Bridges with Full-Span Prestressed Concrete Form Panels," *PCI Journal*, Vol. 43, No. 2, March-April 1998; pp. 80–91.
18. Tadros, M.K., Ficenec, J.A., Einea, A., and Holdsworth, S. "A New Technique to Create Continuity in Prestressed Concrete Members," *PCI Journal*, Vol. 38, No. 5, September-October 1993; pp. 30–37.
19. Ma, Z., Huo, X., Tadros, M.K., and Baishya, M. "Restraint Moments in Precast/Prestressed Concrete Continuous Bridges," *PCI Journal*, Vol. 43, No. 6, November-December 1998; pp. 40–56.
20. "Temperature Gradient Cracks Viaduct Girders," *Engineering News Record;* May 30, 1994; pp. 14–15.
21. *Cracks in Precast Prestressed Bulb Tee Girders on Structure Nos. I-565-45-11.5 A. & B. on I-565 in Huntsville, Alabama.* Alabama DOT, September 1994.
22. Collins, M., Mitchell, D., Felber, A., and Kuchma, D. RESPONSE V 1.0. provided with *Prestressed Concrete Structures.* Prentice Hall: Englewood Cliffs, NJ; 1991.
23. ACI Committee 209. "Prediction of Creep, Shrinkage, and Temperature Effects in Concrete Structures," in *Designing for Creep and Shrinkage in Concrete Structures.* Publication SP-76, American Concrete Institute, 1989; pp. 193–300.
24. *PCI Design Handbook, 5th Edition.* Precast/Prestressed Concrete Institute: Chicago, IL; 1999.
25. Mirmiran, A., Kulkarni, S., Miller, R., Hastak, M., and Castrodale, R. "Nonlinear Continuity Analysis of Precast/Prestressed Girders with Cast-in-Place Deck and Diaphragm," *PCI Journal*, September–October 2001.
26. Russell, H., Ozyildirim, C., Tadros, M., and Miller, R. *Compilation and Evaluation of Results from High-Performance Concrete Bridge Projects.* Project DTFH61-00-C-00009 on compact disc, Federal Highway Administration; Washington, DC; 2003.
27. *ANSYS Reference Manuals.* SAS IP Inc., 1996.
28. Elzanaty, A.H., Nilson, A.H., and Slate, F.O. "Shear Capacity of Prestressed Concrete Beams Using High-Strength Concrete," *ACI Structural Journal*, Vol. 83, 1986; pp. 359–368.
29. Kotsovos M.D., Pavlovic, M.N. "Structural Concrete: Finite Element Analysis for Limit-State Design," *Thomas Telford Publication.* 1995.
30. Holombo, J., Priestley, M.J.N., and Seible, F. "Continuity of Precast Prestressed Spliced-Girder Bridges Under Seismic Loads." *PCI Journal*, Vol. 45, No. 2, 2000; pp. 40–63.

APPENDIX A
RESTRAINT PROGRAM

The RESTRAINT Program is available upon request to NCHRP, Transportation Research Board; call 202-334-3213. Remit payment to NCHRP, Transportation Research Board, Box 289, Washington, DC, 20055.

APPENDIX B
DETAILS OF THE EXPERIMENTAL PROGRAM

GENERAL

The experimental program consisted of two parts: connection capacity tests and full-size tests. The design concrete strength for girders was 4,000 psi at release and 5,500 psi at 28 days. Slabs and diaphragms had design 28-day strengths of 4,000 psi Actual concrete strengths are provided in Table B-1. All mild reinforcing bars were Grade 60, but the actual yield strength was 83 ksi. The prestressing strand was Grade 270 low relaxation.

CONNECTION CAPACITY: STUB SPECIMEN TESTS

Connection Details

The stub specimens consisted of two 16-ft-long AASHTO Type II girders connected by a diaphragm (see Figure B-1). A total of six specimens were tested (see Chapter 2 for details). The original plan was to fabricate six stub girders and to create the six specimens by using both ends of the stubs. Two stubs would be used to create a specimen for a test, and then after the test, the stubs would be cut from the diaphragm. The stub girders could then be turned around, and the other ends used to create a second specimen. This was done for the first four specimens; however, the last two specimens had the girders embedded in the diaphragms, which made cutting them from the diaphragm impractical. Initially, a total of seven stub girders (six for use plus one spare) were fabricated. To make the final specimen, an additional stub beam was fabricated and used with the spare stub girder to make Specimen 6.

The stub specimens were designed to simulate an interior girder in a multispan I-girder bridge. This bridge had 50-ft spans and used AASHTO Type II girders. The live-load inflection points were approximately 15 ft from the diaphragm, so the stub specimens approximated the area between the live-load inflection points. All six specimens used a 10-in. gap between the ends of the girders (see Figure B-1). A 7.5-in.-thick by 8-ft-wide slab was cast on top of the girders.

The diaphragms were 8 ft wide. The thickness of the diaphragms varied from 10 in. to 26 in., depending on whether the girders were embedded in the diaphragm. Except for Specimen 5, the diaphragms had No. 5 stirrups placed 12 in. on center with the first stirrup 3 in. from the face of the bottom flange (see Figure B-1). Specimen 5 had two additional stirrups placed 3 in. on center, just outside of the bottom flange of the girder.

Two types of positive moment connections were used: bent strand or bent bar. All connections were designed to have a nominal capacity of 1.2 M_{cr}. The cracking moment, M_{cr}, was calculated using the composite cross section but assuming the entire section was made from slab/diaphragm concrete. The cracking moment was determined to be 2,950 k-in., so 1.2 M_{cr} is 3,540 k-in.

The bent-strand connection was made by extending the strand extend from the face of the girder and then bending it at a 90° angle. To determine the length of strand, the equations developed by Salmons and others (*1–4*) were used. These equations provide both an ultimate strength and a working stress. The connection was designed to have an ultimate strength capacity of 1.2 M_{cr} and a working stress capacity of M_{cr}. There are two variables: the area of the strand and length of the strand. For the stub specimens, the entire bottom layer of six strands was used. This provided an area of 0.918 in^2.

The original work by Salmons and others allowed for the use of horizontal bars attached to the web and perpendicular to the girder (see Chapter 2). If these horizontal bars are not used, the required working stress in the bent strand is given by

$$f_{ps}(req'd) = \frac{M}{A_{ps} jd_{ps}}$$

where

M = positive moment,
A_{ps} = area of the bent strand crossing the connection joint, and
jd_{ps} = distance between the compressive and tensile resultants.

The required embedment length is then found from

$f_p = (L_e - 8.25 \text{ in.})/0.228 \leq 150$ ksi, and

L_e = embedment length (in.).

Ultimate strength is calculated by

$f_{pu} = (L_e - 8.25 \text{ in.})/0.163$,

$a = (A_{ps} f_{pu} - A_s f_y)/0.85 f'_c b$,

$M_u = (\phi A_{ps} f_{pu} [d_{ps} - a/2] + A_s f_y [d - a/2])$,

b = width of compression face (rectangular section assumed),

f'_c = compressive strength of concrete, and

ϕ = understrength factor.

TABLE B-1 Concrete compressive strength*

Stub Specimens	Concrete Compressive Strength psi (MPa)
Girders	10,500 (73.5)
Diaphragm/Slab 1	7,200 (50.4)
Diaphragm/Slab 2	8,200 (57.3)
Diaphragm/Slab 3	7,500 (52.5)
Diaphragm/Slab 4	5,500 (38.4)
Diaphragm/Slab 5	5,700 (39.9)
Diaphragm/Slab 6	6,400 (44.8)
Full-Size	
Girders	11,500 (80.5)
Partial Diaphragm 1 @ 28 Days	5,300 (37.1)
Partial Diaphragm 1 @ Test	5,500 (38.5)
Slab 1 @ 28 Days	6,550 (45.9)
Slab 1 @ Test	6,750 (47.3)
Diaphragm/Slab 2	7,100 (49.7)

*Strength is at time of test unless noted.

It was assumed that the working stress condition controlled and that the connection should be able to develop M_{cr} at working stress. For six strands, the cracked section has jd = 40 in. with M_{cr} = 243 k-ft, L_e = 26 in. If an L_e of 26 in. is then substituted into the ultimate strength equations, the capacity is found to be 315 k-ft, which exceeds 1.2 M_{cr} = 292 k-ft. For all calculations, the composite cross section is used, but it is assumed to be made entirely of diaphragm concrete. This is consistent with the normal design assumption that failure occurs in the diaphragm concrete. The section is treated as a regular reinforced concrete section and uses 0.9 as the understrength factor.

For the bent-bar connection, the composite cross section was designed as a regular reinforced concrete section with an ultimate capacity of 1.2 M_{cr}. Using the nominal concrete strength of 4 ksi and 60 ksi for yield of the steel, the section required five No. 5 bars.

Experimental Set-Up

Figure B-2 shows the experimental set up. For ease of understanding, the ends of the specimen were designated

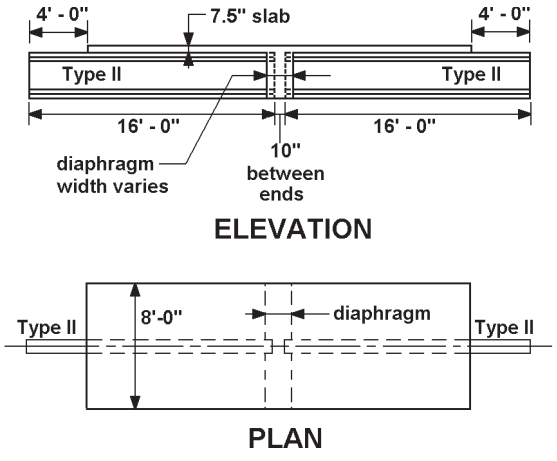

Figure B-1. Stub specimen.

(a)

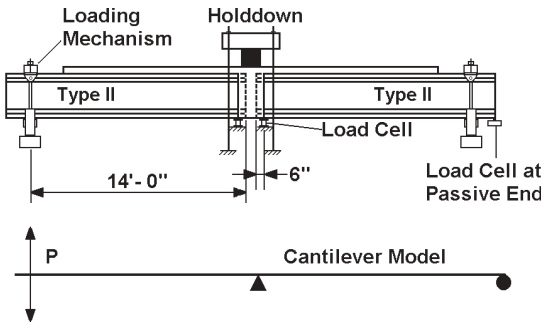

(b)

Figure B-2. Stub experimental setup.

"east" and "west." In Figure B-2, east is foreground. The specimen is held down at the center by a tie down device and is loaded by a yoke system at each end (see Figures B-3 and B-4). Load was applied through two –40 kip hydraulic cylinders. Load cells were attached to the rod of each cylinder. The system was controlled by servohydraulic valves and an electronic controller.

The girders were supported by load cells at the center support placed under the ends of the girders (see Figure B-5). According to data collected in a survey (see Chapter 2), this is the usual method of support. Direct current linear variable differential transformers (DCLVDTs) were attached to the girders and targeted to the diaphragms to measure crack openings (see Figure B-5). Crack openings were measured on both sides of the girders and on both faces of the diaphragm—a total of four joints. The DCLVDTs were placed at the midheight of the top and bottom flanges and at the midheight of the web. Vibrating wire gages were placed in the diaphragm area, as shown in Figure B-6. Vibrating wire strain gages were placed 1.5 in. from the bottom of the diaphragm, at a distance of 3 in. and 12 in. from the outside face of the bottom flange of the girder. Additional external vibrating wire gages were attached to one side of each girder (see Figure B-5).

The original idea was to lift both ends of the specimen, but this proved to be unstable. The same load effect could

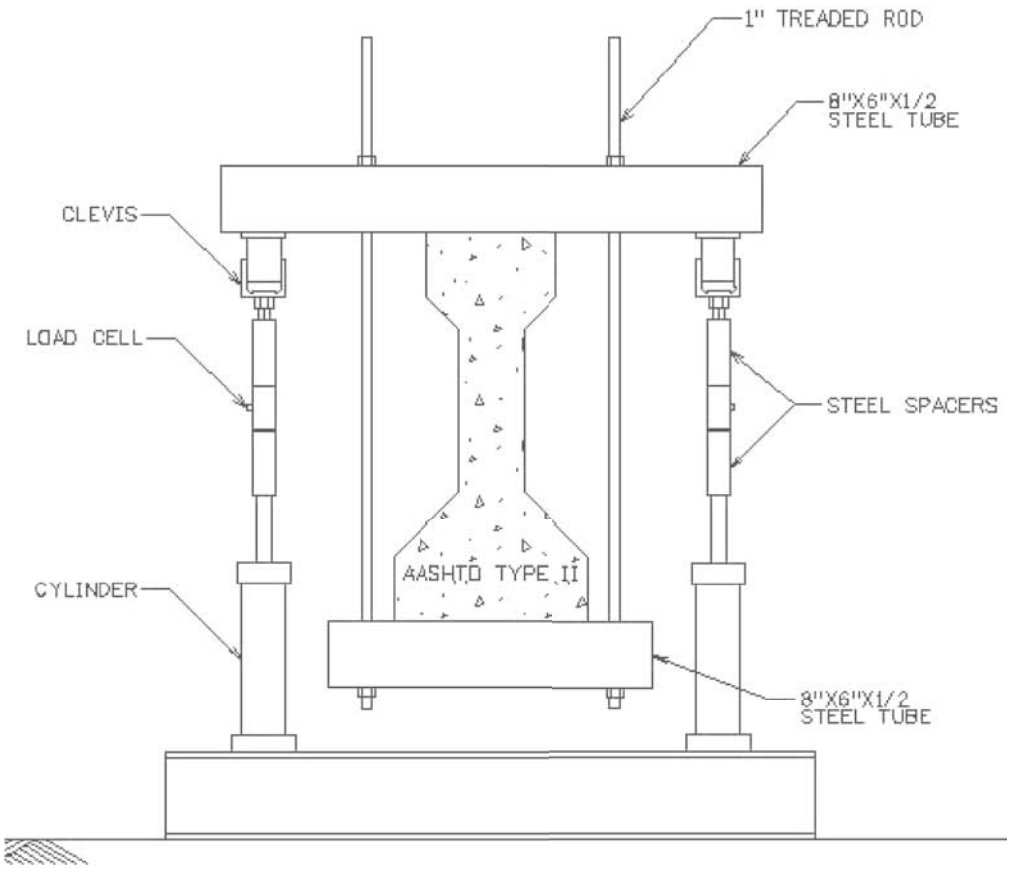

Figure B-3. Schematic of loading yoke.

be obtained by loading the specimen as a cantilever (see Figure B-2). One end was loaded while the other remained stationary. A load cell placed under the stationary end verified that the loading was correct.

The specimen was loaded to simulate a condition where the time dependent and the temperature effects created a positive moment of M_{cr}, and then traffic loads cycled the moment at the connection above or below M_{cr}. As a result, a cyclic loading pattern was developed in which the specimen was loaded between $M_{cr} - M_{LL-}$ and $M_{cr} + M_{LL+}$ where M_{LL-} and M_{LL+} are the positive and negative live-load moments at the connection. From analysis, the maximum negative live-load moment was found to be M_{LL-} = 365 k-ft, and the maximum positive live-load moment was determined to be M_{LL+} = 90 k-ft. All live-load moment values were at the face of the diaphragm. M_{cr} was calculated as 245 k-ft.

Prior to the cyclic loading, the specimen was loaded to develop the negative live load moment and then the positive live-load moment at the joint. This loading was to establish the initial stiffness of connection and was repeated three times. To ensure consistency, the test was done twice. First the east end was loaded and the west end was kept stationary, then the west end was loaded while the east end was kept stationary.

Next, the specimen was loaded to develop M_{cr} at the joint to simulate the assumed time-dependent and temperature effects. This loading was repeated three times for each end by first applying three cycles to one end and then three cycles to the other end.

After the initial loads had been applied, the load was cycled to develop moments between $M_{cr} - M_{LL-}$ and $M_{cr} + M_{LL+}$. This represented an assumed worst-case loading for the connection. The servohydraulic controller applied the load and counted the cycles. The cyclic loading was to last for 1,000,000 cycles or to failure. The intent was to load the east side and keep the west side stationary for 100,000 cycles and then switch sides. However, this was only done for Specimens 5 and 6 because they were the only ones to survive past 100,000 cycles. Load was applied at a rate of 2 hertz as long as the specimen would take the load at that rate. As the connection deteriorated, the cycle length had to be slowed down to ensure the correct loads were applied; however, this only occurred near failure, and the slowest loading rate was 1 hertz.

The cyclic tests were stopped at various intervals, and the specimen was loaded under static loads to $M_{cr} - M_{LL-}$ and $M_{cr} + M_{LL+}$. Even though only one side was being loaded under cyclic load, the static tests were performed twice, once on each side. Static tests were to be performed at 5,000;

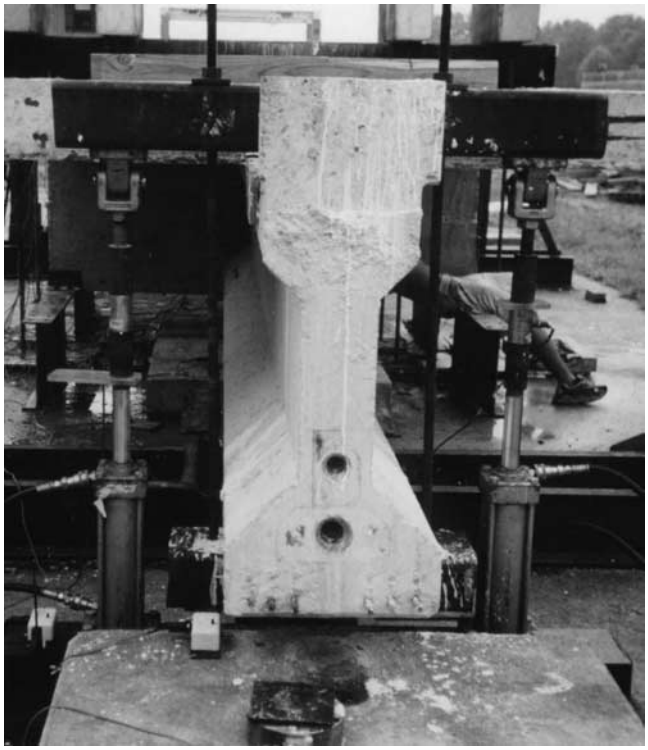

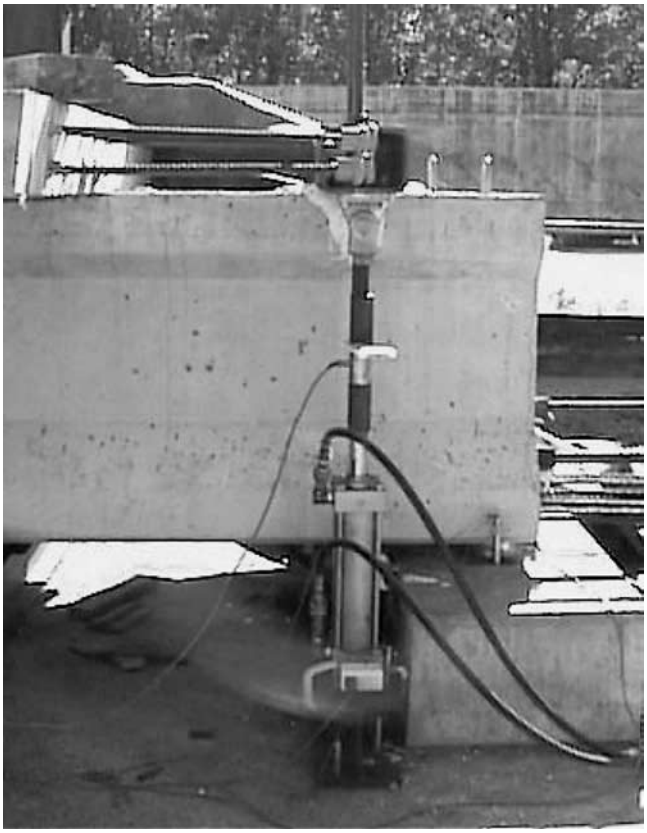

Figure B-4. Loading yoke.

10,000; 15,000; 20,000; 25,000; 30,000; 50,000; 75,000; and 100,000 cycles (if any test had continued beyond 200,000 cycles, static tests would have been conducted every 100,000 cycles).

Failure of the specimen was accompanied by a catastrophic event such as the concrete on the bottom of the diaphragm spalling off or the specimen pulling out of the diaphragm. At this point, the specimen would not hold the required load under static testing.

The stub girders from Specimens 1 and 3 were reused for Specimens 2 and 4. On both Specimens 1 and 3, failure was accompanied by the concrete spalling off the bottom of the diaphragm, exposing the positive moment bar or strand. This bar or strand could then be cut, if needed (in some cases the bar or strand was already broken). The deck was cut on both sides of the diaphragm, and the girders were removed from the diaphragm. The stub girders were turned end-for-end and reused in Specimens 2 and 4.

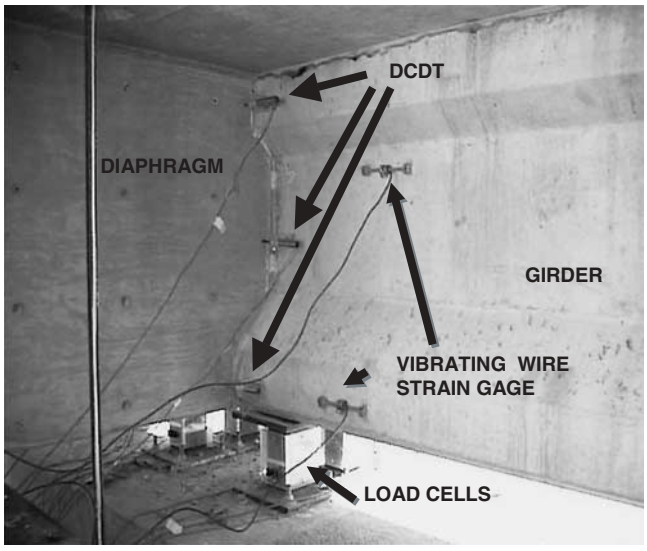

Figure B-5. External instrumentation.

FULL-SIZE SPECIMENS

The full-size specimens were constructed of two 50-ft Type III AASHTO I girders joined with a 10-in. diaphragm. An 8-ft-wide × 7.5-in. thick composite concrete deck slab was cast on top (see Figure B-7). Each end of the girder specimens were cast with both bent-bar and extended strands so that either end could be used for either type of connection.

When the girders were cast, shrinkage specimens were made. One was left with the girder to measure field shrinkage, and the other was used for the standard shrinkage test (AASHTO T160). At 180 days after the girders were fabricated, the field specimen showed a shrinkage of 710 micro-

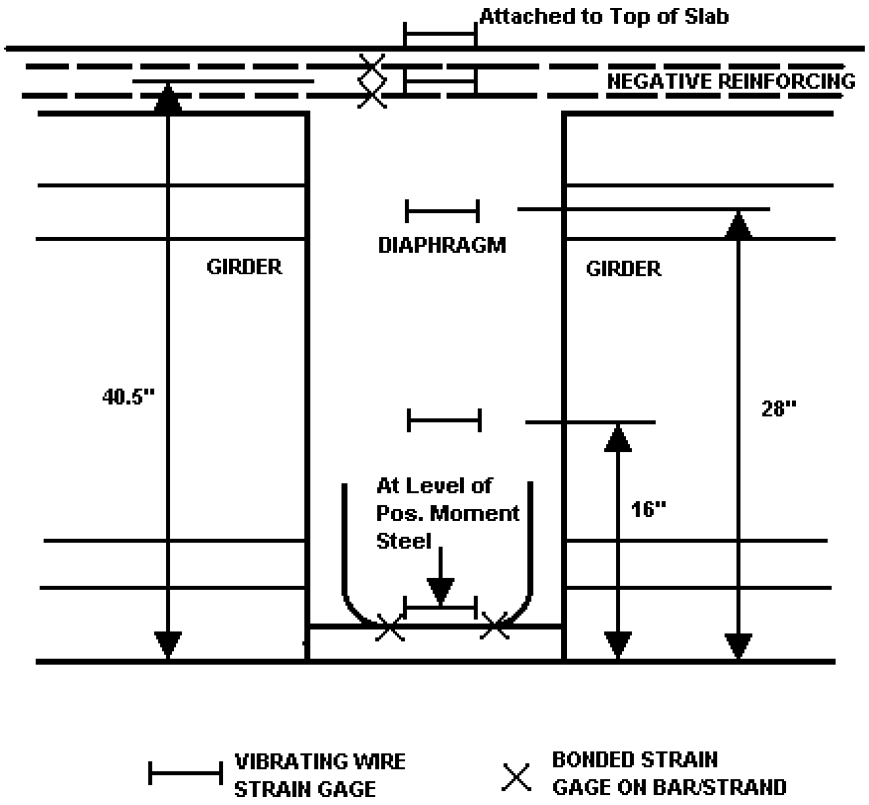

Figure B-6. Placement of instruments in the diaphragm of the stub specimen.

strain and the standard specimen shrank 570 microstrain. Cylinders were cast for creep tests. Two cylinders were used for the standard creep test. At 180 days after the girders were cast, the average creep coefficient (creep strain/elastic strain) was 2.4.

Monitoring Specimen 1

Full-size Specimen 1 used a bent-bar connection with the girders not embedded in the diaphragm. The positive moment connection was designed as a reinforced concrete section using the composite cross section and the strength of the diaphragm concrete. As with the stub specimens, the connection was designed for a capacity of 1.2 M_{cr}. Using the design strengths of the concrete and steel, it was determined that eight No. 5 bars, in two rows of four, were needed to provide a capacity of 1.2 M_{cr} = 500 k-ft (see Figure B-8). The bars had standard hooks. The diaphragm was 10-in. wide.

As noted in Chapter 2, a partial diaphragm was cast for Specimen 1 when the girders were 28 days old. The remainder of the diaphragm and the slab was cast 28 days later. As with the girders, both field and standard shrinkage specimens were made for the slab. At 120 days after the slab was cast, the shrinkage was approximately 560 microstrain for both specimens.

After the slab was cast, the specimen was monitored for approximately 120 days. Girder reactions were monitored by six vibrating wire strain gage–type load cells. These load cells are very stable and do not drift. Three load cells were placed under each girder, two at the end near the diaphragm and one at the far end.

Two vibrating wire strain gages were embedded in each girder at midspan. A vibrating wire strain gage was embedded in the slab at midspan directly above the girders (see Figure B-9). A vibrating wire strain gage was also embedded 6 in. from the end of each girder, 4 in. from the bottom. Vibrating wire strain gages and bonded foil strain gages were placed in the diaphragm, as shown in Figure B-10. Another vibrating wire strain gage was placed 1.5 in. from the bottom of the diaphragm at a distance of 3 in. from the outside edge of the girder bottom flange.

DCLVDTs were installed to measure crack openings. There were four joints, one on each side of the girder on each side of the diaphragm. Three DCLVDTs were placed on each joint at 3 in., 23 in., and 42 in. from the bottom of the girder. The bottom DCLVDTs were placed 1 day after the partial diaphragm was poured by drilling holes in the formwork to allow the DCLVDTs to be targeted on the diaphragm. These DCLVDTs were removed for a few hours when the forms were removed and then reinstalled. The DCLVDT can never be reinstalled to exactly the same reading as before removal, so several data points were taken before and after removal. The difference between these two readings was used to correct future readings. Deflections were monitored by wire potentiometers placed at midspan of the girders. After the

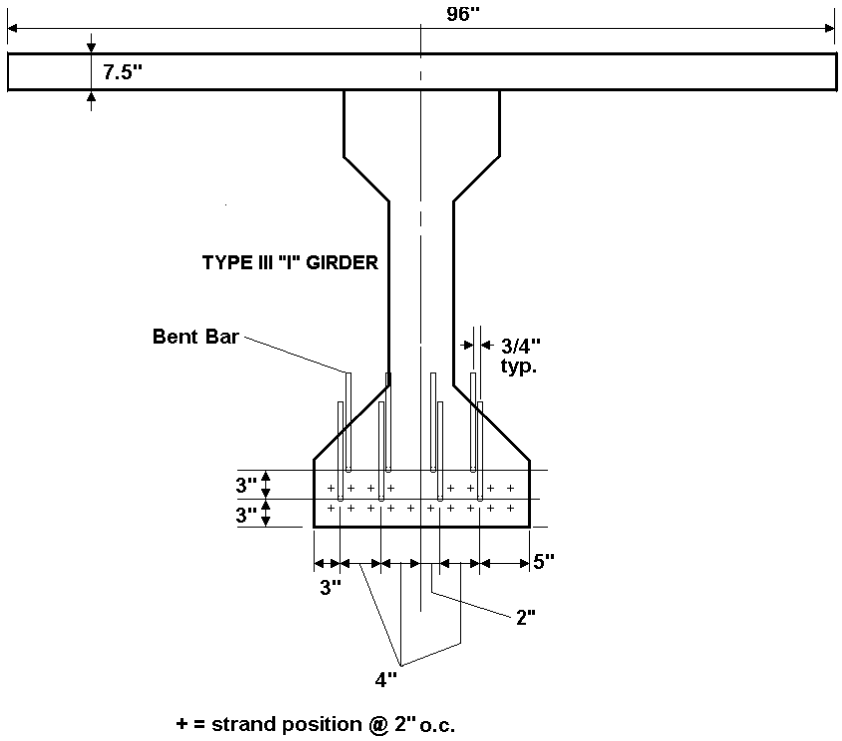

Figure B-7. Full-size composite section.

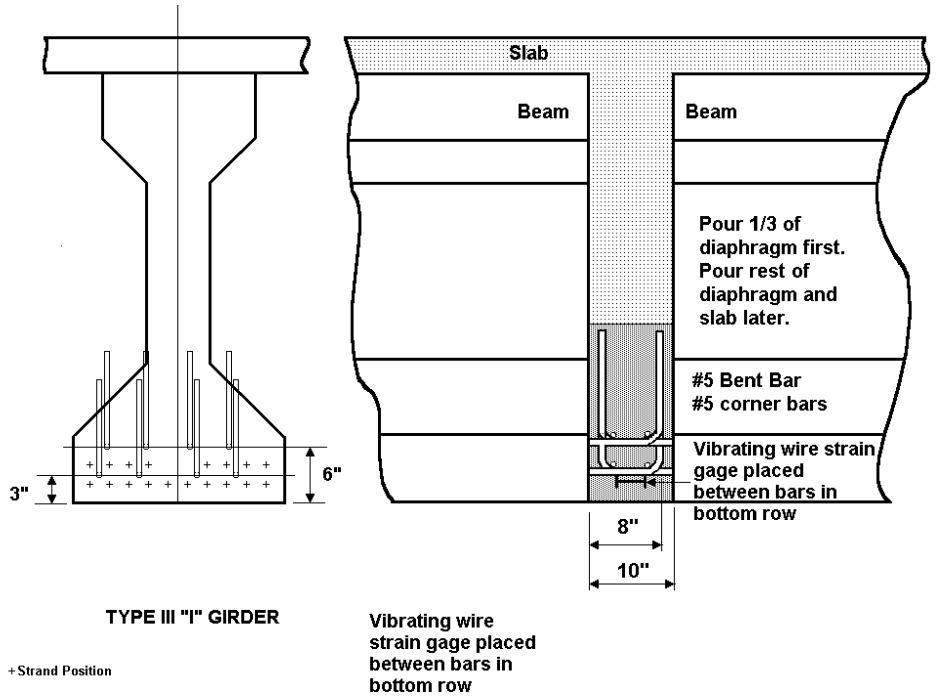

Figure B-8. Full-size bent bar specimen.

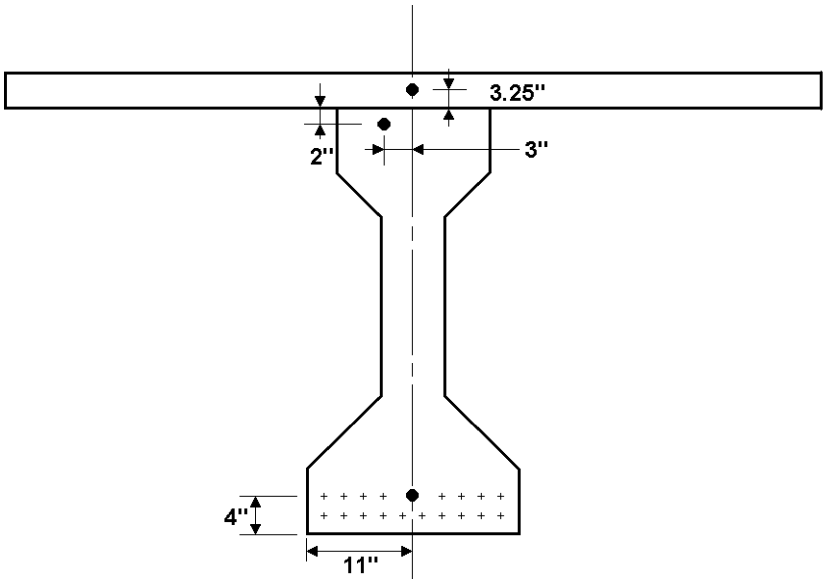

Figure B-9. Location of vibrating wire gages at midspan.

forms were removed, two additional wire potentiometers were attached to the diaphragm.

The instruments were monitored by an electronic data acquisition system, except for the foil gages. The system did not have the ability to monitor the foil gages and the foil gages tend to drift, so any data obtained would have been questionable. The gages were read every hour. The tests were done at an outdoor facility located at Prestress Services in Melbourne, Kentucky. The facility is approximately 16 miles from the University of Cincinnati campus. Because of the distance, data was collected every 3 to 4 days. Although the computers were furnished with battery backups and surge protectors, there were still occasions in which the research team would arrive to collect data and find that one or more of the computers had reset and that the data were lost. This is why some gaps appear in the data in Chapter 2.

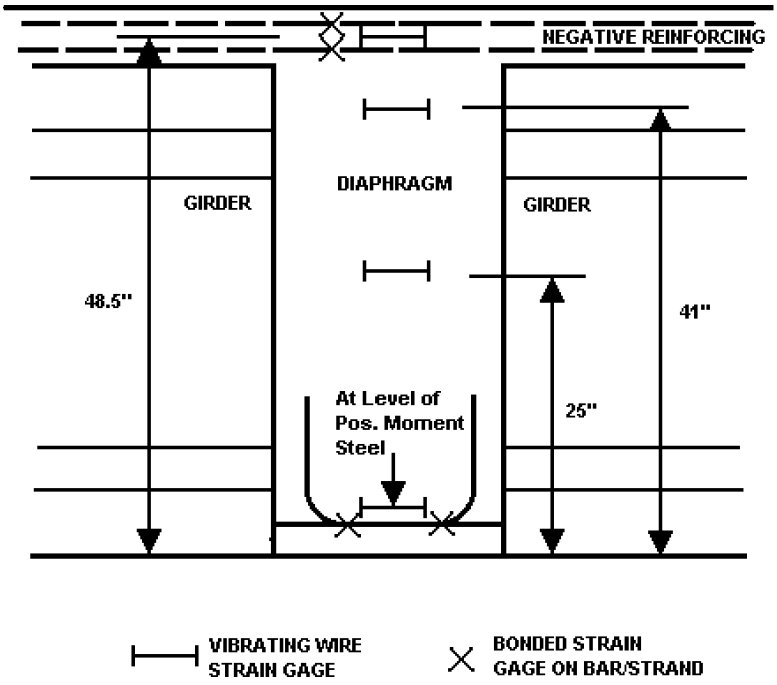

Figure B-10. Location of vibrating wire gages in the full-size specimen diaphragm.

After monitoring the first specimen for 120 days after the slab was cast, the specimen was tested for continuity. These tests are described in a following section.

Full-Size Specimen 2

Full-size Specimen 2 was a bent-strand connection with the girder ends not embedded in the diaphragm. The strand length was kept at 26 in. to match the stub girder specimens. To achieve a capacity of 1.2 M_{cr} = 500 k-ft, 10 strands were needed (see Figure B-11). The number of strands was determined from the same equations used for determining strand capacity for the stub girder specimens.

The second full-size specimen was constructed by cutting the diaphragm out of the first full-size specimen and turning the girders end-for-end. When the deck slab was cast for the first full-size specimen, approximately 12 ft of slab had not been cast at the end of each girder. When the girders were turned end-for-end, there was a gap in the slab over the diaphragm area. When the diaphragm for Specimen 2 was cast, a deck slab was cast in this gap to provide continuity. Reinforcing bars had extended from the end of the existing slab to tie the new slab to the old slab. Full-size Specimen 2 was not monitored, but was tested for continuity when the diaphragm and deck slab were 28 days old. Instrumentation for full-size Specimen 2 was the same as for full-size Specimen 1.

Testing the Full-Size-Specimens for Continuity

One purpose of the full-size specimens was to determine whether cracking at the diaphragm affected continuity. The plan was to apply the cracking moment to connection and then to apply external loads.

In an effort to duplicate the kind of deformation that would occur due to creep and shrinkage of the girders and would crack the diaphragm, a post-tensioning system was used. A post-tensioning bar was placed through the bottom flange of the girder, and a post-tensioning force was applied (see Figures B-12 and B-13). This would cause the girders to camber up—simulating the formation of additional positive moment. Note that the post-tensioning bars only went through the girders and did not go through the diaphragm (i.e., the bar was dead-ended at the end of the girder where the girder was attached to the diaphragm).

To determine the size and placement of the post-tensioning bar, each span was modeled as a propped cantilever (see Figure B-14) with a constant internal moment applied. Note that for each 1 k-ft of internal moment, the moment at the connection increases by 1.5 k-ft. To generate the cracking moment of 417 k-ft, an internal moment of 278 k-ft was required. This could be achieved with a 1.375-in.-diameter Dywidag bar placed as shown in Figure B-12 and tensioned to the maximum allowable force of 160 k.

Four 40-kip-capacity hydraulic cylinders were used to simulate the live load. Two cylinders were placed in each span at 22.5 ft from the face of the diaphragm (see Figures B-15

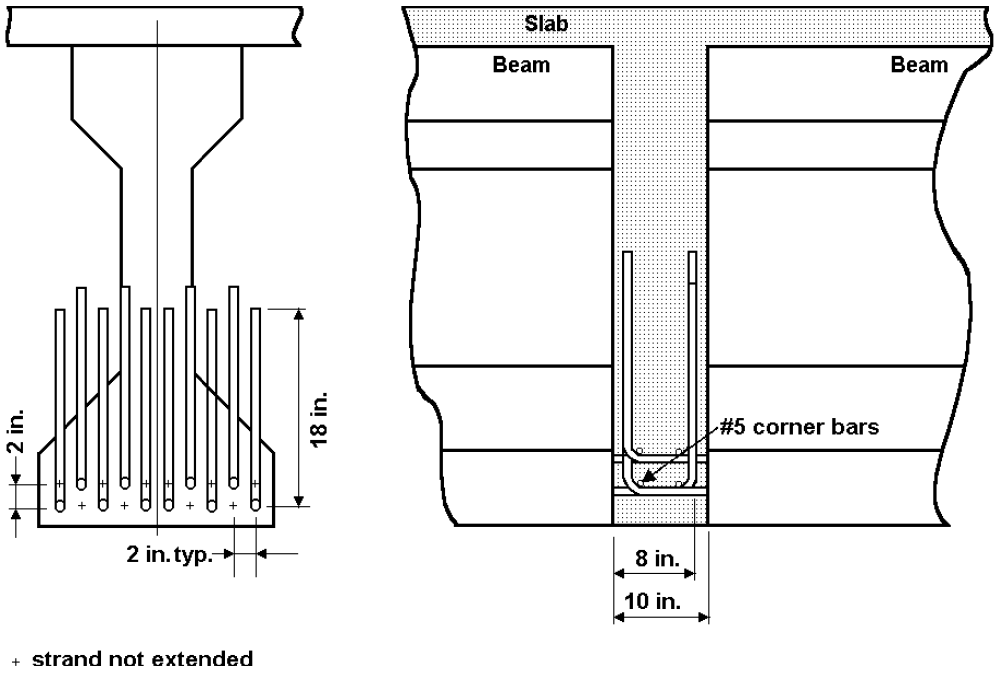

Figure B-11. Full-size bent strand specimen.

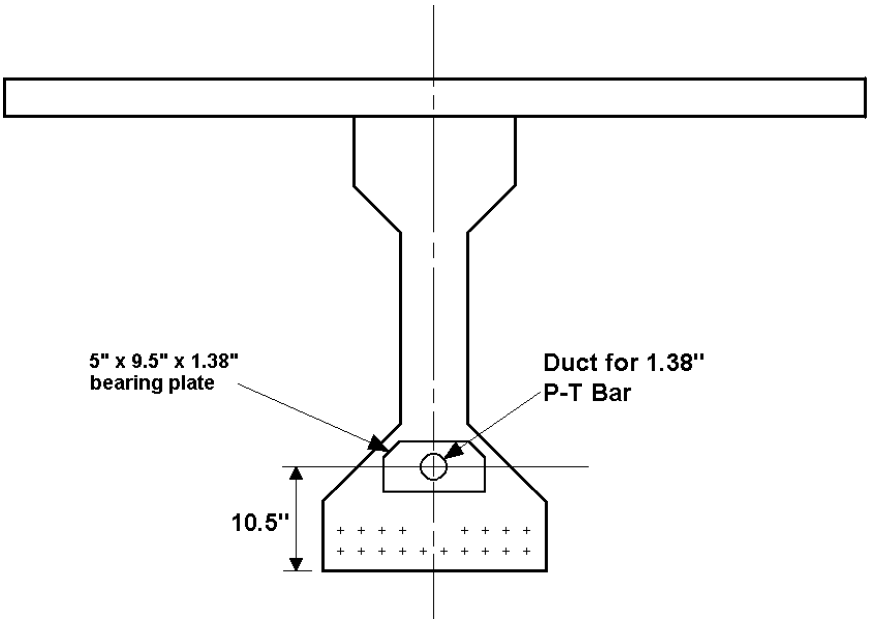

Figure B-12. Positioning of post-tensioning duct in the full-size specimen.

Figure B-13. End of Specimen 1 showing extended bar, extended strand, and post-tensioning bar.

and B-16) because analysis showed that this was the most efficient position for the load. The loading sequence was as follows:

1. Span 1 was loaded,
2. Span 2 was loaded,
3. Span 1 was unloaded, and
4. Span 2 was unloaded.

The upward loads created positive moment, and downward loads created negative moment.

The general steps of testing for both full-size specimens were as follows:

1. The load was applied such that when both spans were loaded, the negative live-load moment (365 k-ft) was developed at the connection.
2. The load was applied such that when both spans were loaded, the positive live-load moment (90 k-ft) was developed at the connection.

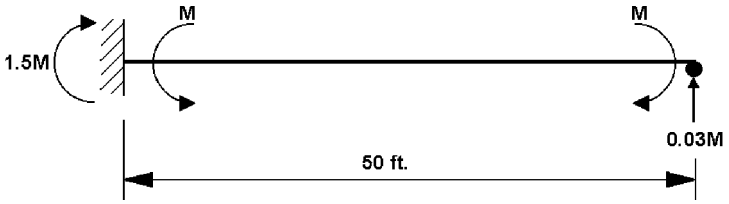

Figure B-14. Model for developing moment from post-tensioning moment.

Figure B-15. Full-size specimen with loading cylinders.

Figure B-16. Overall photograph of the full-size specimen.

3. One-quarter of the post tensioning force (40 kips) was applied to the girders; the girders were post-tensioned one at a time.
4. Steps 1 through 3 were repeated until all the post-tensioning force had been applied.
5. When all the required post-tensioning force has been applied, the specimen was loaded to the negative and positive live-load moments.
6. If the girders still appeared to be continuous, the loading system was used to apply additional positive moment until the specimen failed or the system lifted off the supports.

This sequence was followed for both full-size specimens. For full-size Specimen 2, additional positive moment was generated by jacking up and shimming the ends of the specimen to increase the end reaction (see Chapter 2).

REFERENCES FOR APPENDIX B

1. Salmons, J.R., and McCrate, T.E. *Bond of Untensioned Prestress Strand.* Interim Report 73-5A, Missouri Cooperative Highway Research Program, Missouri State Highway Department, August 1973.
2. Salmons, J.R., and May, G.W. *Strand Reinforcing for End Connections of Pretensioned I-Beam Bridges.* Interim Report 73-5B, Missouri Cooperative Highway Research Program, Missouri State Highway Department, May 1974.
3. Salmons, J.R. *End Connections of Pretensioned I-Beam Bridges.* Final Report 73-5C, Missouri Cooperative Highway Research Program, Missouri State Highway Department, Nov 1974.
4. Salmons, J.R. *Behavior of Untensioned-Bonded Prestressing Strand.* Final Report 77-1, Missouri Cooperative Highway Research Program, Missouri State Highway Department, June 1980.

APPENDIX C

PROPOSED REVISIONS TO THE AASHTO LRFD BRIDGE DESIGN SPECIFICATIONS

INTRODUCTION

A major goal for this research project was to develop proposed revisions to the *AASHTO LRFD Bridge Design Specifications* addressing the design of simple-span precast girders made continuous. Existing Article 5.14.1.2.7 specifically addresses this type of construction. The proposed revisions incorporate many of the existing provisions and provide additional requirements to more fully address design issues and to implement the findings of research.

VERSION OF SPECIFICATIONS USED AS BASIS FOR REVISIONS

The base text for the proposed revisions to Section 5 includes revisions approved at the 2001 and 2002 meetings of the AASHTO Subcommittee on Bridges and Structures and any subsequent minor revisions.

PRESENTATION OF REVISIONS

The proposed revisions are presented in a format as similar to the actual specifications (including the commentary) as possible. Since the existing Article 5.14.1.2.7 is brief and the proposed revisions are much longer, the proposed revisions are presented in their final format without typographical conventions identifying the additions and deletions from the current article.

PROPOSED REVISIONS

SECTION 5—CONTENTS

Replace the current headings for the subarticles of Article 5.14.1.2.7 with the following:

5.14.1.2.7 Bridges Composed of Simple Span Precast Girders Made Continuous

5.14.1.2.7a General
5.14.1.2.7b Restraint Moments
5.14.1.2.7c Material Properties
5.14.1.2.7d Age of Girder when Continuity is Established
5.14.1.2.7e Degree of Continuity at Various Limit States
5.14.1.2.7f Service Limit State
5.14.1.2.7g Strength Limit State
5.14.1.2.7h Negative Moment Connections
5.14.1.2.7i Positive Moment Connections
5.14.1.2.7j Continuity Diaphragms

5.3 NOTATION

Revise or add the following definitions:

A_c = area of core of spirally reinforced compression member measured to the outside diameter of the spiral (IN^2); gross area of concrete deck slab (IN^2) (5.7.4.6) (C5.14.1.2.7c)

A_s = area of nonprestressed tension reinforcement (IN^2); total area of longitudinal deck reinforcement (IN^2) (5.5.4.2.1) (C5.14.1.2.7c)

A_{tr} = area of concrete deck slab with transformed longitudinal deck reinforcement (IN^2) (C5.14.1.2.7c)

$E_{c\ deck}$ = modulus of elasticity of deck concrete (KSI) (C5.14.1.2.7c)

f_{psl} = stress in the strand at the SERVICE limit state. Cracked section shall be assumed. (KSI) (C5.14.1.2.7i)

f_{pul} = stress in the strand at the STRENGTH limit state. (KSI) (C5.14.1.2.7i)

ℓ_{dsh} = total length of extended strand (IN) (C5.14.1.2.7i)

n = modular ratio between deck concrete and reinforcement (C5.14.1.2.7c)

$\varepsilon_{effective}$ = effective concrete shrinkage strain (IN/IN) (C5.14.1.2.7c)

ε_{sh} = concrete shrinkage strain at a given time (IN/IN); unrestrained shrinkage strain for deck concrete (IN/IN) (5.4.2.3.3) (C5.14.1.2.7c)

SPECIFICATIONS

COMMENTARY

Replace the current subarticles of Article 5.14.1.2.7 with the following:

5.14 PROVISIONS FOR STRUCTURE TYPES

5.14.1 Beams and Girders

5.14.1.2 PRECAST BEAMS

5.14.1.2.7 Bridges Composed of Simple-Span Precast Girders Made Continuous

5.14.1.2.7a General

C5.14.1.2.7a

When the requirements of Article 5.14.1.2.7 are satisfied, multi-span bridges composed of simple-span precast girders with continuity diaphragms cast between ends of girders at interior supports may be considered continuous for loads placed on the bridge after the continuity diaphragms are installed and have cured. Continuity diaphragms shall fill the gap between ends of precast girders and shall connect adjacent lines of girders.

The connection between girders at the continuity diaphragm shall be designed for all effects that cause moment at the connection, including restraint moments from time-dependent effects, except as allowed in Article 5.14.1.2.7.

The requirements specified in Article 5.14.1.2.7 supplement the requirements of other sections of these Specifications for fully prestressed concrete components that are not segmentally constructed.

Multi-span bridges composed of precast girders with continuity diaphragms at interior supports that are designed as a series of simple spans are not required to satisfy the requirements of Article 5.14.1.2.7.

This type of bridge is generally constructed with a composite deck slab. However, with proper design and detailing, precast members used without a composite deck may also be made continuous for loads applied after continuity is established. Details of this type of construction are discussed in Miller et al. (2004).

The designer may choose to design a multi-span bridge as a series of simple spans but detail it as continuous with continuity diaphragms to eliminate expansion joints in the deck slab. This approach has been used successfully in several parts of the country.

Where this approach is used, the designer should consider adding reinforcement in the deck adjacent to the interior supports to control cracking that may occur from the continuous action of the structure.

Positive moment connections improve the structural integrity of a bridge, increasing its ability to resist extreme events and unanticipated loadings. These connections also control cracking that may occur in the continuity diaphragm. Therefore, it is recommended that positive moment connections be provided in all bridges detailed as continuous for live load.

If a negative moment connection is provided between precast girders and the continuity diaphragm is installed prior to placement of the deck slab, the girders may be considered to be continuous for the dead load of the deck slab and for any other applied loads placed on the noncomposite girder after continuity is established.

See Article 5.14.1.2.7h.

SPECIFICATIONS

5.14.1.2.7b Restraint Moments

The bridge shall be designed for restraint moments that may develop because of time-dependent or other deformations, except as allowed in Article 5.14.1.2.7d.

COMMENTARY

C5.14.1.2.7b

Deformations that occur after continuity is established from time-dependent effects such as creep, shrinkage, and temperature variation cause restraint moments.

Restraint moments are computed at interior supports of continuous bridges but affect the design moments at all locations on the bridge (Mirmiran et al., 2001 a, b).

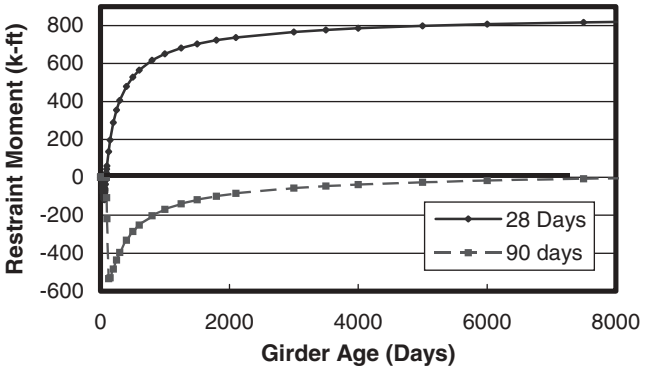

Figure C5.14.1.2.7b-1—Development of Restraint Moments at Interior Support for Two-Span Continuous AASHTO Type III Girder Bridge (Miller et al., 2004)

Figure C-1 shows the predicted development of restraint moments at the interior support for a typical bridge with continuity established at a girder age of 28 and 90 days. The figure demonstrates that the age of the girder when continuity is established has a significant influence on the development of restraint moments.

Positive restraint moments have the most significant effect on bridges of this type because they may cause cracking at the bottom of the continuity diaphragm and they may cause stresses to exceed the stress limits at critical locations in the span. Analysis predicts that positive restraint moments do not develop for all precast girders made continuous.

Analysis also predicts that precast girder bridges with composite deck slabs that are made continuous will develop negative restraint moments because of differential shrinkage between the girders and the deck. The older the girders are at the time the deck is cast, the more severe the predicted negative moment development. However, the consequences of negative restraint moments on these bridges are not generally as significant as for positive restraint moments. Data from various projects (Miller et al., 2004 ; Russell et al., 2003) does not show the effects of differential shrinkage of the decks. Therefore, it is questionable whether negative moments due to differential shrinkage form to the extent predicted by analysis. Since field observations of significant negative moment distress

SPECIFICATIONS

COMMENTARY

have not been reported, negative moments caused by differential shrinkage are often ignored in design.

Even if the negative moment formation in Figure C1 is ignored, the curves still show that the later continuity is formed, the lower the predicted values of positive moment that will form. Therefore, waiting as long as possible after the girders are cast to establish continuity and cast the deck appears to be beneficial.

Several methods have been published for computing restraint moments (Oesterle et al., 1989; Mirmiran et al., 2001 a, b). While these methods may be useful in estimating restraint moments, designers should be aware that these methods may overestimate the restraint moments—both positive and negative. Existing structures do not show the distress that would be expected from the moments computed by some analysis methods.

Restraint moments shall not be included when computing design quantities that are reduced when combined with the restraint moment.

Since estimated restraint moments are highly dependent on actual material properties and project schedules, the computed moment may never develop. Therefore, a critical design moment must not be reduced by a restraint moment in case the restraint moment does not develop.

5.14.1.2.7c Material Properties

C5.14.1.2.7c

Creep and shrinkage properties of the girder concrete and the shrinkage properties of the deck slab concrete shall be determined from either:

- Tests of concrete using the same proportions and materials that will be used in the girders and deck slab. Measurements shall include the time-dependent rate of change of these properties.
- The provisions of Article 5.4.2.3.

The development of restraint moments is highly dependent on the creep and shrinkage properties of the girder and deck concrete. Since these properties can vary widely, measured properties should be used when available to obtain the most accurate analysis. However, these properties are rarely available during design. Therefore, the provisions of Article 5.4.2.3 may be used to estimate these properties.

The restraining effect of reinforcement on concrete shrinkage may be considered.

Because longitudinal reinforcement in the deck slab restrains the shrinkage of the deck concrete, the apparent shrinkage is less than the free shrinkage of the deck concrete. This effect may be estimated using an effective concrete shrinkage strain, $\varepsilon_{effective}$, which may be taken as:

$$\varepsilon_{effective} = \varepsilon_{sh} (A_c/A_{tr}) \qquad \text{(C5.14.1.2.7c-1)}$$

where:

ε_{sh} = unrestrained shrinkage strain for deck concrete (IN/IN)

A_c = gross area of concrete deck slab (IN^2)

A_{tr} = area of concrete deck slab with transformed longitudinal deck reinforcement (IN^2)
= $A_c + A_s(n - 1)$

A_s = total area of longitudinal deck reinforcement (IN^2)

n = modular ratio between deck concrete and reinforcement
= $E_s / E_{c\ deck}$

$E_{c\ deck}$ = modulus of elasticity of deck concrete (KSI)

SPECIFICATIONS

5.14.1.2.7d Age of Girder when Continuity Is Established

The minimum age of the precast girder when continuity is established shall be specified in the contract documents. This age shall be used for calculating restraint moments due to creep and shrinkage. If no age is specified, the girders shall be assumed to be 7 days old at the time continuity is established.

The following simplification may be applied if the owner will permit this simplification to be used and if the contract documents require a minimum girder age of at least 90 days when continuity is established:

- Positive restraint moments caused by girder creep and shrinkage and deck slab shrinkage may be taken to be as 0.
- Computation of restraint moments shall not be required.
- A positive moment connection shall be provided with a factored resistance, fMn, not less than 1.2 Mcr, as discussed in Article 5.14.1.2.7i.

COMMENTARY

Equation C1 is based on simple mechanics (Abdalla et al., 1993). If the amount of longitudinal reinforcement varies along the length of the slab, the average area of longitudinal reinforcement may be used to calculate the transformed area.

C5.14.1.2.7d

Analytical studies show that the age of the precast girder when continuity is established is an important factor in the development of restraint moments (Mirmiran et al., 2001 a, b). These studies suggest that delaying continuity reduces or eliminates time-dependent positive restraint moments (see Figure C5.14.1.2.7b-1). The formation of positive restraint moments is largely the result of creep and shrinkage in the prestressed girder. The creep and shrinkage begin as soon as the prestressing force is applied, which may be less than 1 day after casting. If continuity is delayed, a larger fraction of the creep and shrinkage in the girder will occur prior to establishing continuity, so a lower positive moment will develop in the continuity diaphragm. In addition, allowing the girder to shrink before establishing continuity increases the differential shrinkage between the girder and deck. The differential shrinkage counteracts the formation of positive restraint moments.

According to analysis, establishing continuity when girders are young causes larger positive moments to develop. Therefore, if no minimum girder age for continuity is specified, the earliest reasonable age must be used. Results from surveys of practice (Oesterle et al., 1989; Miller et al., 2004) show a wide variation in girder ages at which continuity is established. An age of 7 days was reported to be a realistic minimum. However, the use of 7 days as the age of girders when continuity is established results in a large positive restraint moment. Therefore, a specified minimum girder age at continuity of at least 28 days is strongly recommended.

If girders are 90 days or older when continuity is established, the provisions of Section 5.4.2.3 predict that approximately 60% of the creep and 70% of the shrinkage in the girders, which could cause positive moments, has already occurred prior to establishing continuity. Since most of the creep and shrinkage in the girder has already occurred before continuity is established, the potential development of time-dependent positive moments is limited. Differential shrinkage between the deck and the girders, to the extent to which it actually occurs (see C5.14.1.2.7b) would also tend to limit positive moment development.

Even if the girders are 90 days old or older when continuity is established, some positive moment may develop at the connection and some cracking may occur. Research (Miller et al., 2004) has shown that if the connection is designed with a capacity of 1.2 M_{cr} , the connection can tolerate this cracking without appreciable loss of continuity.

SPECIFICATIONS

COMMENTARY

This provision provides a simplified approach to design of precast-girder bridges made continuous that eliminates the need to evaluate restraint moments. Some states allow design methods where restraint moments are not evaluated when continuity is established when girders are older than a specified age. These design methods have been used for many years with good success. However, an owner may require the computation of restraint moments for all girder ages.

5.14.1.2.7e Degree of Continuity at Various Limit States

C5.14.1.2.7e

The connection between precast girders at a continuity diaphragm shall be considered fully effective if either of the following are satisfied:

- The calculated stress at the bottom of the continuity diaphragm for the combination of superimposed permanent loads, settlement, creep, shrinkage, 50% live load and temperature gradient, if applicable, is compressive.

- The contract documents require that the age of the precast girders shall be at least 90 days when continuity is established and the positive restraint moments are assumed to be 0 as allowed in Article 5.14.1.2.7d.

A fully effective joint at a continuity diaphragm is a joint that is capable of full moment transfer between spans, resulting in the structure behaving as a continuous structure.

In some cases, especially when continuity is established at an early girder age, continuing upward cambering of the girders due to creep may cause cracking at the bottom of the continuity diaphragm (Mirmiran et al., 2001 a, b). Analysis and tests indicate that such cracking may cause the structure to act as a series of simply supported spans when resisting some portion of the permanent or live loads applied after continuity is established; however, this condition only occurs when the cracking is severe and the positive moment connection is near failure (Miller et al., 2004). Where this occurs, the connections at the continuity diaphragm are partially effective.

If the connection between precast girders at a continuity diaphragm does not satisfy these requirements, the joint shall be considered partially effective.

Theoretically, the portion of the permanent or live loads required to close the cracks would be applied to a simply supported span, neglecting continuity. The remainder of the load would then be applied to the continuous span, assuming full continuity. However, in cases where the portion of the live load required to close the crack is less than 50% of the live load, placing part of the load on simple spans and placing the remainder on the continuous bridge results in only a small change in total stresses at critical sections due to all loads. Tests have shown that the connections can tolerate some positive moment cracking and remain continuous (Miller et. al., 2004). Therefore, if the conditions of the first bullet point are satisfied, it is reasonable to design the member as continuous for the entire load placed on the structure after continuity is established.

The second bullet follows from the requirements of Article 5.14.1.2.7d, where restraint moments may be neglected if continuity is established when the age of the precast girder is at least 90 days. Without positive moment, the potential cracks in the continuity diaphragm would not form and the connection would be fully effective.

Superstructures with fully effective connections at interior supports may be designed as fully continuous structures at all limit states for loads applied after continuity is established.

Superstructures with partially effective connections at interior supports shall be designed as continuous structures for loads applied after continuity is established for strength and extreme event limit states only.

Partially effective construction joints are designed by applying the portion of the permanent and live loads applied after continuity is established required to close the assumed cracks to a simple span (neglecting continuity).

SPECIFICATIONS

COMMENTARY

Only the portion of the loads required to close the assumed cracks are applied. The remainder of the permanent and live loads would then be applied to the continuous span. The load required to close the crack can be taken as the load causing zero tension at the bottom of the continuity diaphragm. Such analysis may be avoided if the contract documents require the age of the girder at continuity to be at least 90 days.

Possible cracking of the deck due to negative moments may be neglected in the analysis, as specified in Article 4.5.2.2.

If the negative moment resistance of the section at an interior support is less than the total amount required, the positive design moments in the adjacent spans shall be increased appropriately for each limit state investigated.

5.14.1.2.7f Service Limit State

C5.14.1.2.7f

Simple-span precast girders made continuous shall be designed to satisfy service limit state stress limits given in Article 5.9.4. For service load combinations that involve traffic loading, tensile stresses in prestressed members shall be investigated using the Service III load combination specified in Table 3.4.1-1.

At the service limit state after losses, when tensile stresses develop at the top of the girders near interior supports, the tensile stress limits specified in Table 5.9.4.1.2-1 for other than segmentally constructed bridges shall apply. The specified compressive strength of the concrete, f'_c, shall be substituted for the compressive strength of concrete at the time of prestressing, f'_{ci}, in the stress limit equations. The Service III load combination shall be used to compute tensile stresses for these locations.

Tensile stresses under service limit state loadings may occur at the top of the girder near interior supports. This region of the girder is not a precompressed tensile zone, so there is not an applicable tensile stress limit in Table 5.9.4.2.2-1. Furthermore, the tensile zone is close to the end of the girder, so adding or debonding pretensioned strands has little effect in reducing the tensile stresses. Therefore, the limits specified for temporary stresses before losses have been used to address this condition, with modification to use the specified concrete strength. This provision provides some relief for the potentially high tensile stresses that may develop at the ends of girders because of negative service load moments.

Alternatively, the top of the precast girders at interior supports may be designed as reinforced concrete members at the strength limit state. In this case, the stress limits for the service limit state shall not apply to this region of the precast girder.

This option allows the top of the girder at the interior support to be designed as a reinforced concrete element using the strength limit state rather than a prestressed concrete element using the service limit state.

A cast-in-place composite deck slab shall not be subject to the tensile stress limits for the service limit state after losses specified in Table 5.9.4.2.2-1.

The deck slab is not a prestressed element. Therefore, the tensile stress limits do not apply. It has been customary to apply the compressive stress limits to the deck slab.

5.14.1.2.7g Strength Limit State

C5.14.1.2.7g

The connections between precast girders and a continuity diaphragm shall be designed for the strength limit state.

The reinforcement in the deck slab shall be proportioned to resist negative design moments at the strength limit state.

The continuity diaphragm is not prestressed concrete, so the stress limits for the service limit state do not apply. Connections to it are therefore designed using provisions for reinforced concrete elements.

5.14.1.2.7h Negative Moment Connections

C5.14.1.2.7h

The reinforcement in a cast-in-place, composite deck slab in a multispan precast girder bridge made continuous

Research at PCA (Kaar et al., 1961) and years of experience show that the reinforcement in a composite

SPECIFICATIONS

shall be proportioned to resist negative design moments at the strength limit state. Requirements of Article 5.7.3 applicable to the strength limit state shall be satisfied.

Longitudinal reinforcement used for the negative moment connection over an interior pier shall be anchored in regions of the slab that are in compression at strength limit states and shall satisfy the requirements of Article 5.11.1.2.3. The termination of this reinforcement shall be staggered. All longitudinal reinforcement in the deck slab may be used for the negative moment connection.

Negative moment connections between precast girders into or across the continuity diaphragm shall satisfy the requirements of Article 5.11.5. These connections shall be permitted when the bridge is designed with a composite deck slab and shall be required when the bridge is designed without a composite deck slab. Additional connection details shall be permitted if the strength and performance of these connections is verified by analysis or testing.

The requirements of Article 5.7.3.4 shall apply to the reinforcement in the deck slab and at negative moment connections at continuity diaphragms.

5.14.1.2.7i Positive Moment Connections

Positive moment connections at continuity diaphragms shall be made with reinforcement developed into both the girder and continuity diaphragm. Two types of connections shall be permitted:

- Mild reinforcement embedded in the precast girders and developed into the continuity diaphragm.
- Pretensioning strands extended beyond the end of the girder and anchored into the continuity diaphragm. These strands shall not be debonded at the end of the girder.

Additional requirements for connections made using each type of reinforcement are given in subsequent articles.

The critical section for the development of positive moment reinforcement into the continuity diaphragm shall be taken at the face of the girder. The critical section for the development of positive moment reinforcement into the precast girder shall consider conditions in the girder as specified in this article for the type of reinforcement used.

Reinforcement for the positive moment connection shall be proportioned to resist the calculated positive moment, except that the positive moment connection shall be proportioned to provide a factored capacity (fM_n) of at least 0.6 M_{cr}.

COMMENTARY

deck slab can be proportioned to resist negative design moments in a continuous bridge.

Limited tests on continuous model and full-size structural components indicate that, unless the reinforcement is anchored in a compressive zone, its effectiveness becomes questionable at the strength limit state (Priestly and Tao, 1993). The termination of the longitudinal deck slab reinforcement is staggered to minimize potential deck cracking by distributing local force effects.

A negative moment connection between precast girders and the continuity diaphragm is not typically provided because the deck slab reinforcement is usually proportioned to resist the negative design moments. However, research (Ma et al., 1998) suggests that mechanical connections between the tops of girders may also be used for negative moment connections, especially when continuity is established prior to placement of the deck slab. If a composite deck slab is not used on the bridge, a negative moment connection between girders is required to obtain continuity. Mechanical reinforcement splices have been successfully used to provide a negative moment connection between box beam bridges that do not have a composite deck slab.

C5.14.1.2.7i

Positive moment connections improve the structural integrity of a bridge, increasing its ability to resist extreme events and unanticipated loadings. Therefore, it is recommended that positive moment connections be provided in all bridges detailed as continuous for live load.

Both embedded bar and extended strand connections have been used successfully to provide positive moment resistance. Test results (Miller et al., 2004) indicate that connections using the two types of reinforcement perform similarly under both static and fatigue loads and both have adequate strength to resist the applied moments.

Analytical studies (Mirmiran et al., 2001 a, b) suggest that a minimum amount of reinforcement, corresponding to a capacity of 0.6 M_{cr}, is needed to develop adequate resistance to positive restraint moments. These same studies show that a positive moment connection with a capacity greater than 1.2 M_{cr} provides only minor improvement in continuity behavior over a connection with

SPECIFICATIONS

The cracking moment, M_{cr}, is computed using Equation 5.7.3.6.2-2 with the gross composite section properties for the girder and the effective width of composite deck slab, if any, and the material properties of the concrete in the continuity diaphragm.

The precast girders must be designed for any positive restraint moments that are used in design. Near the ends of girders, the reduced effect of prestress within the transfer length shall be considered.

Additional positive moment connection details shall be permitted if the strength and performance of these connections are verified by analysis or testing.

The requirements of Article 5.7.3.4 shall apply to the reinforcement at positive moment connections at continuity diaphragms.

- Positive Moment Connection Using Mild Reinforcement

The anchorage of mild reinforcement used for positive moment connections shall satisfy the requirements of Article 5.11 and the additional requirements of this article. Where positive moment reinforcement is added between pretensioned strands, consolidation of concrete and bond of reinforcement shall be considered.

The critical section for the development of positive moment reinforcement into the precast girder shall consider conditions in the girder. The reinforcement shall be developed beyond the inside edge of the bearing area. The reinforcement shall also be detailed so that debonding of strands does not terminate within the development length.

Where multiple bars are used for a positive moment connection, the termination of the reinforcement shall be staggered.

COMMENTARY

a capacity of 1.2 M_{cr}. Therefore, it is recommended that the positive moment capacity of the connection not exceed 1.2 M_{cr}. If the computed positive moment exceeds 1.2 M_{cr}, the section should be modified or steps should be taken to reduce the positive moment.

The cracking moment, M_{cr}, is the moment that causes cracking in the continuity diaphragm. Since the continuity diaphragm is not a prestressed concrete section, the equation for computing the cracking moment for a reinforced section is used. The diaphragm is generally cast with the deck concrete, so the section properties are computed using uniform concrete properties and the deck width is not transformed.

Article 5.7.3.3.2 specifies a minimum capacity for all flexural sections. This is to prevent sudden collapse at the formation of the first crack. However, the positive moment connection that is being discussed here is not intended to resist applied live loads. Even if the positive moment connection were to fail completely, the system may, at worst, become a series of simple spans. Therefore, the minimum reinforcement requirement of Article 5.7.3.3.2 does not apply. Allowing a positive moment connection with lower quantities of reinforcement will relieve congestion in continuity diaphragms.

The positive moment connection is designed to utilize the yield strength of the reinforcement. Therefore, the connection must be detailed to provide full development of the reinforcement. If the reinforcement cannot be detailed for full development, the connection may be designed using a reduced stress in the reinforcement.

Potential cracks are more likely to form in the precast girder at the inside edge of the bearing area and at locations of termination of debonding. Since cracking within the development length reduces the effectiveness of the development, the reinforcement should be detailed to avoid this condition. It is recommended that reinforcement be developed beyond the location where a crack radiating from the inside edge of the bearing may cross the reinforcement.

The termination of the positive moment reinforcement is staggered to reduce the potential for cracking at the ends of the bars.

SPECIFICATIONS

- Positive Moment Connection Using Prestressing Strand

Pretensioning strands that are not debonded at the end of the girder may be extended into the continuity diaphragm as positive moment reinforcement. The extended strands shall be anchored into the diaphragm by bending the strands into a 90° hook or by providing a development length as specified in Article 5.11.4.

COMMENTARY

Strands that are debonded or shielded at the end of a member may not be used as reinforcement for the positive moment connection. There are no requirements for development of the strand into the girder because the strands run continuously through the precast girder.

The following equations for the development length of hooked 0.5 IN diameter prestressing strands were developed by Salmons (1974, 1980), Salmons and May (1974), and Salmons and McCrate (1973). Strands used for a positive moment connection shall project at least 8 IN from the face of the girder before they are bent. The stress in the strands used for design, as a function of the total length of extended strand, shall not exceed:

$$f_{psl} = (\ell_{dsh} - 8)/0.228 \qquad (5.14.1.2.7i\text{-}1)$$

$$f_{pul} = (\ell_{dsh} - 8)/0.163 \qquad (5.14.1.2.7i\text{-}2)$$

where:

ℓ_{dsh} = total length of extended strand (IN)
f_{psl} = stress in the strand at the SERVICE limit state. Cracked section shall be assumed. (KSI)
f_{pul} = stress in the strand at the STRENGTH limit state. (KSI)

Other equations are available to estimate stress in nonprestressed bent strands (Noppakunwijai et al., 2002).

- Details of Positive Moment Connection

Positive moment reinforcement shall be placed in a pattern that is symmetrical, or as nearly symmetrical as possible, about the centerline of the cross section.

Fabrication and erection issues shall be considered in the detailing of positive moment reinforcement in the continuity diaphragm. Reinforcement from opposing girders shall be detailed to mesh during erection without significant conflicts. Reinforcement shall be detailed to enable placement of anchor bars and other reinforcement in the continuity diaphragm.

Tests (Miller et al., 2004) suggest that reinforcement patterns containing significant asymmetry may result in unequal bar stresses that can be detrimental to the performance of the positive moment connection.

With some girder shapes, it may not be possible to install prebent hooked bars without the hook tails interfering with the formwork. In such cases, a straight bar may be embedded and then bent after the girder is fabricated. Such bending is generally accomplished without heating, and the bend must be smooth with a minimum bend diameter conforming to the requirements of Table 5.10.2.3-1. If the engineer allows the reinforcement to be bent after the girder is fabricated, the contract documents shall indicate that field bending is permissible and shall provide requirements for such bending. Since requirements regarding field bending may vary, the preferences of the owner should be considered.

Hairpin bars (a bar with an 180° bend with both legs developed into the precast girder) have been used for positive moment connections to eliminate the need for post-fabrication bending of the reinforcement and to reduce congestion in the continuity diaphragm.

5.14.1.2.7j Continuity Diaphragms

The design of continuity diaphragms at interior supports may be based on the strength of the concrete in the precast girders.

C5.14.1.2.7j

The use of the increased concrete strength is permitted because the continuity diaphragm concrete between girder ends is confined by the girders and by the continuity

SPECIFICATIONS

The continuity diaphragm shall be detailed to provide the required anchorage of reinforcement extending from the precast girders into the continuity diaphragm.

The sequence for concrete placement in the continuity diaphragms and deck slab shall be shown in the contract documents.

Precast girders may be embedded into continuity diaphragms.

If horizontal diaphragm reinforcement is passed through holes in the precast beam or is attached to the precast element using mechanical connectors, the end precast element shall be designed to resist positive moments caused by superimposed dead loads, live loads, creep and shrinkage of the girders, shrinkage of the deck slab, and temperature effects. Design of the end of the girder shall account for the reduced effect of prestress within the transfer length.

Where ends of girders are not directly opposite each other across a continuity diaphragm, the diaphragm must be designed to transfer forces between girders. Continuity diaphragms shall also be designed for situations where an angle change occurs between opposing girders.

COMMENTARY

diaphragm extending beyond the girders. It is recommended that this provision be applied only to conditions where the portion of the continuity diaphragm that is in compression is confined between ends of precast girders.

The width of the continuity diaphragm must be large enough to provide the required embedment for the development of the positive moment reinforcement into the diaphragm. An anchor bar with a diameter equal to or greater than the diameter of the positive moment reinforcement may be placed in the corner of a 90° hook or inside the loop of a 180° hook bar to improve the effectiveness of the anchorage of the reinforcement.

Several construction sequences have been successfully used for the construction of bridges with precast girders made continuous. When determining the construction sequence, the engineer should consider the effect of girder rotations and restraint as the deck slab concrete is being placed.

Test results (Miller et al., 2004) have shown that embedding precast girders 6 IN into continuity diaphragms improves the performance of positive moment connections. The observed stresses in the positive moment reinforcement in the continuity diaphragm were reduced compared with connections without girder embedment.

The connection between precast girders and the continuity diaphragm may be enhanced by passing horizontal reinforcement through holes in the precast beam or attaching the reinforcement to the beam by embedded connectors. Test results (Miller et al., 2004; Salmons, 1974, 1980; Salmons and May, 1974; and Salmons and McCrate, 1973) show that such reinforcement stiffens the connection. The use of such mechanical connections requires that the end of the girder be embedded into the continuity diaphragm. Tests of continuity diaphragms without mechanical connections between the girder and diaphragm show the failure of connection occurs by the beam end pulling out of the diaphragm with all of the damage occurring in the diaphragm. Tests of connections with horizontal bars show that cracks may form in the end of the precast girder outside the continuity diaphragm if the connection is subjected to a significant positive moment. Such cracking in the end region of the girder may not be desirable.

A method such as given in Article 5.6.3 may be used to design a continuity diaphragm for these conditions.

REFERENCES

Add the following references to the list of references currently appearing at the end of Section 5:

Abdalla, O.A., Ramirez, J.A. and, Lee, R.H., "Strand Debonding in Pretensioned Beams: Precast Prestressed Concrete Bridge Girders with Debonded Strands—Continuity Issues", Joint Highway Research Project, Indiana Department of Transportation/Purdue University, FHWA/INDOT/JHRP-92-94, June 1993, 235 p.

Hanson, N. W., "Precast-prestressed Concrete Bridges, 2. Horizontal Shear Connections", Journal of the PCA Research and Development Laboratories, Vol. 2, No. 2, May 1960, pp. 38–58. Also reprinted as PCA Bulletin D35.

Kaar, P.H., Kriz, L.B. and Hognestad, E., "Precast-prestressed Concrete Bridges, 1. Pilot Tests of Continuous Girders", Journal of the PCA Research and Development Laboratories, Vol. 2, No. 2, May 1960, pp. 21–37. Also reprinted as PCA Bulletin D34.

Kaar, P.H., Kriz, L.B. and Hognestad, E., "Precast-prestressed Concrete Bridges, 6. Test of Half-Scale Highway Bridge Continuous over Two Spans", Journal of the PCA Research and Development Laboratories, Vol. 3, No. 3, Sept 1961, pp. 30–70. Also reprinted as PCA Bulletin D51.

Ma, Z., Huo, X., Tadros, M.K. and Baishya, M., "Restraint Moments in Precast/Prestressed Concrete Continuous Bridges," PCI Journal, Vol. 43, No. 6, Nov/Dec 1998, pp. 40–56.

Mattock, A.H and Kaar, P.H., "Precast-prestressed Concrete Bridges, 3. Further Tests of Continuous Girders", Journal of the PCA Research and Development Laboratories, Vol. 2, No. 3, Sept 1960, pp. 51–78. Also reprinted as PCA Bulletin D43.

Mattock, A.H. and Kaar, P.H, "Precast-prestressed Concrete Bridges, 4. Shear Tests of Continuous Girders", Journal of the PCA Research and Development Laboratories, Vol. 3, No. 1, Jan 1961, pp. 19–46. Also reprinted as PCA Bulletin D45.

Mattock, A.H., "Precast-prestressed Concrete Bridges, 5. Creep and Shrinkage Studies", Journal of the PCA Research and Development Laboratories, Vol. 3, No. 2, May 1961, pp. 32–66. Also reprinted as PCA Bulletin D46.

Miller, R.A., Castrodale, R., Mirmiran, A. and Hastak, M., *NCHRP Report 519: Connection of Simple-Span Precast Concrete Girders for Continuity,* National Cooperative Highway Research Program Report, Transportation Research Board, National Research Council, Washington, DC, 2004.

Mirmiran, A., Kulkarni, S., Castrodale, R., Miller, R. and Hastak, M., "Nonlinear Continuity Analysis of Precast, Prestressed Concrete Girders with Cast-in-Place Decks and Diaphragms", PCI Journal, Vol. 46, No. 5, September–October 2001, pp. 60–80.

Mirmiran, A., Kulkarni, S., Miller R.A., Hastak, M., Shahrooz, B. and Castrodale, R.C., "Positive Moment Cracking in Diaphragms of Simple Span Prestressed Girders Made Continuous, SP 204, American Concrete Institute, August 2001.

Noppakunwijai, P., Jongpitakseel, N., Ma, Z. (John), Yehia, S.A., and Tadros, M.K., "Pullout Capacity of Non-Prestressed Bent Strands for Prestressed Concrete Girders," PCI Journal, Vol. 47, No. 4, July–August 2002, pp. 90–103.

Oesterle, R.G., Glikin, J.D. and Larson, S.C., *NCHRP Report 322: Design of Precast-Prestressed Bridge Girders Made Continuous,* Transportation Research Board, National Research Council, Washington, DC, November 1989, 97 p.

Priestley, M.J.N. and Tao, J.R., "Seismic Response of Precast Prestressed Concrete Frames with Partially Debonded Tendons", PCI Journal, Vol. 38, No. 1, January–February 1993, pp. 58–69.

Russell, H., Ozyildirim, C., Tadros, M. and Miller, R., *Compilation and Evaluation of Results from High Performance Concrete Bridge Projects,* Project DTFH61-00-C-00009 Compact Disc, Federal Highway Administration, Washington, DC, 2003.

Salmons, J.R., *Behavior of Untensioned-Bonded Prestressing Strand,* Final Report 77-1, Missouri Cooperative Highway Research Program, Missouri State Highway Department, June 1980, 73 p.

Salmons, J.R., *End Connections of Pretensioned I-Beam Bridges,* Final Report 73-5C, Missouri Cooperative Highway Research Program, Missouri State Highway Department, Nov. 1974, 51 p.

Salmons, J.R. and May, G.W., *Strand Reinforcing for End Connection of Pretensioned I-Beam Bridges,* Interim Report 73-5B, Missouri Cooperative Highway Research Program, Missouri State Highway Department, May 1974, 142 p.

Salmons, J.R. and McCrate, T.E., *Bond of Untensioned Prestress Strand,* Interim Report 73-5A, Missouri Cooperative Highway Research Program, Missouri State Highway Department, Aug. 1973, 108 p.

APPENDIX D
DESIGN EXAMPLES

CONTENTS

INTRODUCTION TO DESIGN EXAMPLES

The following design examples demonstrate the design of precast girder bridges made continuous. The design conforms to the *AASHTO LRFD Bridge Design Specifications* and the proposed design specifications developed as part of this research project (see Appendix C).

LIST OF DESIGN EXAMPLES

All design examples are for bridges with two equal spans. The different girder and bridge types considered in the design examples are listed below, with a brief description of distinguishing features for each:

- **Design Example 1: AASHTO Type III Girder—**This is a detailed design example for a bridge with relatively small conventional prestressed concrete girders and a composite concrete deck. To demonstrate the significant effect of girder age when continuity is established, designs are performed assuming continuity is established at girder ages of 28 days, 60 days, and 90 days.
- **Design Example 2: PCI BT-72 Girder—**This is a brief design example for a bridge with deeper prestressed concrete girders and a composite concrete deck. Only significant differences from Design Example 1 (DE1) are presented. The design assumes that continuity is established at a girder age of at least 90 days. Therefore, according to the simplified approach in the proposed specifications, restraint moments are not computed.
- **Design Example 3: 51-in. Deep Box Girder (Spread)—**This is a brief design example for a bridge with deep box girders and a composite concrete deck. The girders are spaced apart for greater efficiency. Only significant differences from DE1 are presented. The design assumes that continuity is established at a girder age of at least 90 days. Therefore, according to the simplified approach in the proposed specifications, restraint moments are not computed.
- **Design Example 4: AASHTO BIII-48 Box Girder (Adjacent)—**This is a detailed design example for a bridge with box girders placed adjacent to each other. No composite deck is used. An asphalt wearing surface and membrane is placed on the box girders to achieve the desired cross slope. To demonstrate the significant effect of girder age when continuity is established, designs are performed assuming continuity is established at girder ages of 7 days, 28 days, and 90 days.

OTHER FEATURES OF DESIGN EXAMPLES

Other basic features of the design examples are summarized as follows. While the bridges in all design examples have two equal spans, the design is similar with additional spans, unequal spans, or both. For bridges with more than two spans, live load will cause positive moments at the interior supports, which do not develop in these examples.

The precast/prestressed concrete girders are made continuous by the placement of a continuity diaphragm at the interior support, which fills the gap between ends of girders from adjacent spans. For all examples with a composite deck, the continuity diaphragm is placed with the deck concrete. Therefore, the bridge is considered to be continuous for all loads applied after the continuity diaphragm is in place.

Only those details of design that are affected by the use of continuity are presented in the design examples. The focus of the examples is on flexural design, which is most significantly affected by the consideration of restraint moments. Design shears, reactions, and deflections are also affected by continuity, but the procedures for design are not altered.

Continuous bridges may be subject to restraint moments caused by the time-dependent effects of creep and shrinkage. Two approaches have been proposed for considering these effects in design of precast concrete bridges made continuous: the general and simplified. For the complete design examples (DE1 and DE4), both approaches are considered. For the brief design examples, the simplified approach is employed, which does not require the evaluation of restraint moments.

Where required, the restraint moments due to creep and shrinkage are computed using the RESTRAINT spreadsheet developed in this research project. Design moments from sources such as temperature gradient or support settlement may also be considered as required by the owner. Moments from these sources would be combined with the effects considered in the design examples and compared with the same design criteria.

For the detailed design examples—DE1 and DE4—a simple-span design is performed to compare with the two-spans made continuous design.

Both mild reinforcement and pretensioning strands are used to provide the positive moment connection between the precast girder and the continuity diaphragm.

Reinforcement in the composite concrete deck is proportioned to resist negative design moments for design examples

DE1, DE2, and DE3. For the final design example—DE4—negative moments are resisted by a connection between the tops of the box girders.

The design examples represent typical bridges for the cross sections considered. The bridge typical section for DE1 and DE2 are the same. The bridge typical section for DE3 is wider, while the bridge typical section for DE4 is narrower. The girder spacing and span length are fixed for each design example. The examples consider only interior girders.

Each example provides reinforcement details for the connections at the continuity diaphragm. Constructability is considered in developing the details.

Typical design loads are used in the designs. Conventional materials are used for all designs.

DESIGN EXAMPLE 1: AASHTO TYPE III GIRDER

1 INTRODUCTION

This design example demonstrates the design of a typical continuous two-span bridge using the specifications proposed as part of this research. The precast/prestressed concrete girders are made continuous by the placement of a continuity diaphragm at the interior support, which fills the gap between ends of girders from adjacent spans. For this example, the continuity diaphragm is placed with the deck, so the bridge becomes continuous for loads placed on the structure after the deck and continuity diaphragm are in place.

Once made continuous, the bridge is subject to restraint moments that may develop from the time-dependent effects of creep and shrinkage. Restraint moments are caused by restrained deformations in the bridge. Analysis indicates that the restraint moments vary linearly between supports. For this two-span bridge, the restraint moments reach maximum values at the center of the interior pier. Reinforcement is provided at the interior pier to resist moments caused by time-dependent effects and applied loads. Restraint moments also affect the moments within the spans. Therefore, girder designs must be adjusted to account for the additional positive moments caused by restraint.

Variations in temperature also cause restraint moments in continuous bridges. However, this condition will not be considered in this example. If moments from temperature effects were included, girder designs would have to be adjusted in the same way as they are for restraint moments in this example.

Only those details of design that are affected by the use of continuity are presented in this design example. Therefore, the focus of this example will be on flexural design, which is most significantly affected by the consideration of restraint moments. While design shears, reactions, and deflections are also affected when compared with design for simple-span bridges, the procedures for design are not altered; therefore, design for these quantities will not be presented.

In a two-span bridge with simple-span girders made continuous, positive restraint moments may develop at the interior support. Positive moments do not develop from live loads for a two-span bridge, and the effect of support settlement is not considered. The positive design moments at the interior support are resisted by mild reinforcement or pretensioning strands that extend into the continuity diaphragm from the bottom flange of the girder. This positive moment connection is proportioned using strength design methods to resist any restraint moments that may develop or to provide a minimum quantity of reinforcement. The positive moment connection is also provided to enhance the structural integrity of the bridge. Construction details for the positive moment connection are discussed in this example.

Negative moments at the interior pier are caused by dead loads applied to the composite continuous structure, live loads, and restraint moments. However, negative restraint moments are neglected in the design as allowed by the proposed specifications. In this example, negative moments are resisted by mild reinforcement added to the deck slab, which is the most common approach to providing a negative moment connection. The reinforcement in the negative moment connection is proportioned using strength design methods.

1.1 Age of Girders at Continuity

To demonstrate the significant effect of girder age when continuity is established, designs will be performed assuming that continuity is established at the following girder ages:

- 28 days,
- 60 days, and
- 90 days.

If contract documents specify the minimum girder age at continuity, the minimum age is known. If the minimum girder age at continuity is 90 days, the proposed specifications allow the designer to neglect the effect of restraint moments. This is referred to as the "simplified approach." If the minimum girder age at continuity is not specified, the designer must use the "general approach," which considers the effect of restraint moments. See Section 4 for a discussion of the two approaches. Since positive restraint moments have the most significant effect on designs, assuming an early age at continuity will result in higher positive restraint moments. Two early ages for continuity (less than 90 days) are considered in this example to provide information for the designer to make decisions regarding whether to set a minimum girder age at continuity and what that age would be.

1.2 Design Programs Used

Most of the design calculations were performed using a commercially available computer program. This was supplemented by hand and by spreadsheet computations to obtain the quantities needed for this design. Restraint moments were estimated using the Restraint Program. Fatigue design loads were computed using the QConBridge Program, which is available at no cost from the Washington State DOT website (see Subappendix C). Moment-curvature relationships for use

in the nonlinear analysis portion of Restraint were obtained using the Response 2000 Program, which is available at no cost from a website at the University of Toronto (see Subappendix B).

2 DESCRIPTION OF BRIDGE

The bridge is a typical two-span structure with AASHTO Type III girders and a composite deck slab. The span length for this bridge is approaching the maximum achievable for this girder and spacing. The geometry of the bridge is shown in Figures D-2-1 through D-2-3.

The girders are made continuous by a continuity diaphragm that connects the ends of the girders at the interior support. The connection is made when the deck slab is cast. The girders are therefore considered continuous for all loads applied to the composite section.

The distance between centers of bearings (85.00 ft) is used for computing effects of loads placed on the simple-span girders before continuity is established. After continuity, the design span for the continuous girders is assumed to be from the center of bearing at the expansion end of the girder to the center of the interior pier, or 86.00 ft. See Figure D-2-2. The space required between ends of girders to accommodate the positive reinforcement connection should be considered when laying out the bridge (see Section 5.3).

The following design example demonstrates the design of an interior girder. Design of an exterior girder would be similar except for loads. For this bridge, the interior girder design governs.

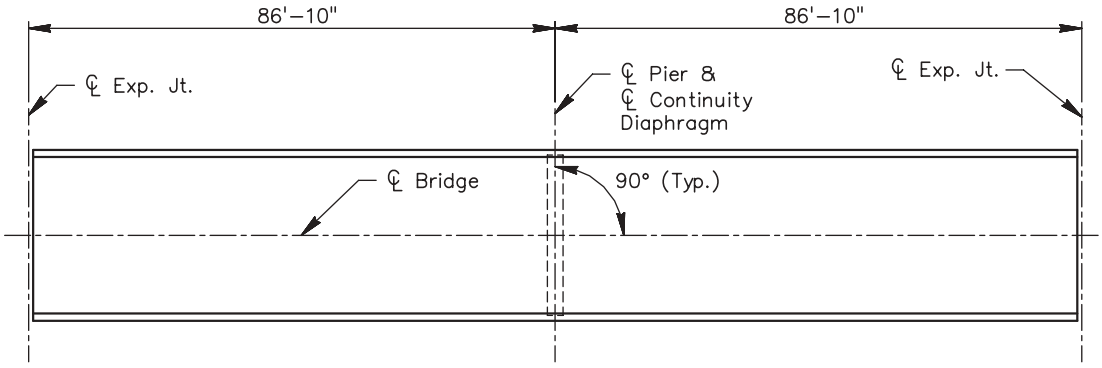

Figure D-2-1. Plan view of bridge.

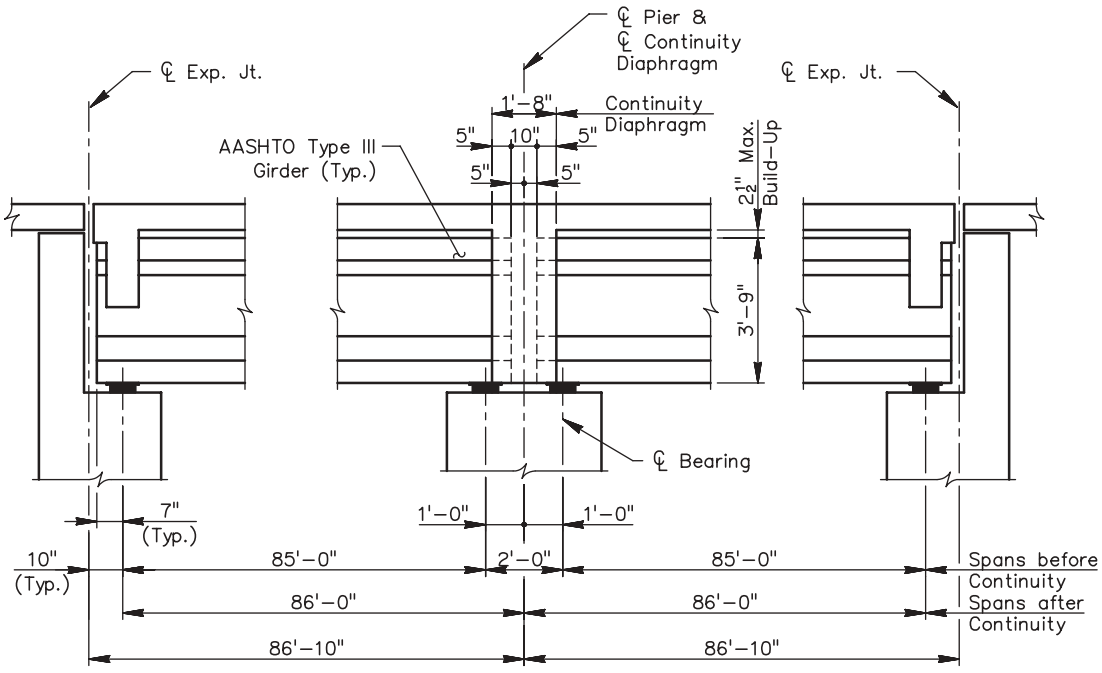

Figure D-2-2. Longitudinal section view of bridge.

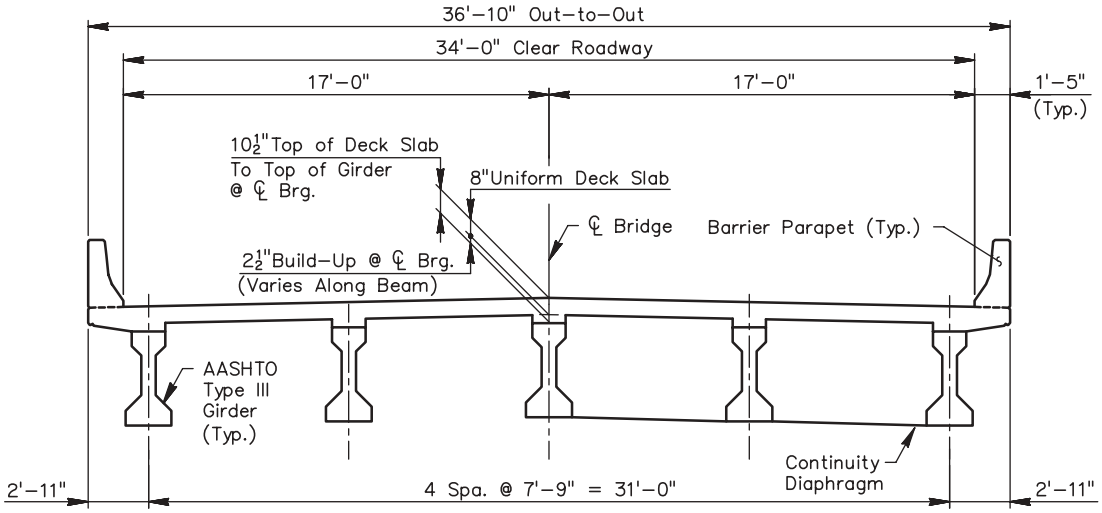

Figure D-2-3. Typical section of bridge.

3 DESIGN ASSUMPTIONS AND INITIAL COMPUTATIONS

3.1 Specifications

AASHTO LRFD Bridge Design Specifications, 2nd Edition with Interims through 2002 is the primary publication to which this appendix will refer (American Assoc. of State Highway and Transportation Officials, 1998). References to articles, equations, and tables in the AASHTO LRFD Specifications will be preceded by the prefix "LRFD" to differentiate them from other references in this design example.

Proposed revisions have been developed as part of this research project (see Subappendix C). References to articles and equations in the proposed specifications will be preceded by the prefix "*proposed*" to differentiate them from references to items in the AASHTO LRFD Specifications.

3.2 Loads

Loads are as follows.

- **Live load:** HL-93 with 33% dynamic allowance (IM) on the design truck. Live-load distribution factors are computed using equations in LRFD Table 4.6.2.2.2b-1 for section type (k) (see LRFD Table 4.6.2.2.1-1):

Distribution of Live Load Moment in Interior Beams		
28 Days	One Design Lane Loaded	0.465 lanes / girder
	Two or More Design Lanes	0.654 lanes / girder
60 & 90 Days	One Design Lane Loaded	0.461 lanes / girder
	Two or More Design Lanes	0.648 lanes / girder

  See Sections 3.3 and 3.6 for values used in computing these factors. The factors are different for the indicated girder ages when continuity is established because the designs require different values for f'_c.
- **Girder self weight:** The unit weight of girder concrete is 0.150 kcf.
  = 0.583 klf
- **Deck slab (structural):** The structural thickness of the deck is 7¾ in. (see Section 3.5).
  = 0.097 ksf on the tributary area for girders
  = 0.751 klf for an interior girder (noncomposite section)
- **Weight of additional deck thickness:** The additional deck slab thickness is ¼ in. (see Section 3.5).
  = 0.003 ksf on the tributary area for girders
  = 0.024 klf for an interior girder (noncomposite section)
- **2½ in. build-up:** The full build-up thickness of 2½ in. is used for dead load computations (see Section 3.5).
  = 0.042 klf for all girders (noncomposite section)
- **Stay-in-place (SIP) deck forms:**
  = 0.016 ksf on formed area between girders
  = 0.103 klf for an interior girder (noncomposite section)
- **Parapet load:**
  = 0.371 klf per parapet, or 0.742 klf for both parapets
  = 0.148 klf for each girder (composite section)
- **Future wearing surface:**
  = 0.025 ksf on roadway width
  = 0.170 klf for each girder (composite section)
- **Dead load:** dead loads placed on the composite girder are distributed equally to all girders in the cross section (LRFD Article 4.6.2.2.1).

3.3 Materials and Material Properties

Material properties used for design are given below.

3.3.1 Girder Concrete

3.3.1.1 Basic Properties. Girder concrete strengths are different for the indicated girder ages at continuity because of design requirements. Initial design was performed using properties shown for a girder age at continuity of 90 days (see Table D-3.3.1.1-1).

3.3.1.2 Time-Dependent Properties. Time-dependent concrete properties (creep and shrinkage) are needed only if restraint moments are being included in the analysis and design. Therefore, the following computations are not required if the simplified approach is being used (see Section 4). Measured values of the ultimate creep coefficient and the ultimate shrinkage strain for the concrete should be used if possible. However, measured creep and shrinkage properties are rarely available; these quantities are usually estimated. For this design example, the equations in LRFD Article 5.4.2.3 are used to estimate creep and shrinkage. See the AASHTO LRFD Specifications for secondary equations and complete definitions of the terms used in the calculations that follow. Restraint moments are very sensitive to variations in creep and shrinkage values, so the best possible estimates should be used. Other methods for estimating creep and shrinkage properties may be used as permitted by LRFD Article 5.4.2.3.1.

3.3.1.2.1 Volume–to–surface area ratio. Both creep and shrinkage equations are dependent upon the volume–to–surface area (*V/S*) ratio. Since the equations are sensitive to this quantity and the analysis for restraint moments is sensitive to creep and shrinkage values, it is important to carefully consider the computation of this ratio.

The *V/S* ratio is generally computed using the equivalent ratio of the cross-sectional area to the perimeter. This quantity can be easily computed for most sections. For the standard AASHTO Type III girder, the area and perimeter can be computed, or they may be obtained from a table of section properties:

TABLE D-3.3.1.1-1 Girder concrete properties

		Girder Age at Continuity		
		28 Days	***60 Days***	***90 Days***
f'_{ci}	(ksi)	7.50	6.00	5.50
f'_c	(ksi)	8.50	7.00	7.00
f_r	(ksi)	0.700	0.635	0.635
E_{ci}	(ksi)	5,520	4,696	4,496
E_c	(ksi)	5,589	5,072	5,072
w_c	(kcf)	0.150	0.150	0.150

Note: E_{ci} and E_c are computed using LRFD Eq. 5.4.2.4-1.
f_r (modulus of rupture) is computed using LRFD Art. 5.4.2.6.

$A = 559.5$ in^2, and

$p = 137.9$ in.

LRFD Article 5.4.2.3.2 suggests that only the surface area exposed to atmospheric drying should be included in the computation of the *V/S* ratio. For the girder, the only surface that is not exposed to drying, for the life of the member, is the top surface of the top flange, which will be in contact with the composite deck slab in the completed structure. However, the girder will be entirely exposed prior to placement of the deck slab concrete. Furthermore, the width of the contact area is relatively small compared with the total girder perimeter. Therefore, the suggestion of LRFD Article 5.4.2.3.2 will be disregarded for this girder. It appears appropriate to neglect the reduction for the contact area between girder and deck in most cases, especially where top flanges are wide and thin. The reduction may be appropriate if the deck will be cast at an early girder age or if the section is stocky, such as a box girder. Please note that for box girders, a fraction of the perimeter of the interior void is included in the perimeter calculation. See DE4 for discussion.

The *V/S* ratio is

$V/S = A/p = 559.5/137.9 = 4.057$ in.

The Commentary (LRFD Article C5.4.2.3.2) indicates that the maximum value of the *V/S* ratio considered in the development of the equations for the creep and shrinkage factors in which *V/S* appears was 6.0 in. This value should be considered a practical upper limit for the ratio when using the equations in the Specifications.

3.3.1.2.2 Ultimate creep coefficient. The creep coefficient may be taken as follows:

$$\psi(t,t_i) = 3.5k_c k_f\left(1.58 - \frac{H}{120}\right)t_i^{-0.118}\frac{(t-t_i)^{0.6}}{10.0+(t-t_i)}0.6. \qquad \text{LRFD Eq. 5.4.2.3.2-1}$$

Significant load is placed on the girder at release. Therefore, t_i, the age of concrete when load is initially applied, is taken to be the age of the girder at release, or typically at 1 day.

To determine the ultimate value for the creep coefficient, ψ_u, where $t = \infty$, the final term in the equation is assumed to approach unity:

$\psi_u = \psi(\infty, 1\text{ day}) = 1.80$ (for continuity at 60 and 90 days)
$= 1.62$ (for continuity at 28 days),

where

k_c = factor for V/S ratio, LRFD Eq. C5.4.2.3.2-1
= 0.781,
k_f = factor for the effect of concrete strength, LRFD Eq. 5.4.2.3.2-2
= 0.691 (using f'_c = 7.00 ksi, for continuity at 60 and 90 days),
= 0.619 (using f'_c = 8.50 ksi, for continuity at 28 days),
H = relative humidity,
= 75% (assumed), and
V/S = 4.057 in. (used to determine k_c).

3.3.1.2.3 Ultimate shrinkage strain. While it is not always known whether the girder will be steam cured during fabrication, the initial strength gain is generally accelerated when compared with "normal" concretes. Therefore, it is reasonable to use the shrinkage equation for steam-cured concrete. The shrinkage strain may therefore be taken as

$$\varepsilon_{sh} = -k_s k_h \left(\frac{t}{55.0 + t}\right) 0.56 \times 10^{-3}. \quad \text{LRFD Eq. 5.4.2.3.3-2}$$

To determine the ultimate shrinkage strain, ε_{shu}, where $t = \infty$, the term in the equation that contains it is assumed to approach unity:

$$\varepsilon_{shu} = \varepsilon_{sh}(\infty) = -395 \times 10^{-6} \text{ in./in.}$$

where

k_s = size factor = 0.760, and LRFD Eq. C5.4.2.3.3-1
k_h = humidity factor = 0.929. LRFD Eq. C5.4.2.3.3-2

3.3.2 Deck and Continuity Diaphragm Concrete

The same concrete properties are used for the deck slab and continuity diaphragm because they are placed at the same time in this example. The subscript *d* is used to indicate properties related to the deck slab or diaphragm concrete.

3.3.2.1 Basic Properties. The same deck slab concrete strength is used for all designs:

f'_{cd} = 4.00 ksi,

f_{rd} = 0.480 ksi, LRFD Art. 5.4.2.6

w_{cd} = 0.150 kcf, and

E_{cd} = 3,834 ksi. LRFD Eq. 5.4.2.4-1

According to *proposed* Article 5.14.1.2.7j, design at the continuity diaphragm will use the concrete strength of the precast girder where noted.

3.3.2.2 Time-Dependent Properties. See Section 3.3.1.2.1 for discussion.

3.3.2.2.1 V/S ratio. As discussed in Section 3.3.1.2.1, determination of the V/S ratio should be carefully considered. The V/S ratio for the composite deck is computed using the equivalent ratio of the cross-sectional area to the perimeter.

For a composite deck slab, the area is computed as the product of the full depth of the deck and the width of the deck extending to the center of the bay between girders or to the exterior edge of the deck. The area of the build-up could also be included in the deck area. However, such a refinement of the computation is not generally justified, since the calculation is not precise. Therefore, the area of the deck for the interior girder being considered will be the product of the girder spacing, S, and the total deck thickness, h_f:

$A = Sh_f = 7.75 \text{ ft} \times 8 \text{ in.} = 7.75(12)(8) = 744 \text{ in.}^2$.

The perimeter of the deck slab used to compute the V/S ratio is subject to some refinement based on the recommendation of LRFD Article 5.4.2.3.2, which indicates that only the surface area exposed to atmospheric drying should be included in the computation of the V/S ratio. Since the area of the deck that is in contact with the girder will never be exposed to drying, it may be eliminated from the computed perimeter. For simplicity and since the top flange of the Type III girder is relatively narrow, this correction will not be taken. It may be appropriate to use the correction for the contact area where the contact area with the girder is wide, such as a bulb-T or box girder. For interior girders, the deck thickness is not considered in computing the perimeter because it is an imaginary boundary not exposed to drying. Therefore, for the interior girder being designed, the perimeter is taken as twice the girder spacing, S:

$p = 2S = 2(7.75)(12) = 186.0$ in.

The V/S ratio is

$V/S = A/p = 744/186 = 4.00$ in.

This calculation demonstrates that, for a uniform thickness deck slab with no deducted surface area, V/S is simply half of the thickness of the deck.

Since stay-in-place deck forms may be used on this bridge, the bottom of the deck slab may not be exposed to drying. This would increase the V/S ratio to 8.00 in., which exceeds the V/S limit used to develop the equations for correction factors, k_c and k_s The increased V/S will reduce the corrections factors, but not significantly. Therefore, the effect of the deck forms is neglected.

3.3.2.2.2 Ultimate creep coefficient. The age of the deck concrete at loading is not as well defined as it is for the girder.

An early age of 14 days is assumed to provide a conservative estimate of deck creep behavior (a larger creep coefficient). An early age at loading is also a reasonable assumption because some load will be transferred to the deck shortly after casting because it restrains the continued downward deflection of the girder under the load of the deck (due to creep):

$$\psi(t, t_i) = 3.5 k_c k_f \left(1.58 - \frac{H}{120}\right) t_i^{-0.118} \frac{(t - t_i)^{0.6}}{10.0 + (t - t_i)} 0.6. \quad \text{LRFD Eq. 5.4.2.3.2-1}$$

As described previously, $t = \infty$ is used to obtain the ultimate value for the creep coefficient, ψ_u:

$\psi_u = \psi\ (\infty, 14 \text{ days}) = 1.70$,

where

k_c = factor for V/S ratio — LRFD Eq. C5.4.2.3.2-1
= 0.775,
k_f = factor for the effect of concrete strength — LRFD Eq. 5.4.2.3.2-2
= 0.897 (using $f'_{cd} = 4.00$ ksi),
H = relative humidity = 75% (assumed), and
V/S = 4.00 in. (used for k_c; this is a simplified value, based on the full 8-in.deck thickness and neglecting any effect of SIP metal forms and the area of contact with the girder).

3.3.2.2.3 Ultimate shrinkage strain. Since deck slab concrete is normally moist cured, the equation for shrinkage for moist-cured concrete is used:

$$\varepsilon_{sh} = -k_s k_h \left(\frac{t}{35.0 + t}\right) 0.51 \times 10^{-3}. \quad \text{LRFD Eq. 5.4.2.3.3-1}$$

To determine the ultimate shrinkage strain, ε_{shu}, where $t = \infty$, the term in the equation that contains t is assumed to approach unity:

$\varepsilon_{shu} = \varepsilon_{sh}\ (\infty) = -353 \times 10^{-6}$ in./in.,

where

k_s = size factor = 0.745, and — LRFD Eq. C5.4.2.3.3-1
k_h = humidity factor = 0.929. — LRFD Eq. C5.4.2.3.3-2

The restraining effect of longitudinal reinforcement in the deck slab on the free shrinkage is not considered in this design example. *Proposed* Article C5.14.1.2.7c states that the effect may be computed by *proposed* Equation C5.14.1.2.7c-1.

3.3.3 Prestressing Strand

The material properties of the prestressing strand are as follows:

0.5-in.- or 0.6-in.-diameter low-relaxation seven-wire strand;

A_{ps} = 0.153 in.^{2} (0.5-in.-diameter strand, for continuity at 60 and 90 days) and
= 0.217 in.^{2} (0.6-in.-diameter strand, for continuity at 28 days);

f_{pu} = 270 ksi;

$f_{py} = 0.90\, f_{pu}$ = 243 ksi;

$f_{pj} = 0.75\, f_{pu}$ = 202.5 ksi; and

E_p = 28,500 ksi.

3.3.3.1 Transfer Length. At the ends of pretensioned girders, the force in the pretensioning strands is transferred from the strands to the girder concrete over the transfer length. The stress in the strands is assumed to vary linearly from zero at the end of the girder to the full effective prestress, f_{pe}, at the transfer length. The transfer length, ℓ_t, may be estimated as

$\ell_t = 60 d_b$, — LRFD Art. 5.11.4.1
= 60(0.5 in.)
= 30 in. (for continuity at 60 and 90 days), and
= 60(0.6 in.) = 36 in. (for continuity at 28 days),

where

d_b = nominal strand diameter.

The location at a transfer length from the end of the girder is a critical stress location at release. Therefore, moments and stresses computed for this location are shown in various tables in this example. These locations are identified in the tables with the heading "Trans" or "Transfer." Values in tables differ for continuity at 28 days and for continuity at 60 and 90 days because the different strand size results in a different transfer length.

3.3.4 Mild Reinforcement

Mild reinforcement is as follows:

f_y = 60 ksi, and

E_s = 29,000 ksi.

3.4 Stress Limits

The following stress limits are used for the design of the girders for the service limit state. For computation of girder

stresses, the sign convention will be compressive stress is positive (+) and tensile stress is negative (–). Signs are not shown for limits in the following, they will be applied in later stress comparisons.

3.4.1 Pretensioned Strands

The stress limits for low relaxation strands are as follows:

Immediately prior to transfer: LRFD Table 5.9.3-1

$f_{pi} = 0.75\, f_{pu} = 202.5$ ksi.

At service limit state after losses: LRFD Table 5.9.3-1

$f_p = 0.80\, f_{py} = 199.4$ ksi.

The stress limits above are not discussed in this example because they do not govern designs.

3.4.2 Concrete

3.4.2.1 Temporary Stresses at Release. See Table D-3.4.2.1-1.

Compression: LRFD Art. 5.9.4.1.1

$f_{cR} = 0.60 f'_{ci}$.

Tension: LRFD Table 5.9.4.1.2-1

$f_{tR1} = 0.0948\sqrt{f'_{ci}} \le 0.2$ ksi, or

$f_{tR2} = 0.24\sqrt{f'_{ci}}$ with reinforcement to resist the tensile force in the concrete.

3.4.2.2 Final Stresses at Service Limit State after Losses. The following stress limits are given for the girder concrete. Compressive stresses may be checked for the deck slab, but never govern, so they are not included here. Tensile stresses in the deck slab at interior supports should not be compared with limits for the service limit state because the deck is not prestressed. Instead, it is designed to satisfy the specified requirements at the strength limit state.

Compression: LRFD Table 5.9.4.2.1-1

$f_{c1} = 0.60\, \phi_w f'_c$, for full-service loads ($\phi_w = 1$ for girders);

$f_{c2} = 0.45 f'_c$, for effective prestress (*PS*) and full dead loads (*DL*); and

$f_{c3} = 0.40 f'_c$, for live load plus one-half of effective *PS* and full *DL*.

Tension: LRFD Table 5.9.4.2.2-1

For the precompressed compression zone, $f_{t1} = 0.19\sqrt{f'_c}$, assuming moderate corrosion conditions. For locations other than the precompressed compression zone, such as at the end of the girder where the top of the girder may go into tension under the effect of the negative live-load moment, the LRFD Specifications give no stress limits. Therefore, the following limits have been proposed, which take the same form as those for temporary tensile stresses at release given in LRFD Table 5.9.4.1.2-1, but with the specified concrete compressive strength, f'_c, rather than the concrete compressive strength at release, f'_{ci}:

$f_{t2} = 0.0948\sqrt{f'_c} \le 0.2$ ksi, or

$f_{t3} = 0.24\sqrt{f'_c}$ with reinforcement to resist the tensile force in the concrete.

Numerical values for the stress limits are given in Table D-3.4.2.2-1.

3.5 Other Design Assumptions

Intermediate diaphragms are not used in the design example. Temporary steel or timber cross frames are generally required during erection to stabilize girders. However, the weight of these temporary components is minor and is neglected in these calculations.

TABLE D-3.4.2.1-1 Temporary stress limits at release

		Girder Age at Continuity		
		28 Days	*60 Days*	*90 Days*
f'_{ci}	(ksi)	7.50	6.00	5.50
f_{cR}	(ksi)	4.500	3.600	3.300
f_{tR1}	(ksi)	–0.200	–0.200	–0.200
f_{tR2}	(ksi)	–0.660	–0.590	–0.560

Note: Values are rounded to two significant digits.

TABLE D-3.4.2.2-1 Final stress limits after losses

		Girder Age at Continuity		
		28 Days	*60 Days*	*90 Days*
f'_c	(ksi)	8.50	7.00	7.00
f_{c1}	(ksi)	5.100	4.200	4.200
f_{c2}	(ksi)	3.830	3.150	3.150
f_{c3}	(ksi)	3.400	2.800	2.800
f_{t1}	(ksi)	–0.550	–0.500	–0.500
f_{t2}	(ksi)	–0.200	–0.200	–0.200
f_{t3}	(ksi)	–0.700	–0.630	–0.630

The top 0.25 in. of the deck is assumed to be a sacrificial wearing surface; the structural deck thickness is taken as 7.75 in. for design purposes. The weight of the remaining 0.25 in. of the deck is included as additional load on the non-composite girder.

For simplicity, the full thickness of the build-up is applied to the full length of the girder for dead-load computations. In most design situations, a value is used that is less than the specified build-up thickness at the center of the bearings because the actual thickness will vary along the length of the girder from the maximum of 2½ in. at the center of bearings.

The build-up is neglected when computing composite section properties that are used to calculate stresses for service limit state design since the build-up will vary along the bridge. However, for computation of section properties and strength calculations related to the reinforcement at the continuity diaphragm, the build-up is included. This is done because the build-up is specified at the center of the bearings, so the full build-up will be provided at the continuity diaphragm location.

Potential deck cracking, if considered in the analysis of this continuous bridge, could increase positive design moments. However, potential deck cracking is neglected as allowed in LRFD Article 4.5.2.2.

3.6 Section Properties

3.6.1 Noncomposite Section (Girder Only)

The section properties for a standard AASHTO Type III girder are as follows (see Figure D-3.6.1-1):

$h = 45.00$ in.,

$A = 559.5$ in.^{2},

$I = 125{,}390$ in.^{4},

$y_b = 20.27$ in.,

$y_t = 24.73$ in.,

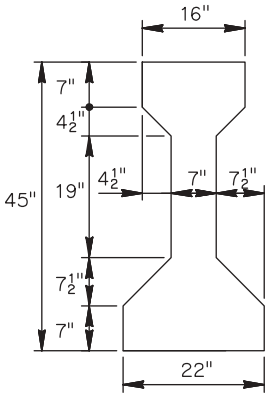

Figure D-3.6.1-1. AASHTO Type III girder.

$S_b = 6{,}185$ in.^{3}, and

$S_t = 5{,}071$ in.^{3}.

3.6.2 Composite Section (Girder with Deck Slab)

3.6.2.1 Effective Deck Width. The effective width for the composite deck at all limit states is determined according to LRFD Article 4.6.2.6.1. The effective deck width for an interior beam is the least of the following:

1. One-quarter of the span length (260 in.);
2. Average spacing of adjacent girders (93 in.) GOVERNS; and
3. Twelve times the average thickness of the slab (93 in.), plus the greater of
   a. The web thickness (7 in.) or
   b. One-half of the width of the top flange of the girder (8 in.).

In the case of this design example, the average spacing of adjacent girders controls, resulting in an effective deck width of 93 in.

3.6.2.2 Transformed Effective Deck Width. The composite deck slab is transformed using the modular ratio, n, for computing stresses at the service limit state. See Table D-3.6.2.3-1.

3.6.2.3 Section Properties. The build-up is neglected when computing section properties because the build-up height varies along the length of the girder, with the minimum height at or near midspan. See Section 3.5. Composite section properties vary for different girder ages at continuity because the girder concrete strength is different.

TABLE D-3.6.2.3-1 Composite section properties

		Girder Age at Continuity		
		28 Days	***60 Days***	***90 Days***
h_c	(in.)	52.75	52.75	52.75
$n = E_{cd}/E_c$		0.686	0.756	0.756
b_{eff}	(in.)	93.00	93.00	93.00
$b_{eff\,tr} = n\,b_{eff}$	(in.)	63.80	70.31	70.31
A_c	(in^2)	1,053.9	1,104.3	1,104.3
I_c	(in^4)	342,585	353,928	353,928
y_{bc}	(in.)	33.69	34.38	34.38
y_{tc}	(in.)	11.31	10.62	10.62
y_{tcd}	(in.)	19.06	18.37	18.37
S_{bc}	(in^3)	10,168	10,293	10,293
S_{tc}	(in^3)	30,294	33,340	33,340
* S_{tcd}	(in^3)	26,203	25,493	25,493
*Note: $S_{tcd} = (I_c / y_{tcd}) / n$, so that $f_{cd} = M / S_{tcd.}$				

3.7 Design Moments

The following sections present the computed design moments for service and strength limit states. All loads applied to the bare girder are thought to act on a simple span. Loads applied after the deck slab and continuity diaphragm are placed are thought to act on a fully continuous structure.

For tables in this section—Tables D-3.7.1-1 through D-3.7.1-3—rows and columns are shaded to indicate quantities that apply only to the design with a girder age at continuity of 28 days. The rows for the transfer length are shaded because the design with continuity at 28 days required 0.6-in.-diameter strands rather than the 0.5-in.-diameter strands used in the other designs. The columns for live load are shaded because the design with continuity at 28 days required a higher concrete strength, f'_c, which altered the live-load distribution factor slightly. See the table in Section 3.2.

Restraint moments are not shown in tables contained in this section. Computations are made later in the example. Moments at the ends of the transfer length are identified in the following tables by "Trans."

TABLE D-3.7.1-1 Service design moments for loads on noncomposite section

	Location from Bearing (ft)	Self Weight (k-ft)	Dead Load on Precast (k-ft)	Dead Load of Deck (k-ft)
Load Factor		*1.0*	*1.0*	*1.0*
Bearing	0.0	0.0	0.0	0.0
Trans. (60 & 90)	1.9	46.4	13.5	59.8
H/2	2.2	53.1	15.4	68.3
Trans. (28 Days)	2.42	58.2	16.9	74.9
0.10 L	8.0	180.3	52.2	232.1
0.20 L	16.7	331.9	96.2	427.2
0.30 L	25.3	440.2	127.5	566.6
0.40 L	33.9	505.2	146.4	650.2
0.50 L	42.5	526.8	152.6	678.0
0.60 L	51.1	505.2	146.4	650.2
0.70 L	59.7	440.2	127.5	566.6
0.80 L	68.4	331.9	96.2	427.2
0.90 L	77.0	180.3	52.2	232.1
Trans. (28 Days)	82.58	58.2	16.9	74.9
H/2	82.8	53.1	15.4	68.3
Trans. (60 & 90)	83.1	46.4	13.5	59.8
Bearing	85.0	0.0	0.0	0.0

3.7.1 Service Limit State

The following tables provide moments for the service limit state. A separate table is given for moments caused by loads applied to the noncomposite section.

3.7.2 Strength Limit State

Table D-3.7.2-1 provides moments for the Strength I limit state.

4 ANALYSIS AND DESIGN OF GIRDERS FOR CONTINUITY

The age at which continuity is established for precast/prestressed concrete girders is a critical factor in the design of bridges of this type. The earlier the age of the girder at continuity, the more girder creep and shrinkage contribute to the development of positive restraint moments. Minimizing the risk of developing positive moments avoids an increase in critical moments and stresses in the girders and avoids cracking of the continuity diaphragm.

It is highly recommended that the minimum age for continuity be specified in the contract documents. Analytical studies and field experience indicate that waiting to establish continuity until the girders are at least 90 days old will significantly reduce or eliminate the development of positive restraint moments.

The proposed specifications recognize the benefit of delaying continuity by allowing two approaches for the design of girders made continuous. The steps in each approach are as follows:

- **General Approach:**
  - The age of girders when continuity is established may or may not be specified;
  - Estimate time-dependent material properties (creep and shrinkage) that will be used to compute restraint moments;
  - Estimate the positive restraint moment, which is strongly dependent on girder age at continuity and time-dependent material properties;
  - Evaluate conditions at the continuity diaphragms to determine whether the connection is fully or partially effective under the effect of the positive restraint moment;
  - If the restraint moment exceeds $1.2M_{cr}$ or if the joint is not fully effective, it is recommended that the design or conditions be altered to improve the situation;
  - Analyze and design the girders for all design loads, including positive restraint moment (positive restraint moment should be neglected when evaluating stresses in regions of negative moment);
  - Design and detail a positive moment connection at continuity diaphragms; and
  - Design and detail reinforcement to resist negative moments from design loads, neglecting both positive and negative restraint moments.
- **Simplified Approach:**
  - Specify the minimum age of the girders when continuity is established in the contract documents; the minimum girder age at continuity must be at least 90 days;

TABLE D-3.7.1-2 Service I design moments for loads on composite section

	Location from Bearing (ft)	Compos. DL (DC) (k-ft)	Compos. DL (DW) (k-ft)	LL+IM (+) [28 Days] (k-ft)	LL+IM (+) [60 & 90] (k-ft)	LL+IM (–) [28 Days] (k-ft)	LL+IM (–) [60 & 90] (k-ft)
Load Factor		*1.0*	*1.0*	*1.0*	*1.0*	*1.0*	*1.0*
Bearing	0.0	0.0	0.0	0.0	0.0	0.0	0.0
Trans. (60 & 90)	1.9	8.9	10.2	N/A	127.6	N/A	–15.1
H/2	2.2	10.2	11.6	147.0	145.7	–17.5	–17.3
Trans. (28 Days)	2.4	11.1	12.8	161.0	N/A	–19.2	N/A
0.10 L	8.0	33.7	38.6	486.8	482.6	–63.9	–63.4
0.20 L	16.7	59.1	67.7	854.9	847.5	–132.5	–131.4
0.30 L	25.3	73.6	84.3	1,073.8	1,064.6	–201.1	–199.4
0.40 L	33.9	77.0	88.2	1,173.7	1,163.6	–269.7	–267.4
0.50 L	42.5	69.4	79.5	1,163.2	1,153.3	–338.3	–335.4
0.60 L	51.1	50.8	58.1	1,044.7	1,035.8	–406.9	–403.4
0.70 L	59.7	21.1	24.2	812.7	805.7	–475.5	–471.4
0.80 L	68.4	–19.5	–22.4	489.5	485.3	–632.2	–626.8
0.90 L	77.0	–71.2	–81.6	187.2	185.6	–738.5	–732.2
Trans. (28 Days)	82.6	–110.8	–126.9	74.8	N/A	–998.1	N/A
H/2	82.8	–112.4	–128.8	71.8	71.2	–1,011.3	–1,002.6
Trans. (60 & 90)	83.1	–114.6	–131.2	N/A	67.5	N/A	–1,019.7
Bearing	85.0	–129.3	–148.1	47.1	46.7	–1,156.1	–1,146.2
CL Pier	86.0	–137.0	–156.9	35.7	35.6	–1221.93	–1,211.6

TABLE D-3.7.1-3 Service III design moments for loads on composite section

	Location from Bearing (ft)	Compos. DL (DC) (k-ft)	Compos. DL (DW) (k-ft)	LL+IM (+) [28 days] Days] (k-ft)	LL+IM (+) [60 & 90] (k-ft)	LL+IM (–) [28 Days] (k-ft)	LL+IM (–) [60 & 90] (k-ft)
Load Factor		*1.0*	*1.0*	*1.0*	*1.0*	*1.0*	*1.0*
Bearing	0.0	0.0	0.0	0.0	0.0	0.0	0.0
Trans. (60 & 90)	1.9	8.9	10.2	N/A	102.1	N/A	–12.1
H/2	2.2	10.2	11.6	117.6	116.6	–14.0	–13.8
Trans. (28 Days)	2.4	11.1	12.8	128.8	N/A	–15.4	N/A
0.10 L	8.0	33.7	38.6	389.4	386.1	–51.2	–50.7
0.20 L	16.7	59.1	67.7	683.9	678.0	–106.0	–105.1
0.30 L	25.3	73.6	84.3	589.0	851.7	–160.9	–159.5
0.40 L	33.9	77.0	88.2	938.9	930.9	–215.8	–213.9
0.50 L	42.5	69.4	79.5	930.6	922.6	–270.6	–268.3
0.60 L	51.1	50.8	58.1	835.8	828.6	–325.5	–322.7
0.70 L	59.7	21.1	24.2	650.2	644.6	–380.4	–377.1
0.80 L	68.4	–19.5	–22.4	391.6	388.2	–505.8	–501.4
0.90 L	77.0	–71.2	–81.6	149.7	148.5	–590.8	–585.8
Trans. (28 Days)	82.6	–110.8	–126.9	59.9	N/A	–798.5	N/A
H/2	82.8	–112.4	–128.8	57.5	57.0	–809.0	–802.1
Trans. (60 & 90)	83.1	–114.6	–131.2	N/A	54.0	N/A	–815.8
Bearing	85.0	–129.3	–148.1	37.7	37.4	–924.8	–917.0
CL Pier	86.0	–137.0	–156.9	28.6	28.6	–975.7	–969.4

TABLE D-3.7.2-1 Strength I design moments

	Location from Bearing (ft)	Self Weight (Max) (k-ft)	Self Weight (Min) (k-ft)	DL on Precast (Max) (k-ft)	DL on Precast (Min) (k-ft)	DL of Deck (Max) (k-ft)	DL of Deck (Min) (k-ft)	Compos. DL (DC) (Max) (k-ft)	Compos. DL (DC) (Min) (k-ft)	Compos. DL (DW) (Max) (k-ft)	Compos. DL (DW) (Min) (k-ft)	LL+IM (+) [28 Days] (k-ft)	LL+IM (+) [60 & 90] (k-ft)	LL+IM (-) [28 Days] (k-ft)	LL+IM (-) [60 & 90] (k-ft)
Load Factor		*1.25*	*0.9*	*1.25*	*0.9*	*1.25*	*0.9*	*1.25*	*0.9*	*1.50*	*0.65*	*1.75*	*1.75*	*1.75*	*1.75*
Bearing	0.0	0.0	0.0	0.0	0.0	0.0	0.0	0.0	0.0	0.0	0.0	0.0	0.0	0.0	0.0
Trans. (60 & 90)	1.9	58.1	41.8	16.8	12.1	74.7	53.8	11.1	8.0	15.3	6.6	N/A	223.3	N/A	–26.5
H/2	2.2	66.4	47.8	19.2	13.8	85.4	61.5	12.7	9.1	17.5	7.6	257.2	255.0	–30.6	–30.4
Trans. (28 Days)	2.4	72.8	52.4	21.1	15.2	93.6	67.4	13.9	10.0	19.1	8.3	281.8	N/A	–33.7	N/A
0.10 L	8.0	225.4	162.3	65.3	47.0	290.1	208.9	42.1	30.3	57.8	25.1	851.9	844.6	–111.9	–110.9
0.20 L	16.7	414.9	298.7	120.2	86.5	534.0	384.5	73.9	53.2	101.6	44.0	1,496.0	1,483.2	–231.9	–229.9
0.30 L	25.3	550.3	396.2	159.4	114.8	708.2	509.9	91.9	66.2	126.4	54.8	1,879.1	1,863.0	–351.9	–348.9
0.40 L	33.9	631.5	454.7	182.9	131.7	812.7	585.2	96.2	69.3	132.3	57.3	2,053.9	2,036.3	–472.0	–467.9
0.50 L	42.5	658.5	474.1	190.8	137.4	847.6	610.2	86.7	62.4	119.2	51.7	2,035.6	2,018.2	–592.0	–586.9
0.60 L	51.1	631.5	454.7	182.9	131.7	812.7	585.2	63.5	45.7	87.2	37.8	1,828.2	1,812.6	–712.0	–705.9
0.70 L	59.7	550.3	396.2	159.4	114.8	708.2	509.9	26.4	19.0	36.3	15.7	1,422.2	1,410.0	–832.0	–824.9
0.80 L	68.4	414.9	298.7	120.2	86.5	534.0	384.5	–24.4	–17.6	–33.6	–14.5	856.6	849.2	–1,106.3	–1,096.9
0.90 L	77.0	225.4	162.3	65.3	47.0	290.1	208.9	–89.0	–64.1	–122.3	–53.0	327.5	324.7	–1,292.4	–1,281.3
Trans. (28 Days)	82.6	72.8	52.4	21.1	15.2	93.6	67.4	–138.5	–99.7	–190.4	–82.5	131.0	N/A	–1,746.7	N/A
H/2	82.8	66.4	47.8	19.2	13.8	85.4	61.5	–140.6	–101.2	–193.2	–83.7	125.7	124.6	–1,769.7	–1,754.6
Trans. (60 & 90)	83.1	58.1	41.8	16.8	12.1	74.7	53.8	–143.2	–103.1	–196.9	–85.3	N/A	118.1	N/A	–1,784.5
Bearing	85.0	0.0	0.0	0.0	0.0	0.0	0.0	–161.6	–116.4	–222.2	–96.3	82.4	81.7	–2,023.1	–2,005.8
CL Pier	86.0	N/A	N/A	N/A	N/A	N/A	N/A	–171.2	–123.3	–235.4	–102.0	62.4	62.3	–2,137.6	–2,120.2

– The connection at continuity diaphragms may be taken to be fully continuous;
– Analyze and design the girders for all design loads (neglect restraint moments);
– Design and detail a positive moment connection at continuity diaphragms; and
– Design reinforcement to resist negative moments from design loads.

This section of the design example is divided into two subsections corresponding to the two approaches listed above. Both approaches are presented for completeness; however, it is anticipated that the simplified approach, with its required specification of a minimum girder age of 90 days when continuity is established, will be the approach used most often by bridge designers. The main benefits of the simplified approach include the simplicity of design and the ability to use standard design aids or software to complete a design. The general approach requires a method for estimating restraint moments. The Restraint software program has been developed for this purpose, and it is used for this example. Few other programs are available, and some may have significant limitations or disadvantages.

The general approach is presented first. In this section, computations and results will be presented for the bridge with continuity established when the age of the girders is 28 and 60 days. Positive restraint moments are estimated, and their effect is considered in the design of the girders. The design for continuity at a girder age of 90 days is also discussed with the initial calculation of restraint moments. The required time-dependent material properties were computed in the previous section of this design example.

The simplified approach will then be presented for the bridge with girders that are at least 90 days old when continuity is established. The calculations only address concrete stresses in the girders at the service limit state. Flexural design at the strength limit state was checked and does not govern the designs, so calculations are not shown.

A summary compares the results of the designs using the general and simplified approaches. The reinforcement for positive and negative continuity connections, which is determined using the same methods for both approaches, is computed in subsequent sections.

4.1 General Approach

The steps in the general approach were summarized in the previous section. The items will be addressed as they appear in the list, except that the determination of the effectiveness of the joint is considered prior to computation of the restraining moment, as discussed in the following section.

4.1.1 Effectiveness of Joint

According to *proposed* Article 5.14.1.2.7e, the connection between spans at the continuity diaphragm may be considered fully effective if one or both of the following conditions are satisfied:

1. The contract documents specify that the girders will be at least 90 days old when continuity is established.
2. The stress in the joint is compressive for the combination of superimposed permanent loads, settlement, creep, shrinkage, 50% live load (with impact), and temperature gradient, if applicable.

The first criterion is addressed by the contract documents. To demonstrate the general approach, girder ages at continuity are selected that do not satisfy the first criterion.

The second criterion is stated in terms of a stress, but since the continuity diaphragm is not prestressed, it can also be expressed in terms of moments. Using moments will simplify manual computations since all of the moments are known, but the stress does not have to be computed. Therefore, the sum of the positive restraint moment, composite dead-load moments (negative), and 50% of the maximum negative live-load (with impact) moment must not be positive since a positive moment would cause tension at the bottom of the diaphragm. (Please note that effects other than permanent and live loads, such as temperature effects, are not considered in this example, but could be included in the calculation.) This summation can also be backsolved to determine the maximum positive restraint moment that can develop before the net moment becomes positive or the stress at the bottom of the diaphragm becomes tensile. This computed maximum positive restraint moment can then be used to facilitate the comparison of different designs and to eliminate the separate computation of joint stress since the restraint moment is computed as part of each design iteration.

The maximum positive restraint moment at the interior support is computed in Table D-4.1.1-1. The live load used in this computation is 50% of the maximum negative service moment. See Table D-3.7.1-2. The Service I load combination is used rather than the Service III load combination because the

TABLE D-4.1.1-1 Calculation of moment limit for joint effectiveness

Composite Dead Load (*DC*)	(k-ft)	–137.0
Composite Dead Load (*DW*)	(k-ft)	–156.9
50 % of Live Load + Impact	(k-ft)	–605.9
TOTAL	**(k-ft)**	**–900.3**
Maximum Positive Restraint Moment for Fully Effective Joint	(k-ft)	900.3

connection at the continuity diaphragm is not prestressed concrete, which is a requirement for use of Service III. When the positive restraint moment computed in the various design iterations remains less than or equal to the computed maximum positive restraint moment (900.3 k-ft), the joint may be considered to be fully effective, and the bridge may be designed using continuity for all loads applied after continuity is established. If the positive restraint moment exceeds the maximum computed moment, the connection must be considered partially effective. In this case, a fraction of the loads applied to the continuous structure are considered to be carried by the girders as simple spans, and the remainder of the loads resisted by the continuous structure.

The computation shown above represents the initial design moments only. Due to various adjustments that are made to the designs throughout the required iterations, the live-load moment changes slightly. Therefore, in the following, the stress at the bottom of the joint is computed as a check.

4.1.2 Initial Design Without Restraint Moments

An initial design of an interior girder was performed without including any restraint moment. The strand pattern required for the specified geometry and loads is shown in Figure D-4.1.2-1.

4.1.3 Compute Restraint Moments

Numerical analysis shows that both positive and negative restraint moments may occur. Positive restraint moments can have a significant effect on the design of precast/prestressed concrete girders made continuous. Negative restraint moments are temporary and are usually ignored in design.

Positive restraint moments are generally larger for two-span bridges than for bridges with a greater number of spans with similar span lengths, given the same span lengths and other conditions. However, two-span bridges have limited positive live-load moments at the interior support, while bridges with a greater number of spans can develop significant positive moments at interior supports from live load. The development of restraint moments with time is computed using the Restraint Program for the initial girder design. The strand pattern shown in Figure D-4.1.2-1 is input to define the creep behavior of the girder. Material properties computed earlier are also used for input, including the ultimate creep coefficient for girder and deck concrete and the ultimate shrinkage strain for the girder concrete. Restraint uses the Dischinger effect to account for the restraining effect of reinforcement on deck shrinkage. A complete listing of input values used in Restraint is presented in Subappendix A.

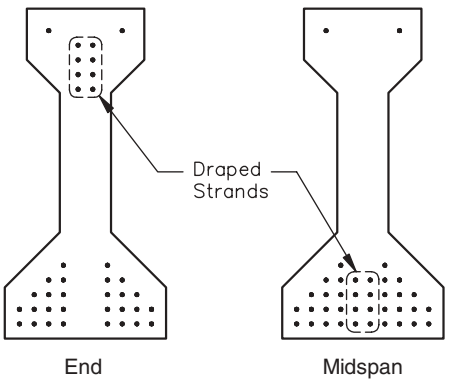

Figure D-4.1.2-1. Strand pattern for initial design.

Results for the restraint moment analysis for continuity established at the girder ages of 28, 60, and 90 days are shown in Figure D-4.1.3-1.

The restraint moment analysis for this initial design indicates that, for continuity established at a girder age of 28 days, a positive restraint moment of about 830 k-ft will eventually develop from the combined effect of creep and shrinkage in the girder and deck concrete. For continuity established at a girder age of 60 days, the analysis indicates that a positive restraint moment of approximately 300 k-ft will eventually develop. The analysis shows that a positive restraint moment of only 3 k-ft develops when continuity is delayed until 90 days after the girder is cast. This very small (negligible) positive moment supports the *proposed* Article 5.14.1.2.7d, which allows positive restraint moments to be neglected in the design of bridges where contract documents require that continuity cannot be established until the girders are at least 90 days old. This initial design will be modified for the positive restraint moments in the next section.

The analysis also indicates that a negative restraint moment develops rapidly after the composite deck slab has been placed. The maximum negative moment varies with the age of the girders at continuity from a negative moment of nearly −120 k-ft for the bridge with continuity at a girder age of 28 days to a moment of about −540 k-ft for continuity established at a girder age of 90 days. However, the negative restraint moments dissipate with time. Because of the temporary nature of this negative restraint moment peak and the lack of observed distress in deck slabs that negative restraint moments would cause, the negative moment is neglected in this example.

4.1.4 Subsequent Design Iterations Including Positive Restraint Moments

Since the analysis indicates that a significant positive restraint moment develops with time for the girders that are 28 and 60 days old when continuity is established, the design of these girders must be revised. The modifications to the initial design are necessary to counteract the increased stresses caused by the additional positive restraint moments, so several iterations are required.

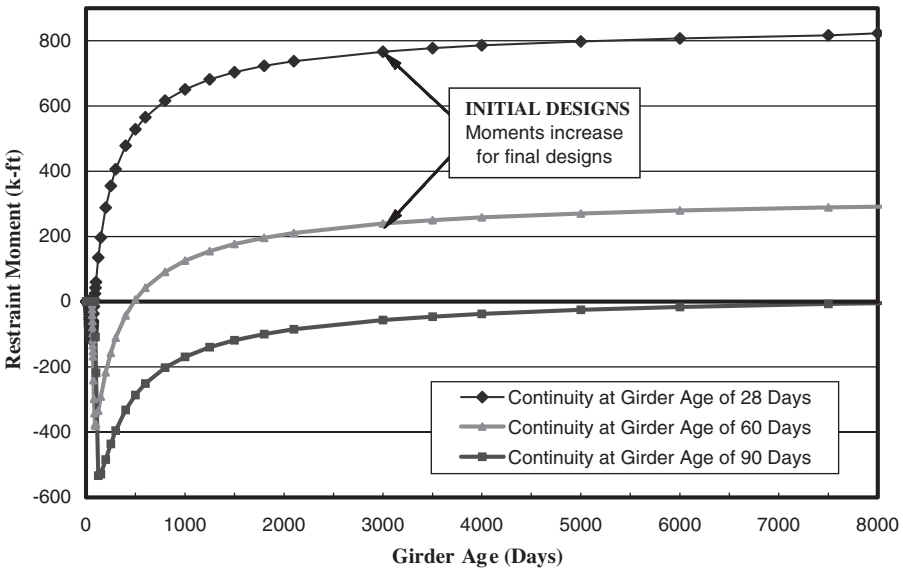

Figure D-4.1.3-1. Development of restraint moment with girder age—initial design.

For each iteration, strands are added or repositioned and other quantities are adjusted as needed to provide a design that includes the positive restraint moment and satisfies the service limit state design criteria. A new positive restraint moment is then computed using the Restraint Program for the new strand pattern, and the process is repeated. The iterations continue until the revised positive restraint moment does not require a change in the strand pattern.

Tables of strand requirements, positive restraint moments, and stresses at the bottom of the continuity diaphragm are given for the designs with girder ages at continuity of 28 and 60 days, respectively. Initial and final concrete strengths were adjusted during the iterations. For the design with continuity at 28 days, the strand size and location of the hold-down are listed because modifications were made during the design iterations.

Strand patterns and other data for the final designs for girder ages of 28 and 60 days at continuity are shown in the summary, Section 4.3. Computations for the strength limit state are not shown since they do not govern. The effect of the positive restraint moment is included when computing the stresses shown.

4.1.4.1 Girder Age at Continuity of 28 Days. In the final iteration, the restraint moment exceeds the maximum positive restraint moment of 900.3 k-ft computed in Table D-4.1.1-1. The computed stress at the bottom of the continuity diaphragm has also gone into tension for the specified loading (see darker-shaded cells), which supports the use of the positive restraint moment limit. Therefore, the joint cannot be considered fully effective for analysis for all loads applied to the continuous structure. If this design were to be carried further, the stresses in the girders must be recomputed by applying a portion of the live load to the continuous structure and applying the remaining live load on the structure as a simple span. This accounts for the change in behavior that would occur if a crack opens in the continuity diaphragm due to the positive restraint moment. This crack must close before continuous behavior can be restored.

The fraction of the live load applied to the simple span would be equal to the ratio of the sum of the net positive service load moment at the center of the interior support caused by dead load and restraint moments to the full live-load moment (including any dynamic allowance) at the center of the interior support. The remainder of the live load would then be applied to the continuous structure. This combination of moments from simple and continuous spans can be accomplished by applying the fractions computed as discussed above to the live-load moment envelopes from the simple and continuous span analyses.

The additional stress that would result from applying some of the live load on the structure acting as a simple span would likely increase stresses to a level where a solution could not be reached using normal design parameters for the bridge in this example. The analysis would also be more complex. Therefore, it is recommended that the design with continuity established at a girder age of 28 days should be abandoned as unreasonable. Further discussion of the design is continued for illustration purposes only.

Table D-4.1.4.1-1 also shows that the positive restraint moments for all iterations following the initial design (see lighter-shaded cells) exceed the quantity $1.2M_{cr} = 550.8$ k-ft as shown in Table D-5.2-1. It is recommended that designs should be reconsidered where the restraint moment exceeds

TABLE D-4.1.4.1-1 Summary of design iterations—continuity at 28 days

Iteration	f'_{ci} (ksi)	f'_c (ksi)	Number of Strands	Strand Diameter (in.)	Positive Restraint Moment (k-ft)	Stress at Bottom of Continuity Diaphragm (ksi)	Hold-down Location from End
1	5.50	7.00	38	0.5	0.0	1.049	0.40 L
2	7.00	8.50	34	0.6	826.8	0.091	0.40 L
3	7.50	9.00	34	0.6	899.6	0.008	0.40 L
4	7.50	8.50	34	0.6	884.3	0.024	0.40 L
5	7.50	8.50	34	0.6	**945.1**	**–0.047**	0.40 L

this limit because analytical studies have shown that increasing the reinforcement beyond levels required to resist a moment of $1.2M_{cr}$ is not effective.

In summary, the design of this girder, with continuity established at a girder age of 28 days, is not recommended because of the positive restraint moment exceeds two significant limits. For further discussion, see the summary and comparison of designs in Section 4.3.

The maximum restraint moment as shown in Table D-4.1.4.1-1 occurs at the center of the interior support and decreases linearly to zero at the center of bearing at the expansion joint. A load factor of 1.0 is applied to the restraint moment for the service limit state, and a load factor of 0.5 is applied to the restraint moment for the strength limit state (LRFD Article 3.4.1). Since the moments vary linearly, a table of restraint moments along the girder is not given.

Tables D-4.1.4.1-2 and D-4.1.4.1-3 present the service limit state stresses for the final design for a girder age at continuity of 28 days. These stresses are compared with stress limits for release and final conditions after losses that are given in Tables D-3.4.2.1-1 and D-3.4.2.2-1.

4.1.4.2 Girder Age at Continuity of 60 Days. The positive restraint moments shown in the table remain below the maximum positive restraint moment of 900.3 k-ft computed in Table D-4.1.1-1 for all iterations. As expected, the stress at the bottom of the diaphragm also remains in compression for all iterations. Therefore, design may be performed considering the joint fully effective for all loads applied to the continuous structure.

Additionally, the moments all remain below the quantity $1.2M_{cr}$ = 550.8 k-ft as shown in Table D-5.2-1. Designs are generally considered unreasonable if this limit is exceeded. Therefore, the design of this girder, with continuity established at a girder age of 60 days, is acceptable. For further discussion, see the summary and comparison of designs in Section 4.3.

The maximum restraint moment as shown in Table D-4.1.4.2-1 occurs at the center of the interior pier and decreases linearly to zero at the center of bearing at the expansion joint. A load factor of 1.0 is applied to the restraint moment for the service limit state and a load factor of 0.5 is applied to the restraint moment for the strength limit state.

TABLE D-4.1.4.1-2 Summary of design stresses for final design at release—continuity at 28 days

	Location from Bearing	(ft)	Brg.	H/2	Trans.	0.10L	0.20L	0.30L	0.40L	0.50L
			0.00	2.20	2.42	8.03	16.65	25.27	33.88	42.50
Prestress at Release	Top Girder	(ksi)	N/A	N/A	1.269	0.819	0.127	–0.564	–0.910	–0.910
	Bottom Girder	(ksi)	N/A	N/A	3.305	3.675	4.241	4.808	5.092	5.092
Self Weight	Top Girder	(ksi)	N/A	N/A	0.172	0.461	0.820	1.076	1.230	1.281
	Bottom Girder	(ksi)	N/A	N/A	–0.141	–0.378	–0.672	–0.882	–1.008	–1.050
Total at Release	Top Girder	(ksi)	N/A	N/A	1.442	1.280	0.947	0.512	0.320	0.371
	Bottom Girder	(ksi)	N/A	N/A	3.164	3.297	3.569	3.926	4.083	4.041

Notes:
1. Critical stresses are shaded.
2. Values for limiting stresses are given in Table D-3.4.2.1-1.
3. Compressive stresses at release are compared with the limit f_{cR} = 4.500 ksi. The maximum compressive stress is 4.083 ksi at 0.40L.
4. Tensile stresses in regions other than the precompressed tensile zone at release are compared with the limiting tensile stress f_{tR1} = –0.200 ksi or f_{tR2} = –0.660 ksi. The latter value requires an area of reinforcement to resist the tensile force. There are no tensile stresses in the concrete at release.
5. In all cases, this design satisfies the specified stress limits at release.

TABLE D-4.1.4.1-3 Summary of design stresses for final design at service limit state after losses—continuity at 28 days

	Location		Brg.	Trans.	H/2	0.10L	0.20L	0.30L	0.40L	0.50L	0.60L	0.70L	0.80L	0.90L	H/2	Trans.	Brg.
		From Brg. (ft)	0.00	2.42	2.20	8.03	16.65	25.27	33.88	42.50	51.12	59.77	68.35	76.97	82.80	82.58	85.00
SERVICE STRESSES (ksi)																	
1	Prestress After Losses	Top Girder	0.221	0.986	0.927	0.636	0.098	-0.440	-0.708	-0.708	-0.708	-0.440	0.098	0.636	0.927	0.986	0.221
		Bottom Girder	0.475	2.568	2.370	2.855	3.296	3.736	3.956	3.956	3.956	3.736	3.296	2.855	2.370	2.568	0.475
2	Self Weight	Top Girder	0.000	0.138	0.126	0.427	0.786	1.042	1.196	1.247	1.196	1.042	0.786	0.427	0.126	0.138	0.000
		Bottom Girder	0.000	-0.113	-0.103	-0.350	-0.644	-0.854	-0.980	-1.022	-0.980	-0.854	-0.644	-0.350	-0.103	-0.113	0.000
3	Non-Comp. DL	Top Girder	0.000	0.217	0.198	0.673	1.239	1.643	1.885	1.966	1.885	1.643	1.239	0.673	0.198	0.217	0.000
		Bottom Girder	0.000	-0.178	-0.162	-0.552	-1.015	-1.346	-1.545	-1.611	-1.545	-1.346	-1.015	-0.552	-0.162	-0.178	0.000
4	Composite DL	Top Girder	0.000	0.009	0.009	0.026	0.050	0.063	0.065	0.059	0.043	0.018	-0.017	-0.061	-0.096	-0.094	-0.110
		Bottom Girder	0.000	-0.028	-0.026	-0.085	-0.150	-0.186	-0.195	-0.176	-0.128	-0.053	0.049	0.180	0.284	0.280	0.327
5	Restraint Mom't (RM) (+)	Top Girder	0.000	0.011	0.010	0.035	0.073	0.111	0.149	0.187	0.225	0.263	0.301	0.339	0.365	0.364	0.375
		Bottom Girder	0.000	-0.032	-0.029	-0.105	-0.218	-0.331	-0.444	-0.557	-0.670	-0.783	-0.896	-1.009	-1.086	-1.083	-1.115
6	LL + IM (+)	Top Girder	0.000	0.064	0.058	0.193	0.339	0.426	0.465	0.461	0.414	0.322	0.194	0.074	0.028	0.030	0.019
		Bottom Girder	0.000	-0.190	-0.173	-0.574	-1.008	-1.266	-1.384	-1.372	-1.232	-0.958	-0.577	-0.221	-0.085	-0.088	-0.056
7	LL + IM (-)	Top Girder	0.000	-0.008	-0.007	-0.025	-0.053	-0.080	-0.107	-0.134	-0.161	-0.188	-0.251	-0.293	-0.401	-0.396	-0.458
		Bottom Girder	0.000	0.023	0.021	0.075	0.156	0.237	0.318	0.399	0.480	0.561	0.746	0.871	1.193	1.177	1.363
TOTAL SERVICE STRESSES (ksi)																	
A = 1-4	Full PS + DL	Top Girder	0.221	1.350	1.260	1.762	2.173	2.308	2.438	2.564	2.416	2.263	2.106	1.675	1.155	1.247	0.111
		Bottom Girder	0.475	2.249	2.079	1.868	1.487	1.350	1.236	1.147	1.303	1.483	1.686	2.133	2.389	2.557	0.802
B = 1-5	Full PS + DL + RM (+)	Top Girder	0.221	1.361	1.270	1.797	2.246	2.419	2.587	**2.751**	2.641	2.526	2.407	2.014	1.520	1.611	0.486
		Bottom Girder	0.475	2.217	2.050	1.763	1.269	1.019	0.792	0.590	0.633	0.700	0.790	1.124	1.303	1.474	-0.313
B + 1.0*6	Service I LL+IM (+) w/RM	Top Girder	0.221	1.425	1.328	1.990	2.585	2.845	3.052	3.212	3.055	2.848	2.601	2.088	1.548	1.641	0.505
		Bottom Girder	0.475	2.027	1.877	1.189	0.261	-0.247	-0.592	-0.782	-0.599	-0.258	0.213	0.903	1.218	1.386	-0.369
A + 1.0*7	Service I LL+IM (-)	Top Girder	0.221	1.342	1.253	1.737	2.120	2.228	2.331	2.430	2.255	2.075	1.855	1.382	0.754	0.851	-0.347
		Bottom Girder	0.475	2.272	2.100	1.943	1.643	1.587	1.554	1.546	1.783	2.044	2.432	3.004	3.582	**3.734**	2.165
B + 0.8*6	Service III LL+IM (+) w/RM	Top Girder	0.221	1.412	1.316	1.951	2.517	2.760	2.959	3.120	2.972	2.784	2.562	2.073	1.542	1.635	0.501
		Bottom Girder	0.475	2.065	1.912	1.304	0.463	0.006	-0.315	**-0.508**	-0.353	-0.066	0.328	0.947	1.235	1.404	-0.358
A + 0.8*7	Service III LL+IM (-)	Top Girder	0.221	1.344	1.254	1.742	2.131	2.244	2.352	2.457	2.287	2.113	1.905	1.441	0.834	0.930	**-0.255**
		Bottom Girder	0.475	2.267	2.096	1.928	1.612	1.540	1.490	1.466	1.687	1.932	2.283	2.830	3.343	3.499	1.892
6 + 0.5*B	Special Service+RM (+)	Top Girder	0.111	0.745	0.693	1.092	1.462	1.636	1.759	1.837	1.735	1.585	1.398	1.081	0.788	0.836	0.262
		Bottom Girder	0.238	0.919	0.852	0.308	-0.374	-0.757	-0.988	-1.077	-0.916	-0.608	-0.182	0.341	0.567	0.649	-0.213
7 + 0.5*A	Special Service (-)	Top Girder	0.111	0.667	0.623	0.856	1.034	1.074	1.112	1.148	1.047	0.944	0.802	0.545	0.177	0.228	-0.403
		Bottom Girder	0.238	1.148	1.061	1.009	0.900	0.912	0.936	0.973	1.132	1.303	1.589	1.938	2.388	**2.456**	1.764

Notes for Table D-4.1.4.1-3:

1. Maximum stresses for each condition are shaded, with the governing stresses also boxed and bolded.
2. Values for limiting stresses are shown in Table D-3.4.2.2-1.
3. Compressive stresses for both dead-load combinations (A and B, see first column) are compared with the limiting compressive stress for full dead load f_{c2} = 3.830 ksi. The maximum stress is 2.751 ksi at 0.50L for the combination with restraint moment (B).
4. Compressive stresses for both Service I LL+IM conditions are compared with the limiting compressive stress for full service conditions f_{c1} = 5.100 ksi. The maximum stress is 3.734 ksi at the interior transfer length location (Trans.).
5. Tensile stresses in the precompressed tensile zone for Service III with RM are compared with the limiting tensile stress f_{t1} = –0.550 ksi. The maximum stress is–0.508 ksi at 0.50L.
6. Tensile stresses in regions other than the precompressed tensile zone for Service III without RM are compared with the limiting tensile stress f_{t2} = –0.200 ksi or f_{t3} = –0.700 ksi. The latter value requires an area of reinforcement to resist the tensile force. The maximum stress is –0.255 ksi at the interior bearing, so reinforcement is required to resist the tensile force in the concrete.
7. Compressive stresses for the special service cases are compared with the limiting compressive stress for that case f_{c3} = 3.400 ksi. The maximum stress is 2.456 ksi at the interior transfer length location.
8. In all cases, this design satisfies the specified stress limits.

TABLE D-4.1.4.2-1 Summary of design iterations—continuity at 60 days

Iteration	f'_{ci} (ksi)	f'_c (ksi)	Number of Strands	Strand Diameter (in.)	Positive Restraint Moment (k-ft)	Stress at Bottom of Continuity Diaphragm (ksi)	Hold-down Location from End
1	5.50	7.00	38	0.5	0	1.049	0.40 L
2	6.00	7.00	40	0.5	299.4	0.700	0.40 L
3	6.00	7.00	42	0.5	372.7	0.615	0.40 L
4	6.00	7.00	42	0.5	455.4	0.542	0.40 L

Since the moments vary linearly, a table of restraint moments along the girder is not given.

Tables D-4.1.4.2-2 and D-4.1.4.2-3 present the service limit state stresses for the final design for a girder age at continuity of 60 days. These stresses are compared with stress limits for release and final conditions after losses that are given in Tables D-3.4.2.1-1 and D-3.4.2.2-1.

4.2 Simplified Approach

If the contract documents require that the girders be at least 90 days old when continuity is established, positive restraint moments may be neglected. This greatly simplifies the design of precast concrete girder bridges made continuous. Once the designer has made this decision, design proceeds assuming that the bridge is fully continuous for loads applied to the continuous structure as specified in *proposed* Article 5.14.1.2.7d; therefore, no iterations are required. The resulting design is the same as the initial design performed without restraint moments in the preceding section.

4.2.1 Girder Age at Continuity of at Least 90 Days

Tables D-4.2.1-1 and D-4.2.1-2 present the service limit state stresses for the final design for a girder age at continuity of at least 90 days. These stresses are compared with stress limits for release and final conditions after losses that are given in Tables D-3.4.2.1-1 and D-3.4.2.2-1.

4.3 Summary of Results for General and Simplified Approaches

Designs for precast/prestressed concrete girders made continuous have been presented in the preceding sections for girder ages at continuity of 28, 60, and 90 days. The designs using earlier girder ages were performed using the general approach, which required the consideration of positive restraint moments. The design for a girder age of 90 days at continuity was performed using the simplified approach, in which positive restraint moments are neglected. The inclusion of positive restraint moments for the designs with earlier

TABLE D-4.1.4.2-2 Summary of design stresses for final design at release—continuity at 60 days

	Location from Bearing	(ft)	Brg.	Trans.	H/2	0.10L	0.20L	0.30L	0.40L	0.50L
			0.00	1.92	2.20	8.03	16.65	25.27	33.88	42.50
Prestress at Release	Top Girder	(ksi)	N/A	0.297	N/A	0.049	–0.301	–0.651	–1.001	–1.001
	Bottom Girder	(ksi)	N/A	3.540	N/A	3.743	4.030	4.317	4.604	4.604
Self Weight	Top Girder	(ksi)	N/A	0.144	N/A	0.461	0.820	1.076	1.230	1.281
	Bottom Girder	(ksi)	N/A	–0.118	N/A	–0.378	–0.672	–0.882	–1.008	–1.050
Total at Release	Top Girder	(ksi)	N/A	0.442	N/A	0.510	0.519	0.425	0.229	0.280
	Bottom Girder	(ksi)	N/A	3.421	N/A	3.365	3.358	3.435	3.595	3.553

Notes:
1. Critical stresses are shaded.
2. Values for limiting stresses are given in Table D-3.4.2.1-1.
3. Compressive stresses at release are compared with the limit f_{cR} = 3.600 ksi. The maximum compressive stress is 3.595 ksi at 0.40L.
4. Tensile stresses in regions other than the precompressed tensile zone at release are compared with the limiting tensile stress f_{tR1} = -0.200 ksi or f_{tR2} = -0.590 ksi. The latter value requires an area of reinforcement to resist the tensile force. There are no tensile stresses in the concrete at release.
5. In all cases, this design satisfies the specified stress limits at release.

TABLE D-4.1.4.2-3 Summary of design stresses for final design at service limit state after losses—continuity at 60 days

	Location		Brg.	Trans.	H/2	0.10L	0.20L	0.30L	0.40L	0.50L	0.60L	0.70L	0.80L	0.90L	H/2	Trans.	Brg.
		From Brg. (ft)	0.00	1.83	2.20	7.97	16.60	25.23	33.87	42.50	51.13	59.77	68.40	77.03	82.80	83.17	85.00
SERVICE STRESSES (ksi)																	
1	Prestress After Losses	Top Girder	0.070	0.238	0.229	0.039	-0.241	-0.522	-0.802	-0.802	-0.802	-0.522	-0.241	0.039	0.229	0.238	0.070
		Bottom Girder	0.651	2.840	2.847	3.003	3.233	3.463	3.692	3.693	3.692	3.463	3.233	3.003	2.847	2.840	0.651
2	Self Weight	Top Girder	0.000	0.110	0.126	0.427	0.786	1.042	1.196	1.247	1.196	1.042	0.786	0.427	0.126	0.110	0.000
		Bottom Girder	0.000	-0.090	-0.103	-0.350	-0.644	-0.854	-0.980	-1.022	-0.980	-0.854	-0.644	-0.350	-0.103	-0.090	0.000
3	Non-Comp. DL	Top Girder	0.000	0.173	0.198	0.673	1.239	1.643	1.885	1.966	1.885	1.643	1.239	0.673	0.198	0.173	0.000
		Bottom Girder	0.000	-0.142	-0.162	-0.552	-1.015	-1.346	-1.545	-1.611	-1.545	-1.346	-1.015	-0.552	-0.162	-0.142	0.000
4	Composite DL	Top Girder	0.000	0.007	0.008	0.026	0.046	0.057	0.059	0.054	0.039	0.016	-0.015	-0.055	-0.087	-0.088	-0.100
		Bottom Girder	0.000	-0.022	-0.025	-0.084	-0.148	-0.184	-0.192	-0.173	-0.127	-0.053	0.049	0.178	0.281	0.286	0.323
5	Restraint Moment (RM) (+)	Top Girder	0.000	0.004	0.004	0.015	0.032	0.049	0.065	0.082	0.099	0.115	0.132	0.148	0.160	0.160	0.164
		Bottom Girder	0.000	-0.012	-0.014	-0.050	-0.104	-0.158	-0.211	-0.265	-0.319	-0.373	-0.427	-0.481	-0.517	-0.519	-0.531
6	LL + IM (+)	Top Girder	0.000	0.046	0.052	0.174	0.305	0.383	0.419	0.415	0.373	0.290	0.175	0.067	0.026	0.024	0.017
		Bottom Girder	0.000	-0.149	-0.170	-0.562	-0.987	-1.240	-1.356	-1.344	-1.207	-0.939	-0.565	-0.216	-0.083	-0.079	-0.054
7	LL + IM (-)	Top Girder	0.000	-0.005	-0.006	-0.023	-0.047	-0.072	-0.096	-0.121	-0.145	-0.170	-0.226	-0.264	-0.361	-0.367	-0.413
		Bottom Girder	0.000	0.018	0.020	0.074	0.153	0.232	0.312	0.391	0.470	0.549	0.730	0.853	1.168	1.188	1.336
TOTAL SERVICE STRESSES (ksi)																	
A = 1-4	Full PS + DL	Top Girder	0.070	0.528	0.561	1.165	1.830	2.220	2.338	2.465	2.318	2.179	1.769	1.084	0.466	0.433	-0.030
		Bottom Girder	0.651	2.586	2.557	2.017	1.426	1.079	0.975	0.887	1.040	1.210	1.623	2.279	2.863	**2.894**	0.974
B = 1-5	Full PS + DL + RM (+)	Top Girder	0.070	0.532	0.565	1.180	1.862	2.269	2.403	2.547	2.417	2.294	1.901	1.232	0.626	0.593	0.134
		Bottom Girder	0.651	2.574	2.543	1.967	1.322	0.921	0.764	0.622	0.721	0.837	1.196	1.798	2.346	2.375	0.443
B + 1.0*6	Service I LL+IM (+) w/RM	Top Girder	0.070	0.578	0.617	1.354	2.167	2.652	2.822	2.962	2.790	2.584	2.076	1.299	0.652	0.617	0.151
		Bottom Girder	0.651	2.425	2.373	1.405	0.335	-0.319	-0.592	-0.722	-0.486	-0.102	0.631	1.582	2.263	2.296	0.389
A + 1.0*7	Service I LL+IM (-)	Top Girder	0.070	0.523	0.555	1.142	1.783	2.148	2.242	2.344	2.173	2.009	1.543	0.820	0.105	0.066	-0.443
		Bottom Girder	0.651	2.604	2.577	2.091	1.579	1.311	1.287	1.278	1.510	1.759	2.353	3.132	4.031	**4.082**	2.310
B + 0.8*6	Service III LL+IM (+) w/RM	Top Girder	0.070	0.569	0.607	1.319	2.106	2.575	2.738	2.879	2.715	2.526	2.041	1.286	0.647	0.612	0.148
		Bottom Girder	0.651	2.455	2.407	1.517	0.532	-0.071	-0.321	**-0.453**	-0.245	0.086	0.744	1.625	2.280	2.312	0.400
A + 0.8*7	Service III LL+IM (-)	Top Girder	0.070	0.524	0.556	1.147	1.792	2.162	2.261	2.368	2.202	2.043	1.588	0.873	0.177	0.139	**-0.360**
		Bottom Girder	0.651	2.600	2.573	2.076	1.548	1.265	1.225	1.200	1.416	1.649	2.207	2.961	3.797	3.844	2.043
6 + 0.5*B	Special (+) Service + RM	Top Girder	0.035	0.312	0.335	0.764	1.236	1.518	1.621	1.689	1.582	1.437	1.126	0.683	0.339	0.321	0.084
		Bottom Girder	0.326	1.138	1.102	0.422	-0.326	-0.780	-0.974	-1.033	-0.847	-0.521	0.033	0.683	1.090	1.109	0.168
7 + 0.5*A	Special (-) Service	Top Girder	0.035	0.259	0.275	0.560	0.868	1.038	1.073	1.112	1.014	0.920	0.659	0.278	-0.128	-0.151	-0.428
		Bottom Girder	0.326	1.311	1.299	1.083	0.866	0.772	0.800	0.835	0.990	1.154	1.542	1.993	2.600	**2.635**	1.823

Notes for Table D-4.1.4.2-3:

1. Maximum stresses for each condition are shaded, with the governing stresses also boxed and bolded.
2. Values for limiting stresses are given in Table D-3.4.2.2-1.
3. Compressive stresses for both dead-load conditions (A and B) are compared with the limiting compressive stress for full dead load f_{c2} = 3.150 ksi. The maximum stress is 2.894 ksi at the interior transfer length location.
4. Compressive stresses for both service I LL+IM conditions are compared with the limiting compressive stress for full-service conditions f_{c1} = 4.200 ksi. The maximum stress is 4.082 ksi at the interior transfer length location.
5. Tensile stresses in the precompressed tensile zone for Service III with RM are compared with the limiting tensile stress f_{t1} = –0.500 ksi. The maximum stress is –0.453 ksi at midspan.
6. Tensile stresses in regions other than the precompressed tensile zone for Service III without RM are compared with the limiting tensile stress f_{t2} = –0.200 ksi or f_{t3} = –0.630 ksi. The latter value requires an area of reinforcement to resist the tensile force. The maximum stress is –0.360 ksi at the interior bearing, so reinforcement is required to resist the tensile force in the concrete.
7. Compressive stresses for the special cases are compared with the limiting compressive stress for that case f_{c3} = 2.800 ksi. The maximum stress is 2.635 ksi at the interior transfer length location.
8. In all cases, this design satisfies the specified stress limits.

TABLE D-4.2.1-1 Summary of design stresses for final design at release—continuity at 90 days

	Location from Bearing	(ft)	Brg. 0.00	Trans. 1.92	H/2 2.20	0.10L 8.03	0.20L 16.65	0.30L 25.27	0.40L 33.88	0.50L 42.50
Prestress at Release	Top Girder	(ksi)	N/A	0.393	N/A	0.142	–0.211	–0.563	–0.916	–0.916
	Bottom Girder	(ksi)	N/A	3.129	N/A	3.334	3.623	3.913	4.202	4.202
Self Weight	Top Girder	(ksi)	N/A	0.144	N/A	0.461	0.820	1.076	1.230	1.281
	Bottom Girder	(ksi)	N/A	–0.118	N/A	–0.378	–0.672	–0.882	–1.008	–1.050
Total at Release	Top Girder	(ksi)	N/A	0.537	N/A	0.603	0.609	0.513	0.314	0.365
	Bottom Girder	(ksi)	N/A	3.011	N/A	2.956	2.951	3.030	3.193	3.151

Notes:
1. Critical stresses are shaded.
2. Values for limiting stresses are given in Table D-3.4.2.1-1.
3. Compressive stresses at release are compared with the limit f_{cR} = 3.300 ksi. The maximum compressive stress is 3.193 ksi at 0.40L.
4. Tensile stresses in regions other than the precompressed tensile zone at release are compared with the limiting tensile stress f_{tR1} = –0.200 ksi or f_{tR2} = –0.560 ksi. The latter value requires an area of reinforcement to resist the tensile force. There are no tensile stresses in the concrete at release.
5. In all cases, this design satisfies the specified stress limits at release.

continuity resulted in larger positive design moments within the spans, which required an increase in the number of prestressing strands and changes to other design parameters.

A simple-span design has also been developed using the same girder dimensions used for the spans made continuous. This design was prepared as a benchmark for comparison to the continuous girder designs. Design moments and stresses for this design as given in Section 4.3.1.

Figure D-4.3-1 summarizes the significant characteristics of the different designs. The figure clearly shows the benefit of continuity for precast/prestressed concrete girders. The girder design for the simple span required over 20% more strands than did the continuous girder design developed using the simplified approach.

The design using girders that were 60 days old when continuity was established required 10.5% more strands than the girders designed using the simplified approach, but less strands than the simple-span design. This design required more effort than the simplified approach, since positive restraint moments were included in the design. However, the design that established continuity when the girders were 28 days old required nearly 27% more strands than did the girder designed using the simplified approach. This design had more strands than did the simple-span design, so designing for continuity provided no structural advantage. The design also required significantly more effort in design because, in addition to including positive restraint moments in the design, the joint was not considered effective in the final design. In fact, as discussed in Section 4.1.4.1, the strand pattern shown will probably not be adequate to satisfy stress limits when the joint is considered partially effective. The positive restraint moments for this design also exceeded the $1.2M_{cr}$ limit, as discussed in Section 4.1.4.1. Based on the significant disadvantages mentioned, this design is not considered to be a viable design. It is recommended to abandon the design for this bridge.

It appears that the simplified approach, with its requirement for girders to be at least 90 days old when continuity is established, would be the best solution, providing economy in both the structure and in the design process. Figure D-4.3-2 compares the development of restraint moments with time for the final designs for the three girder ages at continuity. The increase in restraint moments for the final designs with continuity at earlier ages can be compared with development of restraint moments for the initial designs in Figure D-4.1.3-1. The increase in restraint moment was caused by the increased creep resulting from the increased number of strands. For the design with continuity established at a girder age of 28 days, a portion of the increase was also caused by the change in the ultimate creep coefficient that resulted from in increased concrete strength.

4.3.1 Simple-Span Design for Comparison

A simple-span design using the same girder lengths and bearing locations was performed for comparison to the continuous girder designs. The concrete compressive strength at release was increased to equal the specified concrete compressive strength at 28 days in order to satisfy design requirements—that is, $f'_c = f'_{ci} = 7.00$ ksi. Otherwise, the properties of the concretes used for the simple-span design are the same as for the continuous girder design with a girder age of at least 90 days when continuity is established, as given in Section 3.3.

The following tables of moments and stresses are provided for the simple-span bridge design used for comparison to the continuous girder designs (see Tables D-4.3.1-1 through D-4.3.1-3). Because of symmetry, moments and stresses are only shown for half of the girder. Moments for noncomposite loads on the simple-span design are the same as shown in Table D-3.7.1-1.

TABLE D4.2.1-2 Summary of design stresses for final design at service limit state after losses—continuity at 90 days

	Location		Brg.	Trans.	H/2	0.10L	0.20L	0.30L	0.40L	0.50L	0.60L	0.70L	0.80L	0.90L	H/2	Trans.	Brg.
		From Brg. (ft)	0.00	1.92	2.20	8.03	16.65	25.27	33.88	42.50	51.12	59.73	68.35	76.97	82.80	83.08	85.00
SERVICE STRESSES (ksi)																	
1	Prestress After Losses	Top Girder	0.091	0.324	0.315	0.117	-0.174	-0.465	-0.756	-0.756	-0.756	-0.465	-0.174	0.117	0.315	0.324	0.091
		Bottom Girder	0.590	2.584	2.591	2.753	2.992	3.231	3.469	3.469	3.469	3.231	2.992	2.753	2.591	2.584	0.590
2	Self Weight	Top Girder	0.000	0.110	0.126	0.427	0.786	1.042	1.196	1.247	1.196	1.042	0.786	0.427	0.126	0.110	0.000
		Bottom Girder	0.000	-0.090	-0.103	-0.350	-0.644	-0.854	-0.980	-1.022	-0.980	-0.854	-0.644	-0.350	-0.103	-0.090	0.000
3	Non-Comp. DL	Top Girder	0.000	0.173	0.198	0.673	1.239	1.643	1.885	1.966	1.885	1.643	1.239	0.673	0.198	0.173	0.000
		Bottom Girder	0.000	-0.142	-0.163	-0.551	-1.016	-1.346	-1.545	-1.611	-1.545	-1.346	-1.016	-0.551	-0.163	-0.142	0.000
4	Composite DL	Top Girder	0.000	0.007	0.008	0.026	0.046	0.057	0.059	0.054	0.039	0.016	-0.015	-0.055	-0.087	-0.088	-0.100
		Bottom Girder	0.000	-0.022	-0.025	-0.084	-0.148	-0.184	-0.192	-0.173	-0.127	-0.053	0.049	0.178	0.281	0.286	0.323
5	Restraint Moment (RM) (+)	Top Girder	0.000	0.000	0.000	0.000	0.000	0.000	0.000	0.000	0.000	0.000	0.000	0.000	0.000	0.000	0.000
		Bottom Girder	0.000	0.000	0.000	0.000	0.000	0.000	0.000	0.000	0.000	0.000	0.000	0.000	0.000	0.000	0.000
6	LL + IM (+)	Top Girder	0.000	0.046	0.052	0.174	0.305	0.383	0.419	0.415	0.373	0.290	0.175	0.067	0.026	0.024	0.017
		Bottom Girder	0.000	-0.149	-0.170	-0.562	-0.987	-1.240	-1.356	-1.344	-1.207	-0.939	-0.565	-0.216	-0.083	-0.079	-0.054
7	LL + IM (-)	Top Girder	0.000	-0.005	-0.006	-0.023	-0.047	-0.072	-0.096	-0.121	-0.145	-0.170	-0.226	-0.264	-0.361	-0.367	-0.413
		Bottom Girder	0.000	0.002	0.020	0.074	0.153	0.232	0.312	0.392	0.470	0.549	0.730	0.853	1.168	1.188	1.336
TOTAL SERVICE STRESSES (ksi)																	
A = 1-4	Full PS + DL	Top Girder	0.091	0.614	0.647	1.243	1.897	2.277	2.384	2.511	2.364	2.236	1.836	1.162	0.552	0.519	-0.009
		Bottom Girder	0.590	2.330	2.300	1.768	1.184	0.847	0.752	0.663	0.817	0.978	1.381	2.030	2.606	**2.638**	0.913
B = 1-5	Full PS + DL + RM (+)	Top Girder	0.091	0.614	0.647	1.243	1.897	2.277	2.384	2.511	2.364	2.236	1.836	1.162	0.552	0.519	-0.009
		Bottom Girder	0.590	2.330	2.300	1.768	1.184	0.847	0.752	0.663	0.817	0.978	1.381	2.030	2.606	**2.638**	0.913
B + 1.0*6	Service I LL+IM (+) w/RM	Top Girder	0.091	0.660	0.699	1.417	2.202	2.660	2.803	2.926	2.737	2.526	2.011	1.229	0.578	0.543	0.008
		Bottom Girder	0.590	2.181	2.130	1.206	0.197	-0.393	-0.604	-0.681	-0.390	0.039	0.816	1.814	2.523	2.559	0.859
A + 1.0*7	Service I LL+IM (-)	Top Girder	0.091	0.609	0.641	1.220	1.850	2.205	2.288	2.390	2.219	2.066	1.610	0.898	0.191	0.152	-0.422
		Bottom Girder	0.590	2.332	2.320	1.842	1.337	1.079	1.064	1.055	1.287	1.527	2.111	2.883	3.774	**3.826**	2.249
B + 0.8*6	Service III LL+IM (+) w/RM	Top Girder	0.091	0.651	0.689	1.382	2.141	2.583	2.719	2.843	2.662	2.468	1.976	1.216	0.573	0.538	0.005
		Bottom Girder	0.590	2.211	2.164	1.318	0.394	-0.145	-0.333	**-0.412**	-0.149	0.227	0.929	1.857	2.540	2.575	0.870
A + 0.8*7	Service III LL+IM (-)	Top Girder	0.091	0.610	0.642	1.225	1.859	2.219	2.307	2.414	2.248	2.100	1.655	0.951	0.263	0.225	**-0.339**
		Bottom Girder	0.590	2.331	2.316	1.827	1.306	1.033	1.002	0.977	1.193	1.417	1.965	2.712	3.540	3.588	1.982
6 + 0.5*B	Special (+) Service + RM	Top Girder	0.046	0.353	0.376	0.796	1.254	1.522	1.611	1.671	1.555	1.408	1.093	0.648	0.302	0.284	0.013
		Bottom Girder	0.295	1.016	0.980	0.322	-0.395	-0.817	-0.980	-1.013	-0.799	-0.450	0.126	0.799	1.220	1.240	0.403
7 + 0.5*A	Special (-) Service	Top Girder	0.046	0.302	0.318	0.599	0.902	1.067	1.096	1.135	1.037	0.948	0.692	0.317	-0.085	-0.108	-0.417
		Bottom Girder	0.295	1.167	1.170	0.958	0.745	0.656	0.688	0.724	0.879	1.038	1.421	1.868	2.471	**2.507**	1.793

Notes for Table D-4.2.1-2: 1. Maximum stresses for each condition are shaded, with the governing stresses also boxed and bolded.
2. Values for limiting stresses are given in Table D-3.4.2.2-1.
3. Compressive stresses for both dead-load conditions (A and B) are compared with the limiting compressive stress for full dead load f_{c2} = 3.150 ksi. The maximum stress is 2.638 ksi at the interior transfer length location.
4. Compressive stresses for both Service I LL+IM conditions are compared with the limiting compressive stress for full-service conditions f_{c1} = 4.200 ksi. The maximum stress is 3.826 ksi at the interior transfer length location.
5. Tensile stresses in the precompressed tensile zone for Service III with RM are compared with the limiting tensile stress f_{t1} = –0.500 ksi. The maximum stress is –0.412 ksi at mids pan.
6. Tensile stresses in regions other than the precompressed tensile zone for Service III without RM are compared with the limiting tensile stress f_{t2} = –0.200 ksi or ft3 = –0.630 ksi. The latter value requires an area of reinforcement to resist the tensile force. The maximum stress is –0.339 ksi at the interior bearing, so reinforcement is required to resist the tensile force in the concrete.
7. Compressive stresses for the special cases are compared with the limiting compressive stress for that case f_{c3} = 2.800 ksi. The maximum stress is 2.507 ksi at the interior transfer length location.
8. In all cases, this design satisfies the specified stress limits.

Design	End of Girder	Girder at Midspan	f'_{ci} f'_c	Design Moments**	Number of Strands	Area of Strands
Initial Design 90 Day Final Design ***Simplified Approach***	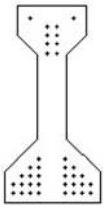	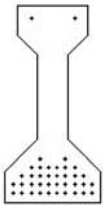	5.5 ksi	0.0 k-ft	*Draped:* 8	1.224 in^2
					Straight: 30	4.590 in^2
			7.0 ksi	2,429.0 k-ft	*Total:* **38**	**5.814 in^2** --
28 Day Final Design ***General Approach***	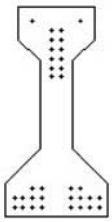	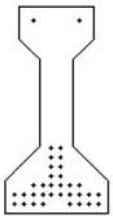	7.5 ksi	945.1 k-ft	*Draped:* 12 *	2.604 in^2
					Straight: 22 *	4.774 in^2
			8.5 ksi	2,909.5 k-ft	*Total:* **34 ***	**7.378 in^2** ***+26.9%***
60 Day Final Design ***General Approach***	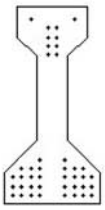	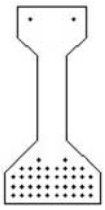	6.0 ksi	455.4 k-ft	*Draped:* 8	1.224 $in.^2$
					Straight: 34	5.202 $in.^2$
			7.0 ksi	2,656.7 k-ft	*Total:* **42**	**6.426 $in.^2$** ***+10.5%***
Simple-Span Design			7.0 ksi	0.0 k-ft	*Draped:* 14	2.142 $in.^2$
					Straight: 32	4.896 $in.^2$
			7.0	2,810.1 k-ft		
	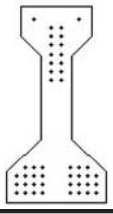	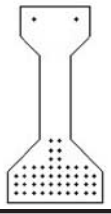	ksi		*Total:* **46**	**7.038 $in.^2$** ***+21.1%***
* 0.6-in.-diameter strands were required for 28 day final design; other designs used 0.5-in.-diameter strands.						
**Top number in cells is positive restraint moment at interior support. Bottom number in cells is Service III maximum positive design moment at midspan.						

Figure D-4.3-1. Summary of designs.

Tables D-4.3.1-2 and D-4.3.1-3 present the service limit state stresses for the simple-span design. The stresses are compared with stress limits in the notes following each table.

5 REINFORCEMENT FOR POSITIVE MOMENTS AT INTERIOR SUPPORTS

The connections between girders at interior supports of bridges made continuous are subject to positive design moments. However, the moments are caused by minor live-load effects (for more than two-span bridges) and restraint of time-dependent effects, including creep, shrinkage, and temperature. Therefore, the positive design moments are not well-defined. Past research has questioned the benefit of providing a positive moment connection.

5.1 Positive Moment Connection

The proposed specifications recommend that positive moment connections be provided between all prestressed concrete girders made continuous (*proposed* Article C5.14.1.2.7a). This recommendation is based on providing the connection to enhance the structural integrity of the structure so that it may be more robust and better able to resist unforeseen or

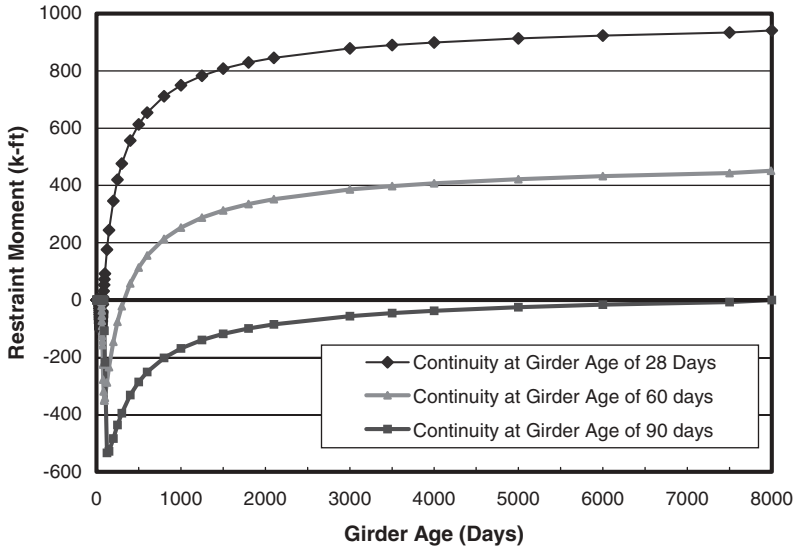

Figure D-4.3-2. Development of restraint moment with girder age—final design.

extreme loads. However, if analysis for restraint moments is required and the analysis indicates that a positive moment will develop, the proposed specifications require that a positive moment connection be provided. While not required, a positive moment connection is provided for the design with continuity at 90 days.

Reinforcement to resist the positive design moment at the interior support may be provided using either mild reinforcement or pretensioning strand, as demonstrated in Sections 5.4 and 5.5.

5.2 Positive Design Moments

For the strength limit state, the reinforcement in the positive moment connection is proportioned to provide a factored resistance, ϕM_n, greater than the larger of the factored moment, M_u, or $0.6M_{cr}$, but not to exceed $1.2M_{cr}$. A design moment of $1.2M_{cr}$ is typically provided because testing and field experience have shown that this quantity of reinforcement, which is also the minimum quantity of reinforcement required by the AASHTO LRFD Specifications in many cases, has performed well. Reinforcement provided in excess of the quantity needed to resist $1.2M_{cr}$ has been shown to be less effective. Therefore, it is not recommended to use a quantity of reinforcement greater than that required for $1.2M_{cr}$.

For the service limit state, the reinforcement is proportioned to resist the larger of the service load moment or M_{cr}. The Service I load combination is used to compute the design moment because the connection is not prestressed.

Since this bridge has two spans, the only positive moment that can be developed at the interior support is caused by restraint (considering the effects included in this design example). Bridges with more spans will develop positive moments at the interior supports from live loads. Because there is no restraint moment for the design with continuity at a girder age of 90 days, there is no positive design moment.

TABLE D-4.3.1-1 Service design moments for loads on composite section for simple-span bridge

	Location from Bearing (ft)	Compos. DL (DC) (k-ft)	Compos. DL (DW) (k-ft)	LL + IM Service I (k-ft)	LL + IM Service III (k-ft)
Bearing	0.0	0.0	0.0	0.0	0.0
Trans.	1.9	11.8	13.5	135.9	108.7
H/2	2.2	13.5	15.5	155.2	124.2
0.10 L	8.0	45.9	52.6	523.7	419.0
0.20 L	16.7	84.4	96.7	952.0	761.6
0.30 L	25.3	112.0	128.3	1,242.1	993.6
0.40 L	33.9	128.5	147.2	1,413.8	1,131.0
0.50 L	42.5	134.0	153.5	1,456.2	1,165.0

5.2.1 Computation of Positive Cracking Moment at Continuity Diaphragm

5.2.1.1 Section Properties for Continuity Diaphragm. The cracking moment is computed using a cross section composed of the girder shape, the build-up, and the effective width of deck. The remainder of the continuity diaphragm could be considered, but the assumed section provides a minimum area that may be effective.

TABLE D-4.3.1-2 Summary of design stresses for simple-span design at release

	Location from Bearing	(ft)	Brg.	Trans.	H/2	0.10L	0.20L	0.30L	0.40L	0.50L
			0.00	1.92	2.20	8.03	16.65	25.27	33.88	42.50
Prestress at Release	Top Girder	(ksi)	N/A	0.884	N/A	0.531	0.033	–0.464	–0.962	–0.962
	Bottom Girder	(ksi)	N/A	3.420	N/A	3.709	4.117	4.525	4.933	4.933
Self Weight	Top Girder	(ksi)	N/A	0.144	N/A	0.461	0.820	1.076	1.230	1.281
	Bottom Girder	(ksi)	N/A	–0.118	N/A	–0.378	–0.672	–0.882	–1.008	–1.050
Total at Release	Top Girder	(ksi)	N/A	1.028	N/A	0.992	0.853	0.612	0.268	0.319
	Bottom Girder	(ksi)	N/A	3.301	N/A	3.331	3.445	3.643	**3.925**	3.883

Notes:
1. Maximum stresses for each condition are shaded, with the governing stresses also boxed and bolded.
2. Values for limiting stresses are given below because they do not appear in any table.
3. Compressive stresses at release are compared with the limit f_{cR} = 4.200 ksi. The maximum compressive stress is 3.925 ksi at 0.40L.
4. Tensile stresses in regions other than the precompressed tensile zone at release are compared with the limiting tensile stress f_{tR1} = –0.200 ksi or f_{tR2} = –0.635 ksi. The latter value requires an area of reinforcement to resist the tensile force. There are no tensile stresses in the concrete at release.
5. In all cases, this design satisfies the specified stress limits at release.

Since the continuity diaphragm (between the ends of opposing girders) is composed entirely of deck concrete, transformation of the deck is not required. The build-up is included in the computation of these section properties because the full depth of the build-up is specified at the center of bearings, immediately adjacent to the continuity diaphragm. Including the build-up will increase the cracking moment.

The composite section properties computed earlier in Section 3.6.2 are similar, but are not used here because the deck has been transformed (deck and girder concrete compressive strengths are different) and the build-up was neglected.

The section properties for the continuity diaphragm are as follows:

h'_c = total depth of diaphragm section; build-up is included since full build-up must be provided at CL bearings;
= 45 + 2.5 + 7.75 = 55.25 in.;

A'_c = 1,320 in.^{2};

I'_c = 436,486 in.^{4};

y'_{bc} = 38.04 in.;

y'_{tcd} = 17.21 in.;

S'_{bc} = 11,475 in.^{3}; and

S'_{tcd} = 25,362 in.^{3}

5.2.1.2 Cracking Moment. The positive cracking moment, M_{cr}, is computed using the section modulus for the bottom of the continuity diaphragm and the modulus of rupture for the deck concrete, f_{rd}, which is given in Section 3.3.2.1:

$M_{cr} = f_{rd} S'_{bc}$;
= 0.480 (11,475); and
= 5,508 k-in = 459.0 k-ft.

The concrete strength of the deck, f'_{cd}, is used for this calculation because the confining effect of the precast girders in the continuity diaphragm is not significant for positive moments, where the deck slab is in compression.

For reinforcement limits, the quantity $1.2M_{cr}$ is also computed:

$1.2M_{cr}$ = 550.8 k-ft.

5.3 Minimum Distance Between the Ends of Girders

The bridge must be laid out to provide adequate distance between the ends of girders in the continuity diaphragm to develop the reinforcement. This distance depends on the type and size of reinforcement that is used. Computations for determining required development lengths into the continuity diaphragm are presented for mild reinforcement and for strands in the next two sections.

For proper meshing of the positive moment connection reinforcement, the distance between the ends of girders must also be adequate to allow movement of the bars or strands during erection. The greater the distance, the less bending would be required to provide clearance, especially for strands that cannot be offset to avoid conflicts. The minimum distance between the ends of girders should be determined early in the design process because design spans and continuity diaphragm dimensions depend on this distance.

5.4 Mild Reinforcement

Mild reinforcement is often used to provide the positive moment connection. The reinforcement for the connection must extend from the end of the girder and must be anchored into the continuity diaphragm. This reinforcement is usually placed among the pretensioned strands near the bottom of the

TABLE D-4.3.1-3 Summary of design stresses for simple-span design at service limit state after losses

	Location from Bearing	(ft)	Brg.	Trans.	H/2	0.10L	0.20L	0.30L	0.40L	0.50L
			0.00	1.92	2.20	8.03	16.65	25.27	33.88	42.50
SERVICE STRESSES (ksi)										
Prestress after Losses	Top Girder	(ksi)	0.183	0.698	0.685	0.419	0.026	–0.367	–0.760	–0.760
	Bottom Girder	(ksi)	0.613	2.700	2.711	2.929	3.251	3.573	3.895	3.895
Self Weight	Top Girder	(ksi)	0.000	0.110	0.126	0.427	0.786	1.042	1.196	1.247
	Bottom Girder	(ksi)	0.000	–0.090	–0.103	–0.350	–0.644	–0.854	–0.980	–1.022
Non-Comp. DL	Top Girder	(ksi)	0.000	0.173	0.198	0.673	1.239	1.643	1.885	1.966
	Bottom Girder	(ksi)	0.000	–0.142	–0.163	–0.551	–1.016	–1.346	–1.545	–1.611
Composite DL	Top Girder	(ksi)	0.000	0.009	0.011	0.036	0.065	0.086	0.099	0.103
	Bottom Girder	(ksi)	0.000	–0.030	–0.034	–0.114	–0.211	–0.279	–0.322	–0.335
LL + IM	Top Girder	(ksi)	0.000	0.049	0.056	0.189	0.343	0.447	0.509	0.524
	Bottom Girder	(ksi)	0.000	–0.158	–0.181	–0.610	–1.109	–1.447	–1.647	–1.697
TOTAL SERVICE STRESSES (ksi)										
Full PS + DL	Top Girder	(ksi)	0.183	0.990	1.019	1.554	2.116	2.404	2.420	**2.557**
	Bottom Girder	(ksi)	0.613	2.439	2.412	1.913	1.381	1.093	1.049	0.927
Service I	Top Girder	(ksi)	0.183	1.039	1.075	1.743	2.458	2.852	2.929	**3.081**
	Bottom Girder	(ksi)	0.613	2.280	2.231	1.303	0.272	–0.354	–0.598	–0.770
Service III	Top Girder	(ksi)	0.183	1.030	1.064	1.705	2.390	2.762	2.828	2.976
	Bottom Girder	(ksi)	0.613	2.312	2.267	1.425	0.493	–0.065	–0.269	**–0.431**
Special Service	Top Girder	(ksi)	0.092	0.544	0.566	0.966	1.401	1.649	1.719	1.803
	Bottom Girder	(ksi)	0.307	**1.061**	1.025	0.346	–0.419	–0.901	–1.123	–1.233

Notes:

1. Maximum stresses for each condition are shaded, with the governing stresses also boxed and bolded.
2. Values for limiting stresses are the same as for the design with continuity at a girder age of 90 days given in Table D-3.4.2.2-1.
3. Compressive stresses for full prestress and dead load are compared with the limiting compressive stress for full deadload f_{c2} = 3.150 ksi. The maximum stress is 2.557 ksi at midspan.
4. Compressive stresses for Service I conditions are compared with the limiting compressive stress for full-service conditions f_{c1} = 4.200 ksi. The maximum stress is 3.081 ksi at the interior transfer length location.
5. Tensile stresses in the precompressed tensile zone for Service III are compared with the limiting tensile stress f_{t1} = –0.500 ksi. The maximum stress is–0.431 ksi at midspan.
6. Tensile stresses in regions other thanthe precompressed tensile zone for Service III are compared with the limiting tensile stress f_{t2} = –0.200 ksi or f_{t3} = –0.630 ksi. The latter value requires an area of reinforcement to resist the tensileforce. There are no tensile stresses in the concrete at release.
7. Compressive stresses for the special service combination are compared with the limiting compressive stress for thatcase f_{c3} = 2.800 ksi. The maximum stress is 1.061 ksi at the interior transfer length location.
8. In all cases, this design satisfies the specified stress limits.

girder in order to maximize the effective depth to the reinforcement. This additional reinforcement inserted between strands that are usually placed on the standard 2-in. × 2-in. grid increases the congestion of reinforcement at the ends of girders. Therefore, extra attention must be given to this area during the placement of concrete to avoid lack of consolidation.

Hooks are generally provided on the projecting reinforcement to improve the development of the reinforcement into the continuity diaphragm and also to shorten the required diaphragm width. The bars may be bent prior to or after fabrication of the girder, depending on fabricator preferences and clearances within the girder forms. Hairpin bars (180° hooks) are sometimes used to address reinforcement issues.

5.4.1 Development and Detailing of Reinforcement into Continuity Diaphragm

It is important that the distance between the ends of opposing girders be great enough within a continuity diaphragm to allow development of the positive reinforcement into the diaphragm. This should be considered during the initial stages of laying out a bridge.

The mild reinforcement is developed into the continuity diaphragm using a standard 90° hook. No. 5 bars will be used for the connection. The required length of embedment, ℓ_{dh}, into the diaphragm to develop the No. 5 hooked bar is computed according to LRFD Article 5.11.2.4:

TABLE D-5.2-1 Summary of positive design moments and limits at center of interior support (critical moments are shaded)

			Girder Age at Continuity		
			28 Days	***60 Days***	***90 Days***
Service I Limit State	M_{sl}	(k-ft)	698.1	202.5	N/A
	M_{cr}	(k-ft)	459.0	459.0	459.0
Strength I Limit State	M_u	(k-ft)	1,147.1	458.7	N/A
	$1.2M_{cr}$	(k-ft)	550.8	550.8	550.8

ℓ_{dh} = 8.3 in.; USE 8½ in. LRFD Eq. 5.11.2.4.1-1

A reduction factor of 0.7 was used because conditions provide the required side and end cover. While the clear distance between the hook and the edge of the diaphragm is 1.5 in. (less than the 2 in. required), the face of the diaphragm is confined by the girder concrete. Therefore, this surface is not an exterior surface, and it appears appropriate to use the reduction. An embedment of the hook into the continuity diaphragm of 8.5 in. will be used. The distance between ends of girders across the continuity diaphragm will be taken as 10 in., so the 8.5-in. projection to the hook can be provided and still allow for construction tolerances.

A small additional reduction in the required hook embedment could be taken since the provided area of reinforcement is slightly more than is required by analysis. Using this reduction, the embedment could be reduced to 8 in., but the design of the connection must be complete before the magnitude of this reduction is known. Therefore, 8.5 in. will be used in this example.

A cross bar should be placed in the corner of the hooks to enhance the development of the hooked reinforcement into the diaphragm. The cross bar should be at least the same size as the hooked bar.

In most cases, bars with 90° hooks cannot be installed in the forms with the hooks prebent. This is because the hooks cannot fit within the girder forms; thus, girders are usually fabricated with straight bars projecting from the ends, and the hooks are bent in the precast plant after fabrication. In some situations, hooked bars may be installed in the forms with the hook tilted to clear the forms. Then, after girder fabrication, the hooked bars can be twisted to make the hooks vertical.

A 180° hooked bar (hairpin) may also be used to provide two legs developed into the continuity diaphragm with only one hook. Also, the hooks are prebent, which simplifies fabrication and eliminates hooks that may not fit within the forms during manufacturing. The use of hairpin bars is especially helpful when a large number of bars is required to satisfy positive moment requirements. The development length for 90° hooked reinforcement should be used to compute the required embedment of 180° hooks into the continuity diaphragm. The placement of anchor bars through the hairpins, as shown in Figure D-5.4.1-1 for 90° hooked bars, is recommended.

5.4.2 Required Area of Reinforcement

Using typical strength design procedures and the design moments given in Table D-5.2-1, the required area of reinforcement is computed to be

A_s = 2.35 in.^{2} (continuity at 60 and 90 days) and

A_s = 4.92 in.^{2} (continuity at 28 days),

where

f'_{cd} = 4.00 ksi;
f_y = 60 ksi ;
M_u = $1.2M_{cr}$ = 550.8 k-ft (continuity at 60 and 90 days)
= 1,147.1 k-ft (continuity at 28 days);
ϕ = 0.9;
b = width of compression face
= effective width of deck slab = 93 in.;
h_c = total section height including build-up = 55.25 in.;
g = distance from bottom of girder to centroid of reinforcement
= 3.00 in. (one row of reinforcement—continuity at 60 and 90 days)
= 4.00 in. (two rows of reinforcement—continuity at 28 days); and
d = effective depth from top of deck including build-up
= $h_c - g$ = 52.25 in.(continuity at 60 and 90 days)
= 51.25 in. (continuity at 28 days).

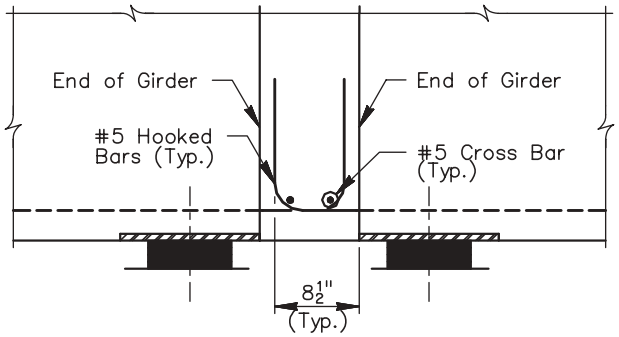

Figure D-5.4.1-1. Detail of reinforcement placement at positive moment connection (section view).

5.4.2.1 Girder Age at Continuity of 60 or 90 Days. For girders that are 60 and 90 days old when continuity is established, the required area of reinforcement, $A_s = 2.35$ in.^{2}, can be provided using eight No. 5 reinforcing bars. This satisfies the assumption that all of the reinforcement can be placed in a single layer:

$A_{s\,prov} = 8\ (0.31\ \text{in.}^2) = 2.48\ \text{in.}^2 > A_s = 2.35\ \text{in.}^2$ OK.

A layout for the reinforcement is shown in Figure D-5.4.2-1 with opposing bars offset to allow meshing.

5.4.2.2 Girder Age at Continuity of 28 Days. For girders that are 28 days old when continuity is established, the required area of reinforcement is 4.92 in.^{2}—nearly twice the area required for continuity established at the later ages. This area can be provided using 15 No. 5 reinforcing bars. To provide a symmetrical connection, the number of reinforcing bars is rounded up to an even number, 16.

$A_{s\,prov} = 4.96\ \text{in.}^2 > A_s = 4.92\ \text{in.}^2$ OK.

Using No. 5 bars, this area requires two layers of reinforcement, which greatly complicates detailing, fabrication, and erection. A larger bar size could also be used to reduce the number of bars, but this would require a greater distance between the ends of girders to properly develop the hooked bars. This large required area of reinforcement and the accompanying complications in detailing are other reasons to require that continuity to be established at girder ages greater than 28 days.

5.4.3 Development and Detailing of Reinforcement into the Girder

The required development length into the girder for the positive moment reinforcement is computed as follows:

$\ell_{dh} = 15.0$ in. LRFD Art. 5.11.2.1.1

This length applies for designs with continuity at all ages considered.

The total length of embedment of the positive moment reinforcement into the girder should be carefully considered. It is recommended that the bar be developed beyond where an assumed crack radiating at a 2:1 slope from the inner edge of the bearing or where an embedded plate intersects the reinforcement. The general concept is illustrated in Figure D-5.4.3-1, with the details of the connection for this bar shown in Figure D-5.4.2-1.

Where multiple bars are required for positive moment reinforcement, at least two different embedment lengths should be used to avoid stress concentrations and potential cracking where the bars terminate in the girder. One bar type should provide the minimum embedment length, with the second bar type providing at least an additional 1.5 ft of embedment. Where hairpin bars are used, the staggering of bar terminations can be accomplished by using a single bar type that is detailed with unequal legs.

5.4.4 Constructability Issues

Reinforcement projecting from the end of a girder is detailed to mesh with the reinforcement projecting from the opposing girder. This is intended to provide an essentially continuous load path for any tension that may develop at the bottom of the connection, requiring that the reinforcement be detailed to mesh. To accomplish this, the bars must be offset or bent so that conflicts between bars are minimized or eliminated.

The use of offset bars is illustrated for the design with continuity at 60 and 90 days in Figure D-5.4.4-1. The bars are placed in a slightly eccentric pattern. This pattern simplifies fabrication and erection by allowing use of a single detail for the placement of reinforcement in all girders, avoiding fabrication errors, and providing a positive offset between bars.

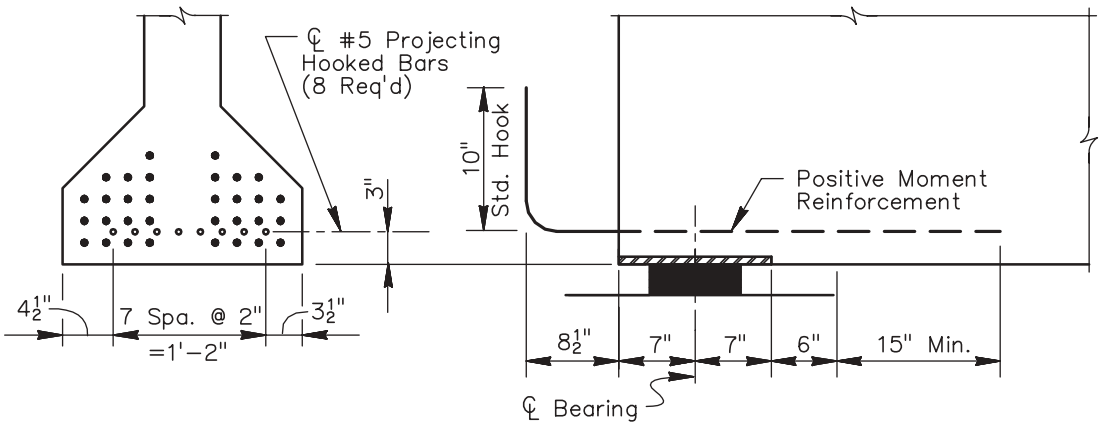

Figure D-5.4.2-1. Details of reinforcement placement at end of girder.

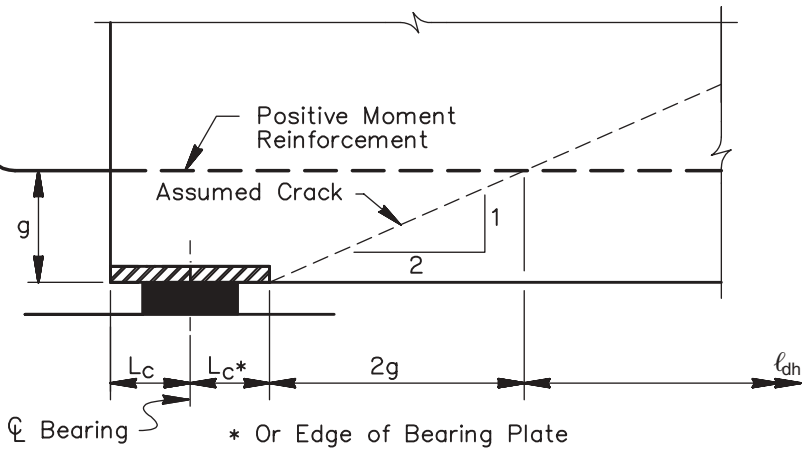

Figure D-5.4.3-1. Detail for embedment of reinforcement into girder.

As mentioned in Section 5.4.2.2, the use of two layers of reinforcement greatly complicates fabrication and erection of the girders, as well as placement of reinforcement in the continuity diaphragm. If possible, a single layer of reinforcement should be detailed. However, the available locations for placement of reinforcement are limited. Furthermore, the use of a larger number of smaller bars allows for a smaller gap between ends of opposing girders than is possible with fewer larger bars. The smaller bars also require a shorter embedment into the girder. These factors tend to lead designers to use a larger number of smaller bars.

The placement of the positive moment connection reinforcement between pretensioning strands increases congestion; this is significant because the congestion can inhibit the proper consolidation of concrete in the critical bearing area. Reinforcement should be positioned to facilitate placement and consolidation of concrete around the strands and bars.

Reinforcement projections must be detailed to allow tolerances in bar projections, girder lengths, and girder placement at erection. In this example, the distance from end of the hook to the face of the opposing girder is detailed as 1½ in., which should provide an adequate tolerance. When developing a layout for the positive moment reinforcement, the locations of all other reinforcement and embedments must be carefully considered to avoid conflicts and provide adequate tolerances for fabrication. One example is that the positive moment reinforcement must avoid locations of headed studs attached to embedded plates.

5.4.5 Control of Cracking by Distribution of Reinforcement

5.4.5.1 Girder Age at Continuity of 60 or 90 Days. According to LRFD Article 5.7.3.4, the reinforcement will be pro-

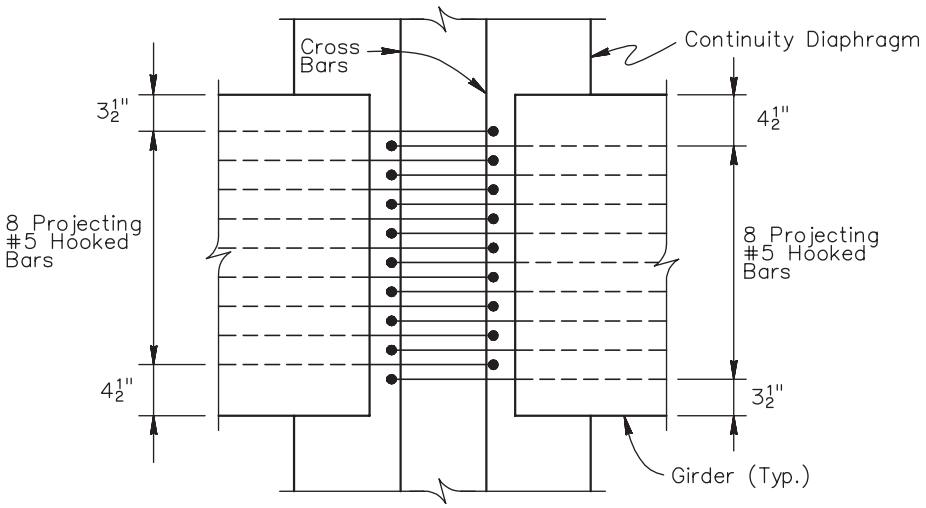

Figure D-5.4.4-1. Detail of reinforcement placement at positive moment connection (plan view).

portioned so that the tensile stress in the mild steel reinforcement at the service limit state does not exceed the stress limit given by LRFD Equation 5.7.3.4-1. The tensile stress in the mild reinforcement at service limit state is computed to be as follows:

$$f_s = \frac{M_{sl}}{A_s jd} = \frac{202.5(12)}{2.48(0.972)(52.25)} = 19.3 \text{ ksi},$$

where

M_{sl} = 202.5 k-ft (from Table D-5.2-1);
A_s = 2.48 in.$^{2;}$
f_y = 60 ksi;
E_s = 29,000 ksi;
E_{cd} = 3,834 ksi;
$n = E_s/E_{cd}$ = 7.564;
b = width of compression face = effective width of deck slab = 93 in.;
d = effective depth to positive moment reinforcement from top of deck, including build-up = 52.25 in. (Note: the height of the build-up is included in this calculation because it is specified at the centerline of the bearings);

$$\rho = \frac{A_s}{bd} = \frac{2.48}{93(52.25)} = 0.00051;$$

$$k = \sqrt{2\rho n + (\rho n)^2}$$
$$-\rho n = \sqrt{2(0.00051)(7.564) + ((0.00051)(7.564))^2}$$
$$-(0.00051)(7.564) = 0.084; \text{ and}$$

$$j = 1 - \frac{k}{3} = 1 - \frac{0.084}{3} = 0.972.$$

The allowable tensile stress in the mild reinforcement is

$$f_{sa} = \frac{Z}{(d_c A)^{1/3}} \le 0.6 f_y$$
$$= \frac{170}{(2.31(12.71))^{1/3}} \le 0.6 \times 60 \qquad \text{LRFD Eq. 5.7.3.4-1}$$
$$= 55.1 > 36.0 \text{ ksi USE } f_{sa} = 36.0 \text{ ksi},$$

where

$d_c = 2.00 + d_b/2 = 2.00 + 0.625/2 = 2.31$ in.;
Z = 170 k/in. (moderate conditions);
b' = width of bottom flange; = 22 in.; and

$$A = \frac{2 d_c b'}{\text{No. of Bars}} = \frac{2(2.31)(22)}{8} = 12.71 \text{ in.}^2.$$

For girders that are 60 and 90 days old when continuity is established, the tensile stress in the mild reinforcement is less than the allowable. Therefore, the distribution of reinforcement for control of cracking is adequate:

f_{sa} = 36.0 ksi > f_s = 19.3 ksi. OK.

5.4.5.2 Girder Age at Continuity of 28 Days. For girders that are 28 days old when continuity is established, the same procedure as shown in Section 5.4.5.1 is used to check distribution of reinforcement. Equations and common values are not repeated here:

M_{sl} = 698.1 k-ft (from Table D-5.2-1);

A_s = 4.96 in.$^{2;}$

d = 51.25 in. (two layers of reinforcement are required);

ρ = 0.00104;

k = 0.118;

j = 0.961;

f_s = 34.3 ksi;

d_c = 3.31 in.;

A = 9.10 in.$^{2;}$ and

f_{sa} = 54.6 > 36.0 ksi; USE f_{sa} = 36.0 ksi. (maximum allowed)

For girders that are 28 days old when continuity is established, the tensile stress in the mild reinforcement is less the allowable stress by 1.7 ksi. Therefore, the distribution of reinforcement for control of cracking is adequate:

f_{sa} = 36.0 ksi > f_s = 34.3 ksi. OK.

5.4.6 Fatigue of Positive Moment Connection Reinforcement

The reinforcement in the positive moment connection is not subjected to tension from the live load for this two-span bridge, so fatigue does not need to be investigated. The positive moments caused from restraint moments or temperature effects do not occur frequently enough to be considered as loadings that cause fatigue. However, for other bridge configurations, where the connection is subjected to tension from live loads, fatigue should be considered. See Section 6.2.5 for the approach used for negative moment connection.

5.5 Pretensioning Strand

An alternate positive moment connection uses pretensioning strands extended into the continuity diaphragm. A positive moment connection that uses the pretensioning strands provides the connection without increasing congestion in the end of the girder. However, girder fabrication may be affected if the required length of extended strand is large. The service load stress limit for strands used in positive moment connections serves to limit the length of strand that can be effectively used for the connection. Extended strands used for the positive moment connection must be bonded at the end of the girder—that is, they cannot be shielded or debonded at the end of the girder.

5.5.1 Development and Detailing of Extended Strands into Continuity Diaphragm

The strands are developed into the continuity diaphragm using a 90° hook. The strand must be bent so the hook projects at least 8 in. from the end of the girder. This distance is required by the equations used in Section 5.5.2. The distance between ends of girders in the continuity diaphragm is detailed as 10 in., so the 8-in. projection to the bent strand can be provided and still allow for construction tolerances.

A cross bar should be placed in the corner of the hooks to enhance the development of the hooked reinforcement into the diaphragm. The cross bar should have an area not less than the area of the strand. A No. 5 bar is shown in Figure D-5.5.1-1.

5.5.2 Required Area of Strands

The area of strands required to resist the positive design moments (see Table D-5.5.2-1) is computed using both the strength design provisions given in *proposed* Article 5.14.1.2.7i and service load (working stress) design procedures. The working stress design procedures may be found in concrete design textbooks. Working stress design is used in addition to strength design for this calculation because the procedure is based on results of research (Salmons, 1974, 1980; Salmons and May, 1974; Salmons and McCrate, 1973). The researchers proposed a design methodology that included both approaches.

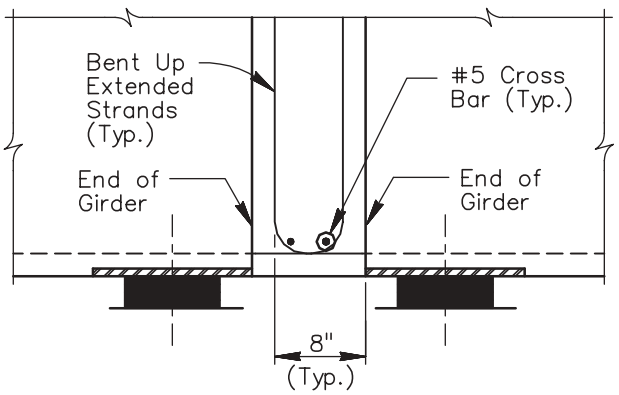

Figure D5.5.1-1. Detail of strand placement at positive moment connection (section view).

The design moment for the working stress check will be M_{cr}, while the design moment for the strength check is $1.2M_{cr}$. Initially, it was assumed that the total length of extended strand, ℓ_{sh}, was 44 in. This provides a length of strand beyond the bend (vertical leg) of 44 − 8 = 36 in. The vertical leg extends for much of the depth of the girder to maximize the development of the strand, while not using so much strand that fabrication of the girders is adversely affected.

The resulting stresses in the 0.5-in.-diameter strands at service and strength conditions are

$f_{psl} = [(44 - 8)/0.228]$ *proposed* Eq. 5.14.1.2.7i-1
$= 158$ ksi > 150 ksi, and

$f_{pul} = [(44 - 8)/0.163]$ *proposed* Eq. 5.14.1.2.7i-2
$= 221$ ksi.

Since f_{psl} exceeds the maximum service load stress of 150 ksi that applies to *proposed* Equation 5.14.1.2.7i-1, the length of strand was reduced to provide a computed f_{psl} just below the limit. The resulting total length of strand extension was 42 in., with a vertical leg of 34 in. The revised stress limits were computed as

$f_{psl} = [(42 - 8)/0.228]$ *proposed* Eq. 5.14.1.2.7i-1
$= 149$ ksi < 150 ksi, and

$f_{pul} = [(42 - 8)/0.163]$ *proposed* Eq. 5.14.1.2.7i-2
$= 209$ ksi.

For the design with continuity at 28 days, 0.6-in.-diameter strands are used. Since the conventional development length for strands increases linearly with increasing strand diameter (LRFD Equation 5.11.4.2-1), the above equations have been modified by introducing the factor $(0.5/d_b)$ to reflect an increased development length beyond the hook for larger strands. These equations are shown below for the 0.6-in.-diameter strands at service and strength conditions:

$f_{psl} = [\{(0.5/0.6)44 - 8/0.228]$ *proposed* Eq. 5.14.1.2.7i-1
$= 126$ ksi < 150 ksi, and

$f_{pul} = [\{(0.5/0.6)\ 44 - 8/0.163]$ *proposed* Eq. 5.14.1.2.7i-2
$= 176$ ksi.

The computed service load stress for the initial strand extension length (44 in.) does not exceed 150 ksi for the larger strand; thus, it is used in the initial design computations.

Based on these stress limits for service and strength limit states, the number of strands required to resist the positive

TABLE D-5.5.2-1 Design information for positive moment connection using strand (critical values are shaded)

		Girder Age at Continuity			
		28 Days		60 & 90 Days	
Iteration:		1	2	1	2
BASIC DESIGN INFORMATION					
l_{dsh}	(in.)	44	39	42	35
b	(in.)	93	93	93	93
d	(in.)	53.25	53.25	53.25	53.25
f'_{cd}	(ksi)	4.00	4.00	4.00	4.00
Strand Diameter	(in.)	0.6	0.6	0.5	0.5
STRENGTH DESIGN					
Design Moment	(k-ft)	1147.1	1147.1	550.8	550.8
f_{pul}	(ksi)	175.9	150.1	208.6	165.6
a	(in.)	0.82	0.82	0.39	0.39
A_{ps}	(in^2)	1.481	1.736	0.597	0.752
No. of Strands Req'd		6.8	8.0	3.9	4.9
WORKING STRESS DESIGN					
Design Moment	(k-ft)	698.1	698.1	459.0	459.0
E_c	(ksi)	3605	3605	3605	3605
E_s	(ksi)	29000	29000	29000	29000
n	8	.04	8.04	8.04	8.04
f_s	(ksi)	125.7	107.5	149.1	118.4
jd	(in.)	52.14	52.05	52.42	52.32
k	0	.062	0.067	0.047	0.052
rho		0.000258	0.000302	0.000142	0.000180
A_s	(in^2)	1.278	1.498	0.705	0.889
No. of Strands Req'd		5.9	6.9	4.6	5.8

design moments are computed for both girders with continuity at 28 days and for 60 and 90 days. Design moments and other parameters are found in Table D-5.2-1. Results are given in Table D-5.5.2-1.

The connection for the design with girder age of 28 days at continuity is governed by strength design; the connection for the design with girders made continuous at later ages is governed by working stress design, as indicated by the shaded cells in the table. A second design iteration is used to determine the least length of extended strand required for the design moments for both girder ages at continuity. The first iterations are performed using the initial length of extended strand. The results indicate an odd number of strands is required for both girder ages at continuity. An even number of extended strands is desirable to provide symmetry in the connection. The number of strands was then rounded up to an even number.

Using the increased number of strands, the required stress in the strands is computed, using the stress equation for whichever design approach governs (working stress or strength). The required stress is then used to compute the required length of strand extension. This new length of strand extension is then used for the second iteration. These calculations are illustrated below for the design of the girders with continuity established at an age of 60 and 90 days, where working stress design governed:

$F = A_{ps} f_{psl} = (0.705)(149.1) = 105.1$ kips;

$A_{ps} = 6\ (0.153) = 0.918$ in.^{2}; and

$f_{psl2} = F/A_{ps} = 105.1/0.918 = 114.5$ ksi.

Solving for the length of extended strand required to develop this stress is as follows:

$f_{psl} = [\ell_{dsh} - 8]/0.228$, then *proposed* Eq. 5.14.1.2.7i-1

$\ell_{dsh} = 0.228 f_{psl} + 8 = 0.228(114.5) + 8$
$= 34.1$ in. USE $\ell_{dsh} = 35$ in.

The stress can then be recomputed using the 35-in.-strand extension:

$f_{psl} = [35 - 8]/0.228 = 118.4$ ksi.

This stress is then used in the working stress computations to compute a required area of strand. The required area of strand is slightly less than the 6 strands determined in the computations above, so no further iterations are required (see Figure D-5.5.2-1).

5.5.3 Constructability Issues

Pretensioning strands are on a fixed layout within the girder. If the number of strands required for the positive moment connection is relatively small, a pattern of strands may be developed that allows strands to mesh when the girders are erected. However, in this example, nearly all of the strands in the bottom row are required to make the connection. The strands must therefore be pushed over during erection to allow proper girder placement, as shown in Figure D-5.5.3-1. The length of strand extension must be adequate to allow this bending during erection of the girder, considering the size of the strand.

5.5.4 Crack Control

The allowable tensile stress in the untensioned pretensioning strands in the connection would be computed using the same procedure as is used in Section 5.4.5.

5.5.5 Fatigue of Positive Moment Connection Reinforcement

For information on fatigue of positive moment connection reinforcement, see Section 5.4.6.

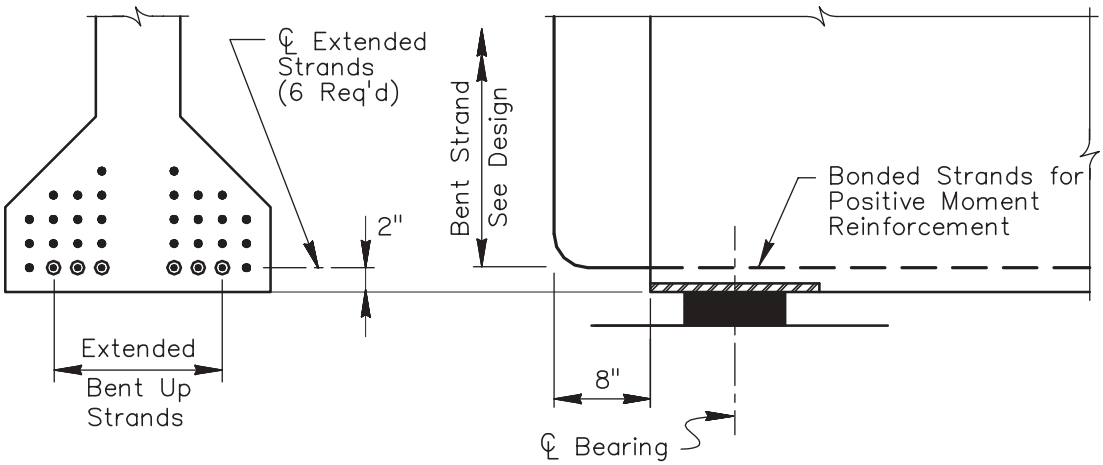

Figure D-5.5.2-1. Details of strand placement at end of girder.

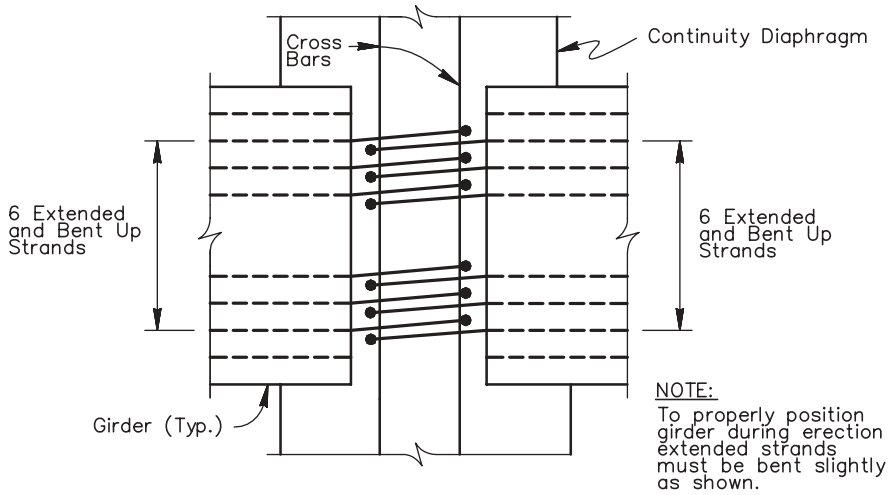

Figure D-5.5.3-1. Detail of strand placement at positive moment connection (plan view).

6 REINFORCEMENT FOR NEGATIVE MOMENTS AT INTERIOR SUPPORTS

The proper design of reinforcement at the negative moment connection is essential for the bridge to behave as a continuous structure and to provide the desired service life with little or no maintenance. This section presents the necessary steps for the design of the reinforcement for the negative moment connection.

6.1 Negative Design Moments

Negative moments at interior supports of precast/prestressed concrete girders made continuous result from dead loads, live loads, and restraint moments. Negative restraint moments, however, are ignored in design, as allowed by the *proposed* Article C5.14.1.2.7b. Therefore, the negative design moments shown below result from dead loads and live loads only (see Table D-6-1). The negative moment connection is proportioned for the strength limit state, so design moments are factored.

6.1.1 Computation of Negative Cracking Moment at Continuity Diaphragm

Section properties for the continuity diaphragm used to compute the cracking moment are discussed and given in Section 5.2.1.1. The negative cracking moment, M_{cr}, is computed using the section modulus for the top of the continuity diaphragm and the modulus of rupture for the deck concrete, f_{rd}, which is given in Section 3.3.2.1:

$$M_{cr} = f_{rd} S'_{tc} = 0.480(25{,}362) = 12{,}174 \text{ k-in} = 1{,}014.5 \text{ k-ft.}$$

For reinforcement limits, the quantity $1.2M_{cr}$ is also computed:

$$1.2M_{cr} = 1{,}217.4 \text{ k-ft.}$$

6.2 Negative Moment Connection

The connections between girders at interior piers of a bridge with precast girders made continuous are subject to significant negative design moments. The portion of the bridge subjected to negative moments must therefore be properly reinforced to resist these negative moments if it is to perform as a continuous member and if the structure is to have good serviceability.

The negative moment connection for precast/prestressed concrete girders made continuous is typically made using reinforcement in the deck. Longitudinal reinforcement in the deck, which includes distribution reinforcement and other minimum reinforcement, can be used for this connection. The total area of reinforcement required to resist the negative design moments is computed using strength design. Fatigue of the reinforcement must also be checked.

Concepts have been proposed in which the negative moment connection may be made prior to deck placement in order to make the girders continuous for the dead load of the deck. However, these concepts are not considered here. Detailing of the deck reinforcement, which is important for economy and to avoid congestion, is also addressed.

TABLE D-6-1 Summary of negative design moments and limits at center of interior support (critical moments are shaded)

			Girder Age at Continuity		
			28 Days	*60 Days*	*90 Days*
Service I Limit State	M_{sl}	(k-ft)	1,515.8	1,505.5	1,505.5
	M_{cr}	(k-ft)	–1,014.5	–1,014.5	–1,014.5
Strength I Limit State	M_u	(k-ft)	–2,544.1	–2,526.8	–2,526.8
	$1.2M_{cr}$	(k-ft)	–1,217.4	–1,217.4	–1,217.4

6.2.1 Required Area of Reinforcement

Longitudinal reinforcement is required in all deck slabs to satisfy distribution or detail reinforcement requirements. For this bridge, the typical longitudinal deck reinforcement satisfying the distribution requirements is shown in Figure D-6.2.1-1. The area of the longitudinal reinforcement within the effective tension flange width (see Section 6.2.2.1) is shown in Table D-6.2.1-1. Based on the factored negative design moment at the interior support and neglecting restraint moments, a total required area of reinforcement is computed as shown in Table D-6.2.1-1. The build-up is included in the effective depth as discussed in Section 5.2.1. The effective depth is taken as the distance from the bottom of the diaphragm to the center of the deck slab, assuming that the area of deck reinforcement is equal on the top and bottom of the slab. The typical longitudinal deck reinforcement is included in this area of reinforcement available to resist the factored negative design moment (LRFD Article 5.14.1.2.7b and *proposed* Article 5.14.1.2.7h).

For girders with continuity established at 60 and 90 days, the total area of deck reinforcement required to resist the factored negative design moment is computed using strength design as follows:

$A_s = 11.52$ in.^{2} (total area within the effective width of 93 in.; see Section 6.2.2.1),

where

$f'_c = 7.00$ ksi (use girder concrete strength, *proposed* Article 5.14.1.2.7j);
$f_y = 60$ ksi;
$M_u = 2{,}526.8$ k-ft;
$\phi = 0.90$ (for reinforced concrete since continuity diaphragm is not prestressed);

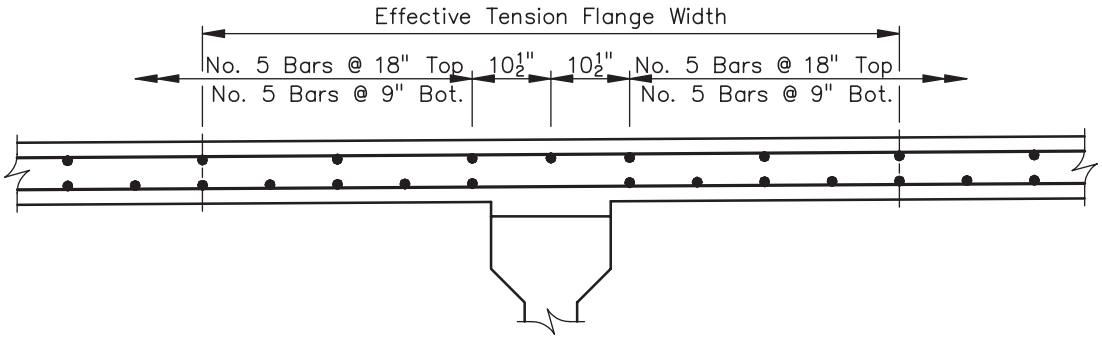

Figure D-6.2.1-1. Typical longitudinal deck reinforcement (partial section view).

b' = width of compression face = width of girder bottom flange = 22.0 in.;
d = effective depth to negative moment reinforcement from the bottom of girder and continuity diaphragm to center of deck including build-up (see discussion in Section 5.4.5.1); the center of the deck is an approximate location that could be refined considering details of deck reinforcement = 51.375 in.;
a = 2.82 in.; and
c = 4.03 in.

Checking the maximum reinforcement limit,

$c/d = 4.03/51.375 = 0.079 < 0.42$ OK

Use 15 No. 5 and 12 No. 7 = 11.85 in.^{2} > 11.52 in.^{2} OK

Results for girders with conditions established at 28 days are shown in Table D-6.2.1-1, which gives the area of additional reinforcement required to resist the negative design moment. This area will be provided by placing bars between the typical longitudinal reinforcement, as shown in Figure D-6.2.1-2.

6.2.2 Details of Deck Reinforcement

Detailing of reinforcement for the negative moment connection is generally simple since the reinforcement consists of straight bars placed in the deck. However, several issues must be considered in detailing this reinforcement.

6.2.2.1 Effective Tension Flange Width. When the deck slab in a typical girder is subjected to tension from the effects of negative moments at the service limit state, tension reinforcement effective in resisting the tension must be placed within the width of deck equal to the lesser of (LRFD Article 5.7.3.4):

1. The effective flange width (LRFD Article 4.6.2.6; see Section 3.6.2.1). For this design example, the average

TABLE D-6.2.1-1 Design of deck reinforcement for negative design moments

		Girder Age at Continuity	
		28 Days	***60 & 90 Days***
Typical Longitudinal Deck Reinforcement (Fig. D6.2.1-1)		No. 5 @ 18 in. Top No. 5 @ 9 in. Bottom	No. 5 @ 18 in. Top No. 5 @ 9 in. Bottom
Total Area of Longitudinal Reinforcement Provided	*(in.^{2})*	4.65	4.65
Factored Negative Design Moment	*(k-ft)*	2,544.1	2,526.8
Total Area Required to Resist Negative Moment	*(in.^{2})*	11.61	11.52
Additional Area of Deck Reinforcement Required	*(in.^{2})*	6.96	6.87
Additional Reinforcement Provided (Fig. D-6.2.1-2)		12 No. 7 Bars	12 No. 7 Bars
Additional Area of Deck Reinforcement Provided	*(in.^{2})*	7.20	7.20
Total A_s Provided	*(in.^{2})*	11.85 > 11.61 OK	11.85 > 11.52 OK
c/d_e		0.079	0.079

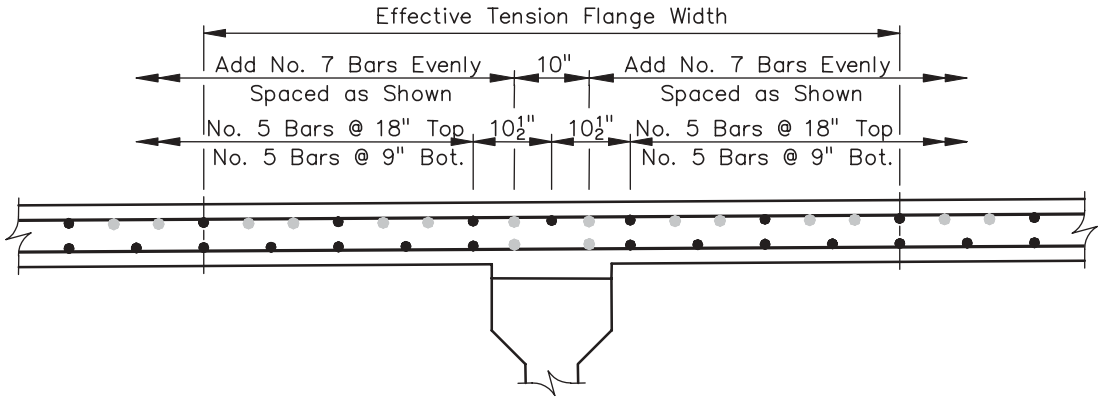

Figure D-6.2.1-2. Longitudinal deck reinforcement for negative moment at interior support (partial section view).

girder spacing controls resulting in an effective deck width of 93 in. GOVERNS.

2. One-tenth of the average of adjacent spans between bearings = 0.10(86)(12) = 103.2 in.

For this design example, the effective flange width computed earlier governs. Therefore, the full width of deck is effective. Where a portion of the flange width is not within the effective width defined above, an area of steel must be provided that is equal to at least 0.4% of the deck outside of the effective flange width.

6.2.2.2 Anchorage of Deck Reinforcement. The LRFD Specifications indicate that the longitudinal reinforcement resisting the negative design moments must be anchored in concrete that is in compression at the strength limit state (LRFD Article 5.14.1.2.7b and *proposed* Article 5.14.1.2.7h). Therefore, the inflection points for the negative moment envelope at the strength limit state must be located.

Figure D-6.2.2.2-1 indicates the extent of the negative moment region at strength limit state. Additional deck reinforcement for the factored negative design moment must be extended past the indicated locations for at least a development length. Therefore, the minimum length of the No. 7 reinforcing bars added at the interior support would be

$$\ell_{min} = 2(22.8 \text{ ft}) + 2\ell_d = 2(22.8 \text{ ft}) + 2(22.5 \text{ in.}/12) = 49.35 \text{ ft},$$

where

ℓ_d = 22.5 in. (for No. 7 reinforcing bars). LRFD Art. 5.11.2.1.1

6.2.2.3 Termination of Deck Reinforcement. Although all of the additional deck reinforcement theoretically can be terminated at the locations shown in Figure D-6.2.2.2-1, this would probably not provide good serviceability. It is recommended that the same reinforcing bar mark be used, but that alternate reinforcing bars be shifted several feet to stagger the terminations. This would require that the minimum length of reinforcing bar computed above would be increased by the amount of the shift.

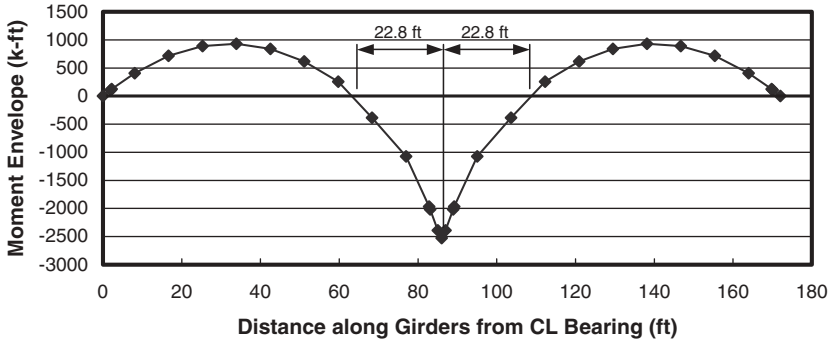

Figure 6.2.2.2-1. Negative moment envelope and location of inflection points—continuity at 60 days.

6.2.3 *Constructability Issues*

In this example, there are no significant constructability issues to address regarding the negative moment reinforcement. In some cases, a large quantity of reinforcement must be added to the typical longitudinal deck reinforcement. This can lead to difficulties in the placement of reinforcement or in placement of splices for the reinforcement.

The distance between layers of reinforcement must be considered when the larger bar sizes are needed to provide a large area of reinforcement.

6.2.4 *Control of Cracking by Distribution of Reinforcement*

6.2.4.1 Girder Age at Continuity of 60 or 90 Days. According to LRFD Article 5.7.3.4, the reinforcement should be proportioned so that the tensile stress in the mild steel reinforcement at the service limit state does not exceed the stress limit given by LRFD Equation 5.7.3.4-1. The tensile stress in the mild reinforcement is computed to be

$$f_s = \frac{M_{sl}}{A_s jd} = \frac{1{,}505.5(12)}{11.85(0.903)(51.375)} = 32.9 \text{ ksi},$$

where

M_{sl} = 1,505.5 k-ft (from Table D-6.1-1);
A_s = 11.85 in.$^{2;}$
f_y = 60 ksi;
E_s = 29,000 ksi;
E_c = 5,072 ksi (use girder concrete strength, *proposed* Article 5.14.1.2.7j);
$n = E_s/E_c = 5.718$;
b' = width of compression face = width of bottom flange of girder = 22 in.;
d = effective depth from bottom of girder and continuity diaphragm to center of deck including build-up = 51.375 in.;

$$\rho = \frac{A_s}{bd} = \frac{11.85}{22(51.375)} = 0.01048;$$

$$k = \sqrt{2\rho n + (\rho n)^2}$$
$$-\rho n = \sqrt{2(0.01048)(5.718) + ((0.01048)(5.718))^2}$$
$$-(0.01048)(5.718) = 0.291; \text{ and}$$

$$j = 1 - \frac{k}{3} = 1 - \frac{0.291}{3} = 0.903.$$

The allowable tensile stress in the mild reinforcement is

$$f_{sa} = \frac{Z}{(d_c A)^{1/3}} \le 0.6 f_y$$
$$= \frac{170}{(2.44(28.37))^{1/3}} \le 0.6 \times 60 \qquad \text{LRFD Eq. 5.7.3.4-1}$$
$$= 41.4 > 36.0 \text{ ksi USE} f_{sa} = 36.0 \text{ ksi},$$

where

d_c = 2.00 + (7/8)/2 (neglecting bottom row of deck reinforcement for simplicity) = 2.44 in.;
Z = 170 k/in. (moderate conditions);
b = 93 in.; and

$$A = \frac{2d_c b'}{\text{No. of Bars}} = \frac{2(2.44)(93)}{16} = 28.37 \text{ in.}^2.$$

For girders that are 60 and 90 days old when continuity is established, the tensile stress in the mild reinforcement is less than is allowable. Thus, the distribution of reinforcement for control of cracking is adequate:

f_{sa} = 36.0 ksi > f_s = 32.9 ksi OK.

6.2.5 *Fatigue of Negative Moment Connection Reinforcement*

LRFD Article 5.5.3.1 states that "fatigue need not be investigated for concrete deck slabs in multigirder applications." However, the commentary for the article indicates that this provision is based on the observation of low measured stresses in deck slabs, which is "most probably due to internal arching action."

The longitudinal reinforcement, which is acting as main reinforcement for the negative design moments at the interior support, is not subject to arching action. Therefore, fatigue of the deck slab reinforcement at the interior support is checked in this example.

Furthermore, the deck slab is not in compression from the design loads (see the second paragraph of LRFD Article 5.5.3.1), so it is not exempt from fatigue considerations. To determine whether cracked section properties must be used to evaluate the stress range, the stress in the concrete is computed under a specified loading combination:

M = sum of unfactored permanent loads
+ prestress + 1.5(fatigue load)
= −294 + 0
+ 1.5(−193) (fatigue moment is computed below)
= −584 k-ft; and

$f_{cd\,\text{top}} = M/S'_{tcd} = M/(I'_c/[h'_c - y'_{bc}])$
= −584(12)/(436,713/(55.25 − 38.03) = −0.276 ksi.

The stress limit is then computed for comparison to computed stress:

$f_{cd\,\max} = 0.095\sqrt{f'_{cd}} = 0.095\sqrt{4.0} = 0.190$ ksi.

Comparing the absolute values of the computed stress and stress limit,

$f_{cd\,\text{top}} = 0.276$ ksi $> f_{cd\,\max} = 0.190$ ksi.

Since the computed tensile stress exceeds the stress limit, the effect of fatigue must be evaluated using cracked section analysis.

The stress in the deck slab reinforcement is computed using the specified fatigue loading and cracked section analysis as required. The following computations are based on the designs for girders made continuous at 60 and 90 days. The results for continuity established at 28 days will differ slightly, due to the difference in live-load distribution factors.

The basic negative fatigue moment is computed to be −582 k-ft, using the QConBridge program (see Subappendix C). The analysis assumes the bridge is fully continuous for live loads. The moment is then factored by the dynamic load allowance for fatigue (1 + 0.15, LRFD Article 3.6.2.1); the live-load distribution factor for one lane loaded (0.461, LRFD Article 3.6.1.4.3b; and LRFD Table 4.6.2.2.2b-1, cross-section type (k), which is divided by the multiple presence factor for one lane loaded (1.2, LRFD Article C3.6.1.1.2) and the load factor for the fatigue limit state, which is 0.75 (LRFD Table 3.4.1-1). Therefore, the design fatigue moment is as follows:

$M_f = 1.15(0.461/1.2)(0.75)(-582) = -193$ k-ft.

The area of reinforcement provided in the deck for the interior girder, as shown in Table D-6.2.1-1, is

$A_s = 11.85$ in.^{2}

The stress range in the reinforcement caused by this design fatigue moment is computed using the principles of working stress design for a cracked section (see Section 6.2.4.1). The compression zone extends through the bottom flange and into the web, so the average of the web and bottom flange width, 14.5 in., is used as a conservative estimate for the width of the compression zone:

$f_f = 4.299$ ksi.

The limiting stress range, $f_{f\,\max}$, is computed as

$f_{f\,\max} = 21 - 0.33 f_{\min} + 8\,(r/h)$ LRFD Eq. 5.5.3.2-1
$= 21 - 0.33(4.299) + 8(0.3)$
$= 22.0$ ksi,

where

$f_{\min} = f_{LLf} + f_{DL} = 0.000 + 4.299 = 4.299$ ksi;
f_{LLf} = minimum live-load stress from fatigue loading = 0.000 ksi;
f_{DL} = stress in reinforcement from permanent loads from working stress analysis = 4.299 ksi;
M_{DL} = total composite dead-load moment (load factor = 1.0) at the center of the pier = −294 k-ft (see Table D-3.7.1-2); and
r/h = ratio of base radius to height of rolled on transverse deformations in the reinforcement; 0.3 may be used if value not known.

Comparing the computed stress range with the limiting stress range,

$f_f = 4.299$ ksi $< f_{f\,\max} = 22.0$ ksi OK.

7 DESIGN WITH NONLINEAR ANALYSIS

This section provides a brief overview of the results of a nonlinear analysis for this example, DE1. Nonlinear analysis takes into account the changing stiffness of the different sections in the girder as loading is increased. This allows a more refined estimate of the behavior of the bridge with time as time-dependent effects develop or as live load is applied. The age of the girders when continuity is established is considered in determining the behavior of the bridge with time and with increasing load.

Several limitations to the nonlinear analysis are discussed. Results from this analysis should be considered as an indication of behavior, but should not be used for design without further development and verification.

7.1 Analysis

The Restraint Program is used to perform the nonlinear analysis of this example. The analyses performed using Restraint in Section 4.1.3 have used linear analysis. The software is only capable of performing nonlinear analysis for two-span bridges. The program first performs an analysis to estimate the development of restraint moments in the girders with time. This is similar to the analysis performed earlier in this example. Then, a live-load analysis is performed, with the live load applied at the final girder age. The live load used in this analysis is a pair of concentrated loads, one at the midspan of each span. Therefore, the loading does not consider moving loads, nor does it consider only one span loaded, which would produce the maximum positive moment in the loaded span.

To perform the nonlinear analysis, the user must define the moment-curvature relationship for the following cross sections and locations:

- The continuity diaphragm, which is not prestressed and is reinforced with untensioned strands or mild reinforcement;
- The precast prestressed concrete girder with composite deck slab at midspan; and
- The precast prestressed concrete girder with composite deck slab at the end of the girder.

The program allows the input of different moment-curvature relationships at the midspan and end of girder locations because the prestressing strand patterns will be different at these locations if draped strands are used.

The Response 2000 Program was used to generate the moment-curvature relationships for use in Restraint. Information regarding the website from which the program can be obtained and results from the various analyses, including plots of the required moment-curvature relationships, are presented in Subappendix B.

7.2 Results

The results of the linear and nonlinear analyses are shown in Figure D-7.2-1 for girders with continuity established at the ages of 28, 60, and 90 days. The lines representing linear behavior shown in this figure are the same lines shown in Figure D-4.3-2 for the final designs discussed in the section summarizing the general and simplified approaches. The final restraint moments corresponding to the restraint moments at 7,500 days (see Figure D-7.2-1) are summarized in Table D-7.2-1. The results for linear analysis shown in this table differ slightly from the results reported earlier because these are for girder ages of 7,500 days, while the previous results were for 10,000 days. The nonlinear analysis does not extend to 10,000 days. As shown in Figure D-7.2-1 and Table D-7.2-1, results of the nonlinear analysis are not significantly different from the results of the linear analysis used for design earlier in this example.

In general, the results of the nonlinear analysis are less than the results from the linear analysis. This is true for all situations for both positive and negative moments, except for the final positive restraint moment for continuity at 90 days. The final moments at 90 days for the two analysis methods are on both sides of the origin, making a relative comparison of values meaningless. Using nonlinear analysis, the positive moments were reduced by 11.1%, while the negative moments were reduced by a maximum of 9.1%. However, the reduction of the final positive moment for the design with continuity established when the girder is 28 days old is significant. It reduces the moment below the moment limit used as an indication of whether the joint (continuity diaphragm) is fully effective. While this is an important change, it would not make

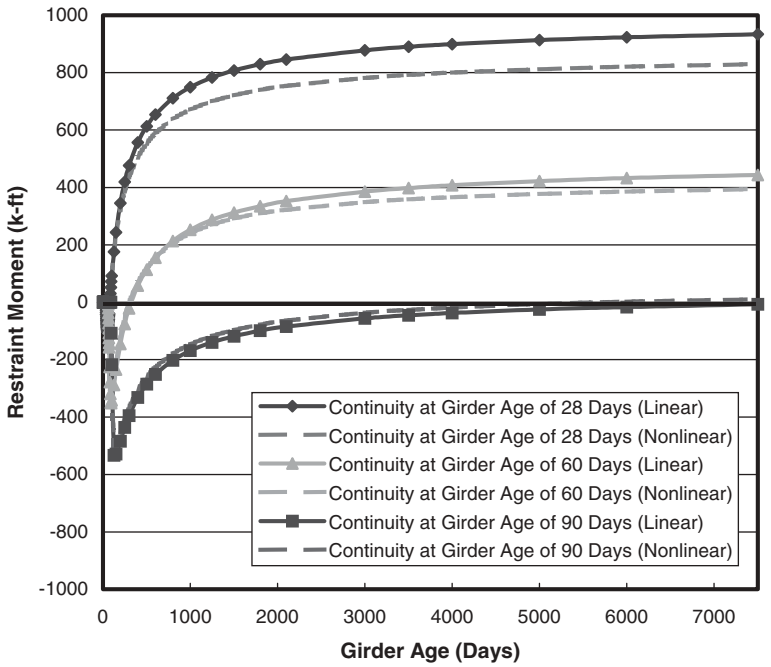

Figure D-7.2-1. Development of restraint moment with girder age—comparison of linear and nonlinear analysis results.

TABLE D-7.2-1 Comparison of restraint moments at interior support for linear and nonlinear analyses

		Girder Age at Continuity		
		28 Days	***60 Days***	***90 Days***
Maximum Positive Restraint Moment—Final Design				
Linear Analysis	*(k-ft)*	933.7	443.4	–7.3
Nonlinear Analysis	*(k-ft)*	829.7	394.2	10.1
% Change from Linear to Nonlinear		*–11.1%*	*–11.1%*	—
Peak Negative Restraint Moment—Final Design				
Linear Analysis	*(k-ft)*	–104.8	–351.5	–533.4
Nonlinear Analysis	*(k-ft)*	–95.3	–325.9	–503.5
% Change from Linear to Nonlinear		*–9.1%*	*–7.3%*	*–5.6%*

Note: Positive restraint moments are shown at a girder age of 7,500 days. Moments shown earlier were for a girder age of 10,000 days.

the design viable because the positive restraint moment is still well above the $1.2M_{cr}$ limit of 550.8 k-ft (see Section 5.2.1.2).

It appears that the nonlinear analysis reveals that the structure is not as stiff as would be assumed using the conventional elastic analysis. This may explain the reduction in both the maximum positive and negative moments because restraint moments are developed in response to deformations in the structure and because a less stiff structure will not develop as large a moment. Further work needs to be done to better understand the results of the nonlinear analysis for restraint moments, as well as the live-load analysis that is not discussed here.

DESIGN EXAMPLE 2: PCI BT-72 GIRDER

1 INTRODUCTION

This design example demonstrates the design and detailing of the positive moment connection for a typical continuous two-span bridge. The contract documents specify that the minimum girder age at continuity is 90 days. Therefore, this bridge is designed for continuity using the simplified approach (see DE1). Details of the girder design are not given here (again, see DE1, which is for an AASHTO Type III girder, for a description of the simplified approach and guidance in all other details of the design of this girder). This example is limited to a discussion of the design and detailing of the positive moment connection because some issues for this topic differ from those found in DE1. The design is based on the *AASHTO LRFD Specifications*, 2nd Edition with Interims through 2002, and the specifications proposed as part of this research.

2 DESCRIPTION OF BRIDGE

The bridge is a typical two-span structure with PCI BT-72 (bulb-T) girders and a composite deck slab. The span length for this bridge is approaching the maximum achievable for this girder and spacing. The geometry of the bridge is shown in Figures D-2-1 through D-2-3.

The girders are made continuous by a continuity diaphragm that connects the ends of the girders at the interior support. The connection is made when the deck slab is cast. Therefore, the girders are considered continuous for all loads applied to the composite section. A typical interior girder is considered.

The distance between centers of bearings (124.75 ft) is used for computing effects of loads placed on the simple-span girders before continuity is established. After continuity, the design span for the continuous girders is assumed to be from the center of the bearing at the expansion end of the girder to the center of the interior pier, or 126.00 ft (see Figure D-2-2). The space required between the ends of girders to accommodate the positive reinforcement connection should be considered when laying out the bridge (see Section 5.3 in DE1).

3 DESIGN PARAMETERS

3.1 Loads

For simplified design, loads are required for the design of the girder, but the positive moment connection is designed for $1.2M_{cr}$. Therefore, the loads are not required for this design example.

3.2 Materials and Material Properties

Material properties used for design are given below.

3.2.1 Girder Concrete

Material properties required for this design example are

$f'_c = 7.00$ ksi, and

$w_c = 0.150$ kcf.

3.2.2 Deck and Continuity Diaphragm Concrete

The same concrete properties are used for the deck and continuity diaphragm because they will be cast at the same time. Material properties required for this design example are given below. The subscript *d* is used to indicate properties related to the deck or diaphragm concrete:

$f_{cd} = 4.00$ ksi,

$f_{rd} = 0.480$ ksi, and LRFD Art. 5.4.2.6

$w_{cd} = 0.150$ kcf.

3.2.3 Prestressing Strand

For this example, the properties of the 0.6-in.-diameter low-relaxation seven-wire strand are:

$A_{ps} = 0.217$ in.$^{2;}$

$f_{pu} = 270$ ksi;

$f_{py} = 0.90\, f_{pu} = 243$ ksi;

$f_{pj} = 0.75\, f_{pu} = 202.5$ ksi; and

$E_p = 28{,}500$ ksi.

3.2.4 Mild Reinforcement

Mild reinforcement is as follows:

$f_y = 60$ ksi, and

$E_s = 29{,}000$ ksi.

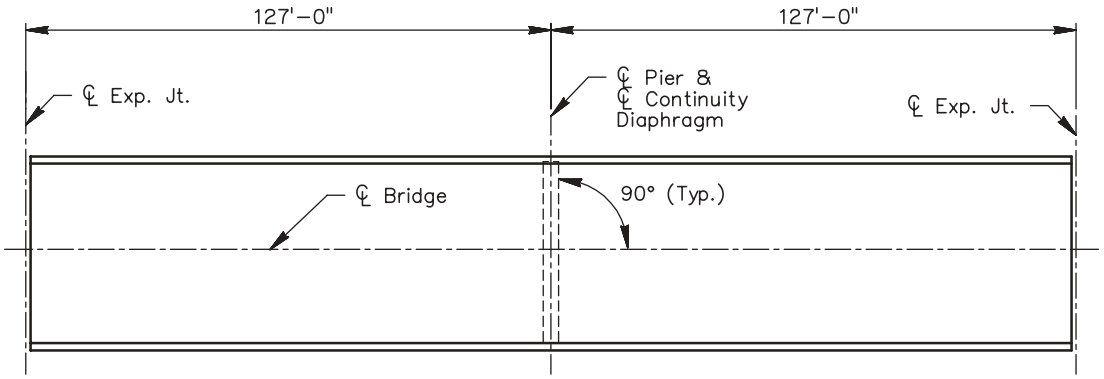

Figure D-2.1. Plan view of bridge.

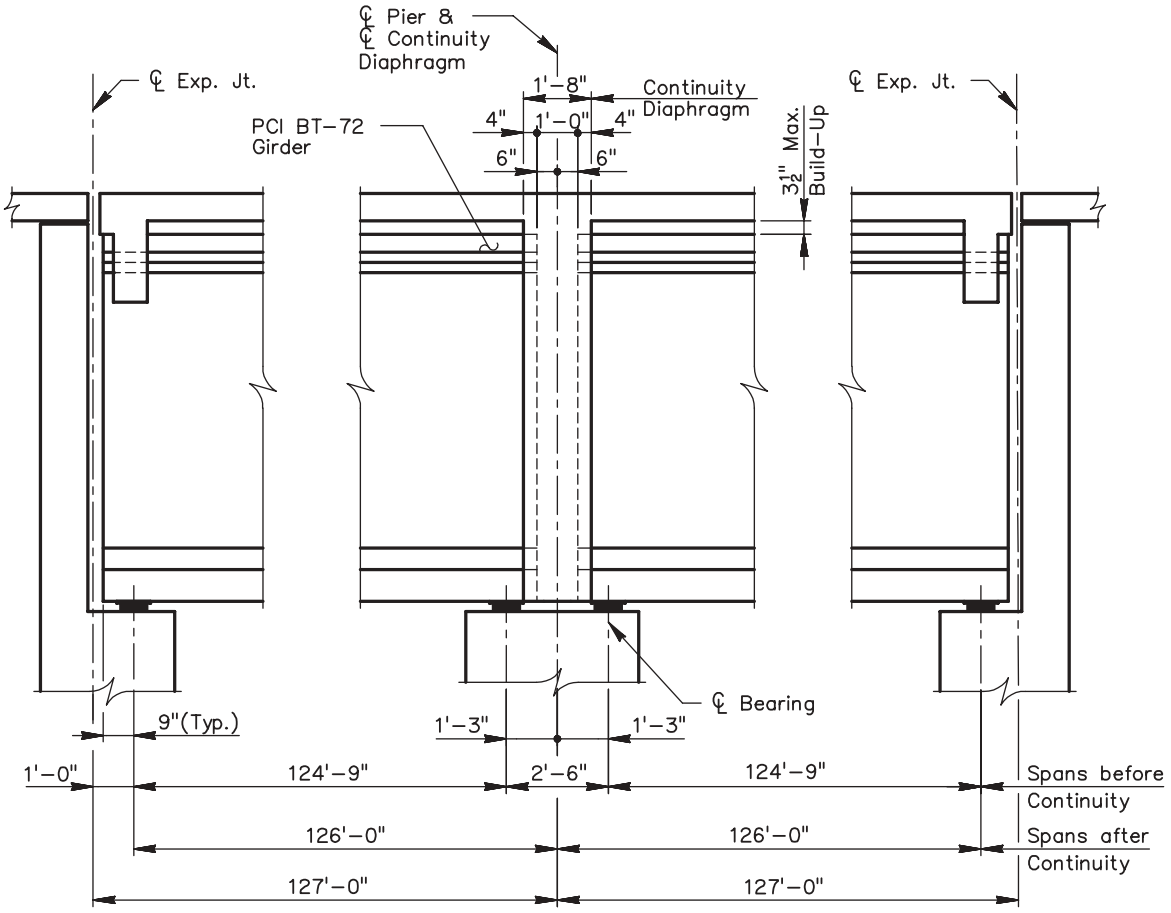

Figure D-2.2. Longitudinal section view of bridge.

3.3 Section Properties

3.3.1 Girder

The section properties for a standard PCI BT-72 are

$h = 72.00$ in.,

$A = 767.0$ in.^{2},

$I = 545{,}894$ in.^{4},

$y_b = 36.60$ in.,

$y_t = 35.40$ in.,

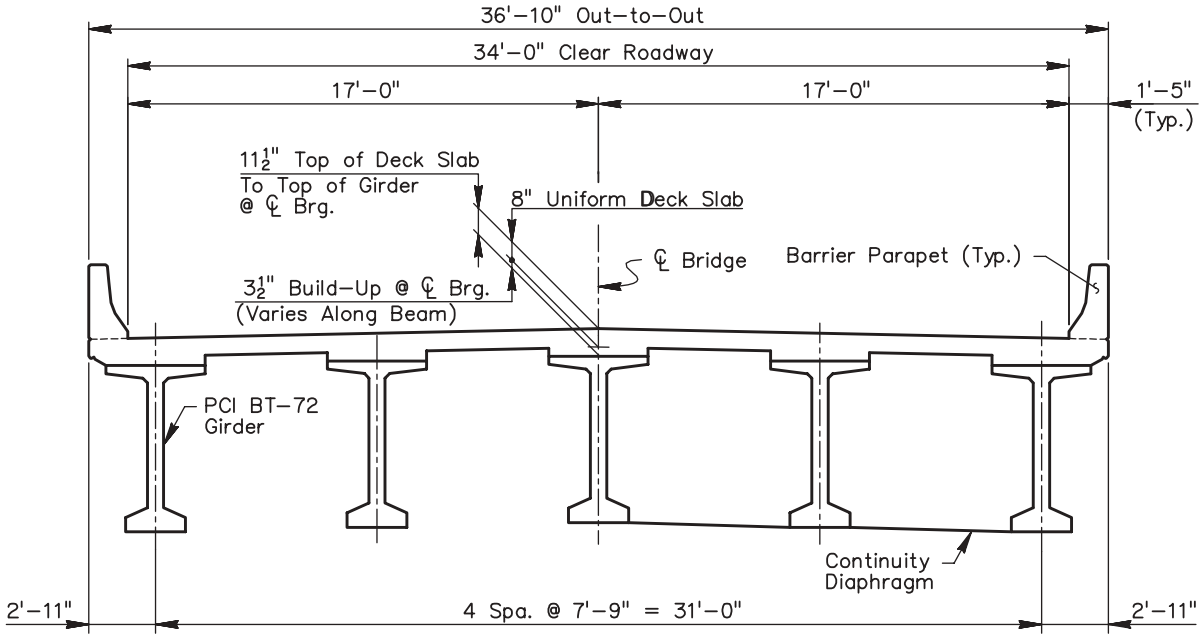

Figure D-2-3. Typical section of bridge.

S_b = 14,915 in.^{3}, and

S_t = 15,421 in.^{3}.

3.3.2 Continuity Diaphragm

The section properties of the continuity diaphragm are required to compute the cracking moment. The cross section of the continuity diaphragm is assumed to be composed of the girder shape, the build-up, and the effective width of deck for an interior girder. The remainder of the continuity diaphragm could be considered, but the assumed section provides a minimum area that may be effective.

Since the continuity diaphragm (between the ends of opposing girders) is composed entirely of deck concrete, transformation of the deck is not required. The build-up is included in the computation of these section properties because the full depth of the build-up is specified at the center of bearings, immediately adjacent to the continuity diaphragm. Including the build-up will increase the cracking moment.

The composite section properties used for girder design are similar, but are not used here because the deck has been transformed (deck and girder concrete compressive strengths are different) and the build-up was neglected.

The section properties for the continuity diaphragm are as follows:

h'_c = total depth of diaphragm section; the full 3½-in. build-up is included because the full build-up must be provided at CL bearings = 72 + 3.5 + 7.75 = 83.25 in.;

A'_c = 1,635 in.^{2};

I'_c = 1,265,630 in.^{4};

y'_{bc} = 58.80 in.;

y'_{tcd} = 24.45 in.;

S'_{bc} = 21,524 in.^{3}; and

S'_{tcd} = 51,764 in.^{3}.

4 REINFORCEMENT FOR POSITIVE MOMENTS AT INTERIOR SUPPORTS

The connections between girders at interior supports of bridges made continuous are subject to positive design moments. However, the positive moments are caused by minor live-load effects (for more than two-span bridges) and the restraint of time-dependent effects including creep, shrinkage, and temperature. Therefore, the positive design moments are not well-defined. Past research has questioned the benefit of providing a positive moment connection.

4.1 Positive Moment Connection

The proposed specifications recommend that positive moment connections be provided for all prestressed concrete bridges that are made continuous. This recommendation is based on providing the connection to enhance the

structural integrity of the structure so that it may be more robust and may be better able to resist unforeseen or extreme loads. Since the simplified approach is being used, where restraint moments are not computed, a positive moment connection is not required. However, a connection will be provided for this bridge as recommended by the proposed specifications.

The positive moment connection can be made using either an extended strand detail or a mild reinforcement detail. The design method for the extended strand detail is identical to that presented in DE-1, so it is not repeated here. Due to the small size of the bottom flange of the bulb-T girder, special detailing is needed for the mild reinforcement connection. Therefore, the design of the mild reinforcement detail is presented here.

4.2 Positive Design Moments

Since this bridge has two spans, the only positive moment that can be developed at the interior support is caused by restraint (considering the effects included in this design example). Bridges with more spans will develop positive moments at the interior supports from live loads. Because the simplified approach is being used for this design example, restraint moment is not considered, so there is no positive design moment.

In general, the reinforcement in the positive moment connection is proportioned using strength design to provide a factored resistance, ϕM_n, greater than the larger of the factored moment, M_u or $0.6M_c$, but not to exceed $1.2M_{cr}$. A design moment of $1.2M_{cr}$ is typically provided because testing and field experience have shown that this quantity of reinforcement, which is also the minimum quantity of reinforcement required by the AASHTO LRFD Specifications in many cases, has performed well. Reinforcement provided in excess of the quantity needed to resist $1.2M_{cr}$ has been shown to be less effective. Therefore, the positive moment connection for this design example will be taken as $1.2M_{cr}$.

4.2.1 Computation of Positive Cracking Moment at the Continuity Diaphragm

The positive cracking moment, M_{cr}, is computed using the section modulus for the bottom of the continuity diaphragm and the modulus of rupture for the deck concrete, f_{rd}, which is given in Section 3.2.2:

$$M_{cr} = f_{rd}\, S'_{bc} = 0.480(21{,}524) = 10{,}332 \text{ k-in} = 861 \text{ k-ft.}$$

The concrete strength of the deck, f'_{cd}, is used for this calculation because the confining effect of the precast girders in the continuity diaphragm is not significant for positive moments, where the deck slab is in compression. For reinforcement limits, the quantity $1.2M_{cr}$ is also computed:

$$1.2M_{cr} = 1{,}033 \text{ k-ft.}$$

4.3 Mild Reinforcement

Mild reinforcement will be used for this example to provide the positive moment connection. See DE1 for a more complete discussion of the issues to be considered in design of the positive moment connection using mild reinforcement, including development of the reinforcement into the girder and constructability issues.

4.3.1 Development and Detailing of Reinforcement into the Continuity Diaphragm

It is important that the distance between ends of opposing girders be great enough within a continuity diaphragm to allow the development of the positive reinforcement into the diaphragm. This should be considered during the initial stages of laying out a bridge.

The mild reinforcement is developed into the continuity diaphragm using a standard 90° hook. A No. 6 bar will be used for the connection. The required length of embedment, ℓ_{dh}, into the diaphragm to develop the hooked bar is computed according to LRFD Article 5.11.2.4:

$$\ell_{dh} = 9.98 \text{ in.; USE } 10 \text{ in.} \qquad \text{LRFD Eq. 5.11.2.4.1-1}$$

A reduction factor of 0.7 was used because conditions provide the required side and end cover. An embedment of the hook into the continuity diaphragm of 10 in. will be used. The distance between ends of girders across the continuity diaphragm will be taken as 12 in., so the 10-in. projection to the hook can be provided and still allow for construction tolerances. A standard hook length of 12 in. is used for the vertical leg (see Figure D-4.3.3-1).

A small additional reduction in the required hook embedment could be taken if the provided area of reinforcement is more than that required by analysis, but the design of the connection must be complete before the magnitude of this reduction is known. Therefore, 10 in. will be used in this example.

A cross bar of at least the same size as the hooked bar will be placed in the corner of the hooks, as shown in Figure D-4.3.1-1, to enhance the development of the hooked reinforcement into the diaphragm. A 180° hooked bar (hairpin) may also be used to provide two legs developed into the continuity diaphragm with only one hook, as shown in Figure D-4.3.3-2. The hooks are prebent, which simplifies fabrication and eliminates the tails of 90° hooks that may not fit within the forms during manufacturing. The use of hairpin bars is especially helpful when a large number of bars is required to satisfy positive moment requirements. The development length for 90° hooked reinforcement should be used to compute the required embedment of 180° hooks into the continuity diaphragm.

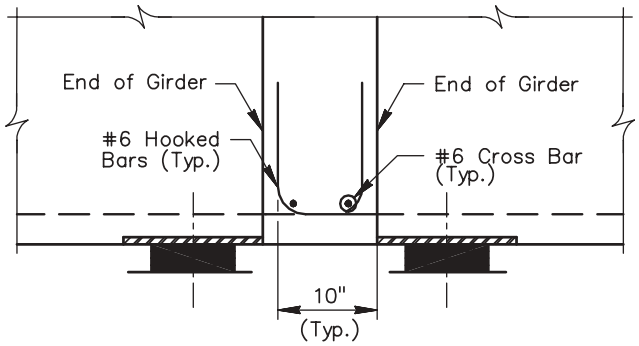

Figure D-4.3.1-1. Detail of reinforcement placement at positive moment connection (section view).

4.3.2 Required Area of Reinforcement

Using typical strength design procedures and the assumed design moment of 1.2 M_{cr}, the required area of reinforcement is computed to be

$A_s = 2.90$ in.^{2}

where

$f'_{cd} = 4.00$ ksi;
$f_y = 60$ ksi;
$M_u = 1.2M_{cr} = 1{,}033$ k-ft;
$\phi = 0.9$;
b' = width of compression face = width of bottom flange of girder = 26 in.;
$h'_c = 83.25$ in.;
g = distance from bottom of girder to centroid of reinforcement = 3.00 in. (one row of reinforcement centered between bottom rows of strands); and
d = effective depth from top of deck including build-up = $h'_c - g = 80.25$ in.

4.3.3 Reinforcement Layout

The required area of reinforcement, $A_s = 2.90$ in.^{2}, can be provided using seven No. 6 reinforcing bars. An odd number of bars can be used since the bars are already placed asymmetrically in order to facilitate meshing of the reinforcement from opposing girders. The seven bars can be placed in a single layer, satisfying the assumption that all of the reinforcement can be placed in a single layer. The actual area of reinforcement provided is as follows:

$A_{s\,prov} = 7(0.44 \text{ in.}^2) = 3.08 \text{ in.}^2 > A_s = 2.90 \text{ in.}^2$ OK

A layout for the reinforcement is shown in Figure D-4.3.3-1. If hairpin bars are used, the dimension g would have to be adjusted. For a No. 6 hairpin, the outside dimension of a standard 180° bend is 6 in. Therefore, if the bottom leg of the hairpin remained centered at 3 in. from the bottom of the girder, the new value for g would be located at the center of the hairpin, which would yield

$g = 3 - (5/8)/2 + (6/2) = 5.69$ in.;

$d = 77.56$ in.; and

$A_s = 3.00$ in.^{2}.

The required area of reinforcement for the No. 6 hairpins require four hairpins, with

$A_{s\,prov} = 8(0.44 \text{ in.}^2) = 3.52 \text{ in.}^2 > A_s = 3.00 \text{ in.}^2$ OK

However, it would be difficult to provide four hairpin bars in the bottom flange of a bulb-T girder and to place them so that bars from the opposing girder would mesh. The height of the flange is insufficient to place the hairpins far from the center of the girder.

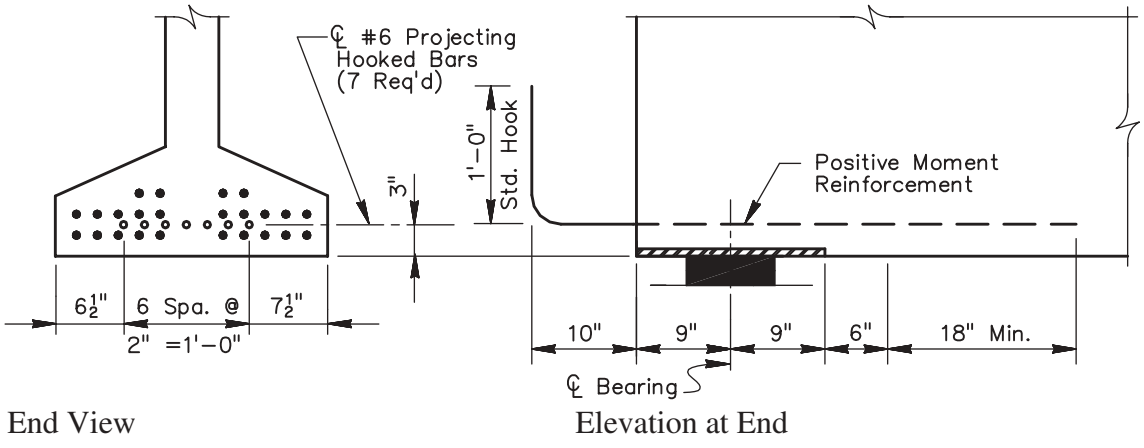

Figure D-4.3.3-1. Details of hooked reinforcement placement at end of girder.

A combination of bar sizes may prove more practical. Using two No. 5 and two No. 6 bars (the development of the No. 5 bars will be adequate since they are smaller than the No. 6 bars) provides

$A_{s\ prov} = 4(0.44\ \text{in.}^2) + 4(0.31\ \text{in.}^2)$
$= 3.00\ \text{in.}^2 = A_s = 3.00\ \text{in.}^2$ OK

The alternate reinforcement layout using hairpin bars is shown in Figure D-4.3.3-2. Two cross bars should be passed through the projecting loops of the hairpins to enhance the development, similar to the cross bars shown in Figure D-4.3.1-1.

When developing a layout for the positive moment reinforcement, the locations of all other reinforcement and embedments must be carefully considered to avoid conflicts and to provide adequate tolerances for fabrication. One example is that the positive moment reinforcement must avoid locations of headed studs attached to embedded plates.

4.3.4 Development of Reinforcement into Girder

The positive moment reinforcement must be developed into the girder (see discussion in DE1). The development lengths for the No. 5 and No. 6 bars are 15 in. and 18 in., respectively.

4.3.5 Termination of Positive Moment Reinforcement

The termination of positive moment reinforcement in the girder should be staggered. For hooked bars, two bar marks should be used with different horizontal leg lengths. For hairpin bars, the two legs of the hairpin should be detailed with different lengths, as shown in Figure D-4.3.3-2.

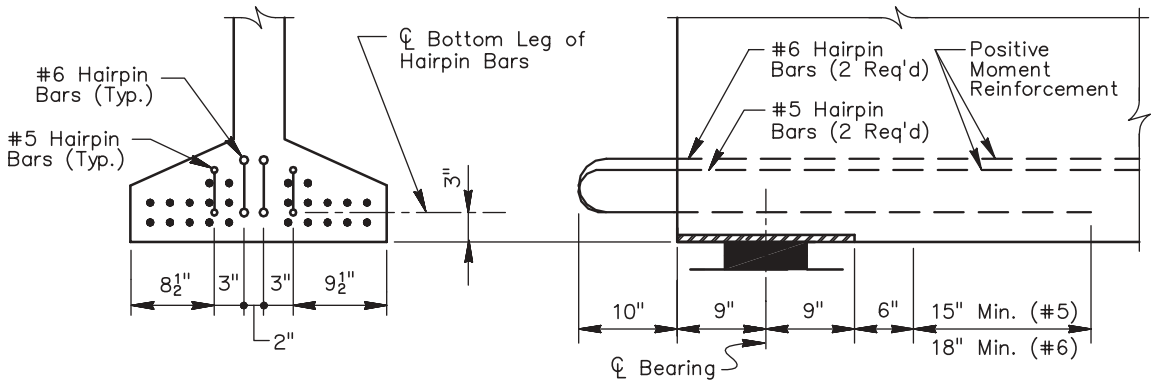

Figure D-4.3.3-2. Details of hairpin reinforcement placement at end of girder.

DESIGN EXAMPLE 3: 51-IN. DEEP BOX GIRDER SPREAD

1 INTRODUCTION

This design example demonstrates the design and detailing of the positive moment connection for a typical continuous two-span bridge. The contract documents specify that the minimum girder age at continuity is 90 days. Therefore, this bridge is designed for continuity using the simplified approach (see DE1).

Details of the girder design are not given here. See DE1, which is for an AASHTO Type III girder, for a description of the simplified approach and guidance in all other details of the design of this girder. This example is limited to a discussion of the design and detailing of the positive moment connection because some issues for this topic differ from those found in DE1. The design is based on the AASHTO LRFD Specifications, 2nd Edition with Interims through 2002, and the specifications proposed as part of this research.

2 DESCRIPTION OF BRIDGE

The bridge is a typical two-span structure with spread 51-in.-deep box girders and a composite deck slab. The geometry of the bridge is shown in Figures D-2-1 through D-2-3. The girders are made continuous by a continuity diaphragm that connects the ends of the girders at the interior support. The connection is made when the deck slab is cast. Therefore, the girders are considered continuous for all loads applied to the composite section. A typical interior girder is considered.

The distance between centers of bearings (84.83 ft) is used for computing the effects of loads placed on the simple-span girders before continuity is established. After continuity, the design span for the continuous girders is assumed to be from the center of bearing at the expansion end of the girder to the center of the interior pier, or 86 ft. (see Figure D-2-2). The space required between ends of girders to accommodate the positive reinforcement connection should be considered when laying out the bridge (see Section 5.3 in DE1).

3 DESIGN PARAMETERS

3.1 Loads

For simplified design, loads are required for the design of the girder, but the positive moment connection is designed for $1.2M_{cr}$. Therefore, the loads are not required for this design example.

3.2 Materials and Material Properties

Material properties used for design are given below.

3.2.1 Girder Concrete

Material properties required for this design example are as follows:

$f'_c = 6.00$ ksi, and

$w_c = 0.150$ kcf.

3.2.2 Deck and Continuity Diaphragm Concrete

The same concrete properties are used for the deck and continuity diaphragm because they will be cast at the same time. Material properties required for this design example are given below. The subscript *d* is used to indicate properties related to the deck or diaphragm concrete:

$f'_{cd} = 4.50$ ksi,

$f_{rd} = 0.509$ ksi, and LRFD Art. 5.4.2.6

$w_{cd} = 0.150$ kcf.

3.2.3 Prestressing Strand

For this example, the properties of the 0.5-in.-diameter low-relaxation seven-wire strand are:

$A_{ps} = 0.153$ in.^{2};

$f_{pu} = 270$ ksi;

$f_{py} = 0.90\, f_{pu} = 243$ ksi;

$f_{pj} = 0.75\, f_{pu} = 202.5$ ksi; and

$E_p = 28{,}500$ ksi.

3.2.4 Mild Reinforcement

Mild reinforcement is as follows:

$f_y = 60$ ksi, and

$E_s = 29{,}000$ ksi.

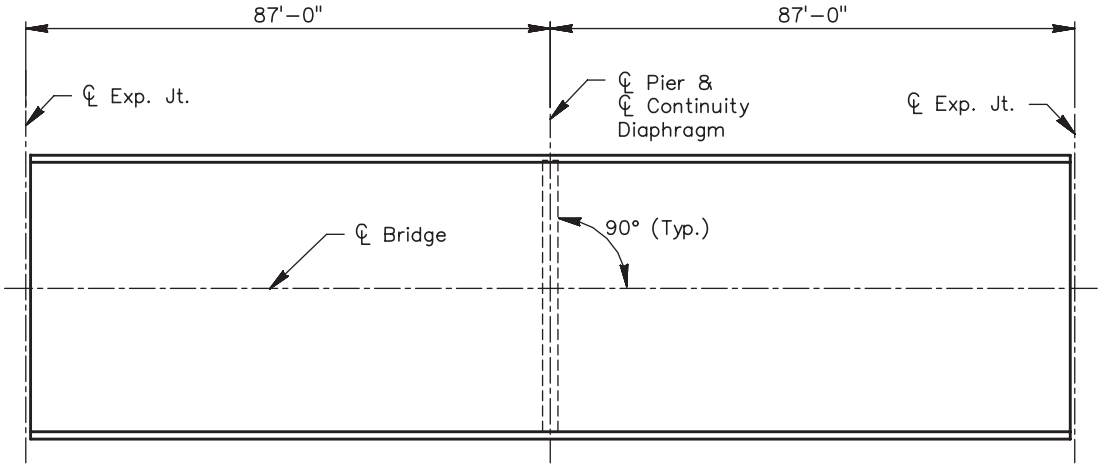

Figure D-2-1. Plan view of bridge.

3.3 Section Properties

3.3.1 Girder

The section properties for the 51-in. box girder are as follows (see Figure D-3.3.1-1):

$h = 51.0$ in.,

$A = 908.0$ in.^{2},

$I = 309{,}865$ in.^{4},

$y_b = 22.95$ in.,

$y_t = 28.05$ in.,

$S_b = 13{,}502$ in.^{3}, and

$S_t = 11{,}047$ in.^{3}.

3.3.2 Continuity Diaphragm

The section properties of the continuity diaphragm are required to compute the cracking moment. The cross section

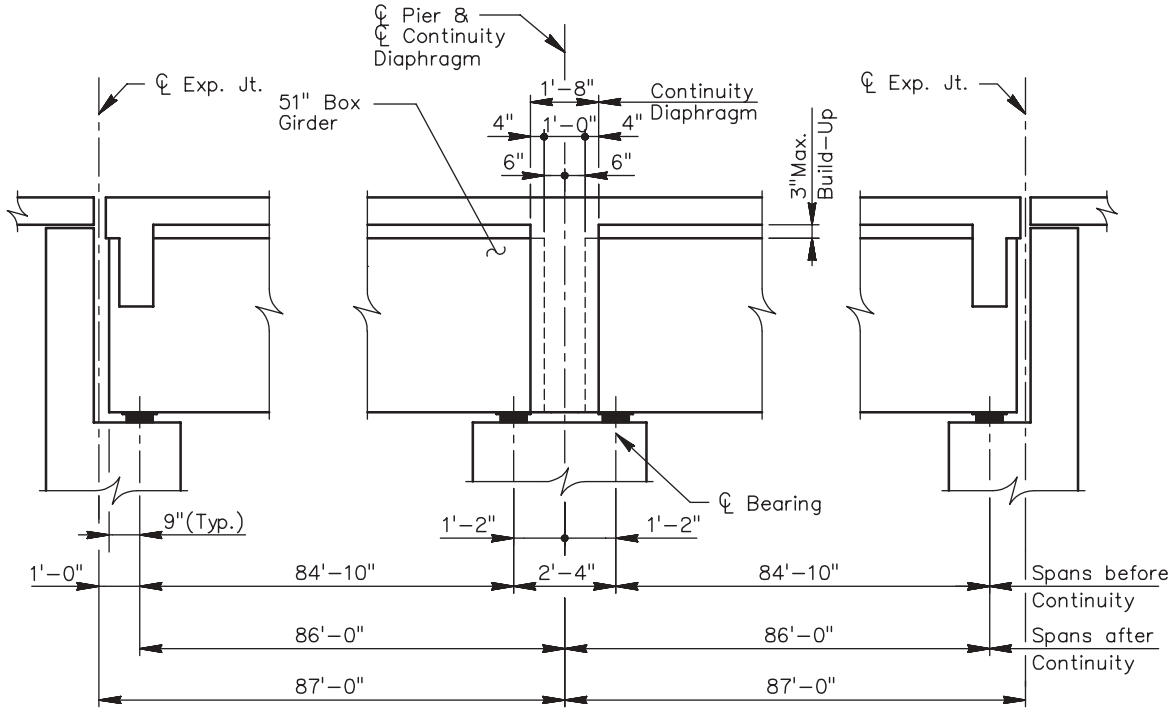

Figure D-2-2. Longitudinal section view of bridge.

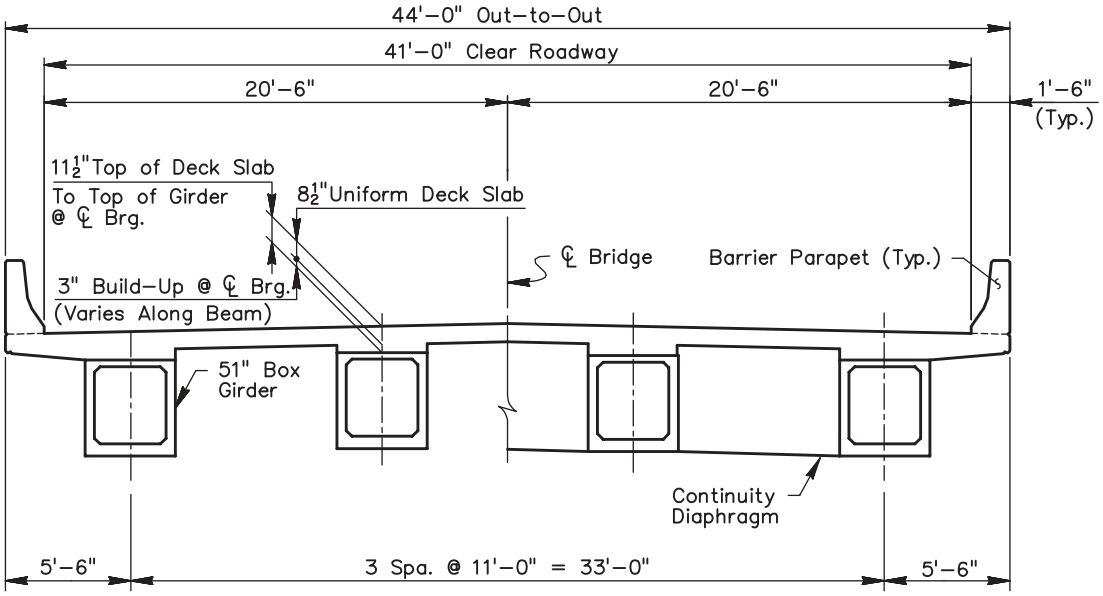

Figure D-2-3. Typical section of bridge.

of the continuity diaphragm is assumed to be composed of the outer dimensions of the box girder shape, the build-up, and the effective width of deck for an interior girder. The section properties for the box girder given above in Section 3.3.1 are for the box girder including the void. However, the end of the girder at the continuity diaphragm is a solid rectangle, so the properties of the solid section must be used in computing the properties of the diaphragm. The remainder of the continuity diaphragm outside the limits of the box girder could be considered, but the assumed section provides a minimum area that may be effective.

Since the continuity diaphragm (between the ends of opposing girders) is composed entirely of deck concrete, transformation of the deck is not required. The build-up is included in the computation of these section properties because the full depth of the build-up is specified at the center of the bearings, immediately adjacent to the continuity diaphragm. Including the build-up will increase the cracking moment.

The composite section properties used for girder design are similar, but are not used here because the deck has been transformed (deck and girder concrete compressive strengths are different) and the build-up was neglected. The section properties for the continuity diaphragm are

h_c' = total depth of diaphragm section; the full 3-in. build-up is included because the full build-up must be provided at CL bearings; = 51 + 3 + 8.25 = 62.25 in.;

$A_c' = 3{,}681$ in.^{2};

$I_c' = 1{,}517{,}929$ in.^{4};

$y_{bc}' = 34.51$ in.;

$y_{tcd}' = 27.74$ in.;

$S_{bc}' = 43{,}982$ in.^{3}; and

$S_{tcd}' = 54{,}724$ in.^{3}.

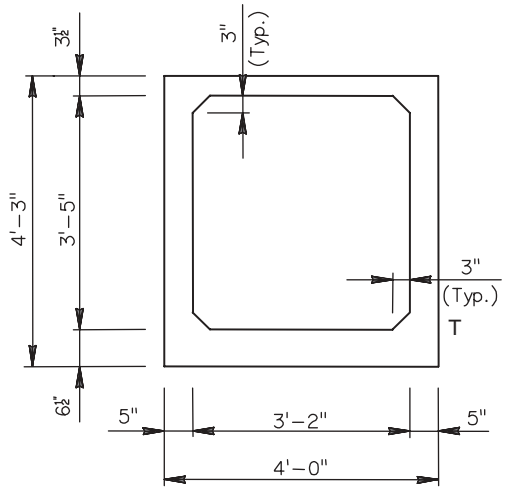

Figure D-3.3.1-1. 51-in. box girder dimensions.

4 REINFORCEMENT FOR POSITIVE MOMENTS AT INTERIOR SUPPORTS

The connections between girders at interior supports of bridges made continuous are subject to positive design

moments. However, the positive moments are caused by minor live-load effects (for more than two-span bridges) and the restraint of time-dependent effects including creep, shrinkage, and temperature. Therefore, the positive design moments are not well defined. Past research has questioned the benefit of providing a positive moment connection.

4.1 Positive Moment Connection

The proposed specifications recommend that positive moment connections be provided between all prestressed concrete girders made continuous. This recommendation is based on providing the connection to enhance the structural integrity of the structure so that it may be more robust and better able to resist unforeseen or extreme loads. Since the simplified approach is being used, where restraint moments are not computed, a positive moment connection is not required. However, a connection will be provided for this bridge as recommended by the proposed specifications.

As with DE-1 and DE-2, either an extended strand or mild reinforcement detail could be used for the positive moment connection. A mild reinforcement detail is shown here. The extended strand connection would be designed and detailed exactly as in DE-1, so it is not repeated here.

4.2 Positive Design Moments

Since this bridge has two spans, the only positive moment that can be developed at the interior support is caused by restraint (considering the effects included in this design example). Bridges with more spans will develop positive moments at the interior supports from live loads. Because the simplified approach is being used for this design example, restraint moment is not considered, so there is no positive design moment.

In general, the reinforcement in the positive moment connection is proportioned using strength design to provide a factored resistance, ϕM_n, greater than the larger of the factored moment, M_u, or $0.6M_{cr}$, but not to exceed $1.2M_{cr}$. A design moment of $1.2M_{cr}$ is typically provided because testing and field experience have shown that this quantity of reinforcement, which is also the minimum quantity of reinforcement required by the AASHTO LRFD Specifications in many cases, has performed well. Reinforcement provided in excess of the quantity needed to resist $1.2M_{cr}$ has been shown to be less effective. Therefore, the positive moment connection for this design example will be taken as $1.2M_{cr}$.

4.2.1 Computation of Positive Cracking Moment at the Continuity Diaphragm

The positive cracking moment, M_{cr}, is computed using the section modulus for the bottom of the continuity diaphragm and the modulus of rupture for the deck concrete, f_{rd}, which is given in Section 3.2.2:

$$M_{cr} = f_{rd} S'_{bc} = 0.509(43{,}982) = 22{,}387 \text{ k-in} = 1{,}866 \text{ k-ft.}$$

The concrete strength of the deck, f'_{cd}, is used for this calculation because the confining effect of the precast girders in the continuity diaphragm is not significant for positive moments, where the deck slab is in compression. For reinforcement limits, the quantity $1.2M_{cr}$ is also computed:

$$1.2M_{cr} = 2{,}239 \text{ k-ft.}$$

4.3 Mild Reinforcement

Mild reinforcement will be used for this example to provide the positive moment connection. See DE1 for a more complete discussion of the issues to be considered in design of the positive moment connection using mild reinforcement, including development of the reinforcement into the girder and constructability issues.

4.3.1 Development and Detailing of Reinforcement into the Continuity Diaphragm

It is important that the distance between ends of opposing girders be great enough within a continuity diaphragm to allow development of the positive reinforcement into the diaphragm. This should be considered during the initial stages of laying out a bridge.

The mild reinforcement is developed into the continuity diaphragm using a standard 90° hook. A No. 6 bar will be used for the connection. The required length of embedment, ℓ_{dh}, into the diaphragm to develop the hooked bar is computed according to LRFD Article. 5.11.2.4:

$$\ell_{dh} = 9.98 \text{ in.; USE } 10 \text{ in.} \qquad \text{LRFD Eq. 5.11.2.4.1-1}$$

A reduction factor of 0.7 was used because conditions provide the required side and end cover. An embedment of the hook into the continuity diaphragm of 10 in. will be used. The distance between ends of girders across the continuity diaphragm will be taken as 12 in., so the 10-in. projection to the hook can be provided and still allow for construction tolerances. A standard hook length of 12 in. is used for the vertical leg (see Figure D-4.3.3-1).

A small additional reduction in the required hook embedment could be taken if the provided area of reinforcement is more than required by analysis, but the design of the connection must be complete before the magnitude of this reduction is known. Therefore, 10 in. will be used in this example.

A cross bar of at least the same size as the hooked bar will be placed in the corner of the hooks, as shown in Figure D-4.3.1-1, to enhance the development of the hooked reinforcement into the diaphragm.

A 180° hooked bar (hairpin) may also be used to provide two legs developed into the continuity diaphragm with only one hook. However, hairpin bars are not generally practical for box girder sections because the top leg of the hairpin would typically extend beyond the end of the solid portion of the section and into the void. Therefore, adequate development may not be available for the top leg without altering the dimensions of the end block.

4.3.2 Required Area of Reinforcement

Using typical strength design procedures and the assumed design moment of 1.2 M_{cr}, the required area of reinforcement is computed to be

$A_s = 8.60$ in.^{2}

where

$f'_{cd} = 4.50$ ksi;
$f_y = 60$ ksi;

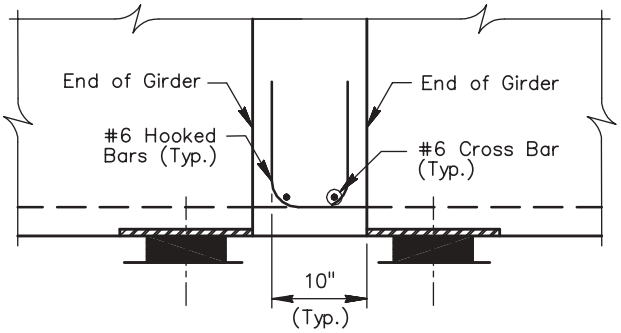

Figure D-4.3.1-1. Detail of reinforcement placement at positive moment connection (section view).

$M_u = 1.2M_{cr} = 2{,}239$ k-ft;
$\phi = 0.9$;
b' = width of compression face = width of bottom flange of box girder = 48 in.;
$h'_c = 62.25$ in.;
g = distance from bottom of girder to centroid of reinforcement
= 3.00 in. (one row of reinforcement centered between bottom rows of strands); and
d = effective depth from top of deck including build-up
$= h'_c - g = 59.25$ in.

The much larger section of the continuity diaphragm results in a larger design moment than for the other sections considered in these design examples. However, the area in which the reinforcement can be placed is also much greater.

4.3.3 Reinforcement Layout

The required area of reinforcement, $A_s = 8.60$ in.^{2}, can be provided using twenty No. 6 reinforcing bars. Due to the width of the girder, the twenty bars can be placed in a single layer, satisfying the assumption that all of the reinforcement can be placed in a single layer. The actual area of reinforcement provided is as follows:

$A_{s\,prov} = 20(0.44 \text{ in.}^2) = 8.80 \text{ in.}^2 > A_s = 8.60 \text{ in.}^2$ OK

A layout for the reinforcement is shown in Figure D-4.3.3-1.

Alternate positive reinforcement layouts could be developed using two layers of reinforcement or using hairpin bars. When developing a layout for the positive moment reinforcement, the locations of all other reinforcement and embedments must be carefully considered to avoid conflicts and to provide adequate tolerances for fabrication. One example is that the positive moment reinforcement must avoid locations of headed studs attached to embedded plates.

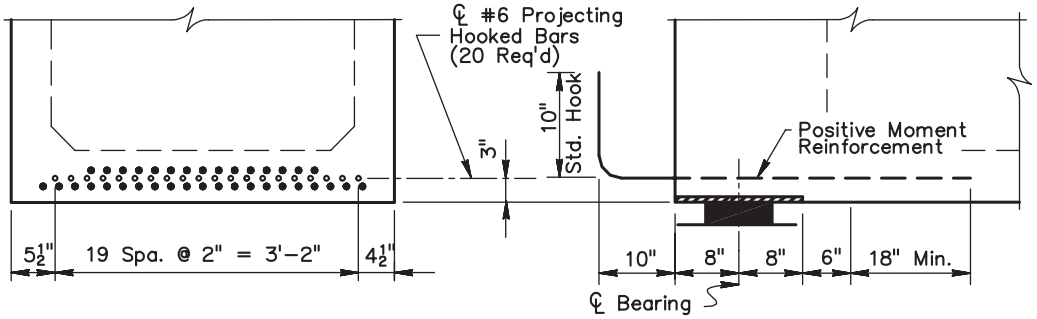

Figure D-4.3.3-1. Details of reinforcement placement at end of girder.

4.3.4 Development of Reinforcement into Girder

The positive moment reinforcement must be developed into the girder (see discussion in DE1). The development length for the No. 6 bars is 18 in.

4.3.5 Termination of Positive Moment Reinforcement

The termination of positive moment reinforcement in the girder should be staggered. For hooked bars, two bar marks should be used with different horizontal leg lengths. For hairpin bars, the two legs of the hairpin should be detailed with different lengths, as shown in Figure D-4.3.3-2 of DE2.

DESIGN EXAMPLE 4: AASHTO BIII-48 BOX GIRDER (ADJACENT)

1 INTRODUCTION

This example demonstrates the design of a continuous two-span bridge using the specifications proposed as part of this research. The precast/prestressed concrete box girders are made continuous by the placement of a continuity diaphragm at the interior support, which fills the gap between ends of girders from adjacent spans.

This example illustrates the design of an adjacent box girder bridge that does not have a composite deck. Therefore, continuity is established when the continuity diaphragm is placed. The bridge then becomes continuous for loads placed on the structure after the continuity diaphragm is in place. This is an experimental concept that has not been built or tested, so this design example is intended to explore the feasibility of its use.

Once made continuous, the bridge is subject to restraint moments that may develop from the time-dependent effects of creep and shrinkage. Restraint moments are caused by restrained deformations in the bridge. Analysis indicates that the restraint moments vary linearly between supports. For this two-span bridge, the restraint moments reach maximum values at the center of the interior pier. Reinforcement is provided at the interior pier to resist moments caused by time-dependent effects and applied loads. Restraint moments also affect the moments within the spans. Therefore, girder designs must be adjusted to account for the additional positive moments caused by restraint.

Because this bridge does not have a composite deck, a negative restraint moment due to creep and shrinkage effects does not develop since the differential shrinkage between the deck and precast girder is the source of the negative moment. This also means that the initial negative moment spike that is experienced by conventional bridges with a composite deck will not occur, and negative restraint moment will not be available to reduce the effect of the creep in the girder that produces the positive restraint moment.

Variations in temperature also cause restraint moments in continuous bridges. This would be the only typical source of negative restraint moments for this bridge. However, this condition will not be considered in this example. The application of any moment from temperature effects would be combined with the effects considered in this example, and the same design criteria must be satisfied.

Only those details of design that are affected by the use of continuity are presented in this design example. The focus of the example will therefore be on flexural design, which is most significantly affected by the consideration of restraint moments. While the design shears, reactions, and deflections are also affected when compared with design for simple-span bridges, the procedures for design are not altered. Therefore, design for these quantities will not be presented.

In a two-span bridge made continuous, positive moments at the interior pier develop only from restraint moments. These positive design moments are resisted by mild reinforcement or strands that are extended into the continuity diaphragm from the bottom flange of the girder. This positive moment connection is proportioned using strength design methods to resist any developed restraint moments or to provide a minimum quantity of reinforcement. The positive moment connection is also provided to enhance the structural integrity of the bridge. Construction details for the positive moment connection will be discussed in this example.

Negative moments at the interior pier of this bridge are caused by dead loads applied to the composite continuous structure and live loads. Negative restraint moments cannot form due to creep and shrinkage. However, this design is similar to the design of other precast/prestressed concrete girder bridges made continuous because negative restraint moments are neglected in conventional designs as allowed by the proposed specifications. In this example, negative moments are resisted by mild reinforcement added to the top of the prestressed concrete girder rather than being placed in a composite deck, which is the most common approach to providing a negative moment connection. The reinforcement in the negative moment connection is proportioned using strength design methods.

1.1 Age of Girders at Continuity

To demonstrate the significance of girder age when continuity is established, designs will be performed assuming that continuity is established at the following girder ages:

- 7 days,
- 28 days, and
- 90 days.

If contract documents specify the minimum girder age at continuity, the minimum age is known. If the minimum girder age at continuity is 90 days, the proposed specifications allow the designer to neglect the effect of restraint moments. This is referred to as the "simplified approach." If the minimum girder age at continuity is not specified, the designer must use the "general approach," which considers the effect of restraint moments. See Section 4 for a discussion of the two approaches. Since positive restraint moments have the most significant effect on designs, assuming an early age at continuity will result in higher positive restraint moments.

Two early ages for continuity (less than 90 days) are considered in this example to provide information for the designer to decide whether to set a minimum girder age at continuity and what that age would be. A girder age of 7 days at continuity is used in this example because continuity could be established very early as there is no deck or continuity diaphragm forming or reinforcement to place prior to casting the continuity diaphragm.

1.2 Design Programs Used

Most of the design calculations were performed using a commercially available computer program. This was supplemented by hand and spreadsheet computations to obtain the quantities needed for this design. Restraint moments were estimated using the RESTRAINT Program that was developed as part of this research project. Fatigue design loads were computed using the QConBridge Program, which is available free of charge from the Washington State DOT website (see Subappendix C).

2 DESCRIPTION OF BRIDGE

The bridge is a two-span structure in which AASHTO Type BIII-48 box girders (see Figure D-3.6.1-1) are placed side-by-side (adjacent). An asphalt wearing surface is applied after continuity is established to create the riding surface and cross slope on the bridge. The span length for this bridge is in the middle of the usual span range for this girder in a side-by-side configuration. The geometry of the bridge is shown in Figures D-2-1 through D-2-3.

The girders are made continuous by a continuity diaphragm that connects the ends of the girders at the interior support. For this bridge, the continuity diaphragm will require no forming except at the end of the diaphragm, since the girders are placed side by side. The continuity connection is made when the continuity diaphragm is cast; therefore, the girders are considered continuous for all loads applied after the diaphragm is placed.

During or after the girders are erected, grout keys between girders are filled and transverse ties are installed. Details and sequencing of installation for the transverse ties and grout keys are not discussed here because they are not a feature affected by continuity. Details of such construction can be found in the *PCI Bridge Design Manual*.

The AASHTO LRFD Specifications mention two types of connection between adjacent box girders. The type of connection affects the live-load distribution (see AASHTO LRFD Specifications Table 4.6.2.2.2b-1). The first type of connection assumes that the transverse connection between girders is only capable of preventing relative vertical displacement at the interface. A second, more-effective type of connection between boxes causes the entire bridge to function as a unit. However, the use of the more-effective (and sophisticated) connection details has not yet become widespread. Therefore, the first type of connection, which is the more typical and conservative type of connection between adjacent box members, will be used for this design example.

The distance between the centers of bearings (84.83 ft.) is used for computing effects of loads placed on the simple-span girders before continuity is established. After continuity, the design span for the continuous girders is assumed to be from the center of bearing at the expansion end of the girder to the center of the interior pier, or 86.00 ft. See Figure D-2-2. The space required between ends of girders to accommodate the positive reinforcement connection should be considered when laying out the bridge. See Section 5.3.

This design example demonstrates the design of an interior girder. Design of an exterior girder would be similar except for loads. For this bridge, the interior girder design governs.

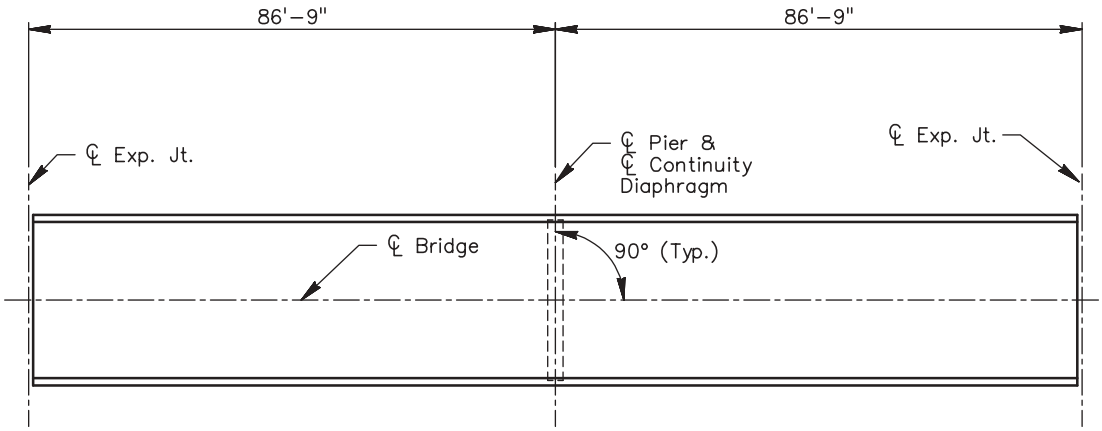

Figure D-2-1. Plan view of bridge.

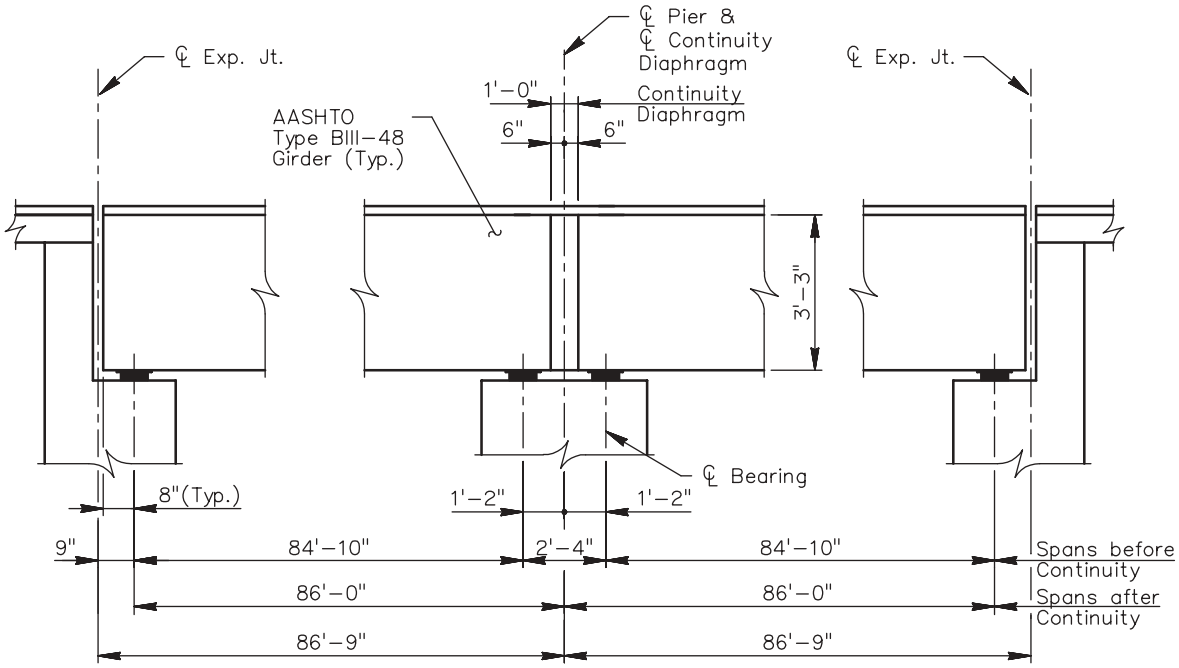

Figure D-2-2. Longitudinal section view of bridge.

3 DESIGN ASSUMPTIONS AND INITIAL COMPUTATIONS

3.1 Specifications

AASHTO LRFD Bridge Design Specifications, 2nd Edition with Interims through 2002, is used for this design example**.** References to articles, equations and tables in the AASHTO LRFD Specifications will be preceded by the prefix "LRFD" to differentiate them from other references in this design example.

Proposed revisions have been developed as part of this research project (see Subappendix C). References to articles and equations in the proposed specifications will be preceded by the prefix "*proposed*" to differentiate them from references to items in the AASHTO LRFD Specifications.

3.2 Loads

The loads are as follows.

- **Live load:** HL-93 with 33% dynamic allowance (IM) on the design truck. Live-load distribution factors are computed using equations in LRFD Table 4.6.2.2.2b-1 for

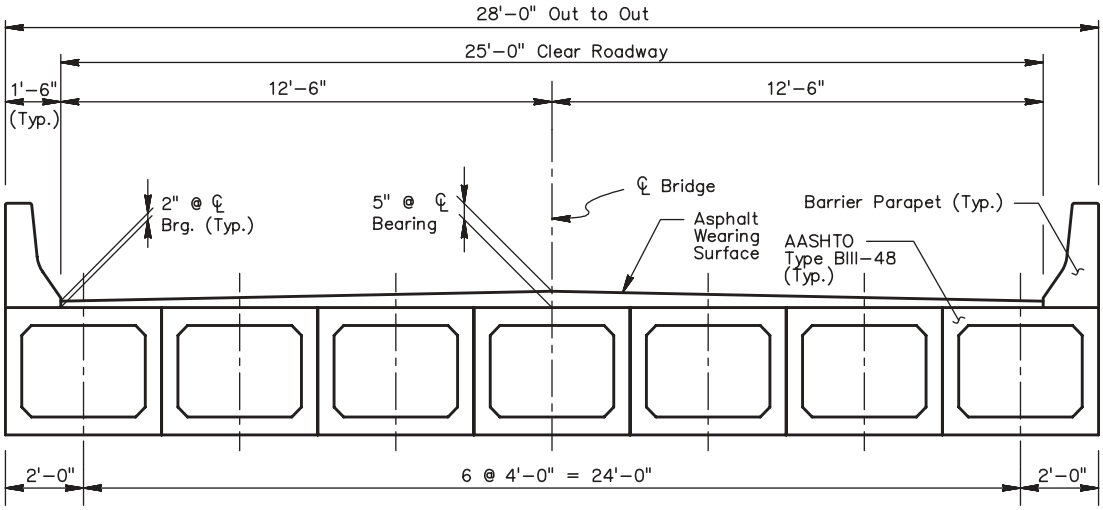

Figure D-2-3. Typical section of bridge.

section type (g) (see LRFD Table 4.6.2.2.1-1), assuming that the girders are connected only enough to prevent relative vertical displacement at the interface.
= 0.333 lanes per girder, regardless of number of lanes loaded

- **Girder self weight:** The unit weight of girder concrete is 0.150 kcf. The weight of the grout in the shear keys is neglected.
  = 0.847 klf
- **Internal diaphragms:** Internal diaphragms, 9 in. thick, are placed at quarter points. The area of each diaphragm is 7.26 sf.
  = 0.817 kips each at 3 locations within the span
- **Asphalt wearing surface:** An average asphalt thickness of 4 in. is used for dead load of the wearing surface, with a unit weight of 0.140 kcf (LRFD Table 3.5.1-1). This weight is considered as a wearing surface for strength design (use a load factor of 1.5).
  = 0.047 ksf on each 4 ft wide girder
  = 0.187 klf for an interior girder (on continuous span)
- **Parapet load:**
  = 0.371 klf per parapet, or 0.742 klf for both parapets
  Assume the load of each parapet is distributed to three girders on each side of bridge.
  = 0.124 klf for an interior girder (on continuous span)
- **Future wearing surface:**
  = 0.025 ksf on each 4-ft-wide girder
  = 0.100 klf for each girder (on continuous span)

3.3 Materials and Material Properties

Material properties used for design are given below.

3.3.1 Girder Concrete

3.3.1.1 Basic Properties. Girder concrete strengths and properties remain the same for all designs considered in this design example.

f'_{ci} = 4.50 ksi,

f'_c = 6.00 ksi,

f_r = 0.587 ksi, LRFD Art. 5.4.2.6

E_{ci} = 4,067 ksi, LRFD Eq. 5.4.2.4-1

E_C = 4,696 ksi, and LRFD Eq. 5.4.2.4-1

w_c = 0.150 kcf.

3.3.1.2 Time-Dependent Properties. Time-dependent concrete properties (creep and shrinkage) are needed only if restraint moments are being included in the analysis and design. Therefore, the following computations are not required if the simplified approach (see Section 4) is being used.

Measured values of the ultimate creep coefficient and the ultimate shrinkage strain for the concrete should be used if possible. However, measured creep and shrinkage properties are rarely available. Therefore, these quantities are usually estimated. For this design example, the equations in LRFD Article 5.4.2.3 are used to estimate creep and shrinkage. See the AASHTO LRFD Specifications for secondary equations and complete definitions of the terms used in the calculations that follow.

Restraint moments are very sensitive to variations in creep and shrinkage values, so possible estimates should be used. Other methods for estimating creep and shrinkage properties may be used as permitted by LRFD Article 5.4.2.3.1.

3.3.1.2.1 Volume–to–surface area ratio. Both creep and shrinkage equations are dependent upon the volume–to–surface area ratio (*V/S*). Since the equations are sensitive to this quantity and the analysis for restraint moments is sensitive to creep and shrinkage values, it is important to carefully consider the computation of this ratio.

The *V/S* is generally computed using the equivalent ratio of the cross-sectional area to the perimeter. This quantity can be easily computed for most sections. For the standard AASHTO Type BIII-48 girder, the area may be obtained from a table of section properties:

A = 812.5 in.^{2}.

The area above includes deductions for the shear keys, but these could be neglected.

LRFD Article 5.4.2.3.2 indicates that only the surface area exposed to atmospheric drying should be included in the computation of *V/S*. Prior to installation in the bridge, the entire exterior surface of the girder is exposed to drying. Once the bridge is completed with the wearing surface in place, it could be reasoned that the top of the girder would not be exposed to drying. However, this refinement will be neglected for this example.

The computation of the perimeter exposed to drying requires consideration of the enclosed void. LRFD Article 5.4.2.3.2 indicates that only 50% of the perimeter of a poorly ventilated interior void should be included in the perimeter. The void in the box girder will have one or more small vents, so it can be considered as poorly ventilated. Therefore, the reduction of the perimeter for the interior void will be included in computing the perimeter. The side faces of the boxes, since they are placed very close to one another, could also be considered as poorly ventilated. However, this adjustment will not be considered here since the side faces will be exposed to drying prior to completion of the bridge. The slight modification

of the exterior perimeter for shear keys will be neglected. Therefore, the perimeter will be computed as follows:

p = Exterior perimeter + 50% of interior perimeter
= 2(48 + 39) + 50%[2(38 + 28) − 4(2(3) − 4.24)]
= 236.5 in.

Therefore, *V/S* will be

$V/S = A/p = 812.5/236.5 = 3.44$ in.

It should be noted that the commentary to the specifications indicates that the maximum value of *V/S* considered in the development of the equations for the creep and shrinkage factors in which *V/S* appears was 6.0 in. Therefore, it would appear that this value may be considered a practical upper limit for the ratio when using the equations in the specifications.

3.3.1.2.2 Ultimate creep coefficient. The creep coefficient may be taken as follows:

$$\psi(t, t_i) = 3.5 k_c k_f \left(1.58 - \frac{H}{120}\right) t_i^{-0.118} \frac{(t - t_i)^{0.6}}{10.0 + (t - t_i)} 0.6. \qquad \text{LRFD Eq. 5.4.2.3.2-1}$$

Significant load is placed on the girder at release. Therefore, t_i, the age of concrete when load is initially applied, is taken to be the age of the girder at release, or typically 1 day. To determine the ultimate value for the creep coefficient, ψ_u, where $t = \infty$, the final term in the equation is assumed to approach unity:

$\psi_u = \psi(\infty, 1 \text{ day}) = 2.00$

where

k_c = factor for $V/S = 0.800$; LRFD Eq. C5.4.2.3.2-1
k_f = factor for the effect of concrete strength = 0.748 (using $f'_c = 6.00$ ksi); LRFD Eq. 5.4.2.3.2-2
H = relative humidity = 75% (assumed); and
V/S = 3.44 in. (used to determine k_c; ratio is computed for nominal box dimensions, using 50% of interior void area as directed by LRFD Article 5.4.2.3.2; top surface of box in contact with the wearing surface is neglected for simplicity).

3.3.1.2.3 Ultimate shrinkage strain. While it is not always known whether the girder will be steam cured during fabrication, the initial strength gain is generally accelerated when compared with "normal" concretes. It is reasonable to use the shrinkage equation for steam-cured concrete. The shrinkage strain may therefore be taken as

$$\varepsilon_{sh} = -k_s k_h \left(\frac{t}{55.0 + t}\right) 0.56 \times 10^{-3}. \qquad \text{LRFD Eq. 5.4.2.3.3-2}$$

To determine the ultimate shrinkage strain, $\varepsilon_{sh\,u}$, where $t = \infty$, the term in the equation that contains it is assumed to approach unity.

$\varepsilon_{sh\,u} = \varepsilon_{sh}(\infty) = -415 \times 10^{-6}$ in./in.

where

k_s = size factor = 0.797 and LRFD Eq. C5.4.2.3.3-1
k_h = humidity factor = 0.929. LRFD Eq. C5.4.2.3.3-2

3.3.2 Continuity Diaphragm Concrete

The subscript "d" will be used to indicate properties related to the concrete in the continuity diaphragm.

3.3.2.1 Basic Properties. The same diaphragm concrete strength is used for all designs:

$f'_{cd} = 4.00$ ksi,

$f_{rd} = 0.480$ ksi, LRFD Art. 5.4.2.6

$w_{cd} = 0.150$ kcf, and

$E_{cd} = 3{,}834$ ksi.LRFD Eq. 5.4.2.4-1

3.3.2.2 *Time-Dependent Properties*. Since the continuity diaphragm is such a limited segment when compared with the remainder of the span, the time-dependent properties of the diaphragm concrete are neglected.

3.3.3 Prestressing Strand

The properties of the prestressing strand are as follows:

0.5-in.-diameter low-relaxation seven-wire strand,

$A_{ps} = 0.153$ in.^{2},

$f_{pu} = 270$ ksi,

$f_{py} = 0.90 f_{pu} = 243$ ksi,

$f_{pj} = 0.75 f_{pu} = 202.5$ ksi, and

$E_p = 28{,}500$ ksi.

3.3.3.1 Transfer Length. The stress in the pretensioning strands is transferred from the strands to the girder concrete over the transfer length. The stress in the strands is assumed to vary linearly from zero at the end of the girder to the full effective prestress, f_{pe}, at the transfer length. The transfer length, ℓ_t, may be estimated as

$\ell_t = 60 d_b$ LRFD Art. 5.11.4.1
$= 60(0.5 \text{ in.})$
$= 30 \text{ in.}$

The location at a transfer length from the end of the girder is a critical stress location at release. Therefore, moments and stresses are computed for this location and are shown in various tables in this example. These locations are identified in the tables with the heading "Trans." or "Transfer."

3.3.4 Mild Reinforcement

The properties of the mild reinforcing bars are as follows:

$f_y = 60$ ksi and

$E_s = 29{,}000$ ksi.

3.4 Stress Limits

The following stress limits are used for the design of the girders for the service limit state. For computation of girder stresses, the sign convention will be compressive stress is positive (+) and tensile stress is negative (–). Signs are not shown for stress limits computed below, but will be applied in later stress comparisons.

3.4.1 Pretensioned Strands

The stress limits for low relaxation strands are

Immediately prior to transfer: LRFD Table 5.9.3-1

$f_{pi} = 0.75 f_{pu} = 202.5$ ksi.

At service limit state after losses: LRFD Table 5.9.3-1

$fp = 0.80 fpy = 199.4$ ksi.

The stress limits above are not discussed in this example because they do not govern designs.

3.4.2 Concrete

3.4.2.1 Temporary Stresses at Release.

Compression: LRFD Art. 5.9.4.1.1

$f_{cR} = 0.60 f'_{ci} = 0.60(4.50) = 2.700$ ksi.

Tension: LRFD Table 5.9.4.1.2-1

$f_{tR1} = 0.0948 \sqrt{f'_{ci}} \le 0.2$ ksi
$= 0.0948 \sqrt{4.50}$
$= 0.201 \le 0.2$ ksi; USE $f_{tR1} = 0.200$ ksi (minimum allowed)

or

$f_{tR2} = 0.24 \sqrt{f'_{ci}}$ with reinforcement to resist the tensile force in the concrete
$= 0.24$ (4.50
$= 0.509$ ksi.

3.4.2.2 Final Stresses at Service Limit State after Losses. The following stress limits are given for the girder concrete.

Compression: LRFD Table 5.9.4.2.1-1

$f_{c1} = 0.60 \phi_w f'_c$, for full service loads ($\phi_w = 1$ for girders)
$= 0.60(1)(6.00)$
$= 3.600$ ksi

$f_{c2} = 0.45 f'_c$, for effective prestress (PS) and full dead loads (DL)
$= 0.45(6.00)$
$= 2.700$ ksi

$f_{c3} = 0.40 f'_c$, for live load plus one-half of effective PS and full DL
$= 0.40(6.00)$
$= 2.400$ ksi.

Tension: LRFD Table 5.9.4.2.2-1

For the precompressed compression zone,

$f_{t1} = 0.19 \sqrt{f'_c}$, assuming moderate corrosion conditions
$= 0.19$ (6.00
$= 0.465$ ksi.

For locations other than the precompressed compression zone, such as at the end of the girder where the top of the girder may go into tension under the effect of the negative live-load moment, the specifications give no stress limits. The following limits have been proposed, which take the same form as those for temporary tensile stresses at release given in LRFD Table 5.9.4.1.2-1, but with the specified concrete compressive strength, f'_c, substituted for the concrete compressive strength at release, f'_{ci}:

$f_{t2} = 0.0948 \sqrt{f'_c} \le 0.2$ ksi
$= 0.0948 \sqrt{6.00}$
$= 0.232 \le 0.2$ ksi; USE $f_{t2} = 0.200$ ksi (minimum allowed)

or

$f_{t3} = 0.24\sqrt{f'_c}$ with reinforcement to resist the tensile force in the concrete
$= 0.24\sqrt{6.00}$
$= 0.588$ ksi.

3.5 Other Design Assumptions

Internal intermediate diaphragms are placed at quarter points in the bridge. No other bracing is required due to the stability of the section. The weight of the grout in the shear keys is neglected.

3.6 Section Properties

With no composite concrete deck, the structural properties of the bridge are defined by the girder alone.

3.6.1 Girder

The section properties for a standard AASHTO BIII-48 box girder are as follows (see Figure D-3.6.1.1):

$h = 39.00$ in.,

$A = 812.5$ in.^{2},

$I = 168{,}367$ in.^{4},

$y_b = 19.29$ in.,

$y_t = 19.71$ in.,

$S_b = 8{,}728$ in.^{3}, and

$S_t = 8{,}542$ in^3.

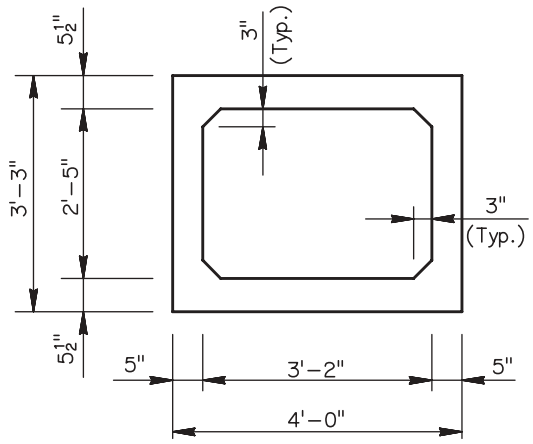

Figure D-3.6.1-1. AASHTO BIII-48 box girder dimensions.

3.7 Design Moments

The following sections present the computed design moments for service and strength limit states. All loads applied to the bare girder are considered to act on a simple span. Loads applied after the continuity diaphragm is placed are considered to act on a fully continuous structure. Restraint moments are not shown in tables contained in this section. Computations are made later in the example.

3.7.1 Service Limit State

Tables D-3.7.1-1 through D-3.7.1-3 provide moments for the service limit state. Table D-3.7.1-1 gives moments caused by loads applied to the noncomposite section (simple span). Tables D-3.7.1-2 and D-3.7.1-3 give moments caused by loads applied to the composite section (continuous span).

3.7.2 Strength Limit State

Table D-3.7.2-1 provides moments for the Strength I limit state.

4 ANALYSIS AND DESIGN OF GIRDERS FOR CONTINUITY

The age of precast/prestressed concrete girders when continuity is established is a critical factor in the design of bridges of this type. The earlier the age of the girder at continuity, the more girder creep and shrinkage contribute to the development

TABLE D-3.7.1-1 Service design moments for loads on simple span

	Location from Bearing (ft)	*Self Weight (k-ft)*	*Internal Diaphragms (k-ft)*
Load Factor		*1.0*	*1.0*
Bearing	0.0	0.0	0.0
H/2	1.6	57.2	2.0
Transfer	1.8	64.4	2.3
0.10 L	8.0	258.8	9.8
0.20 L	16.6	478.8	20.4
0.30 L	25.2	636.0	27.7
0.40 L	33.8	730.3	31.2
0.50 L	42.42	761.7	34.8
0.60 L	51.0	730.3	31.2
0.70 L	59.7	636.0	27.7
0.80 L	68.3	478.8	20.4
0.90 L	76.9	258.8	9.8
Transfer	83.0	64.4	2.2
H/2	83.2	57.2	2.0
Bearing	84.8	0.0	0.0

TABLE D-3.7.1-2 Service I design moments for loads on continuous span

	Location from Bearing (ft)	*Parapet DL (DC) (k–ft)*	*Wrg. Surf. DL (DW) (k–ft)*	*LL+IM (+) (k–ft)*	*LL+IM (–) (k–ft)*
Load Factor		*1.0*	*1.0*	*1.0*	*1.0*
Bearing	0.0	0.0	0.0	0.0	0.0
H/2	1.6	6.3	15.3	55.8	–6.6
Transfer	1.8	7.1	17.2	62.8	–7.4
0.10 L	8.0	27.8	67.4	245.5	–32.2
0.20 L	16.6	49.1	119.1	433.5	–67.2
0.30 L	25.2	61.2	148.5	545.7	–102.1
0.40 L	33.8	64.1	155.6	597.0	–137.1
	42.42	57.9	140.4	592.7	–172.0
0.60 L	51.0	42.5	103.0	532.8	–207.0
0.70 L	59.7	17.9	43.4	415.1	–241.9
0.80 L	68.3	–15.9	–38.6	250.8	–321.7
0.90 L	76.9	–58.8	–142.8	96.4	–374.5
Transfer	83.0	–94.9	–230.2	36.8	–521.3
H/2	83.2	–96.2	–233.4	35.5	–527.9
Bearing	84.8	–106.6	–258.6	27.0	–583.0
CL Pier	86.0	–114.1	–276.8	20.8	–622.5

of positive restraint moments. Minimizing the risk of developing positive moments avoids an increase in critical moments and stresses near midspan and avoids cracking of the continuity diaphragm.

It is highly recommended that the minimum age for continuity be specified in the contract documents. Analytical studies and field experience indicate that waiting to establish continuity until the girders are at least 90 days old will significantly reduce or eliminate the development of positive restraint moments.

The proposed specifications recognize the benefit of delaying continuity by allowing two approaches for the design of

TABLE D-3.7.1-3 Service III design moments for loads on continuous span

	Location from Bearing (ft)	*Parapet DL (DC) (k–ft)*	*Wrg. Surf. DL (DW) (k–ft)*	*LL+IM (+) (k–ft)*	*LL+IM (–) (k–ft)*
Load Factor		*1.0*	*1.0*	*1.0*	*1.0*
Bearing	0.0	0.0	0.0	0.0	0.0
H/2	1.6	6.3	15.3	44.6	–5.3
Transfer	1.8	7.1	17.2	50.2	–5.9
0.10 L	8.0	27.8	67.4	196.4	–25.8
0.20 L	16.6	49.1	119.1	346.8	–53.8
0.30 L	25.2	61.2	148.5	436.5	–81.7
0.40 L	33.8	64.1	155.6	477.6	–109.7
0.50 L	42.42	57.9	140.4	474.2	–137.6
0.60 L	51.0	42.5	103.0	426.2	–165.6
0.70 L	59.7	17.9	43.4	332.1	–193.59
0.80 L	68.3	–15.9	–38.6	200.7	–257.4
0.90 L	76.9	–58.8	–142.8	77.1	–299.6
Transfer	83.0	–94.9	–230.2	29.5	–417.0
H/2	83.2	–96.2	–233.4	28.4	–422.3
Bearing	84.8	–106.6	–258.6	21.6	–466.4
CL Pier	86.0	–114.1	–276.8	16.6	–498.1

TABLE D-3.7.2-1 Strength I design moments

	Loc. from Brg. (ft)	*Self Weight (Max)* (k–ft)	*Self Weight (Min)* (k–ft)	*Intern. Diaphr. (Max)* (k–ft)	*Intern. Diaphr. (Min)* (k–ft)	*Parapet DL (DC) (Max)* (k–ft)	*Parapet DL (DC) (Min)* (k–ft)	*Wrg. Surf. DL (DW) (Max)* (k–ft)	*Wrg. Surf. DL (DW) (Min)* (k–ft)	*LL+IM (+)* (k–ft)	*LL+IM (–)* (k–ft)
Load Factor		*1.25*	*0.9*	*1.25*	*0.9*	*1.25*	*0.9*	*1.50*	*0.65*	*1.75*	*1.75*
Bearing	0.0	0.0	0.0	0.0	0.0	0.0	0.0	0.0	0.0	0.0	0.0
H/2	1.6	71.6	51.5	2.5	1.8	7.9	5.7	23.0	10.0	55.8	–6.6
Transfer	1.8	80.5	58.0	2.8	2.0	8.9	6.4	25.8	11.2	62.8	–7.4
0.10 L	8.0	323.5	232.9	12.2	8.8	34.7	25.0	101.1	43.8	245.5	–32.2
0.20 L	16.6	598.5	430.9	25.5	18.3	61.4	44.2	178.6	77.4	433.5	–67.2
0.30 L	25.2	795.0	572.4	34.6	24.9	76.5	55.1	222.7	96.5	545.7	–102.1
0.40 L	33.8	912.9	657.3	39.1	28.1	80.2	57.7	233.4	101.1	597.0	–137.1
0.50 L	42.42	952.2	685.61	43.5	31.3	72.4	52.1	210.7	91.3	592.7	–172.0
0.60 L	51.0	912.9	657.3	39.1	28.1	53.1	38.2	154.6	67.0	532.8	–207.0
0.70 L	59.7	795.0	572.4	34.6	24.9	22.4	16.1	65.1	28.2	415.1	–241.9
0.80 L	68.3	598.5	430.9	25.5	18.3	–19.9	–14.3	–57.8	–25.1	250.8	–321.7
0.90 L	76.9	323.5	232.9	12.2	8.8	–73.6	–53.0	–214.1	–92.8	96.4	–374.5
Transfer	83.0	80.5	58.0	2.8	2.0	–118.6	–85.4	–345.3	–149.7	36.8	521.3
H/2	83.2	71.6	51.5	2.5	1.8	–120.3	–86.6	–350.1	–151.7	35.5	–527.9
Bearing	84.8	0.0	0.0	0.0	0.0	–133.3	–96.0	–388.0	–168.1	27	–583.0
CL Pier	86.0	N/A	N/A	N/A	N/A	–142.7	–102.8	–415.3	–179.9	20.8	–622.5

girders made continuous. The steps in each approach are summarized below.

- **General Approach:**
  - The age of girders when continuity is established may or may not be specified;
  - Estimate time-dependent material properties (creep and shrinkage) that will be used to compute restraint moments;
  - Estimate the positive restraint moment, which is strongly dependent on girder age at continuity and time-dependent material properties;
  - Evaluate conditions at the continuity diaphragms to determine whether the connection is fully or partially effective under the effect of the positive restraint moment;
  - If the restraint moment exceeds $1.2M_{cr}$ or if the joint is not fully effective, it is recommended that the design or conditions be altered to improve the situation;
  - Analyze and design the girders for all design loads, including positive restraint moment (positive restraint moment should be neglected when evaluating stresses in regions of negative moment);
  - Design and detail a positive moment connection at continuity diaphragms; and
  - Design and detail reinforcement to resist negative moments from design loads, neglecting both positive and negative restraint moments.
- **Simplified Approach:**
  - Specify the minimum age of the girders when continuity is established in the contract documents; the minimum girder age at continuity must be at least 90 days;
  - The connection at continuity diaphragms may be taken to be fully continuous;
  - Analyze and design the girders for all design loads (neglect restraint moments);
  - Design and detail a positive moment connection at continuity diaphragms; and
  - Design reinforcement to resist negative moments from design loads.

This section of the design example is divided into two subsections corresponding to the two approaches listed above. Both approaches are presented for completeness; however, it is anticipated that the simplified approach, with its required specification of a minimum girder age of 90 days when continuity is established, will be the approach used most often by bridge designers. The main benefits of the simplified approach include the simplicity of design and the ability to use standard design aids or software to complete a design. The general approach requires a method for estimating restraint moments. The RESTRAINT Program has been developed for this purpose and will be used for this example. Few other programs are available, and some may have significant limitations or disadvantages.

The general approach will be presented first. In this section, computations and results will be presented for the bridge with continuity established when the age of the girders is 7 and 28 days. Positive restraint moments are estimated, and their effect is considered in the design of the girders. The design for continuity at a girder age of 90 days is also discussed with the initial calculation of restraint moments. The required time-dependent material properties were computed in the previous section of this design example. The simplified approach will then be presented for the bridge with girders that are at least 90 days old when continuity is established.

The calculations only address concrete stresses in the girders at the service limit state. Flexural design at the strength limit state was checked and does not govern these designs, so calculations are not shown. A summary compares the results of the designs using the general and simplified approaches. The reinforcement for positive and negative continuity connections, which is determined using the same methods for both approaches, is computed in subsequent sections.

4.1 General Approach

The steps in the general approach were summarized in the previous section. The items will be addressed as they appear in the list, except that the determination of the effectiveness of the joint is considered prior to computation of the restraining moment, as discussed in the following section.

4.1.1 Effectiveness of Joint

According to *proposed* Article 5.14.1.2.7e, the joint (continuity diaphragm) may be considered fully effective if one or both of the following conditions are satisfied:

- The contract documents specify that the girders will be at least 90 days old when continuity is established.
- The stress in the joint is compressive for the combination of superimposed permanent loads, settlement, creep, shrinkage, 50% live load (with impact), and temperature gradient, if applicable.

The first criterion is addressed by the contract documents. To demonstrate the general approach, girder ages at continuity are selected that do not satisfy the first criterion.

The second criterion is stated in terms of a stress, but since the continuity diaphragm is not prestressed, it can also be expressed in terms of moments. Using moments will simplify manual computations since all of the moments are known, but the stress does not have to be computed. Therefore, the sum of the positive restraint moment, composite dead-load moments (negative), and 50% of the maximum negative live-load (with impact) moment must not be positive since a positive moment would cause tension at the bottom of the diaphragm. (Effects other than permanent and live loads, such as temperature effects, are not considered in this example, but could be included in the calculation.) This summation can also be backsolved to determine the maximum positive restraint moment that can develop before the net moment becomes positive or the stress at the bottom of the diaphragm becomes tensile. This computed maximum positive restraint moment can then be used to facilitate the comparison of different designs and eliminate the separate computation of joint stress since the restraint moment is computed as part of each design iteration.

The maximum positive restraint moment at the interior support is computed in Table D-4.1.1-1. The live load used in this computation is 50% of the maximum negative service moment (see Service I, Table D-3.7.1-2). The Service I load combination is used rather than Service III because the joint (continuity diaphragm) is not prestressed concrete, which is a requirement for use of Service III.

When the positive restraint moment computed in the various design iterations remains less than or equal to the computed maximum positive restraint moment (702.2 k-ft), the joint may be considered to be fully effective and the bridge may be designed using continuity for all loads applied after continuity is established. If the positive restraint moment exceeds the maximum computed moment, the connection must be considered partially effective. In this case, a fraction of the loads applied to the continuous structure are considered to be carried by the girders as simple spans, and the remainder of the loads resisted by the continuous structure.

The computation shown above represents the initial design moments only. Due to various adjustments that are made to the designs throughout the required iterations, the live-load moment changes slightly. Therefore, in the following, the stress at the bottom of the joint is computed as a check.

4.1.2 Initial Design Without Restraint Moments

An initial design of an interior girder was performed without including any restraint moment. The strand pattern required for the specified geometry and loads is shown in Figure D-4.1.2-1.

TABLE D-4.1.1-1 Calculation of moment limit for joint effectiveness

Continuous Dead Load (DC)	(k-ft)	–114.1
Continuous Dead Load (DW)	(k-ft)	–276.8
50 % of Live Load + Impact	(k-ft)	–311.3
TOTAL	***(k-ft)***	***–702.2***
Maximum Positive Restraint Moment for Fully Effective Joint	(k-ft)	702.2

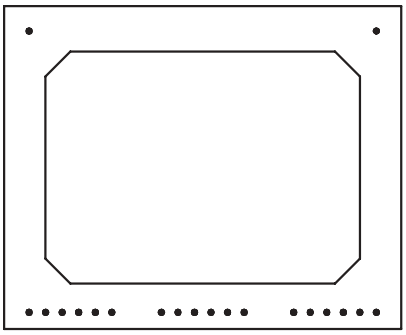

Figure D-4.1.2-1. Strand pattern for initial design.

4.1.3 Compute Restraint Moments

For this bridge without a composite deck, numerical analysis shows that only positive restraint moments develop. Positive restraint moments can have a significant effect on the design of precast/prestressed concrete girder bridges made continuous.

Positive restraint moments are generally larger for two span bridges than for bridges with a greater number of spans with similar span lengths, given the same span lengths and other conditions. However, two-span bridges have limited positive live-load moments at the interior support, while bridges with a greater number of spans can develop significant positive moments at interior supports from live load.

The development of restraint moments with time is computed using the RESTRAINT Program for the initial girder design. The strand pattern shown in Figure D-4.1.2-1 is input to define the creep behavior of the girder. Material properties computed earlier are also used for input, including the ultimate creep coefficient and the ultimate shrinkage strain for the girder concrete. A complete listing of input values used in RESTRAINT is presented in Subappendix A.

Results for the restraint moment analysis for continuity established at girder ages of 7, 28, and 90 days are shown in Figure D-4.1.3-1.

The restraint moment analysis for this initial design indicates that, for continuity established at a girder age of 7 days, a positive restraint moment of about 89 k-ft will eventually develop from the combined effect of creep and shrinkage in the girder concrete. For continuity established at a girder age of 28 days, the analysis indicates that a positive restraint moment of approximately 54 k-ft will eventually develop. The analysis shows that a positive restraint moment of 29 k-ft develops when continuity is delayed until 90 days after the girder is cast. This small positive moment supports *proposed* Article 5.14.1.2.7d, which allows positive restraint moments to be neglected in the design of bridges for which continuity cannot be established until the girders are 90 or more days old. This initial design will be modified for the positive restraint moments in the next section. Since there is no composite deck slab, the analysis indicates that no negative restraint moment develops.

4.1.4 Subsequent Design Iterations Including Positive Restraint Moments

Since the analysis indicates that a significant positive restraint moment develops with time for the girders that are 7 and 28 days old when continuity is established, the design of these girders must be revised. The modifications to the

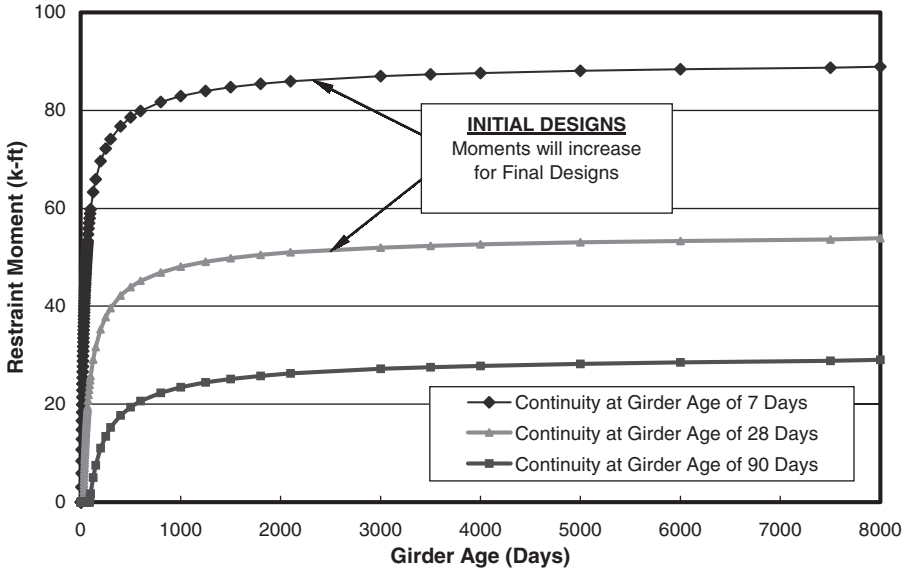

Figure D-4.1.3-1. Development of restraint moment with girder age—initial design.

initial design are necessary to counteract the increased stresses caused by the additional positive restraint moments, so several iterations are required.

For each iteration, strands are added or repositioned to provide a design that includes the positive restraint moment and satisfies the service limit state design criteria. A new positive restraint moment is then computed using RESTRAINT for the new strand pattern, and the process is repeated. The iterations continue until the revised positive restraint moment does not require a change in the strand pattern. While other quantities, such as strand size or concrete strengths, had to be adjusted in DE1 during the iterations, only the strand pattern was revised for this problem.

Tables of strand requirements, positive restraint moments, and stresses at the bottom of the continuity diaphragm are given below for the designs with girder ages at continuity of 7 and 28 days. Strand patterns and other data for the final designs for girder ages of 7 and 28 days at continuity are shown in the summary Section 4.3. Computations for the strength limit state are not shown since they do not govern. The positive restraint moment is included.

4.1.4.1 Girder Age at Continuity of 7 Days. In the final iteration, the restraint moment remains below the maximum positive restraint moment of 702.2 k-ft computed in Table D-4.1.1-1. The computed stress at the bottom of the continuity diaphragm also remains in compression for the specified loading, in agreement with the positive restraint moment limit. Therefore, the joint can be considered fully effective for analysis for all loads applied to the continuous structure.

Table D-4.1.4.1-1 also shows that the positive restraint moments for all iterations remain below the quantity $1.2M_{cr}$ = 584.1 k-ft (see Table D-5.2-1). This indicates that the reinforcement used in the positive moment connection will be effective and that the design is reasonable.

TABLE D-4.1.4.1-1 Summary of design iterations—continuity at 7 days

Iteration	*No. of Strands*	*Positive Restraint Moment (k-ft)*	*Stress at Bottom of Continuity Diaphragm (ksi)*
1	20	0.0	0.818
2	21	89.1	0.714
3	22	151.2	0.642
4	22	213.2	0.570

In summary, the design of this girder, even with continuity established at the very early girder age of 7 days, meets all of the requirements of the proposed specification and is a viable design. For further discussion, see the summary and comparison of designs in Section 4.3, which also contains a table displaying the strand pattern and other characteristics of the final design.

The maximum restraint moment shown in Table D-4.1.4.1-1 occurs at the center of the interior support and decreases linearly to zero at the center of bearing at the expansion joint. A load factor of 1.0 is applied to the restraint moment for the service limit state, and a load factor of 0.5 is applied to the restraint moment for the strength limit state (LRFD Article 3.4.1.) Since the moments vary linearly, a table of restraint moments along the girder is not given.

Tables D-4.1.4.1-2 and D-4.1.4.1-3 present the service limit state stresses for the final design for a girder age at continuity of 7 days. These stresses are compared with stress limits for release, and final conditions after losses that are given in Sections 3.4.2.1 and 3.4.2.2.

4.1.4.2 Girder Age at Continuity of 28 Days. The positive restraint moments shown in Table D-4.1.4.2-1 remain below

TABLE D-4.1.4.1-2 Summary of design stresses for final design at release—continuity at 7 days

	Location from Bearing	*(ft)*	*Brg.*	*H/2*	*Trans.*	*0.10L*	*0.20L*	*0.30L*	*0.40L*	*0.50L*
			0.00	*1.63*	*1.83*	*7.95*	*16.57*	*25.18*	*33.80*	*42.42*
Prestress at Release	Top Girder	(ksi)	N/A	N/A	–0.284	–0.284	–0.284	–0.284	–0.284	–0.284
	Bottom Girder	(ksi)	N/A	N/A	1.880	1.880	1.880	1.880	1.880	1.880
Self Weight	Top Girder	(ksi)	N/A	N/A	0.127	0.411	0.736	0.966	1.104	1.153
	Bottom Girder	(ksi)	N/A	N/A	–0.125	–0.402	–0.719	–0.946	–1.080	–1.128
Total at Release	Top Girder	(ksi)	N/A	N/A	–0.157	0.127	0.452	0.682	0.820	0.869
	Bottom Girder	(ksi)	N/A	N/A	1.755	1.478	1.161	0.934	0.800	0.752

Notes:
1. Critical stresses are shaded.
2. Values for limiting stresses are given in Section 3.4.2.1.
3. Compressive stresses at release are compared with the limit f_{cR} = 2.700 ksi. The maximum compressive stress is 1.755 ksi at the transfer location.
4. Tensile stresses in regions other than the precompressed tensile zone at release are compared with the limiting tensile stress f_{tR1} = –0.200 ksi or f_{tR2} = –0.509 ksi. The latter value requires an area of reinforcement to resist the tensile force. The maximum tensile stress is –0.157 at the transfer location.
5. In all cases, this design satisfies the specified stress limits at release.

TABLE D-4.1.4.1-3 Summary of design stresses for final design at service limit state after losses—continuity at 7 days

	Location		Brg.	Trans.	H/2	0.10L	0.20L	0.30L	0.40L	0.50L	0.60L	0.70L	0.80L	0.90L	H/2	Trans.	Brg.
		From Brg. (ft)	0.00	2.42	2.20	8.03	16.65	25.27	33.88	42.50	51.12	59.77	68.35	76.97	82.80	82.58	85.00
SERVICE STRESSES (ksi)																	
1	Prestress After Losses	Top Girder	-0.070	-0.261	-0.239	-0.261	-0.261	-0.261	-0.261	-0.261	-0.261	-0.261	-0.261	-0.261	-0.239	-0.261	-0.070
		Bottom Girder	0.460	1.724	1.581	1.724	1.724	1.724	1.724	1.724	1.724	1.724	1.724	1.724	1.581	1.724	0.460
2	Self Weight	Top Girder	0.000	0.090	0.080	0.364	0.673	0.893	1.026	1.070	1.026	0.893	0.673	0.364	0.080	0.090	0.000
		Bottom Girder	0.000	-0.089	-0.079	-0.356	-0.658	-0.874	-1.004	-1.047	-1.004	-0.874	-0.658	-0.356	-0.079	-0.089	0.000
3	Non-Comp. DL	Top Girder	0.000	0.003	0.003	0.014	0.029	0.039	0.044	0.049	0.044	0.039	0.029	0.014	0.003	0.003	0.000
		Bottom Girder	0.000	-0.003	-0.003	-0.013	-0.028	-0.038	-0.043	-0.048	-0.043	-0.038	-0.028	-0.013	-0.003	-0.003	0.000
4	Composite DL	Top Girder	0.000	0.010	0.009	0.039	0.069	0.086	0.090	0.081	0.060	0.025	-0.022	-0.083	-0.135	-0.133	-0.150
		Bottom Girder	0.000	-0.010	-0.009	-0.038	-0.068	-0.084	-0.088	-0.080	-0.058	-0.025	0.022	0.081	0.132	0.130	0.147
5	Restraint Mom't (RM) (+)	Top Girder	0.000	0.006	0.006	0.028	0.058	0.089	0.119	0.150	0.180	0.211	0.241	0.271	0.294	0.293	0.300
		Bottom Girder	0.000	-0.006	-0.006	-0.027	-0.057	-0.087	-0.117	-0.147	-0.176	-0.206	-0.236	-0.266	-0.287	-0.287	-0.293
6	LL + IM (+)	Top Girder	0.000	0.071	0.063	0.276	0.487	0.613	0.671	0.666	0.599	0.467	0.282	0.108	0.040	0.041	0.030
		Bottom Girder	0.000	-0.069	-0.061	-0.270	-0.477	-0.600	-0.657	-0.652	-0.586	-0.457	-0.276	-0.106	-0.039	-0.041	-0.030
7	LL + IM (-)	Top Girder	0.000	-0.008	-0.007	-0.036	-0.076	-0.115	-0.154	-0.193	-0.233	-0.272	-0.362	-0.421	-0.593	-0.586	-0.655
		Bottom Girder	0.000	0.008	0.007	0.035	0.074	0.112	0.151	0.189	0.228	0.266	0.354	0.412	0.581	0.573	0.641
TOTAL SERVICE STRESSES (ksi)																	
A = 1-4	Full PS + DL	Top Girder	-0.070	-0.157	-0.147	0.155	0.509	0.758	0.899	0.939	0.869	0.697	0.418	0.034	-0.291	-0.301	-0.220
		Bottom Girder	0.460	1.623	1.491	1.316	0.970	0.728	0.589	0.550	0.619	0.787	1.060	1.436	1.632	**1.763**	0.607
B = 1-5	Full PS + DL + RM (+)	Top Girder	-0.070	-0.151	-0.141	0.183	0.568	0.846	1.018	1.089	1.049	0.907	0.659	0.305	0.003	-0.008	0.080
		Bottom Girder	0.460	1.616	1.485	1.289	0.913	0.641	0.473	0.403	0.443	0.581	0.824	1.170	1.344	1.476	0.313
B + 1.0*6	Service I LL+IM (+) w/RM	Top Girder	-0.070	-0.080	-0.079	0.459	1.055	1.460	1.689	1.755	1.648	1.374	0.941	0.413	0.043	0.034	0.110
		Bottom Girder	0.460	1.547	1.424	1.019	0.436	0.041	-0.184	-0.249	-0.143	0.125	0.548	1.064	1.305	1.435	0.284
A + 1.0*7	Service I LL+IM (-)	Top Girder	-0.070	-0.166	-0.154	0.119	0.434	0.643	0.745	0.746	0.636	0.425	0.057	-0.387	-0.884	-0.886	-0.875
		Bottom Girder	0.460	1.631	1.498	1.352	1.044	0.840	0.740	0.739	0.847	1.053	1.414	1.847	2.212	**2.336**	1.248
B + 0.8*6	Service III LL+IM (+) w/RM	Top Girder	-0.070	-0.094	-0.091	0.404	0.958	1.337	1.555	1.622	1.528	1.280	0.885	0.392	0.035	0.026	0.104
		Bottom Girder	0.460	1.561	1.436	1.073	0.532	0.161	-0.053	**-0.118**	-0.026	0.216	0.603	1.085	1.313	1.444	0.290
A + 0.8*7	Service III LL+IM (-)	Top Girder	-0.070	-0.164	-0.153	0.126	0.449	0.666	0.776	0.785	0.683	0.479	0.129	-0.303	-0.766	**-0.769**	-0.744
		Bottom Girder	0.460	1.629	1.497	1.345	1.030	0.818	0.710	0.701	0.801	1.000	1.343	1.765	2.096	2.221	1.120
6 + 0.5*B	Special Service+RM (+)	Top Girder	-0.035	-0.005	-0.008	0.368	0.771	1.036	1.180	1.211	1.123	0.920	0.612	0.261	0.041	0.038	0.070
		Bottom Girder	0.230	0.739	0.681	0.374	-0.020	-0.280	-0.420	-0.450	-0.365	-0.166	0.136	0.479	0.633	0.697	0.127
7 + 0.5*A	Special Service (-)	Top Girder	-0.035	-0.087	-0.081	0.041	0.179	0.264	0.295	0.276	0.202	0.077	-0.153	-0.404	-0.739	-0.736	-0.765
		Bottom Girder	0.230	0.819	0.753	0.694	0.559	0.476	0.445	0.464	0.537	0.660	0.884	1.130	1.397	**1.455**	0.945

Notes:

1. Maximum stresses are shaded, with the governing stresses boxed and bolded.
2. Values for limiting stresses are given in Section 3.4.2.2.
3. Compressive stresses for both dead-load combinations (A and B) are compared with the limiting compressive stress for full dead load f_{c2} = 2.700 ksi. The maximum stress is 1.763 ksi at the transfer length location for the combination without restraint moment (A).
4. Compressive stresses for both Service I LL+IM conditions are compared with the limiting compressive stress for full-service conditions f_{c1} = 3.600 ksi. The maximum stress is 2.336 ksi at the interior transfer length location for the combination without restraint moment.
5. Tensile stresses in the precompressed tensile zone for Service III with RM are compared with the limiting tensile stress f_{t1} = –0.465 ksi. The maximum stress is –0.118 ksi at 0.50L.
6. Tensile stresses in regions other than the precompressed tensile zone for Service III without RM are compared with the limiting tensile stress f_{t2} = –0.200 ksi or f_{t3} = –0.588 ksi. The latter value requires an area of reinforcement to resist the tensile force. The maximum stress is –0.769 ksi at the interior bearing. This stress exceeds both stress limits. This region of the girder will be designed for the strength limit state.
7. Compressive stresses for the Special Service cases are compared with the limiting compressive stress for that case f_{c3} = 2.400 ksi. The maximum stress is 1.455 ksi at the interior transfer location for the combination without restraint moment.
8. In all cases, this design satisfies the specified stress limits, with the exception of tension at the interior support, which will be dealt with as noted.

TABLE D-4.1.4.2-1 Summary of design iterations—continuity at 28 days

Iteration	*No. of Strands*	*Positive Restraint Moment (k-ft)*	*Stress at Bottom of Continuity Diaphragm (ksi)*
1	20	0	0.818
2	21	54.0	0.755
3	21	96.5	0.706

the maximum positive restraint moment of 702.2 k-ft computed in Table D-4.1.1-1 for all iterations. As expected, the stress at the bottom of the diaphragm also remains in compression for all iterations. Therefore, design may be performed considering the joint fully effective for all loads applied to the continuous structure.

Additionally, the moments all remain below the quantity $1.2M_{cr}$ = 584.1 k-ft as shown in Section 5.2.1.2. Therefore, the design of this girder, with continuity established at the fairly early girder age of 28 days, is acceptable. This is expected, since the design with continuity at 7 days was also viable. For further discussion, see the summary and comparison of designs in Section 4.3.

The maximum restraint moment as shown in Table D-4.1.4.2-1 occurs at the center of the interior pier and decreases linearly to zero at the center of bearing at the expansion joint. A load factor of 1.0 is applied to the restraint moment for the service limit state, and a load factor of 0.5 is applied to the restraint moment for the strength limit state. Since the moments vary linearly, a table of restraint moments along the girder is not given.

Tables D-4.1.4.2-2 and D-4.1.4.2-3 present the service limit state stresses for the final design for a girder age at continuity of 28 days. These stresses are compared with stress limits for release, and final conditions after losses that are given in Sections 3.4.2.1 and 3.4.2.2.

4.2 Simplified Approach

If the contract documents require that the girders be at least 90 days old when continuity is established, positive restraint moments may be neglected. This greatly simplifies the design of bridges with precast concrete girders made continuous.

Once the designer has made this decision, design proceeds assuming that the bridge is fully continuous for loads applied to the continuous structure (*proposed* Article 5.14.1.2.7d); therefore, no iterations are required. The resulting design is the same as the initial design performed without restraint moments in the preceding section.

Although it was not required, a restraint moment analysis was also performed for the bridge with continuity established at a girder age of 90 days (see Figure D-4.1.3-1). The maximum positive restraint moment was nearly 30 k-ft. However, a design iteration was run for the girder with this additional positive moment, and it was found that the initial strand pattern was adequate to resist the additional moment without any revisions. This result appears to support the provisions in the proposed specifications allowing positive restraint moments to be neglected for a design with continuity established at a girder age of at least 90 days, even when a composite deck slab is not used.

TABLE D-4.1.4.2-2 Summary of design stresses for final design at release—continuity at 28 days

	Location from Bearing	*(ft)*	*Brg.* *0.00*	*H/2* *1.63*	*Trans.* *1.83*	*0.10L* *7.95*	*0.20L* *16.57*	*0.30L* *25.18*	*0.40L* *33.80*	*0.50L* *42.42*
Prestress at Release	Top Girder	(ksi)	N/A	N/A	–0.190	–0.190	–0.261	–0.261	–0.261	–0.261
	Bottom Girder	(ksi)	N/A	N/A	1.500	1.500	1.789	1.789	1.789	1.789
Self Weight	Top Girder	(ksi)	N/A	N/A	0.127	0.411	0.736	0.966	1.104	1.153
	Bottom Girder	(ksi)	N/A	N/A	–0.125	–0.402	–0.719	–0.946	–1.080	–1.128
Total at Release	Top Girder	(ksi)	N/A	N/A	–0.063	0.221	0.475	0.705	0.843	0.892
	Bottom Girder	(ksi)	N/A	N/A	1.375	1.098	1.070	0.843	0.709	0.661

Notes:
1. Critical stresses are shaded.
2. Values for limiting stresses are given in Section 3.4.2.1.
3. Compressive stresses at release are compared with the limit f_{cR} = 2.700 ksi. The maximum compressive stress is 1.375 ksi at the transfer length location.
4. Tensile stresses in regions other than the precompressed tensile zone at release are compared with the limiting tensile stress f_{tR1} = –0.200 ksi or f_{tR2} = –0.509 ksi. The latter value requires an area of reinforcement to resist the tensile force. The maximum tensile stress is –0.063 ksi at the transfer length location.
5. In all cases, this design satisfies the specified stress limits at release.

TABLE D-4.1.4.2-3 Summary of design stresses for final design at service limit state after losses—continuity at 28 days

	Location		Brg.	Trans.	H/2	0.10L	0.20L	0.30L	0.40L	0.50L	0.60L	0.70L	0.80L	0.90L	H/2	Trans.	Brg.
		From Brg. (ft)	0.00	1.83	2.20	7.97	16.60	25.23	33.87	42.50	51.13	59.77	68.40	77.03	82.80	83.17	85.00
SERVICE STRESSES (ksi)																	
1	Prestress After Losses	Top Girder	-0.047	-0.175	-0.160	-0.175	-0.241	-0.241	-0.241	-0.241	-0.241	-0.241	-0.241	-0.175	-0.160	-0.175	-0.047
		Bottom Girder	0.369	1.382	1.267	1.382	1.648	1.648	1.648	1.648	1.648	1.648	1.648	1.382	1.267	1.382	0.369
2	Self Weight	Top Girder	0.000	0.090	0.080	0.364	0.673	0.893	1.026	1.070	1.026	0.893	0.673	0.364	0.080	0.090	0.000
		Bottom Girder	0.000	-0.089	-0.079	-0.356	-0.658	-0.874	-1.004	-1.047	-1.004	-0.874	-0.658	-0.356	-0.079	-0.089	0.000
3	Non-Comp. DL	Top Girder	0.000	0.003	0.003	0.014	0.029	0.039	0.044	0.049	0.044	0.039	0.029	0.014	0.003	0.003	0.000
		Bottom Girder	0.000	-0.003	-0.003	-0.013	-0.028	-0.038	-0.043	-0.048	-0.043	-0.038	-0.028	-0.013	-0.003	-0.003	0.000
4	Composite DL	Top Girder	0.000	0.010	0.009	0.039	0.069	0.086	0.090	0.081	0.060	0.025	-0.022	-0.083	-0.135	-0.133	-0.150
		Bottom Girder	0.000	-0.010	-0.009	-0.038	-0.068	-0.084	-0.088	-0.080	-0.058	-0.025	0.022	0.081	0.132	0.130	0.147
5	Restraint Moment (RM) (+)	Top Girder	0.000	0.003	0.003	0.013	0.026	0.040	0.054	0.068	0.082	0.095	0.109	0.123	0.133	0.133	0.136
		Bottom Girder	0.000	-0.003	-0.002	-0.012	-0.026	-0.039	-0.053	-0.066	-0.080	-0.093	-0.107	-0.120	-0.130	-0.130	-0.133
6	LL + IM (+)	Top Girder	0.000	0.071	0.063	0.276	0.487	0.613	0.671	0.666	0.599	0.467	0.282	0.108	0.040	0.041	0.030
		Bottom Girder	0.000	-0.069	-0.061	-0.270	-0.477	-0.600	-0.657	-0.652	-0.586	-0.457	-0.276	-0.106	-0.039	-0.041	-0.030
7	LL + IM (-)	Top Girder	0.000	-0.008	-0.007	-0.036	-0.076	-0.115	-0.154	-0.193	-0.233	-0.272	-0.362	-0.421	-0.593	-0.586	-0.655
		Bottom Girder	0.000	0.008	0.007	0.035	0.074	0.112	0.151	0.189	0.228	0.266	0.354	0.412	0.581	0.573	0.641
TOTAL SERVICE STRESSES (ksi)																	
A = 1-4	Full PS + DL	Top Girder	-0.047	-0.071	-0.068	0.241	0.530	0.778	0.919	0.960	0.889	0.717	0.438	0.120	-0.212	-0.215	-0.197
		Bottom Girder	0.369	1.281	1.177	0.974	0.894	0.652	0.513	0.473	0.543	0.711	0.984	1.094	1.318	**1.421**	0.516
B = 1-5	Full PS + DL + RM (+)	Top Girder	-0.047	-0.068	-0.065	0.254	0.556	0.818	0.973	1.027	0.970	0.812	0.547	0.243	-0.079	-0.082	-0.061
		Bottom Girder	0.369	1.278	1.174	0.962	0.868	0.612	0.460	0.407	0.463	0.618	0.877	0.973	1.188	1.291	0.383
B + 1.0*6	Service I LL+IM (+) w/RM	Top Girder	-0.047	0.002	-0.003	0.530	1.043	1.431	1.644	1.693	1.569	1.279	0.829	0.351	-0.039	-0.041	-0.031
		Bottom Girder	0.369	1.209	1.113	0.692	0.392	0.012	-0.196	-0.245	-0.123	0.161	0.601	0.867	1.149	1.250	0.353
A + 1.0*7	Service I LL+IM (-)	Top Girder	-0.047	-0.080	-0.075	0.205	0.454	0.663	0.765	0.766	0.656	0.445	0.077	-0.301	-0.805	-0.800	-0.852
		Bottom Girder	0.369	1.289	1.184	1.010	0.968	0.764	0.664	0.663	0.770	0.977	1.338	1.505	1.898	**1.994**	1.157
B + 0.8*6	Service III LL+IM (+) w/RM	Top Girder	-0.047	-0.012	-0.015	0.475	0.946	1.308	1.510	1.560	1.449	1.185	0.773	0.329	-0.047	-0.049	-0.037
		Bottom Girder	0.369	1.222	1.125	0.746	0.487	0.132	-0.065	**-0.114**	-0.006	0.252	0.656	0.888	1.156	1.259	0.359
A + 0.8*7	Service III LL+IM (-)	Top Girder	-0.047	-0.078	-0.074	0.212	0.469	0.686	0.796	0.805	0.703	0.499	0.149	-0.217	-0.687	-0.683	**-0.721**
		Bottom Girder	0.369	1.287	1.183	1.003	0.954	0.741	0.634	0.625	0.725	0.924	1.267	1.423	1.782	1.879	1.029
6 + 0.5*B	Special (+) Service + RM	Top Girder	-0.024	0.036	0.030	0.403	0.765	1.022	1.157	1.180	1.084	0.873	0.556	0.230	0.000	0.000	0.000
		Bottom Girder	0.185	0.570	0.526	0.211	-0.043	-0.294	-0.426	-0.448	-0.355	-0.148	0.163	0.381	0.555	0.605	0.162
7 + 0.5*A	Special (-) Service	Top Girder	-0.024	-0.044	-0.041	0.084	0.189	0.274	0.305	0.287	0.212	0.087	-0.142	-0.361	-0.699	-0.693	-0.754
		Bottom Girder	0.185	0.648	0.596	0.523	0.521	0.438	0.407	0.426	0.499	0.622	0.846	0.959	1.240	**1.284**	0.899

Notes:

1. Maximum stresses are shaded, with the governing stresses boxed and bolded.
2. Values for limiting stresses are given in Section 3.4.2.2.
3. Compressive stresses for both dead-load combinations (A and B) are compared with the limiting compressive stress for full dead load f_{c2} = 2.700 ksi. The maximum stress is 1.421 ksi at the transfer length location for the combination without restraint moment (A).
4. Compressive stresses for both Service I LL+IM conditions are compared with the limiting compressive stress for full-service conditions f_{c1} = 3.600 ksi. The maximum stress is 1.994 ksi at the interior transfer length location for the combination without restraint moment.
5. Tensile stresses in the precompressed tensile zone for Service III with RM are compared with the limiting tensile stress f_{t1} = –0.465 ksi. The maximum stress is –0.114 ksi at midspan.
6. Tensile stresses in regions other than the precompressed tensile zone for Service III without RM are compared with the limiting tensile stress f_{t2} = –0.200 ksi or f_{t3} = –0.588 ksi. The latter value requires an area of reinforcement to resist the tensile force. The maximum stress is –0.721 ksi at the interior bearing. This stress exceeds both stress limits. This region of the girder will be designed for the strength limit state.
7. Compressive stresses for the special service cases are compared with the limiting compressive stress for that case f_{c3} = 2.400 ksi. The maximum stress is 1.284 ksi at the interior transfer length location for the combination without restraint moment.
8. In all cases, this design satisfies the specified stress limits, with the exception of tension at the interior support, which will be dealt with as noted.

4.2.1 Girder Age at Continuity of at Least 90 Days

Tables D-4.2.1-1 and D-4.2.1-2 present the service limit state stresses for the final design for a girder age at continuity of at least 90 days. These stresses are compared with stress limits for release and final conditions after losses that are given in Sections 3.4.2.1 and 3.4.2.2.

4.3 Summary of Results for General and Simplified Approaches

Designs for precast/prestressed concrete girders made continuous have been presented in the preceding sections for girder ages at continuity of 7, 28, and 90 days. The designs using earlier girder ages were performed using the general approach, which required the consideration of positive restraint moments. The design for a girder age of 90 days at continuity was performed using the simplified approach, in which positive restraint moments are neglected. The inclusion of positive restraint moments for the designs with earlier continuity resulted in larger positive design moments within the spans, which required an increase in the number of prestressing strands.

A simple-span design has also been developed using the same girder dimensions that are used for the spans made continuous. This design was prepared as a benchmark for comparison to the continuous girder designs. Design moments and stresses for this design are as given in Section 4.3.1.

Figure D-4.3-1 summarizes the significant characteristics of the different designs. The figure clearly shows the benefit of continuity for precast/prestressed concrete girders. The girder design for the simple span required 30% more strands than did the continuous girder design developed using the simplified approach. For this bridge, all of the designs, even the design with continuity established at a girder age of 7 days, required fewer strands than did the simple-span design.

The design using girders that were 28 days old when continuity was established required 5% (1) more strands than did the girders designed using the simplified approach. This design required more effort than did the simplified approach since positive restraint moments were included in the design, although the increase was minor. This is a much less significant increase than was noticed for the Type III design in DE1 for a design using girders of the same age.

Even the design that established continuity when the girders were only 7 days old required only two more strands (a 10% increase) than did the girder designed using the simplified approach. Since this design still had fewer strands than did the simple-span design, designing for continuity provided a significant structural advantage.

The simplified approach, with its requirement for girders to be at least 90 days old when continuity is established, still appeared to be the best solution, with the least strands and the least effort in design. However, if speed were needed, it would still be possible to design a bridge of this type with continuity established at a very early age.

Figure D-4.3-2 compares the development of restraint moments with time for the final designs for the three girder ages at continuity. The increase in restraint moments for the designs with continuity at earlier ages can be seen if the figure is compared with development of restraint moments for the initial designs in Figure D-4.1.3-1. The increase in restraint moment was caused by the increased creep resulting from the increased number of strands. While the increase from the initial design was relatively large, the absolute value of the increase was still small enough that all designs were still viable.

TABLE D-4.2.1-1 Summary of design stresses for final design at release—continuity at 90 days

	Location from Bearing	*(ft)*	*Brg.* *0.00*	*H/2* *1.63*	*Trans.* *1.83*	*0.10L* *7.95*	*0.20L* *16.57*	*0.30L* *25.18*	*0.40L* *33.80*	*0.50L* *42.42*
Prestress at Release	Top Girder	(ksi)	N/A	N/A	–0.143	–0.143	–0.238	–0.238	–0.238	–0.238
	Bottom Girder	(ksi)	N/A	N/A	1.311	1.311	1.697	1.697	1.697	1.697
Self Weight	Top Girder	(ksi)	N/A	N/A	0.127	0.411	0.736	0.966	1.104	1.153
	Bottom Girder	(ksi)	N/A	N/A	–0.125	–0.402	–0.719	–0.946	–1.080	–1.128
Total at Release	Top Girder	(ksi)	N/A	N/A	–0.016	0.268	0.498	0.728	0.866	0.915
	Bottom Girder	(ksi)	N/A	N/A	1.186	0.909	0.978	0.751	0.617	0.569

Notes:
1. Critical stresses are shaded.
2. Values for limiting stresses are given in Section 3.4.2.1.
3. Compressive stresses at release are compared with the limit f_{cR} = 2.700 ksi. The maximum compressive stress is 1.186 ksi at the transfer length location.
4. Tensile stresses in regions other than the precompressed tensile zone at release are compared with the limiting tensile stress f_{tR1} = –0.200 ksi or f_{tR2} = –0.509 ksi. The latter value requires an area of reinforcement to resist the tensile force. The maximum tensile stress is –0.016 ksi at the transfer length location.
5. In all cases, this design satisfies the specified stress limits at release.

TABLE D-4.2.1-2 Summary of design stresses for final design at service limit state after losses—continuity at 90 days

	Location		Brg.	Trans.	H/2	0.10L	0.20L	0.30L	0.40L	0.50L	0.60L	0.70L	0.80L	0.90L	H/2	Trans.	Brg.
		From Brg. (ft)	0.00	1.92	2.20	8.03	16.65	25.27	33.88	42.50	51.12	59.73	68.35	76.97	82.80	83.08	85.00
SERVICE STRESSES (ksi)																	
1	Prestress After Losses	Top Girder	-0.035	-0.132	-0.121	-0.132	-0.220	-0.220	-0.220	-0.220	-0.220	-0.220	-0.220	-0.132	-0.121	-0.132	-0.035
		Bottom Girder	0.324	1.213	1.112	1.213	1.571	1.571	1.571	1.571	1.571	1.571	1.571	1.213	1.112	1.213	0.324
2	Self Weight	Top Girder	0.000	0.090	0.080	0.364	0.673	0.893	1.026	1.070	1.026	0.893	0.673	0.364	0.080	0.090	0.000
		Bottom Girder	0.000	-0.089	-0.079	-0.356	-0.658	-0.874	-1.004	-1.047	-1.004	-0.874	-0.658	-0.356	-0.079	-0.089	0.000
3	Non-Comp. DL	Top Girder	0.000	0.003	0.003	0.014	0.029	0.039	0.044	0.049	0.044	0.039	0.029	0.014	0.003	0.003	0.000
		Bottom Girder	0.000	-0.003	-0.003	-0.013	-0.028	-0.038	-0.043	-0.048	-0.043	-0.038	-0.028	-0.013	-0.003	-0.003	0.000
4	Composite DL	Top Girder	0.000	0.010	0.009	0.039	0.069	0.086	0.090	0.081	0.060	0.025	-0.022	-0.083	-0.135	-0.133	-0.150
		Bottom Girder	0.000	-0.010	-0.009	-0.038	-0.068	-0.084	-0.088	-0.080	-0.058	-0.025	0.022	0.081	0.132	0.130	0.147
5	Restraint Moment (RM) (+)	Top Girder	0.000	0.001	0.001	0.004	0.008	0.012	0.016	0.021	0.025	0.029	0.033	0.037	0.040	0.040	0.041
		Bottom Girder	0.000	-0.001	-0.001	-0.004	-0.008	-0.012	-0.016	-0.020	-0.024	-0.028	-0.032	-0.036	-0.039	-0.039	-0.040
6	LL + IM (+)	Top Girder	0.000	0.071	0.063	0.276	0.487	0.613	0.671	0.666	0.599	0.467	0.282	0.108	0.040	0.041	0.030
		Bottom Girder	0.000	-0.069	-0.061	-0.270	-0.477	-0.600	-0.657	-0.652	-0.586	-0.457	-0.276	-0.106	-0.039	-0.041	-0.030
7	LL + IM (-)	Top Girder	0.000	-0.008	-0.007	-0.036	-0.076	-0.115	-0.154	-0.193	-0.233	-0.272	-0.362	-0.421	-0.593	-0.586	-0.655
		Bottom Girder	0.000	0.008	0.007	0.035	0.074	0.112	0.151	0.189	0.228	0.266	0.354	0.412	0.581	0.573	0.641
TOTAL SERVICE STRESSES (ksi)																	
A = 1-4	Full PS + DL	Top Girder	-0.035	-0.028	-0.029	0.284	0.550	0.798	0.939	0.980	0.909	0.737	0.459	0.163	-0.173	-0.172	-0.185
		Bottom Girder	0.324	1.112	1.022	0.805	0.817	0.574	0.436	0.396	0.465	0.634	0.906	0.925	1.163	**1.252**	0.471
B = 1-5	Full PS + DL + RM (+)	Top Girder	-0.035	-0.027	-0.028	0.288	0.558	0.810	0.956	1.000	0.934	0.766	0.491	0.200	-0.133	-0.132	-0.144
		Bottom Girder	0.324	1.111	1.021	0.802	0.809	0.562	0.420	0.376	0.441	0.606	0.874	0.888	1.124	1.213	0.431
B + 1.0*6	Service I LL+IM (+) w/RM	Top Girder	-0.035	0.043	0.035	0.564	1.045	1.423	1.627	1.667	1.532	1.232	0.773	0.308	-0.093	-0.090	-0.114
		Bottom Girder	0.324	1.042	0.960	0.532	0.332	-0.038	-0.237	-0.276	-0.145	0.149	0.598	0.782	1.085	1.172	0.401
A + 1.0*7	Service I LL+IM (-)	Top Girder	-0.035	-0.037	-0.036	0.248	0.474	0.683	0.785	0.787	0.676	0.465	0.097	-0.258	-0.766	-0.757	-0.840
		Bottom Girder	0.324	1.120	1.029	0.841	0.891	0.687	0.587	0.585	0.693	0.900	1.260	1.336	1.743	**1.825**	1.112
B + 0.8*6	Service III LL+IM (+) w/RM	Top Girder	-0.035	0.029	0.022	0.509	0.948	1.301	1.492	1.533	1.413	1.139	0.717	0.286	-0.101	-0.098	-0.120
		Bottom Girder	0.324	1.055	0.972	0.586	0.428	0.082	-0.105	**-0.145**	-0.027	0.240	0.653	0.803	1.092	1.180	0.407
A + 0.8*7	Service III LL+IM (-)	Top Girder	-0.035	-0.035	-0.035	0.255	0.489	0.706	0.816	0.825	0.723	0.520	0.169	-0.174	-0.648	-0.640	**-0.709**
		Bottom Girder	0.324	1.118	1.028	0.834	0.876	0.664	0.556	0.548	0.648	0.847	1.190	1.254	1.627	1.710	0.984
6 + 0.5*B	Special (+) Service + RM	Top Girder	-0.018	0.057	0.049	0.420	0.766	1.018	1.149	1.166	1.066	0.849	0.528	0.208	-0.027	-0.024	-0.042
		Bottom Girder	0.162	0.486	0.449	0.131	-0.072	-0.319	-0.447	-0.464	-0.365	-0.154	0.161	0.338	0.523	0.566	0.186
7 + 0.5*A	Special (-) Service	Top Girder	-0.018	-0.022	-0.022	0.106	0.199	0.284	0.316	0.297	0.222	0.097	-0.132	-0.340	-0.680	-0.672	-0.748
		Bottom Girder	0.162	0.564	0.518	0.438	0.482	0.399	0.369	0.387	0.460	0.583	0.807	0.874	1.162	**1.199**	0.877

Notes:

1. Maximum stresses are shaded, with the governing stresses boxed and bolded.
2. Values for limiting stresses are given in Section 3.4.2.2.
3. Compressive stresses for both dead-load combinations (A and B) are compared with the limiting compressive stress for full dead load f_{c2} = 2.700 ksi. The maximum stress is 1.252 ksi at the transfer location for the combination without restraint moment (A).
4. Compressive stresses for both Service I LL+IM conditions are compared with the limiting compressive stress for full-service conditions f_{c1} = 3.600 ksi. The maximum stress is 1.825 ksi at the interior transfer length location for the combination without restraint moment.
5. Tensile stresses in the precompressed tensile zone for Service III with RM are compared with the limiting tensile stress f_{t1} = –0.465 ksi. The maximum stress is –0.145 ksi at midspan.
6. Tensile stresses in regions other than the precompressed tensile zone for Service III without RM are compared with the limiting tensile stress f_{t2} = –0.200 ksi or f_{t3} = –0.588 ksi. The latter value requires an area of reinforcement to resist the tensile force. The maximum stress is –0.709 ksi at the interior bearing. This stress exceeds both stress limits. This region of the girder will be designed for the strength limit state.
7. Compressive stresses for the special service cases are compared with the limiting compressive stress for that case f_{c3} = 2.400 ksi. The maximum stress is 1.199 ksi at the interior transfer length location for the combination without restraint moment.
8. In all cases, this design satisfies the specified stress limits, with the exception of tension at the interior support, which will be dealt with as noted.

Design	Strand Pattern	Design Moments*	Number of Strands	Area of Strands
Initial Design 90 Day Final Design ***Simplified Approach***	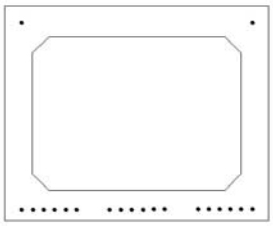	0 k-ft** 1,483.6 k-ft	**20**	**3.060 in^2** --
7 Day Final Design ***General Approach***	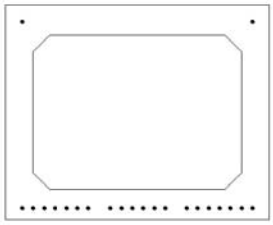	213.2 k-ft 1,575.6 k-ft	**22**	**3.366 in^2** ***+10.0%***
28 Day Final Design ***General Approach***	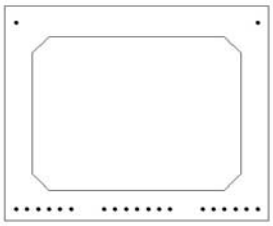	96.5 k-ft 1,517.3 k-ft	**21**	**3.213 in^2** ***+5.0%***
Simple-span Design	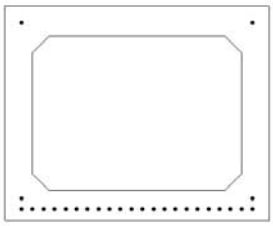	0.0 k-ft 1,772.7 k-ft	**26**	**3.978 in^2** ***+30.0%***
*Top number in cells is positive restraint moment at interior support. Bottom number in cells is Service III maximum positive design moment at midspan.				
**The initial design (same as continuity at 90 days) developed a minor positive restraint moment of 29.1 k-ft, which was neglected for the simplified approach.				

Figure D-4.3.1. Summary of designs.

4.3.1 Simple-Span Design for Comparison

A simple-span design using the same girder lengths and bearing locations was performed for comparison to the continuous girder designs. The properties of the concretes used for the simple-span design are the same as for the continuous design with a girder age of at least 90 days when continuity is established. See Table D-4.3.1-1.

The following tables of moments and stresses are provided for the simple-span bridge design used for comparison to the continuous girder designs. Because of symmetry, moments and stresses are only shown for half of the girder. Moments for noncomposite loads on the simple-span design are the same as shown in Table D-3.7.1-1.

Tables D-4.3.1-2 and D-4.3.1-3 present the service limit state stresses for the simple-span design. These stresses are compared with stress limits for final conditions after losses that are given in Section 3.4.2.2. Stress limits for release are given in the footnotes of Table D-4.3.1-2.

5 REINFORCEMENT FOR POSITIVE MOMENTS AT INTERIOR SUPPORTS

The connections between girders at interior supports of bridges made continuous are subject to positive design moments. The positive moments are caused by minor live-load effects (for bridges with more than two spans) and by restraint

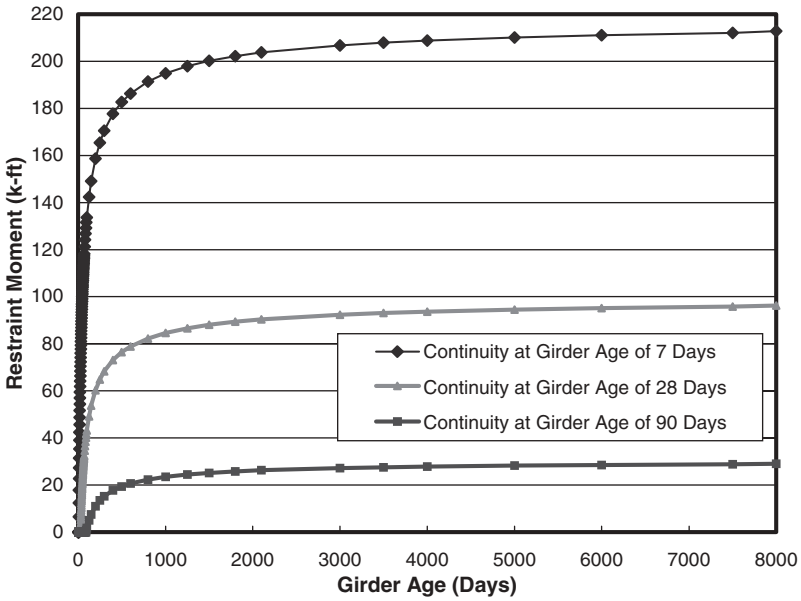

Figure D-4.3-2. Development of restraint moment with girder age—final design.

of time-dependent effects including creep, shrinkage, and temperature. Therefore, the positive design moments are not well-defined. Past research has questioned the benefit of providing a positive moment connection.

5.1 Positive Moment Connection

The proposed specifications recommend that positive moment connections be provided between all prestressed concrete girders made continuous. This recommendation is based on providing the connection to enhance the structural integrity of the structure so that it may be more robust and better able to resist unforeseen or extreme loads. However, if analysis for restraint moments is required and the analysis indicates that a positive moment will develop, the proposed specifications require that a positive moment connection be provided. While not required, a positive moment connection is provided for the design with continuity at 90 days.

Reinforcement to resist the positive design moment at the interior support may be provided using either mild reinforcement or pretensioning strand, as demonstrated in Sections 5.4 and 5.5. A combination of reinforcement types could also be used to provide the positive moment connection. The use of combined reinforcement types can be accomplished by combining the procedures for using each reinforcement type separately.

TABLE D-4.3.1-1 Service design moments for loads on composite section for simple-span bridge

	Location from Bearing (ft)	*Parapet DL (DC) (k-ft)*	*Wrg. Surf. DL (DW) (k-ft)*	*LL + IM Service I (k-ft)*	*LL + IM Service III (k-ft)*
Bearing	0.0	0.0	0.0	0.0	0.0
H/2	1.63	8.4	20.3	59.1	47.3
Transfer	1.83	9.4	22.8	66.5	53.2
0.10 L	8.0	37.8	91.6	265.4	212.3
0.20 L	16.6	69.9	169.6	485.0	388.0
0.30 L	25.2	92.8	225.2	633.9	507.1
0.40 L	33.8	106.6	258.6	722.1	577.7
0.50 L	42.4	111.2	269.8	744.0	595.2

5.2 Positive Design Moments

For the strength limit state, the reinforcement in the positive moment connection is proportioned to provide a factored resistance, (M_n, greater than the larger of the factored moment, M_u, or $0.6M_{cr}$, but not to exceed $1.2M_{cr}$. A design moment of $1.2M_{cr}$ is typically provided because testing and field experience have shown that this quantity of reinforcement, which is also the minimum quantity of reinforcement required by the AASHTO LRFD Specifications in many cases, has performed well. Reinforcement provided in excess of the quantity needed to resist $1.2M_{cr}$ has been shown to be less effective. It is therefore not recommended to use a quantity of reinforcement greater than that required for $1.2M_{cr}$.

For the service limit state, the reinforcement is proportioned to resist the larger of the service load moment or M_{cr}. The Service I load combination is used to compute the design moment because the connection is not prestressed.

Since this bridge has two spans, the only positive moment that can be developed at the interior support is caused by

TABLE D-4.3.1-2 Summary of design stresses for simple-span design at release

	Location from Bearing	*(ft)*	*Brg.*	*H/2*	*Trans.*	*0.10L*	*0.20L*	*0.30L*	*0.40L*	*0.50L*
			0.00	*1.63*	*1.83*	*7.95*	*16.57*	*25.18*	*33.80*	*42.42*
Prestress at Release	Top Girder	(ksi)	N/A	N/A	–0.361	–0.361	–0.361	–0.361	–0.361	–0.361
	Bottom Girder	(ksi)	N/A	N/A	2.226	2.226	2.226	2.226	2.226	2.226
Girder DL	Top Girder	(ksi)	N/A	N/A	0.127	0.411	0.736	0.966	1.104	1.153
	Bottom Girder	(ksi)	N/A	N/A	–0.125	–0.402	–0.719	–0.946	–1.080	–1.128
Total at Release	Top Girder	(ksi)	N/A	N/A	–0.234	0.050	0.375	0.605	0.743	0.792
	Bottom Girder	(ksi)	N/A	N/A	2.101	1.824	1.507	1.280	1.146	1.098

Notes:
1. Critical stresses are shaded.
2. Values for limiting stresses are given in Section 3.4.2.1.
3. Compressive stresses at release are compared with the limit f_{cR} = 2.700 ksi. The maximum compressive stress is 2.101 ksi at the transfer length location.
4. Tensile stresses in regions other than the precompressed tensile zone at release are compared with the limiting tensile stress f_{tR1} = –0.200 ksi or f_{tR2} = –0.509 ksi. The latter value requires an area of reinforcement to resist the tensile force. The maximum tensile stress is –0.234 ksi at the transfer length location. This stress exceeds the lower limit, so reinforcement is required to resist the tensile force in the concrete.
5. In all cases, this design satisfies the specified stress limits at release.

restraint (considering the effects included in this design example). Bridges with more spans will develop positive moments at the interior supports from live loads. Because there is no restraint moment for the design with continuity at a girder age of 90 days, there is no positive design moment.

5.2.1 Computation of Positive Cracking Moment at Continuity Diaphragm

5.2.1.1 Section Properties for Continuity Diaphragm. The cracking moment is computed using a solid rectangular cross section with dimensions equal to the nominal outside dimensions of the box girder. The section properties for the continuity diaphragm are as follows:

h = 39.00 in.;

$A' = h \times b = 39(48) = 1{,}872$ in.^{2};

$I' = bh^3/12 = 48(39)^3/12 = 237{,}276$ in.^{4};

y'_b = 19.50 in.;

y'_t = 19.50 in.;

S'_b = 12,168 in^3; and

S'_t = 12,168 in^3.

5.2.1.2 Cracking Moment. The positive cracking moment, M_{cr}, is computed using the section modulus for the bottom of the continuity diaphragm and the modulus of rupture for the diaphragm concrete, f_{rd}, which is given in Section 3.3.2.1:

$M_{cr} = f_{rd}\, S'_b = 0.480(12{,}168) = 5{,}841$ k-in. = 486.7 k-ft.

For reinforcement limits, the quantity $1.2M_{cr}$ is also computed:

$1.2M_{cr}$ = 584.1 k-ft.

5.3 Minimum Distance Between Ends of Girders

The bridge must be laid out to provide adequate distance between the ends of girders in the continuity diaphragm to develop the reinforcement. This distance depends on the type and size reinforcement that is used. Computations for determining the required development lengths into the continuity are presented for mild reinforcement and strands in the next two sections.

The distance between ends of girders must also be adequate to allow movement of bars or strands during erection for proper meshing of the positive moment connection reinforcement. The greater the distance, the less bending would be required to provide clearance, especially for strands that cannot be offset to avoid conflicts.

This minimum distance between ends of girders should be determined early in the design process because design spans and continuity diaphragm dimensions depend on this distance.

5.4 Mild Reinforcement

Mild reinforcement is often used to provide the positive moment connection. The reinforcement for the connection must extend from the end of the girder and be anchored into the continuity diaphragm. This reinforcement is usually placed among the pretensioned strands near the bottom of the girder

TABLE D-4.3.1-3 Summary of design stresses for simple-span design at service limit state after losses

	Location from Bearing	*(ft)*	*Brg.*	*Trans*	*H/2*	*0.10L*	*0.20L*	*0.30L*	*0.40L*	*0.50L*
			0.00	*1.63*	*1.83*	*7.95*	*16.57*	*25.18*	*33.80*	*42.42*
SERVICE STRESSES (ksi)										
Prestress after Losses	Top Girder	(ksi)	–0.327	–0.300	–0.327	–0.327	–0.327	–0.327	–0.327	–0.327
	Bottom Girder	(ksi)	0.538	1.850	2.018	2.018	2.018	2.018	2.018	2.018
Self Weight	Top Girder	(ksi)	0.000	0.080	0.091	0.364	0.673	0.893	1.026	1.070
	Bottom Girder	(ksi)	0.000	–0.079	–0.089	–0.356	–0.658	–0.874	–1.004	–1.047
Noncomp. DL	Top Girder	(ksi)	0.000	0.003	0.003	0.014	0.029	0.039	0.044	0.049
	Bottom Girder	(ksi)	0.000	–0.003	–0.003	–0.013	–0.028	–0.038	–0.043	–0.048
Composite DL	Top Girder	(ksi)	0.000	0.040	0.045	0.182	0.336	0.446	0.513	0.535
	Bottom Girder	(ksi)	0.000	–0.039	–0.044	–0.178	–0.329	–0.438	–0.503	–0.524
LL + IM	Top Girder	(ksi)	0.000	0.083	0.093	0.373	0.681	0.890	1.014	1.045
	Bottom Girder	(ksi)	0.000	–0.081	–0.091	–0.365	–0.667	–0.871	–0.993	–1.023
TOTAL SERVICE STRESSES (ksi)										
Full PS + DL	Top Girder	(ksi)	–0.087	–0.177	–0.189	0.232	0.71	1.052	1.255	1.327
	Bottom Girder	(ksi)	0.538	1.729	**1.882**	1.470	1.002	0.668	0.468	0.399
Service I	Top Girder	(ksi)	–0.087	–0.094	–0.095	0.604	1.392	1.942	2.270	**2.372**
	Bottom Girder	(ksi)	0.538	1.647	1.790	1.106	0.335	–0.204	–0.524	–0.624
Service III	Top Girder	(ksi)	**–0.087**	–0.111	–0.114	0.531	1.256	1.763	2.067	2.163
	Bottom Girder	(ksi)	0.538	1.664	1.809	1.179	0.469	–0.029	–0.326	**–0.419**
Special Service	Top Girder	(ksi)	–0.044	–0.005	–0.001	0.489	1.036	1.416	1.642	**1.708**
	Bottom Girder	(ksi)	0.269	0.783	0.849	0.370	–0.166	–0.538	–0.759	–0.824

Notes:
1. Maximum stresses are shaded, with the governing stresses boxed and bolded.
2. Values for limiting stresses are given in Section 3.4.2.2.
3. Compressive stresses for full prestress and dead load are compared with the limiting compressive stress for full dead load f_{c2} = 2.700 ksi. The maximum stress is 1.882 ksi at 0.50L.
4. Compressive stresses for Service I conditions are compared with the limiting compressive stress for full-service conditions f_{c1} = 3.600 ksi. The maximum stress is 2.372 ksi at 0.50L.
5. Tensile stresses in the precompressed tensile zone for Service III are compared with the limiting tensile stress f_{t1} = –0.465 ksi. The maximum stress is –0.419 ksi at 0.50L.
6. Tensile stresses in regions other than the precompressed tensile zone for Service III are compared with the limiting tensile stress f_{t2} = –0.200 ksi or f_{t3} = –0.588 ksi. The latter value requires an area of reinforcement to resist the tensile force. The maximum stress is –0.087 ksi at the bearing.
7. Compressive stresses for the special service combination are compared with the limiting compressive stress for that case f_{c3} = 2.400 ksi. The maximum stress is 1.708 ksi at 0.50L.
8. In all cases, this design satisfies the specified stress limits.

TABLE D-5.2-1 Summary of positive design moments and limits at center of interior support (critical moments are shaded)

			Girder Age at Continuity		
			7 Days	*28 Days*	*90 Days*
Service I Limit State	M_{sl}	(k-ft)	N/A	N/A	N/A
	M_{cr}	(k-ft)	486.7	486.7	486.7
Strength I Limit State	M_u	(k-ft)	*	*	N/A
	$1.2M_{cr}$	(k-ft)	584.1	584.1	584.1

*Load combinations at strength limit state do not result in positive design moments.

in order to maximize the effective depth to the reinforcement. This additional reinforcement inserted between strands that are usually placed on the standard 2 in. × 2 in. grid increases the congestion of reinforcement at the ends of girders. Extra attention must be given to this area during placement of concrete to avoid a lack of consolidation. However, the fact that the girder in this design example is a box section greatly improves the ability to provide positive moment reinforcement without a significant increase in congestion.

Hooks are generally provided on the projecting reinforcement to improve the development of the reinforcement into

the continuity diaphragm and also to shorten the required diaphragm width. The bars may be bent prior to or after fabrication of the girder, depending on fabricator preferences and clearances within the girder forms. Hairpin bars (180° hooks) are sometimes used to address reinforcement issues, although with box girders, this should not be required.

5.4.1 Development and Detailing of Reinforcement into the Continuity Diaphragm

The mild reinforcement is developed into the continuity diaphragm using a standard 90° hook. No. 5 bars will be used for the connection. The required length of embedment, ℓ_{dh}, into the diaphragm to develop the No. 5 hooked bar is computed according to LRFD Article 5.11.2.4:

ℓ_{dh} = 8.3 in.; USE 8½ in. LRFD Eq. 5.11.2.4.1-1

A reduction factor of 0.7 was used because conditions provide the required side and end cover. While the clear distance between the hook and the edge of the diaphragm is 1.5 in. (less than the 2 in. required), the face of the diaphragm is confined by the girder concrete. Therefore, this surface is not an exterior surface, and it appears appropriate to use the reduction. An embedment of the hook into the continuity diaphragm of 8.5 in. will be used. The distance between ends of girders in the continuity diaphragm will be taken as 10 in., so the 8.5-in. projection to the hook can be provided and still allow for construction tolerances. A standard hook of 10 in. is used for the vertical leg (see Figure D-5.4.2-1).

A small additional reduction in the required hook embedment could be taken if the provided area of reinforcement is more than required by analysis, but the design of the connection must be complete before the magnitude of this reduction is known. Therefore, 8.5 in. will be used in this example.

A cross bar of at least the same size as the hooked bar should be placed in the corner of the hooks to enhance the development of the hooked reinforcement into the diaphragm. See Figure D-5.4.1-1.

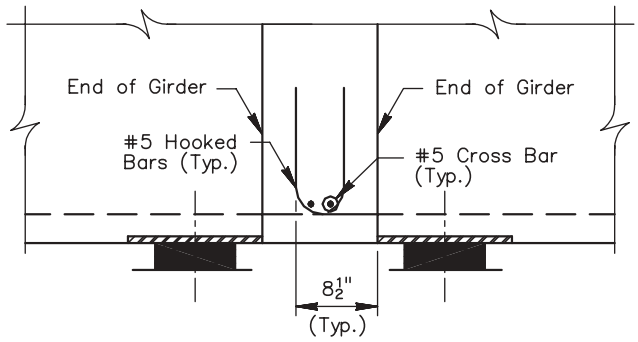

Figure D-5.4.1-1. Detail of reinforcement placement at positive moment connection (section view).

A 180° hooked bar (hairpin) may also be used for positive moment reinforcement, but many of the conditions that encourage use of hairpins are eliminated for box girders.

5.4.2 Required Area of Reinforcement

Using typical strength design procedures and the design moments given in the table above, the required area of reinforcement is computed to be as follows:

A_s = 3.67 in.^{2}

where

f'_{cd} = 4.00 ksi;
f_y = 60 ksi;
M_u = 1.2M_{cr} = 584.1 k-ft;
ϕ = 0.9;
b = 48 in.;
h = total depth of diaphragm, which is the same as h for the girder
= 39.00 in.;
g = distance from bottom of girder to centroid of reinforcement
= 3.00 in. (one row of reinforcement); and
d = effective depth from top of diaphragm = $h - g$ = 36.00 in.

For all girder designs, the required area of reinforcement, A_s = 3.67 in.^{2}, can be provided using twelve No. 5 reinforcing bars. This satisfies the assumption that all of the reinforcement can be placed in a single layer.

$A_{s\,prov}$ = 12(0.31 in.^{2}) = 3.72 in.^{2} > A_s = 3.67 in.^{2} OK.

A layout for the reinforcement is shown in Figure D-5.4.2-1.

5.4.3 Control of Cracking by Distribution of Reinforcement

According to LRFD Article 5.7.3.4, the reinforcement will be proportioned so that the tensile stress in the mild steel reinforcement at the service limit state does not exceed the stress limit given by LRFD Equation 5.7.3.4-1. Since there are no positive service limit state moments, this calculation is not necessary.

5.4.4 Development and Detailing of Reinforcement into Girder

The required development length into the girder for the No. 5 bars used for the positive moment reinforcement is computed as follows:

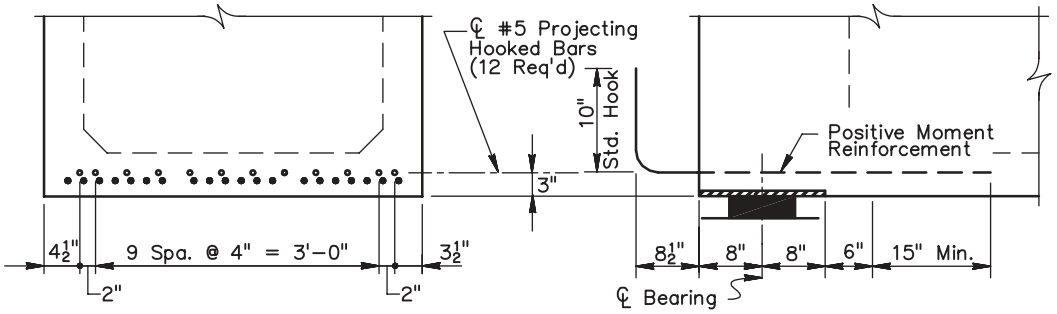

Figure D-5.4.2-1. Details of reinforcement placement at end of girder.

ℓ_{dh} = 15.0 in. LRFD Art. 5.11.2.1.1

This length applies for designs with continuity at all ages considered. The total length of embedment of the positive moment reinforcement into the girder should be carefully considered. It is recommended that the bar be developed beyond where an assumed crack radiating at a 2:1 slope from the inner edge of the bearing or embedded plate intersects the reinforcement. The general concept is illustrated in Figure D-5.4.4-1. The details of the connection for this bar are shown in Figure D-5.4.2-1. Where multiple bars are required for positive moment reinforcement, at least two different embedment lengths should be used to avoid stress concentrations and potential cracking where the bars terminate in the girder. One bar type should provide the minimum embedment length, with the second bar type providing at least an additional 1.5 ft of embedment. Where hairpin bars are used, the staggering of bar terminations can be accomplished by using a single bar type that is detailed with unequal legs.

5.4.5 Constructability Issues

Reinforcement projecting from the end of a girder is detailed to mesh with the reinforcement projecting from the opposing girder. This is intended to provide an essentially continuous load path for any tension that may develop at the bottom of the connection. This requires that the reinforcement be detailed to mesh. To accomplish this, the bars must be offset or bent so that conflicts between bars are minimized or eliminated.

The use of offset bars is illustrated for this design in Figure D-5.4.5-1. The bars are placed in a slightly eccentric pattern. This pattern simplifies fabrication and erection by allowing use of a single detail for the placement of reinforcement in all girders, which avoids fabrication errors and provides a positive offset between bars. As mentioned above, the use of two layers of reinforcement greatly complicates fabrication and erection of the girder, as well as placement of reinforcement in the continuity diaphragm. If possible, a single layer of reinforcement should be detailed; however, the available locations for placement of reinforcement are limited. Furthermore, the use of a larger number of smaller bars allows for a smaller gap between ends of opposing girders than is possible with fewer larger bars. The smaller bars also require a shorter embedment into the girder. These factors tend to lead designers to use a larger number of smaller bars.

The placement of the positive moment connection reinforcement between pretensioning strands increases congestion. This is significant because the congestion can inhibit the proper consolidation of concrete in the critical bearing area. Reinforcement should be positioned to facilitate placement and consolidation of concrete around the strands and bars.

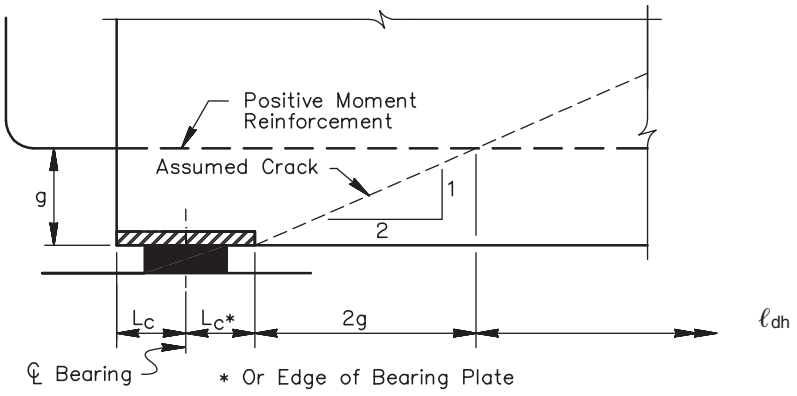

Figure D-5.4.4-1. Detail for embedment of reinforcement into girder.

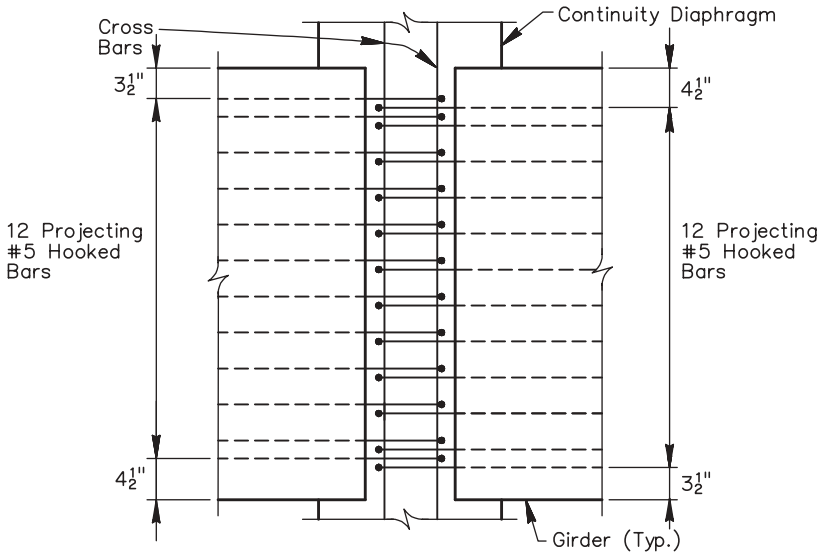

Figure D-5.4.5-1. Detail of reinforcement placement at positive moment connection (plan view).

Reinforcement projections must be detailed to allow tolerances in bar projections, girder lengths, and girder placement at erection. In this example, the distance from the end of the hook to the face of opposing girder was detailed as 3½ in., which should provide an adequate tolerance.

5.5 Pretensioning Strand

An alternate positive moment connection uses pretensioning strands extended into the continuity diaphragm. Because a positive moment connection with strands uses existing reinforcement (strands), the connection is provided without increasing congestion. However, girder fabrication may be complicated if the required length of extended strand is large. The limit on the service load stress of strands serves to limit the length of strand that can be effectively used for the connection. Extended strands used for the positive moment connection must be bonded at the end of the girder—that is, they cannot be shielded or debonded at the end of the girder.

5.5.1 Development and Detailing of Extended Strands into Continuity Diaphragm

The strands are developed into the continuity diaphragm using a 90° hook. The strand must be bent so that after bending, the hook projects at least 8 in. from the end of the girder. This distance is required by the equation used in Section 5.5.2.

The distance between ends of girders in the continuity diaphragm is detailed as 10 in., so the 8-in. projection to the bent strand can be provided and still allow for construction tolerances.

A cross bar should be placed in the corner of the hooks to enhance the development of the hooked reinforcement into the diaphragm. The cross bar should have an area not less than the area of a strand. See Figure D-5.5.1-1.

5.5.2 Required Area of Strands

The area of strands required to resist the positive design moments (see Table D-5.5.2-1) is computed using both the strength design provisions given in LRFD Article 5.14.1.2.7h and service load (working stress) design procedures. The working stress design procedures may be found in concrete design textbooks.

Working stress design is used in addition to strength design for this calculation because the procedure is based on results

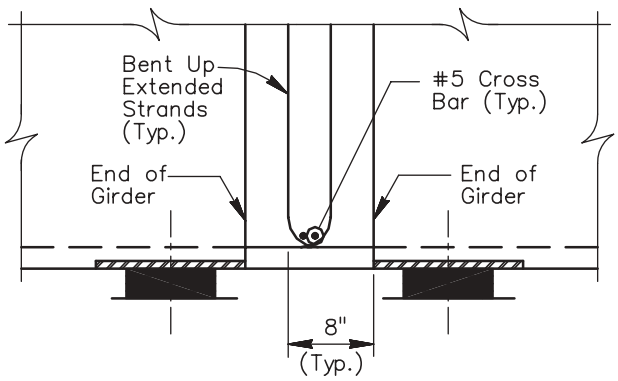

Figure D-5.5.1-1. Detail of strand placement at positive moment connection (section view).

TABLE D-5.5.2-1 Design information for positive moment connection using strand (critical values are shaded)

BASIC DESIGN INFORMATION		
l_{dsh}	(in.)	42
b	(in.)	48
d	(in.)	37
f'_{cd}	(ksi)	4.00
Strand Diameter	(in.)	0.5
STRENGTH DESIGN		
Design Moment	(k-ft)	584.1
f_{pul}	(ksi)	208.6
a	(in.)	1.18
A_{ps}	(in^2)	0.923
No. of Strands Req'd		6.03
WORKING STRESS DESIGN		
Design Moment	(k-ft)	486.7
E_c	(ksi)	3605
E_s	(ksi)	29000
n	8	.04
f_s	(ksi)	149.1
jd	(in.)	35.83
k	0	.095
rho		0.000615
A_s	(in^2)	1.093
No. of Strands Req'd		7.1

of research. The researchers proposed a design methodology that included both approaches.

The design moment for the working stress check will be M_{cr}, while the design moment for the strength check is 1.2 M_{cr}. Initially, it was assumed that the total length of extended strand, ℓ_{sh}, was 42 in. This provides a length of strand beyond the bend (vertical leg) of 42 − 8 = 34 in. The vertical leg extends for much of the depth of the girder to maximize the development of the strand, while not using so much strand that fabrication of the girders is adversely affected. This length of strand is effectively the maximum that can be used for this depth of box girder, allowing approximately 3 in. cover over the tip of the strand.

Using ℓ_{sh} = 42 in., stresses in strands are computed for the available length of strand. The resulting stresses in the 0.5-in.-diameter strands at service and strength conditions are

f_{psl} = [(42 − 8)/0.228] *Proposed* Eq. 5.14.1.2.7i-1
= 149 ksi < 150 ksi and

f_{pul} = [(42 − 8)/0.163] *Proposed* Eq. 5.14.1.2.7i-2
= 209 ksi.

Since f_{psl} does not exceed the maximum service load stress of 150 ksi that applies to *proposed* Equation 5.14.1.2.7i-1, this length of strand and the corresponding stresses may be used.

Based on these stress limits for service and strength limit states, the number of strands required to resist the positive design moments is computed. The design moments are governed by the minimum limits of M_{cr} = 486.7 k-ft and 1.2M_{cr} = 584.1 k-ft for service and strength design, respectively. Design moments are found in Table D-5.2-1. Results are given in Table D-5.5.2-1.

Eight strands will be provided for the connection. Since there are many strands that can be extended, these strands could be offset as shown in Figure D-5.5.2-1 in order to facilitate erection, using details similar to those for the mild reinforcement connection. Since an excess area of strands is being provided, the length of the strand extension could be reduced. See DE1 for the iterative process that can be used. Strands with debonding cannot be used for the positive moment connection.

5.5.3 Constructability Issues

Offsetting the pattern of extended strands enables meshing of the bent-up strands as shown in Figure D-5.5.3-1. This simplifies erection of the girders.

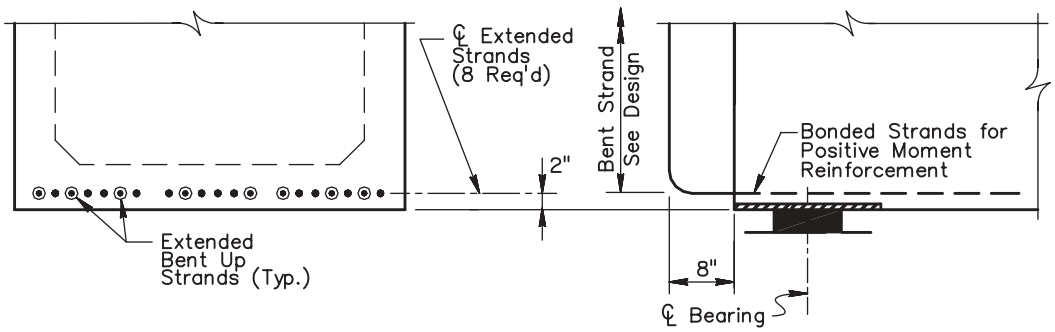

Figure D-5.5.2-1. Details of strand placement at end of girder.

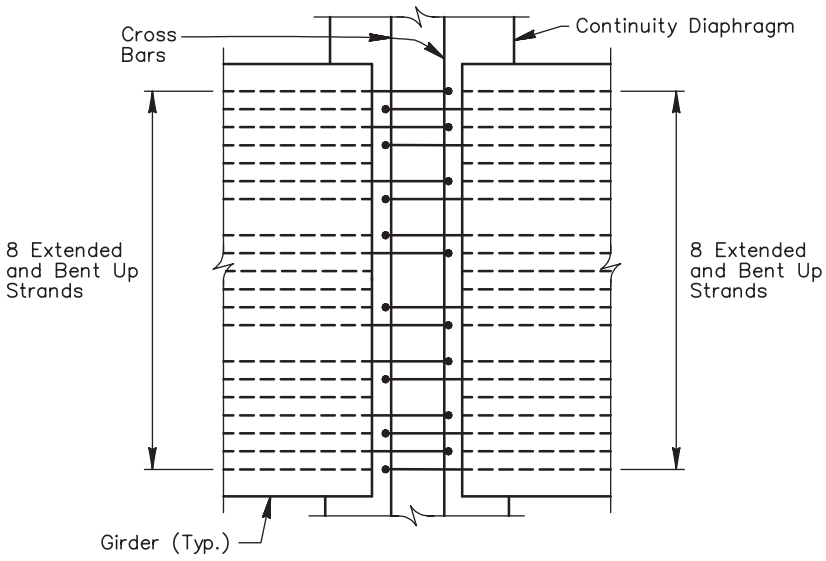

Figure D-5.5.3-1. Detail of strand placement at positive moment connection (plan view).

5.5.4 Fatigue of Positive Moment Connection Reinforcement

Because the reinforcement in the positive moment connection is not subjected to tension from the live load for this two-span bridge, fatigue does not need to be investigated. The positive moments caused from restraint moments or temperature effects do not occur frequently enough to be considered as loadings that cause fatigue. However, for other bridge configurations, where the connection is subjected to tension from live loads, fatigue should be considered. See Section 5.3.2.2.3 for the approach.

6 REINFORCEMENT FOR NEGATIVE MOMENTS AT INTERIOR SUPPORTS

The proper design of reinforcement at the negative moment connection is essential for the bridge to behave as a continuous structure and to provide the desired service life with little or no maintenance. This section presents the necessary steps for the design of the reinforcement for the negative moment connection.

6.1 Negative Design Moments

Negative moments at interior supports of precast/prestressed concrete girders made continuous result from dead loads, live loads, and restraint moments. Negative restraint moments, however, are ignored in design, as allowed by *proposed* Article 5.14.1.2.7b. Therefore, the negative design moments shown below in Table D-6.1-1 result from dead loads and live loads only. The negative moment connection is designed using strength methods, so design moments are factored.

TABLE D-6.1-1 Summary of negative design moments and limits at center of interior support (critical moments are shaded)

			Girder Age at Continuity		
			7 Days	***28 Days***	***90 Days***
Service I Limit State	M_{sl}	(k-ft)	–1,013.1	–1,013.1	–1,013.1
	M_{cr}	(k-ft)	–486.7	–486.7	–486.7
Strength I Limit State	M_u	(k-ft)	–1,180.6	–1,180.6	–1,180.6
	$1.2M_{cr}$	(k-ft)	–584.1	–584.1	–584.1

6.1.1 Computation of Negative Cracking Moment at Continuity Diaphragm

Section properties for the continuity diaphragm used to compute the cracking moment are discussed and given in Section 5.2.1.1. The negative cracking moment, M_{cr}, is computed using the section modulus for the top of the continuity diaphragm and the modulus of rupture for the diaphragm concrete, f_{rd}, which is given in Section 3.3.2.1:

$$M_{cr} = f_{rd} S'_t = 0.480(12{,}168) = 5{,}841 \text{ k-in} = 486.7 \text{ k-ft.}$$

For reinforcement limits, the quantity $1.2M_{cr}$ is also computed:

$$1.2M_{cr} = 584.1 \text{ k-ft.}$$

6.2 Negative Moment Connection

The connections between girders at interior piers of a bridge with precast girders made continuous are subject to significant negative design moments. The portion of the bridge subjected to negative moments must be properly reinforced to resist

these negative moments if it is to perform as a continuous member and if the structure is to have good serviceability.

Since this bridge does not have a composite deck, the negative moment connection cannot be made using reinforcement in the deck, which is the typical approach. Instead, the reinforcement must be provided in the top of the box girder and developed into the continuity diaphragm in the same way as the positive moment reinforcement. Fatigue of the reinforcement must also be checked. Detailing of the negative moment reinforcement, which is important for economy and to avoid congestion, is also addressed.

6.2.1 Required Area of Reinforcement

Reinforcement for the negative moment connection could be provided by mild reinforcement, strands, or a combination of both. For this example, only mild reinforcement will be considered. Computations for a connection using strand would employ the same procedures used for the positive moment connection.

Based on the factored negative design moment at the interior support, a total required area of reinforcement is computed:

b = 48.0 in. (width at bottom of diaphragm = width of girder bottom flange);

d = 36.50 in. (providing 2 in. minimum clear to top reinforcement);

f'_{cd} = 4.00 ksi;

f_y = 60 ksi; and

M_u = –1,180.6 k-ft.

Using this information, the area of reinforcement required to resist the factored negative design moment is computed using strength design to give the following results:

A_s = 7.47 in.^{2}

where

a = 2.75 in. and
c = 3.23 in.

Checking the maximum reinforcement limit,

c/d = 3.23/36.50 = 0.088 < 0.42. OK

Using No. 6 bars, which can be developed into the diaphragm with a 10-in. extension (see DE2), 17 bars are required. Therefore,

$A_{s\,prov}$ = 17(0.44) = 7.48 in.^{2}.

The layout of the negative moment reinforcement in the top of the girder is shown in Figure D-6.2.1-1.

6.2.2 Details of Negative Moment Reinforcement

The negative moment connection reinforcement can be detailed using the same details that are used for the positive moment connection with mild reinforcement except that the hooks are turned down into the continuity diaphragm as shown in Figure D-6.2.1-1.

An alternate negative moment connection may be made by splicing straight bars across the continuity diaphragm. A blockout at the top of the beam may be required to provide the length of exposed reinforcement required to make the connection. Negative moment connections of this type have been made successfully using commercially available grouted splice connections. Requirements for mechanical splices are given in LRFD Article 5.11.5.2.2. Another option is to use high-strength threaded rods that are "coupled" with offset bars from the opposing beam by bolting at a plate (Ma et al., 1998 and Hennessey and Bexten, 2003). Welded splices conforming to the requirements of LRFD Article 5.11.5.2.3 may also be used.

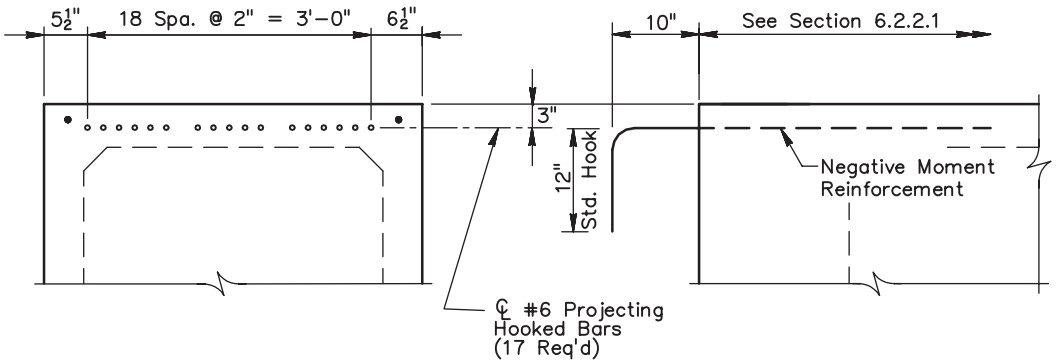

Figure D-6.2.1-1. Details of strand placement at end of girder—negative moment connection.

Using any of these mechanical connection options instead of splicing hooked bars in the continuity diaphragm would permit the use of larger bars, which would reduce the number of bars required to extend from the end of the beam. This would reduce the congestion at the end of the beam and in the continuity diaphragm.

6.2.2.1 Anchorage of Negative Moment Reinforcement. The specifications indicate that the longitudinal reinforcement resisting the negative design moments must be anchored in concrete that is in compression at the strength limit state (LRFD Article 5.14.1.2.7b and *proposed* Art. 5.14.1.2.7h). Therefore, the inflection points for the negative moment envelope at the strength limit state must be located.

Figure D-6.2.2.1-1 indicates the extent of the negative moment region at strength limit state. The reinforcement for the factored negative design moment must be extended past the indicated locations for at least a development length. Therefore, the minimum length of the No. 6 bars placed in the top of the girder would be

$$\ell_{min} = 17.3 \text{ ft} + \ell_d = 17.3 \text{ ft} + (25.2 \text{ in.}/12) = 19.4 \text{ ft}$$

where

ℓ_d = 25.2 in. (for No. 6 bar, "top bar" designation). LRFD Art. 5.11.2.1.1

6.2.2.2 Terminations of Negative Moment Reinforcement. Although all negative moment reinforcement can theoretically be terminated at one location, as shown in Figure D-6.2.2.1-1, this would probably not provide good serviceability. It is recommended that the same bar mark be used, but that alternate reinforcing bars be shifted several feet to stagger the terminations. This would require that the minimum length of bar computed above would be increased by the amount of the shift.

6.2.3 Constructability Issues

In this example, constructability issues for negative moment reinforcement are the same as for the positive moment reinforcement, although congestion issues are not as significant since the reinforcement is in the top of the girder where consolidation is easier. The connection shown uses bars that are hooked into the continuity diaphragm. However, the top of the girder could also be blocked out, and a bar could be placed to lap with the negative moment reinforcement.

6.2.4 Control of Cracking by Distribution of Reinforcement

According to LRFD Article 5.7.3.4, the reinforcement will be proportioned such that the tensile stress in the mild steel reinforcement at the service limit does not exceed the allowable given by LRFD Equation 5.7.3.4-1. The tensile stress in the negative moment reinforcement is computed to be

$$f_s = \frac{M_{sl}}{A_s jd} = \frac{1,013.1(12)}{7.48(0.931)(36.0)} = 48.5 \text{ ksi}$$

where

M_{sl} = 1013.1 k-ft;
A_s = 7.48 in.^{2};
f_y = 60 ksi;
E_s = 29,000 ksi;

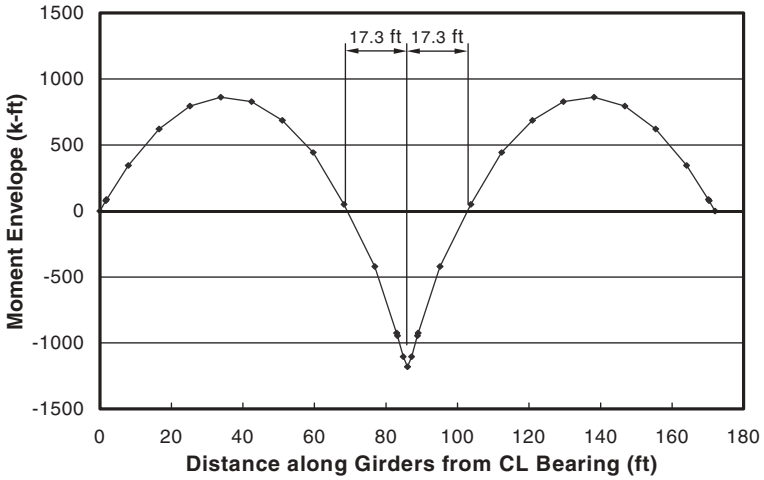

Figure D-6.2.2.1-1. Negative moment envelope and location of inflection points.

E_c = 4,696 ksi;
$n = E_s/E_{cd}$ = 6.175;
b' = width of compression face = 48 in.;
d = effective depth from bottom of girder including build-up = 36.0 in.;

$$\rho = \frac{A_s}{bd} = \frac{7.48}{48(36.0)} = 0.0043;$$

$$k = \sqrt{2\rho n + (\rho n)^2}$$

$$-\rho n = \sqrt{2(0.0043)(6.175) + ((0.0043)(6.175))^2}$$

$$-(0.0043)(6.175) = 0.206; \text{ and}$$

$$j = 1 - \frac{k}{3} = 1 - \frac{0.206}{3} = 0.931.$$

The allowable tensile stress in the mild reinforcement is

$$f_{sa} = \frac{Z}{(d_c A)^{1/3}} \le 0.6 f_y \qquad \text{LRFD Eq. 5.7.3.4-1}$$

$$= \frac{170}{(2.22(12.54))^{1/3}} \le 0.6 \times 60$$

$$= 56.1 > 36.0 \text{ ksi USE } f_{sa} = 36.0 \text{ ksi (maximum allowed)}$$

where

d_c = 2.22 in.;
Z = 170 k/in.; and

$$A = \frac{2 d_c b}{\text{No. of Bars}} = \frac{2(2.22)(48)}{17} = 12.54 \text{ in.}^2.$$

For the girders, the tensile stress in the mild reinforcement is more than the allowable. Thus, the distribution of reinforcement for control of cracking is inadequate and more reinforcement is required:

f_{sa} = 36.0 ksi < f_s = 48.5 ksi. NG (no good)

Using No. 7 bars instead of No. 6 bars, the tensile stress in the mild reinforcement would be 35.4 ksi, which is less then the allowable stress of 36.0 ksi.

6.2.5 Fatigue of Negative Moment Reinforcement

Fatigue of the negative moment reinforcement is evaluated according to LRFD Article 5.5.3.1. The conditions in this design do not meet the requirements to be exempt from evaluation. To determine whether cracked section properties must be used to evaluate the stress range, the stress in the concrete is computed under a specified loading combination:

M = sum of unfactored permanent loads + prestress + 1.5(fatigue load) = −391 + 0 + 1.5(−139.3) (fatigue moment is computed below) = −600 k-ft; and

$f_{cd\,\text{top}} = M/S'_t = M/(I'/[h' - y'_b]) = -600(12)/(237{,}276/(39.00 - 19.50)) = -0.592$ ksi.

Stress limit is then computed for comparison to computed stress:

$$f_{cd\,\max} = -0.095\sqrt{f'_{cd}} = -0.095\sqrt{4.0} = -0.190 \text{ ksi.}$$

Comparing the absolute values of the computed stress and stress limit,

$$f_{cd\,\text{top}} = 0.592 \text{ ksi} > f_{cd\,\max} = 0.190 \text{ ksi.}$$

Since the computed stress exceeds the stress limit, the effect of fatigue must be evaluated using cracked section analysis. The stress in the reinforcement is computed using the specified fatigue loading and cracked section analysis as required.

The basic negative fatigue moment is −582 k-ft, using the QConBridge Program (see Subappendix C). The analysis assumes the bridge is fully continuous for live loads. This moment is factored by the dynamic load allowance for fatigue (1 + 0.15) (LRFD Article 3.6.2.1); by the live-load distribution factor for one lane loaded (0.333) (LRFD Article 3.6.1.4.3b; and by LRFD Table 4.6.2.2.2b-1 (cross-section type g), which is divided by the multiple presence factor for one lane loaded (1.2) (LRFD Article C3.6.1.1.2) and the load factor for the fatigue limit state, which is 0.75 (LRFD Table 3.4.1-1). Therefore, the design fatigue moment is

$$M_f = 1.15(0.333/1.2)(0.75)(-582) = -139.3 \text{ k-ft.}$$

The area of reinforcement provided in the top of the girder is

$$A_{sd} = 7.48 \text{ in.}^2.$$

The stress range in the reinforcement caused by this design fatigue moment is computed using the principles of working stress design for a cracked section. The width of the compression zone is the width of the box girder = 48 in.:

$$f_f = 6.63 \text{ ksi.}$$

The limiting stress range, $f_{f\max}$, is computed as

$$f_{f\max} = 21 - 0.33 f_{\min} + 8(r/h) \qquad \text{LRFD Eq. 5.5.3.2-1}$$

$$= 21 - 0.33(18.61) + 8(0.3)$$

$$= 17.3 \text{ ksi}$$

where

$f_{min} = f_{LLf} + f_{DL} = 0.00 + 18.61 = 18.61$ ksi;

f_{LLf} = minimum live-load stress from fatigue loading = 0.00 ksi;

f_{DL} = stress in reinforcement from permanent loads from working stress analysis = 18.61 ksi;

M_{DL} = total composite dead-load moment (load factor = 1.0) at the center of the pier = −391 k-ft (see Table D-3.7.1-2); and

r/h = ratio of base radius to height of rolled on transverse deformations in the reinforcement = 0.3 may be used if value not known.

Comparing the computed stress range to the limiting stress range,

$f_f = 6.63$ ksi $< f_{f\,max} = 17.3$ ksi. OK

REFERENCES AND BIBLIOGRAPHY FOR APPENDIX D

AASHTO LRFD Bridge Design Specifications, 2nd Edition. American Assoc. of State Highway and Transportation Officials; Washington, DC; 1998.

Hennessey, S.A. and Bexten, K.A. "Value Engineering Results In Successful Precast Bridge Solution," Proceedings of the 2002 Concrete Bridge Conference, Precast/Prestressed Concrete Institute, Chicago, 2003.

Ma, Z., Huo, X., Tadros, M.K., and Baishya, M. "Restraint Moments in Precast/Prestressed Concrete Continuous Bridges," PCI Journal, Vol. 43, No. 6, Nov/Dec 1998; pp. 40–56.

Salmons, J.R. Behavior of Untensioned-Bonded Prestressing Strand, Final Report 77-1, Missouri Cooperative Highway Research Program, Missouri State Highway Department, June 1980.

Salmons, J.R. *End Connections of Pretensioned I-Beam Bridges,* Final Report 73-5C, Missouri Cooperative Highway Research Program, Missouri State Highway Department, Nov. 1974.

Salmons, J.R. and May, G.W. *Strand Reinforcing for End Connection of Pretensioned I-Beam Bridges,* Interim Report 73-5B, Missouri Cooperative Highway Research Program, Missouri State Highway Department, May 1974.

Salmons, J.R. and McCrate, T.E. *Bond of Untensioned Prestress Strand,* Interim Report 73-5A, Missouri Cooperative Highway Research Program, Missouri State Highway Department, Aug. 1973.

SUBAPPENDIX A: INPUT DATA FOR RESTRAINT

DA.1 DESIGN EXAMPLE 1: AASHTO TYPE III GIRDER BRIDGE

DA.1.1 Initial Design

TABLE DA.1.1-1 Initial design

Input			
Span Data		**Strand Data**	
Select Girder Type	III	Centroid of Straight Strands (in)	7.3333
Number of spans	2	Centroid of Draped Strands at Girder End (in)	37
Exterior Span Length (ft)	85	Centroid of Draped Strands at Midspan (in)	5
First Interior Span Length (ft) (for 3,4,5 spans)	100	Number of Straight Strands	30
Second Interior Span Length (5 spans)	0	Number of Draped Strands	8
Strand Draping Length / Span Length	0.4	Cross Sectional Area of Strand (in^2)	0.153
Girder Spacing (ft)	7.75	Initial Strand Tension (psi)	202500
Deck Thickness (in)	7.75	Type of Strand (SR or LL)	LL
Additional Dead Load (psf)	50	Eps	28500
Concrete Data		**Time Data**	
Girder Concrete Compressive Stress at Transfer (psi)	5500	Strand Age at Prestress Transfer (days)	1
Girder Concrete Compressive Stress at 28 Days (psi)	7000	Girder Age at Continuity (days)	
Deck Concrete Compressive Stress at 28 Days (psi)	4000	Girder Age at Time Deck is in Place (days)	
Girder Concrete Unit Weight (pcf)	150	Include Dischinger Effect? (Y/N)	Y
Deck Concrete Unit Weight (pcf)	150	If Yes, Deck Age for Dischinger Modification (days)	30
Girder Concrete Utlimate Creep Coefficient	1.8		
Girder Concrete Ultimate Shrinkage (millionths)	395.4		
Deck Concrete Ultimate Shrinkage (millionths)	353		
Relative Humidity (%)	75		

DA.1.2 Girder Age at Continuity of 90 Days – Simplified Approach

TABLE DA.1.2-1 Final design for girder age at continuity of 90 days

Input			
Span Data		**Strand Data**	
Select Girder Type	III	Centroid of Straight Strands (in)	7.3333
Number of spans	2	Centroid of Draped Strands at Girder End (in)	37
Exterior Span Length (ft)	85	Centroid of Draped Strands at Midspan (in)	5
First Interior Span Length (ft) (for 3,4,5 spans)	100	Number of Straight Strands	30
Second Interior Span Length (5 spans)	0	Number of Draped Strands	8
Strand Draping Length / Span Length	0.4	Cross Sectional Area of Strand (in^2)	0.153
Girder Spacing (ft)	7.75	Initial Strand Tension (psi)	202500
Deck Thickness (in)	7.75	Type of Strand (SR or LL)	LL
Additional Dead Load (psf)	50	Eps	28500
Concrete Data		**Time Data**	
Girder Concrete Compressive Stress at Transfer (psi)	5500	Strand Age at Prestress Transfer (days)	1
Girder Concrete Compressive Stress at 28 Days (psi)	7000	Girder Age at Continuity (days)	90
Deck Concrete Compressive Stress at 28 Days (psi)	4000	Girder Age at Time Deck is in Place (days)	90
Girder Concrete Unit Weight (pcf)	150	Include Dischinger Effect? (Y/N)	Y
Deck Concrete Unit Weight (pcf)	150	If Yes, Deck Age for Dischinger Modification (days)	30
Girder Concrete Utlimate Creep Coefficient	1.8		
Girder Concrete Ultimate Shrinkage (millionths)	395.4		
Deck Concrete Ultimate Shrinkage (millionths)	353		
Relative Humidity (%)	75		

DA.1.3 Girder Age at Continuity of 60 Days

TABLE DA.1.3-1 Run 2—Design for girder age at continuity of 60 days

Input

Span Data		Strand Data	
Select Girder Type	III	Centroid of Straight Strands (in)	7.5
Number of spans	2	Centroid of Draped Strands at Girder End (in)	37
Exterior Span Length (ft)	85	Centroid of Draped Strands at Midspan (in)	5
First Interior Span Length (ft) (for 3,4,5 spans)	100	Number of Straight Strands	32
Second Interior Span Length (5 spans)	0	Number of Draped Strands	8
Strand Draping Length / Span Length	0.4	Cross Sectional Area of Strand (in^2)	0.153
Girder Spacing (ft)	7.75	Initial Strand Tension (psi)	202500
Deck Thickness (in)	7.75	Type of Strand (SR or LL)	LL
Additional Dead Load (psf)	50	Eps	28500
Concrete Data		**Time Data**	
Girder Concrete Compressive Stress at Transfer (psi)	6000	Strand Age at Prestress Transfer (days)	1
Girder Concrete Compressive Stress at 28 Days (psi)	7000	Girder Age at Continuity (days)	60
Deck Concrete Compressive Stress at 28 Days (psi)	4000	Girder Age at Time Deck is in Place (days)	60
Girder Concrete Unit Weight (pcf)	150	Include Dischinger Effect? (Y/N)	Y
Deck Concrete Unit Weight (pcf)	150	If Yes, Deck Age for Dischinger Modification (days)	30
Girder Concrete Utlimate Creep Coefficient	1.8		
Girder Concrete Ultimate Shrinkage (millionths)	395.4		
Deck Concrete Ultimate Shrinkage (millionths)	353		
Relative Humidity (%)	75		

DA.1.4 Girder Age at Continuity of 28 Days

TABLE DA.1.3-2 Run 3 (final)—Design for girder at age continuity of 60 days

Input

Span Data		Strand Data	
Select Girder Type	III	Centroid of Straight Strands	7.294
Number of spans	2	Centroid of Draped Strands at Girder End	37
Exterior Span Length (ft)	85	Centroid of Draped Strands at Midspan	5
First Interior Span Length (ft) (for 3,4,5	100	Number of Straight	34
Second Interior Span Length (5 spans)	0	Number of Draped	8
Strand Draping Length / Span	0.4	Cross Sectional Area of Strand (in^2)	0.153
Girder Spacing (ft)	7.75	Initial Strand Tension	202500
Deck Thickness (in)	7.75	Type of Strand (SR or LL)	LL
Additional Dead Load (psf)	50	Eps	28500
Concrete Data		**Time Data**	
Girder Concrete Compressive Stress at Transfer (psi)	6000	Strand Age at Prestress Transfer (days)	1
Girder Concrete Compressive Stress at 28 Days	7000	Girder Age at Continuity (days)	60
Deck Concrete Compressive Stress at 28 Days	4000	Girder Age at Time Deck is in Place	60
Girder Concrete Unit Weight (pcf)	150	Include Dischinger Effect?	Y
Deck Concrete Unit Weight	150	If Yes, Deck Age for Dischinger Modification	30
Girder Concrete Utlimate Creep	1.8		
Girder Concrete Ultimate Shrinkage	395.4		
Deck Concrete Ultimate Shrinkage	353		
Relative Humidity	75		

DA.1.4 Girder Age at Continuity of 28 Days

TABLE DA.1.4-1 Run 2—Design for girder age at continuity of 28 days

Input

Span Data	
Select Girder Type	III
Number of spans	2
Exterior Span Length (ft)	85
First Interior Span Length (ft) (for 3,4,5 spans)	100
Second Interior Span Length (5 spans)	0
Strand Draping Length / Span Length	0.4
Girder Spacing (ft)	7.75
Deck Thickness (in)	7.75
Additional Dead Load (psf)	50

Strand Data	
Centroid of Straight Strands (in)	7.4
Centroid of Draped Strands at Girder End (in)	37.0
Centroid of Draped Strands at Midspan (in)	5.0
Number of Straight Strands	30
Number of Draped Strands	8
Cross Sectional Area of Strand (in^2)	0.153
Initial Strand Tension (psi)	202500
Type of Strand (SR or LL)	LL
Eps	28500

Concrete Data	
Girder Concrete Compressive Stress at Transfer (psi)	5500
Girder Concrete Compressive Stress at 28 Days (psi)	7000
Deck Concrete Compressive Stress at 28 Days (psi)	4000
Girder Concrete Unit Weight (pcf)	150
Deck Concrete Unit Weight (pcf)	150
Girder Concrete Utlimate Creep Coefficient	1.8
Girder Concrete Ultimate Shrinkage (millionths)	395.4
Deck Concrete Ultimate Shrinkage (millionths)	353
Relative Humidity (%)	75

Time Data	
Strand Age at Prestress Transfer (days)	1
Girder Age at Continuity (days)	28
Girder Age at Time Deck is in Place (days)	28
Include Dischinger Effect? (Y/N)	y
If Yes, Deck Age for Dischinger Modification (days)	30

TABLE DA.1.4-2 Run 3—Design for girder age at continuity of 28 days

Input

Span Data	
Select Girder Type	III
Number of spans	2
Exterior Span Length (ft)	85
First Interior Span Length (ft) (for 3,4,5 spans)	100
Second Interior Span Length (5 spans)	0
Strand Draping Length / Span Length	0.4
Girder Spacing (ft)	7.75
Deck Thickness (in)	7.75
Additional Dead Load (psf)	50

Strand Data	
Centroid of Straight Strands (in)	7.2
Centroid of Draped Strands at Girder End (in)	34.0
Centroid of Draped Strands at Midspan (in)	8.0
Number of Straight Strands	20
Number of Draped Strands	14
Cross Sectional Area of Strand (in^2)	0.217
Initial Strand Tension (psi)	202500
Type of Strand (SR or LL)	LL
Eps	28500

Concrete Data	
Girder Concrete Compressive Stress at Transfer (psi)	7000
Girder Concrete Compressive Stress at 28 Days (psi)	8500
Deck Concrete Compressive Stress at 28 Days (psi)	4000
Girder Concrete Unit Weight (pcf)	150
Deck Concrete Unit Weight (pcf)	150
Girder Concrete Utlimate Creep Coefficient	1.62
Girder Concrete Ultimate Shrinkage (millionths)	395.4
Deck Concrete Ultimate Shrinkage (millionths)	353
Relative Humidity (%)	75

Time Data	
Strand Age at Prestress Transfer (days)	1
Girder Age at Continuity (days)	28
Girder Age at Time Deck is in Place (days)	28
Include Dischinger Effect? (Y/N)	y
If Yes, Deck Age for Dischinger Modification (days)	30

TABLE DA.1.4-3 Run 4—Design for girder age at continuity of 28 days

Input			
Span Data		**Strand Data**	
Select Girder Type	III	Centroid of Straight Strands (in)	7.09
Number of spans	2	Centroid of Draped Strands at Girder End (in)	35.0
Exterior Span Length (ft)	85	Centroid of Draped Strands at Midspan (in)	9.0
First Interior Span Length (ft) (for 3,4,5 spans)	100	Number of Straight Strands	22
Second Interior Span Length (5 spans)	0	Number of Draped Strands	12
Strand Draping Length / Span Length	0.4	Cross Sectional Area of Strand (in^2)	0.217
Girder Spacing (ft)	7.75	Initial Strand Tension (psi)	202500
Deck Thickness (in)	7.75	Type of Strand (SR or LL)	LL
Additional Dead Load (psf)	50	Eps	28500
Concrete Data		**Time Data**	
Girder Concrete Compressive Stress at Transfer (psi)	7500	Strand Age at Prestress Transfer (days)	1
Girder Concrete Compressive Stress at 28 Days (psi)	9000	Girder Age at Continuity (days)	28
Deck Concrete Compressive Stress at 28 Days (psi)	4000	Girder Age at Time Deck is in Place (days)	28
Girder Concrete Unit Weight (pcf)	150	Include Dischinger Effect? (Y/N)	y
Deck Concrete Unit Weight (pcf)	150	If Yes, Deck Age for Dischinger Modification (days)	30
Girder Concrete Utlimate Creep Coefficient	1.56		
Girder Concrete Ultimate Shrinkage (millionths)	395.4		
Deck Concrete Ultimate Shrinkage (millionths)	353		
Relative Humidity (%)	75		

TABLE DA.1.4-4 Run 5 (final)—Design for girder age at continuity of 28 days

Input			
Span Data		**Strand Data**	
Select Girder Type	III	Centroid of Straight Strands (in)	7.09
Number of spans	2	Centroid of Draped Strands at Girder End (in)	35.0
Exterior Span Length (ft)	85	Centroid of Draped Strands at Midspan (in)	9.0
First Interior Span Length (ft) (for 3,4,5 spans)	100	Number of Straight Strands	22
Second Interior Span Length (5 spans)	0	Number of Draped Strands	12
Strand Draping Length / Span Length	0.4	Cross Sectional Area of Strand (in^2)	0.217
Girder Spacing (ft)	7.75	Initial Strand Tension (psi)	202500
Deck Thickness (in)	7.75	Type of Strand (SR or LL)	LL
Additional Dead Load (psf)	50	Eps	28500
Concrete Data		**Time Data**	
Girder Concrete Compressive Stress at Transfer (psi)	7500	Strand Age at Prestress Transfer (days)	1
Girder Concrete Compressive Stress at 28 Days (psi)	8500	Girder Age at Continuity (days)	28
Deck Concrete Compressive Stress at 28 Days (psi)	4000	Girder Age at Time Deck is in Place (days)	28
Girder Concrete Unit Weight (pcf)	150	Include Dischinger Effect? (Y/N)	y
Deck Concrete Unit Weight (pcf)	150	If Yes, Deck Age for Dischinger Modification (days)	30
Girder Concrete Utlimate Creep Coefficient	1.62		
Girder Concrete Ultimate Shrinkage (millionths)	395.4		
Deck Concrete Ultimate Shrinkage (millionths)	353		
Relative Humidity (%)	75		

DA.2 DESIGN EXAMPLE 2 – PCI BT-72 GIRDER BRIDGE

DA.2.1 Initial Design

TABLE DA.2.1-1 Initial design

Input			
Span Data		**Strand Data**	
Select Girder Type	BT 72	Centroid of Straight Strands	8.615
Number of spans	2	Centroid of Draped Strands at Girder End	66
Exterior Span Length (ft)	124.75	Centroid of Draped Strands at Midspan	4
First Interior Span Length (ft) (for 3,4,5)	100	Number of Straight	26
Second Interior Span Length (5 spans)	0	Number of Draped	6
Strand Draping Length / Span	0.4	CrossSectional Area of Strand (in^2)	0.217
Girder Spacing (ft)	7.75	Initial Strand Tension	202500
Deck Thickness (in)	7.75	Type of Strand (SR or LL)	LL
Additional Dead Load (psf)	50	Eps	28500
Concrete Data		**Time Data**	
Girder Concrete Compressive Stress at Transfer (psi)	5500	Strand Age at Prestress Transfer (days)	1
Girder Concrete Compressive Stress at 28 Days	7000	Girder Age at Continuity (days)	
Deck Concrete Compressive Stress at 28 Days	4000	Girder Age at Time Deck is in Place	
Girder Concrete Unit Weight (pcf)	150	Include Dischinger Effect?	y
Deck Concrete Unit Weight	150	If Yes, Deck Age for Dischinger Modification	30
Girder Concrete Utlimate Creep	1.889		
Girder Concrete Ultimate Shrinkage	430.7		
Deck Concrete Ultimate Shrinkage	353		
Relative Humidity	75		

DA.2.2 Girder Age at Continuity of 90 Days – Simplified Approach

TABLE DA.2.2-1 Final design for girder age at continuity of 90 days

Input			
Span Data		**Strand Data**	
Select Girder Type	BT 72	Centroid of Straight Strands	8.615
Number of spans	2	Centroid of Draped Strands at Girder End	66
Exterior Span Length (ft)	124.75	Centroid of Draped Strands at Midspan	4
First Interior Span Length (ft) (for 3,4,5)	100	Number of Straight	26
Second Interior Span Length (5 spans)	0	Number of Draped	6
Strand Draping Length / Span	0.4	Cross Sectional Area of Strand (in^2)	0.217
Girder Spacing (ft)	7.75	Initial Strand Tension	202500
Deck Thickness (in)	7.75	Type of Strand (SR or LL)	LL
Additional Dead Load (psf)	50	Eps	28500
Concrete Data		**Time Data**	
Girder Concrete Compressive Stress at Transfer (psi)	5500	Strand Age at Prestress Transfer (days)	1
Girder Concrete Compressive Stress at 28 Days	7000	Girder Age at Continuity (days)	90
Deck Concrete Compressive Stress at 28 Days	4000	Girder Age at Time Deck is in Place	90
Girder Concrete Unit Weight (pcf)	150	Include Dischinger Effect?	y
Deck Concrete Unit Weight	150	If Yes, Deck Age for Dischinger Modification	30
Girder Concrete Utlimate Creep	1.889		
Girder Concrete Ultimate Shrinkage	430.7		
Deck Concrete Ultimate Shrinkage	353		
Relative Humidity	75		

DA.2.3 Girder Age at Continuity of 60 Days

TABLE DA.2.3-1 Final design for girder age at continuity of 60 days

Input			
Span Data		**Strand Data**	
Select Girder Type	BT 72	Centroid of Straight Strands	8.62
Number of spans	2	Centroid of Draped Strands at Girder End	64
Exterior Span Length (ft)	124.75	Centroid of Draped Strands at Midspan	6
First Interior Span Length (ft) (for 3,4,5)	100	Number of Straight	26
Second Interior Span Length (5 spans)	0	Number of Draped	10
Strand Draping Length / Span	0.4	Cross Sectional Area of Strand (in^2)	0.217
Girder Spacing (ft)	7.75	Initial Strand Tension	202500
Deck Thickness (in)	7.75	Type of Strand (SR or LL)	LL
Additional Dead Load (psf)	50	Eps	28500
Concrete Data		**Time Data**	
Girder Concrete Compressive Stress at Transfer (psi)	5600	Strand Age at Prestress Transfer (days)	1
Girder Concrete Compressive Stress at 28 Days	7000	Girder Age at Continuity (days)	60
Deck Concrete Compressive Stress at 28 Days	4000	Girder Age at Time Deck is in Place	60
Girder Concrete Unit Weight (pcf)	150	Include Dischinger Effect?	y
Deck Concrete Unit Weight	150	If Yes, Deck Age for Dischinger Modification	30
Girder Concrete Utlimate Creep	1.889		
Girder Concrete Ultimate Shrinkage	430.7		
Deck Concrete Ultimate Shrinkage	353		
Relative Humidity	75		

DA.2.4 Girder Age at Continuity of 28 Days

TABLE DA.2.4-1 Final design for girder age at continuity of 28 days

Input			
Span Data		**Strand Data**	
Select Girder Type	BT 72	Centroid of Straight Strands	8.4
Number of spans	2	Centroid of Draped Strands at Girder End	61
Exterior Span Length (ft)	124.75	Centroid of Draped Strands at Midspan	9
First Interior Span Length (ft) (for 3,4,5)	100	Number of Straight	30
Second Interior Span Length (5 spans)	0	Number of Draped	16
Strand Draping Length / Span	0.4	Cross Sectional Area of Strand (in^2)	0.217
Girder Spacing (ft)	7.75	Initial Strand Tension	202500
Deck Thickness (in)	7.75	Type of Strand (SR or LL)	LL
Additional Dead Load (psf)	50	Eps	28500
Concrete Data		**Time Data**	
Girder Concrete Compressive Stress at Transfer (psi)	7500	Strand Age at Prestress Transfer (days)	1
Girder Concrete Compressive Stress at 28 Days	8000	Girder Age at Continuity	28
Deck Concrete Compressive Stress at 28 Days	4000	Girder Age at Time Deck is in Place	28
Girder Concrete Unit Weight (pcf)	150	Include Dischinger Effect?	y
Deck Concrete Unit Weight	150	If Yes, Deck Age for Dischinger Modification	30
Girder Concrete Utlimate Creep	1.754		
Girder Concrete Ultimate Shrinkage	430.7		
Deck Concrete Ultimate Shrinkage	353		
Relative Humidity	75		

DA.3 DESIGN EXAMPLE 3 – 51-IN. DEEP SPREAD BOX GIRDER BRIDGE

DA.3.1 Initial Design

TABLE DA.3.1-1 Initial design

Input			
Span Data		**Strand Data**	
Select Girder Type		Centroid of Straight Strands	7.33
Number of spans	2	Centroid of Draped Strands at Girder End	0
Exterior Span Length (ft)	84.83333	Centroid of Draped Strands at Midspan	0
First Interior Span Length (ft) (for 3,4,5	100	Number of Straight	39
Second Interior Span Length (5 spans)	0	Number of Draped	0
Strand Draping Length / Span	0.4	Cross Sectional Area of Strand (in^2)	0.153
Girder Spacing (ft)	11	Initial Strand Tension	202500
Deck Thickness (in)	8.25	Type of Strand (SR or LL)	LL
Additional Dead Load (psf)	50	Eps	28500
Concrete Data		**Time Data**	
Girder Concrete Compressive Stress at Transfer (psi)	5000	Strand Age at Prestress Transfer (days)	1
Girder Concrete Compressive Stress at 28 Days	6000	Girder Age at Continuity	
Deck Concrete Compressive Stress at 28 Days	4500	Girder Age at Time Deck is in Place	
Girder Concrete Unit Weight (pcf)	150	Include Dischinger Effect?	y
Deck Concrete Unit Weight	150	If Yes, Deck Age for Dischinger Modification	30
Girder Concrete Utlimate Creep	2.025		
Girder Concrete Ultimate Shrinkage	423.6		
Deck Concrete Ultimate Shrinkage	359.6		
Relative Humidity	75		

DA.3.2 Girder Age at Continuity of 90 Days – Simplified Approach

TABLE DA.3.2-1 Final design for girder age at continuity of 90 days

Input			
Span Data		**Strand Data**	
Select Girder Type		Centroid of Straight Strands	7.33
Number of spans	2	Centroid of Draped Strands at Girder End	0
Exterior Span Length (ft)	84.83333	Centroid of Draped Strands at Midspan	0
First Interior Span Length (ft) (for 3,4,5)	100	Number of Straight	39
Second Interior Span Length (5 spans)	0	Number of Draped	0
Strand Draping Length / Span	0.4	Cross Sectional Area of Strand (in^2)	0.153
Girder Spacing (ft)	11	Initial Strand Tension	202500
Deck Thickness (in)	8.25	Type of Strand (SR or LL)	LL
Additional Dead Load (psf)	50	Eps	28500
Concrete Data		**Time Data**	
Girder Concrete Compressive Stress at Transfer (psi)	5000	Strand Age at Prestress Transfer (days)	1
Girder Concrete Compressive Stress at 28 Days	6000	Girder Age at Continuity	90
Deck Concrete Compressive Stress at 28 Days	4500	Girder Age at Time Deck is in Place	90
Girder Concrete Unit Weight (pcf)	150	Include Dischinger Effect?	y
Deck Concrete Unit Weight	150	If Yes, Deck Age for Dischinger Modification	30
Girder Concrete Utlimate Creep	2.025		
Girder Concrete Ultimate Shrinkage	423.6		
Deck Concrete Ultimate Shrinkage	359.6		
Relative Humidity	75		

DA.3.3 Girder Age at Continuity of 60 Days

TABLE DA.3.3-1 Final design for girder age at continuity of 60 days

Input

Span Data		Strand Data	
Select Girder Type		Centroid of Straight Strands	7.25
Number of spans	2	Centroid of Draped Strands at Girder End	0
Exterior Span Length (ft)	84.83333	Centroid of Draped Strands at Midspan	0
First Interior Span Length (ft) (for 3,4,5)	100	Number of Straight	40
Second Interior Span Length (5 spans)	0	Number of Draped	0
Strand Draping Length / Span	0.4	Cross Sectional Area of Strand (in^2)	0.153
Girder Spacing (ft)	11	Initial Strand Tension	202500
Deck Thickness (in)	8.25	Type of Strand (SR or LL)	LL
Additional Dead Load (psf)	50	Eps	28500
Concrete Data		**Time Data**	
Girder Concrete Compressive Stress at Transfer (psi)	5000	Strand Age at Prestress Transfer (days)	1
Girder Concrete Compressive Stress at 28 Days	6000	Girder Age at Continuity	60
Deck Concrete Compressive Stress at 28 Days	4500	Girder Age at Time Deck is in Place	60
Girder Concrete Unit Weight (pcf)	150	Include Dischinger Effect?	y
Deck Concrete Unit Weight	150	If Yes, Deck Age for Dischinger Modification	30
Girder Concrete Utlimate Creep	2.025		
Girder Concrete Ultimate Shrinkage	423.6		
Deck Concrete Ultimate Shrinkage	359.6		
Relative Humidity	75		

DA.3.4 Girder Age at Continuity of 28 Days

TABLE DA.3.4-1 Final design for girder age at continuity of 28 days

Input

Span Data		Strand Data	
Select Girder Type		Centroid of Straight Strands	6.68
Number of spans	2	Centroid of Draped Strands at Girder End	0
Exterior Span Length (ft)	84.83333	Centroid of Draped Strands at Midspan	0
First Interior Span Length (ft) (for 3,4,5)	100	Number of Straight	56
Second Interior Span Length (5 spans)	0	Number of Draped	0
Strand Draping Length / Span	0.4	Cross Sectional Area of Strand (in^2)	0.153
Girder Spacing (ft)	11	Initial Strand Tension	202500
Deck Thickness (in)	8.25	Type of Strand (SR or LL)	LL
Additional Dead Load (psf)	50	Eps	28500
Concrete Data		**Time Data**	
Girder Concrete Compressive Stress at Transfer (psi)	5250	Strand Age at Prestress Transfer (days)	1
Girder Concrete Compressive Stress at 28 Days	6000	Girder Age at Continuity	28
Deck Concrete Compressive Stress at 28 Days	4500	Girder Age at Time Deck is in Place	28
Girder Concrete Unit Weight (pcf)	150	Include Dischinger Effect?	y
Deck Concrete Unit Weight	150	If Yes, Deck Age for Dischinger Modification	30
Girder Concrete Utlimate Creep	2.025		
Girder Concrete Ultimate Shrinkage	423.6		
Deck Concrete Ultimate Shrinkage	359.6		
Relative Humidity	75		

DA.4 DESIGN EXAMPLE 4 – AASHTO BIII-48 ADJACENT BOX GIRDER BRIDGE

DA.4.1 Initial Design

TABLE DA.4.1-1 Final design for girder age at continuity of 28 days

Input			
Span Data		**Strand Data**	
Select Girder Type	BIII-48	Centroid of Straight Strands	5.4
Number of spans	2	Centroid of Draped Strands at Girder End	0.0
Exterior Span Length (ft)	85	Centroid of Draped Strands at Midspan	0.0
First Interior Span Length (ft) (for 3,4,5)	100	Number of Straight	20
Second Interior Span Length (5 spans)	0	Number of Draped	0
Strand Draping Length / Span	0.4	Cross Sectional Area of Strand (in^2)	0.153
Girder Spacing (ft)	4	Initial Strand Tension	202500
Deck Thickness (in)	0	Type of Strand (SR or LL)	LL
Additional Dead Load (psf)	50	Eps	28500
Concrete Data		**Time Data**	
Girder Concrete Compressive Stress at Transfer (psi)	4500	Strand Age at Prestress Transfer (days)	1
Girder Concrete Compressive Stress at 28 Days	6000	Girder Age at Continuity	
Deck Concrete Compressive Stress at 28 Days	4500	Girder Age at Time Deck is in Place	
Girder Concrete Unit Weight (pcf)	150	Include Dischinger Effect?	y
Deck Concrete Unit Weight	150	If Yes, Deck Age for Dischinger Modification	30
Girder Concrete Utlimate Creep	1.999		
Girder Concrete Ultimate Shrinkage	414.5		
Deck Concrete Ultimate Shrinkage	100		
Relative Humidity	75		

DA.4.2 Girder Age at Continuity of 90 Days – Simplified Approach

TABLE DA.4.2-1 Final design for girder age at continuity of 90 days

Input			
Span Data		**Strand Data**	
Select Girder Type	BIII-48	Centroid of Straight Strands	5.4
Number of spans	2	Centroid of Draped Strands at Girder End	0.0
Exterior Span Length (ft)	85	Centroid of Draped Strands at Midspan	0.0
First Interior Span Length (ft) (for 3,4,5)	100	Number of Straight	20
Second Interior Span Length (5 spans)	0	Number of Draped	0
Strand Draping Length / Span	0.4	Cross Sectional Area of Strand (in^2)	0.153
Girder Spacing (ft)	4	Initial Strand Tension	202500
Deck Thickness (in)	0	Type of Strand (SR or LL)	LL
Additional Dead Load (psf)	50	Eps	28500
Concrete Data		**Time Data**	
Girder Concrete Compressive Stress at Transfer (psi)	4500	Strand Age at Prestress Transfer (days)	1
Girder Concrete Compressive Stress at 28 Days	6000	Girder Age at Continuity	90
Deck Concrete Compressive Stress at 28 Days	4500	Girder Age at Time Deck is in Place	90
Girder Concrete Unit Weight (pcf)	150	Include Dischinger Effect?	y
Deck Concrete Unit Weight	150	If Yes, Deck Age for Dischinger Modification	30
Girder Concrete Utlimate Creep	1.999		
Girder Concrete Ultimate Shrinkage	414.5		
Deck Concrete Ultimate Shrinkage	100		
Relative Humidity	75		

DA.4.3 Girder Age at Continuity of 28 Days

TABLE DA.4.3-1 Final design for girder age at continuity of 28 days

Input			
Span Data		**Strand Data**	
Select Girder Type	BIII-48	Centroid of Straight Strands	5.4
Number of spans	2	Centroid of Draped Strands at Girder End	0.0
Exterior Span Length (ft)	85	Centroid of Draped Strands at Midspan	0.0
First Interior Span Length (ft) (for 3,4,5	100	Number of Straight	20
Second Interior Span Length (5 spans)	0	Number of Draped	0
Strand Draping Length / Span	0.4	Cross Sectional Area of Strand (in^2)	0.153
Girder Spacing (ft)	4	Initial Strand Tension	202500
Deck Thickness (in)	0	Type of Strand (SR or LL)	LL
Additional Dead Load (psf)	50	Eps	28500
Concrete Data		**Time Data**	
Girder Concrete Compressive Stress at Transfer (psi)	4500	Strand Age at Prestress Transfer (days)	1
Girder Concrete Compressive Stress at 28 Days	6000	Girder Age at Continuity	28
Deck Concrete Compressive Stress at 28 Days	4500	Girder Age at Time Deck is in Place	28
Girder Concrete Unit Weight (pcf)	150	Include Dischinger Effect?	y
Deck Concrete Unit Weight	150	If Yes, Deck Age for Dischinger Modification	30
Girder Concrete Utlimate Creep	1.999		
Girder Concrete Ultimate Shrinkage	414.5		
Deck Concrete Ultimate Shrinkage	100		
Relative Humidity	75		

SUBAPPENDIX B: INPUT AND OUTPUT FROM RESPONSE 2000

DB.1 PROGRAM INFORMATION

The Response 2000 Program was developed at the University of Toronto and is available free of charge at www.ecf.utoronto.ca/~bentz/r2k.htm. The version of the program used for this study is shown in the figure below taken from the program.

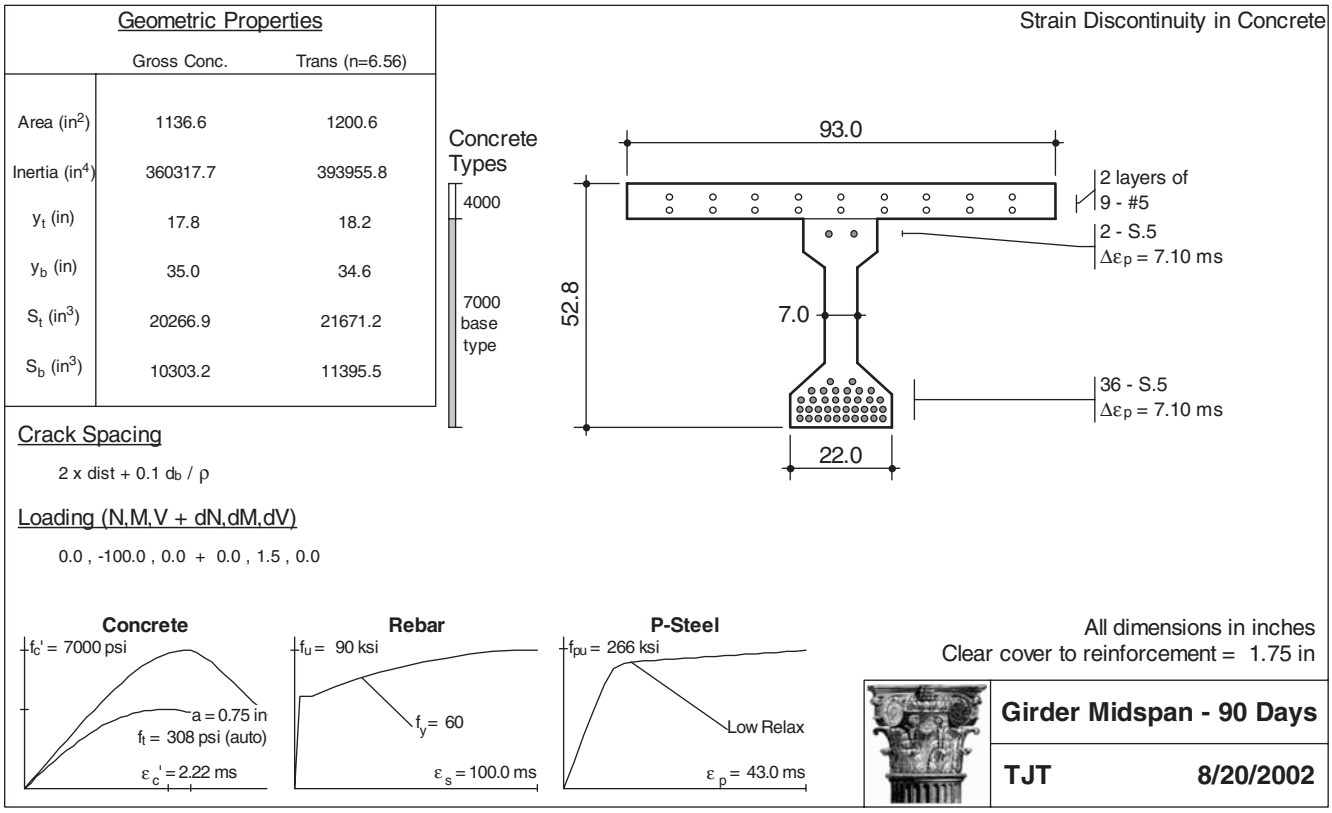

Figure DB.2.1.1-1. Cross section and material information.

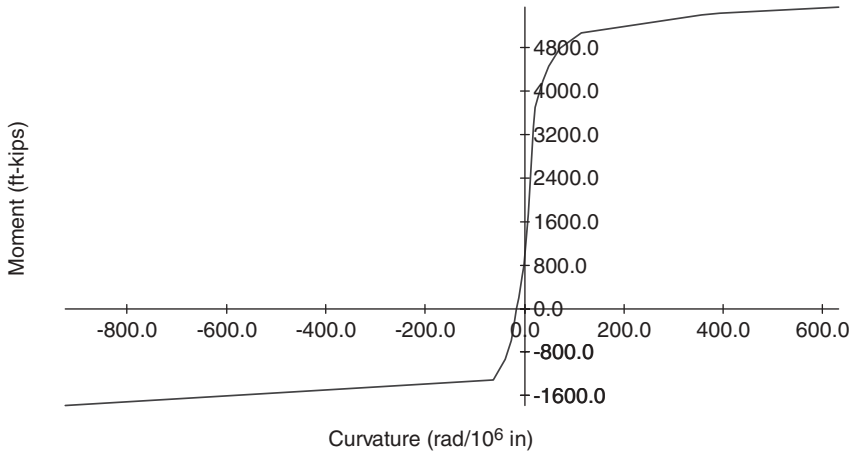

Figure DB.2.1.1-2. Moment curvature analysis plot.

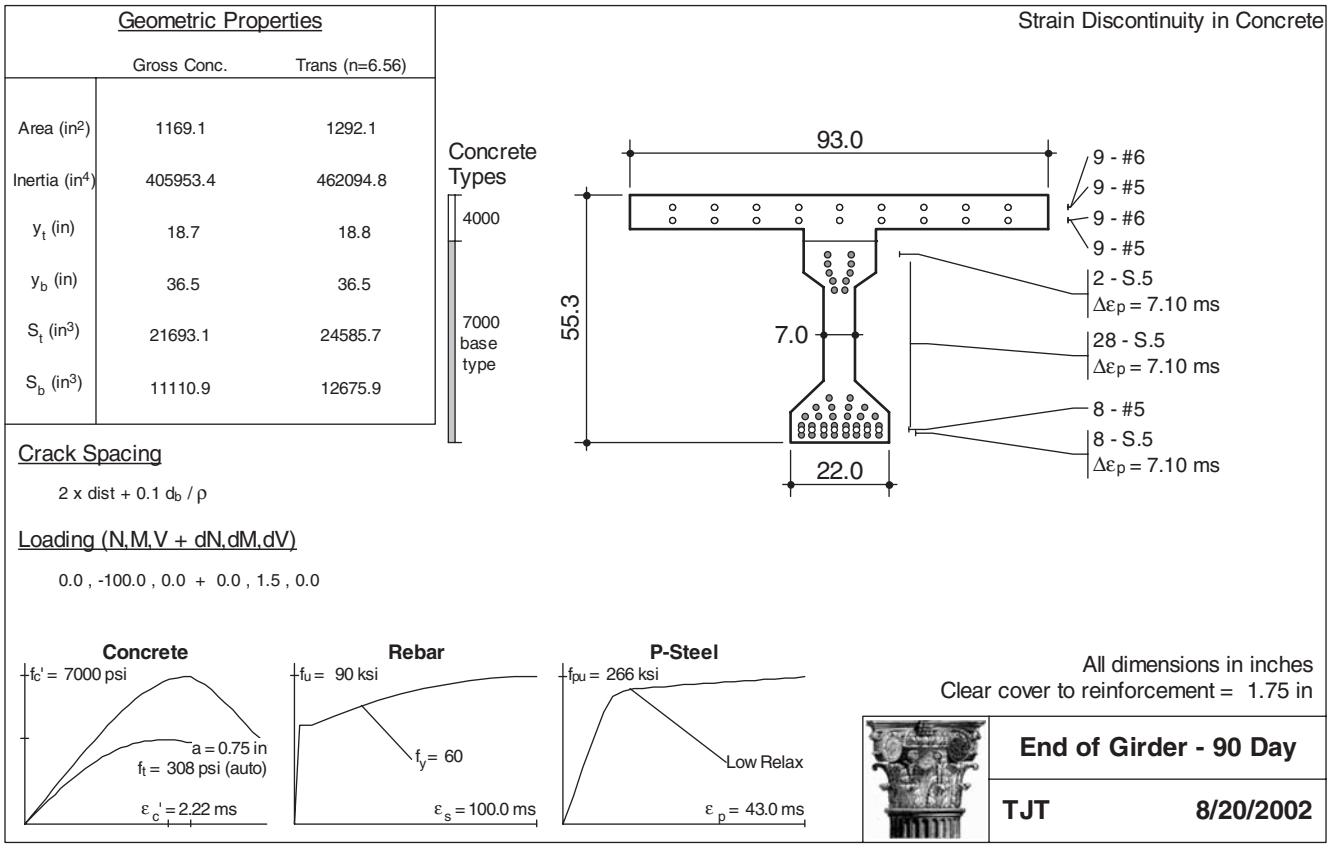

Figure DB.2.1.2-1. Cross section and material information.

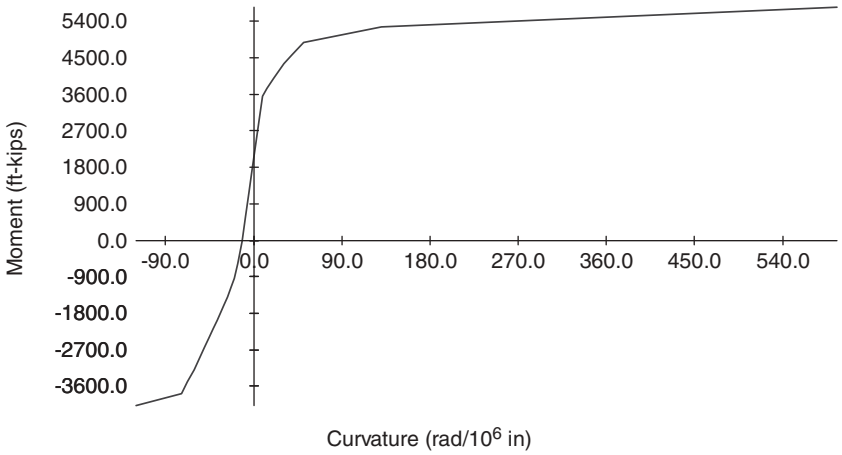

Figure DB.2.1.2-2. Moment curvature analysis plot.

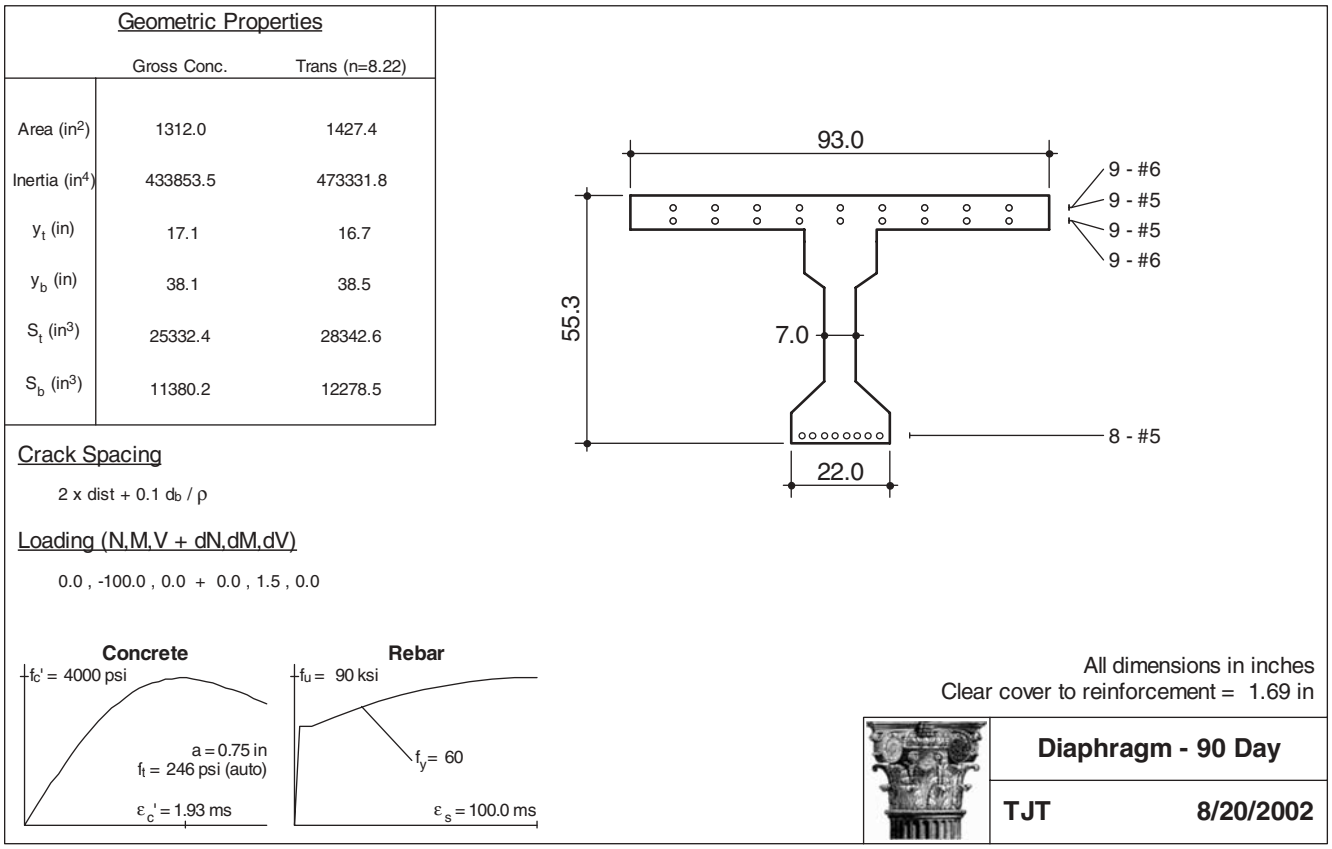

Figure DB.2.1.3-1. Cross section and material information.

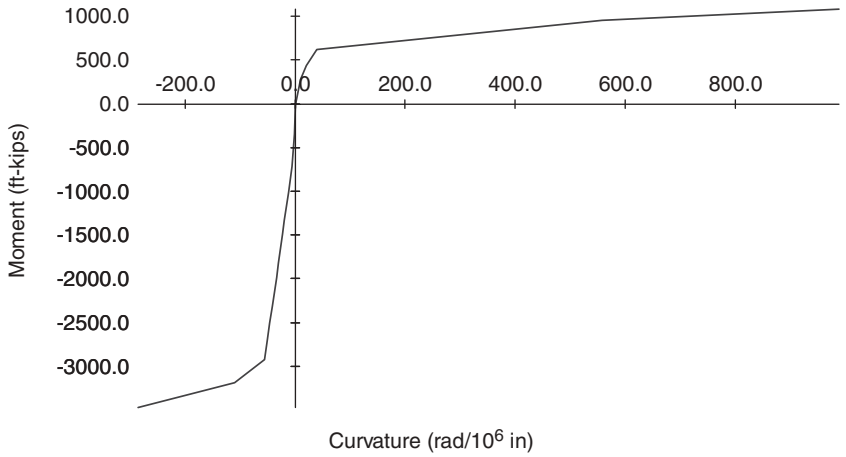

Figure DB.2.1.3-2. Moment curvature analysis plot.

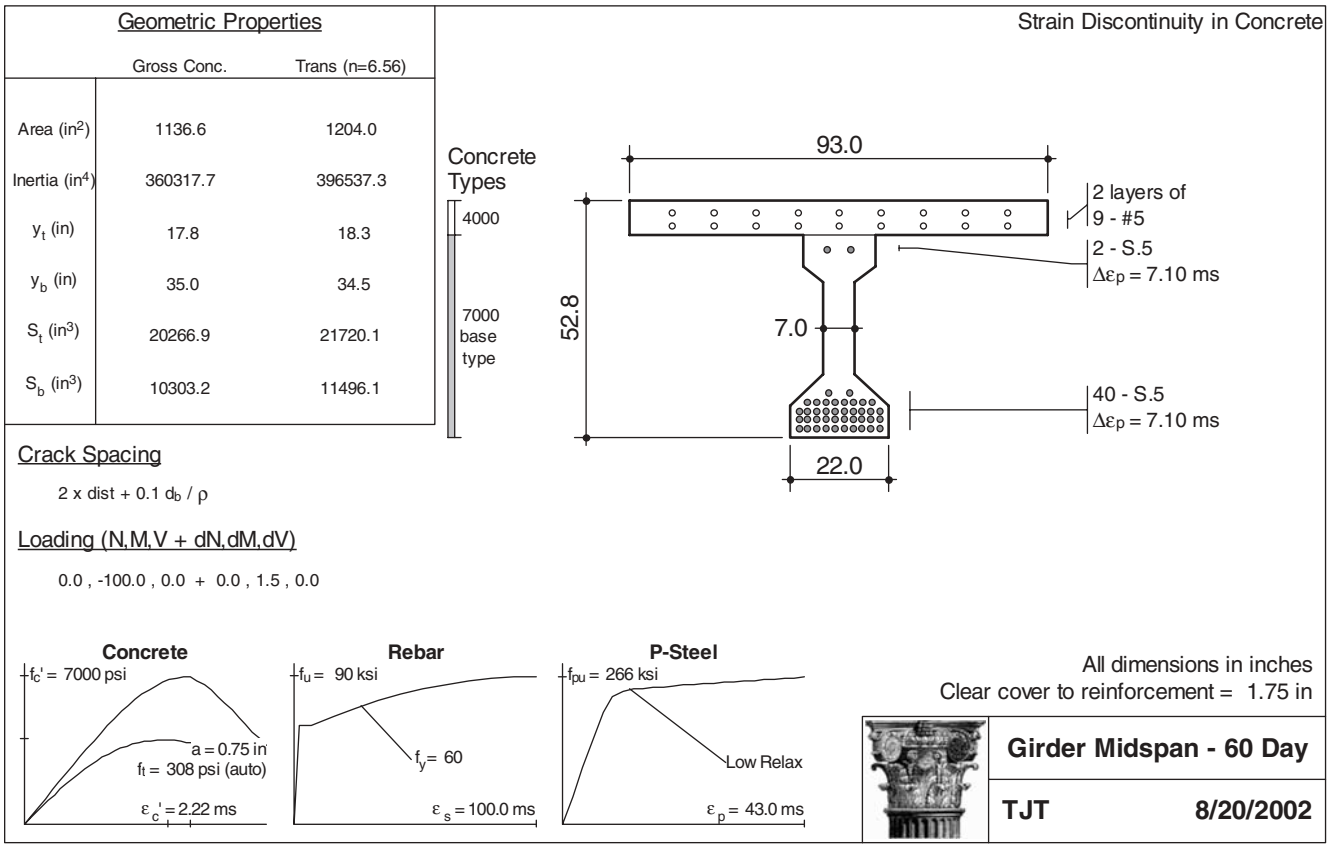

Figure DB.2.2.1-1. Cross section and material information.

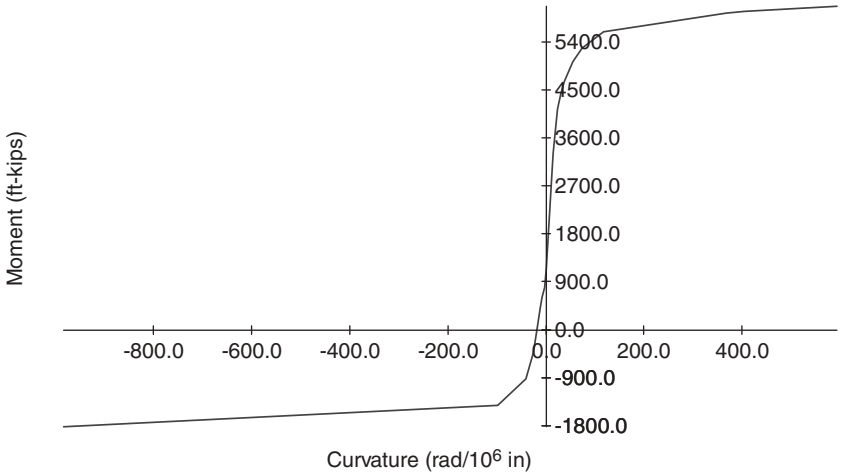

Figure DB.2.2.1-2. Moment curvature analysis plot.

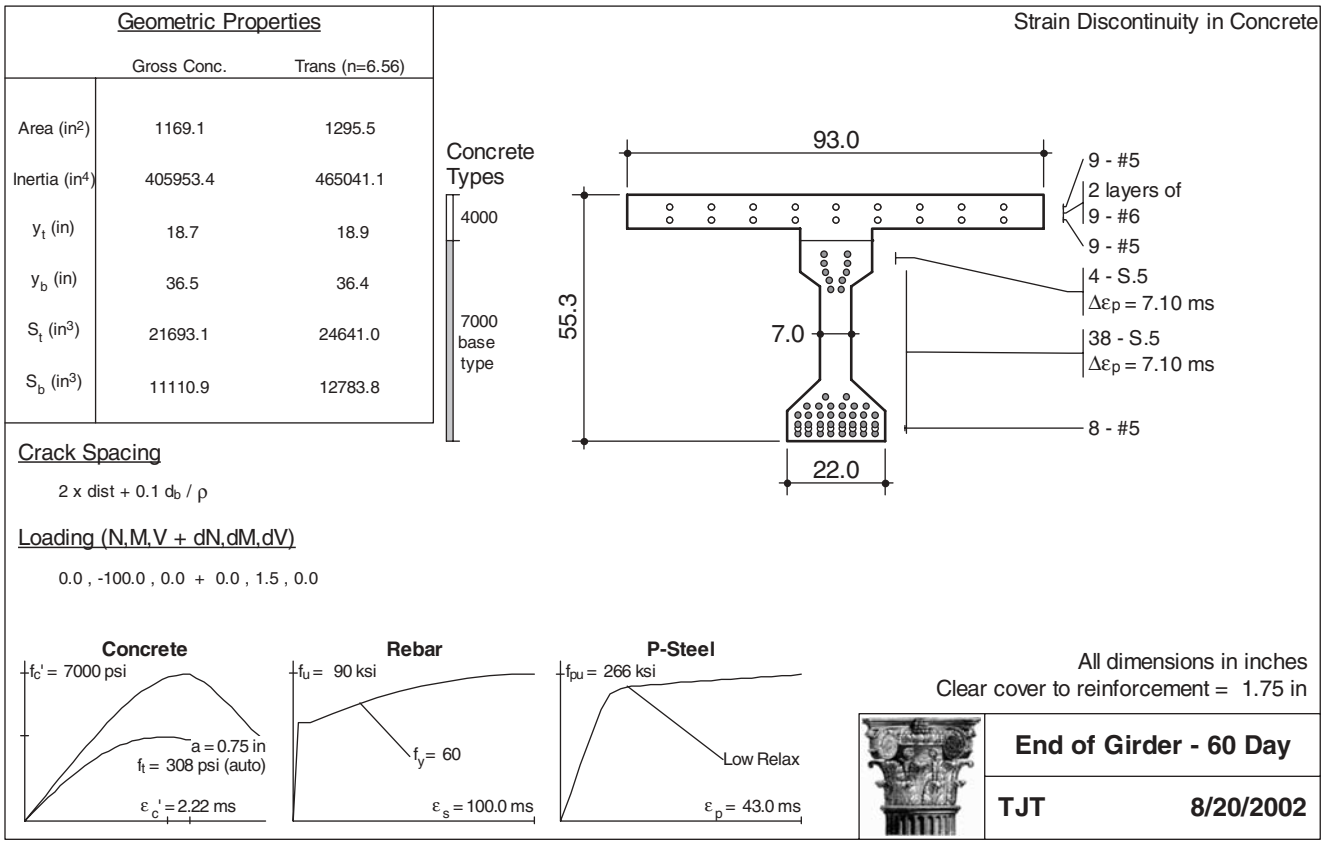

Figure DB.2.2.2-1. Cross section and material information.

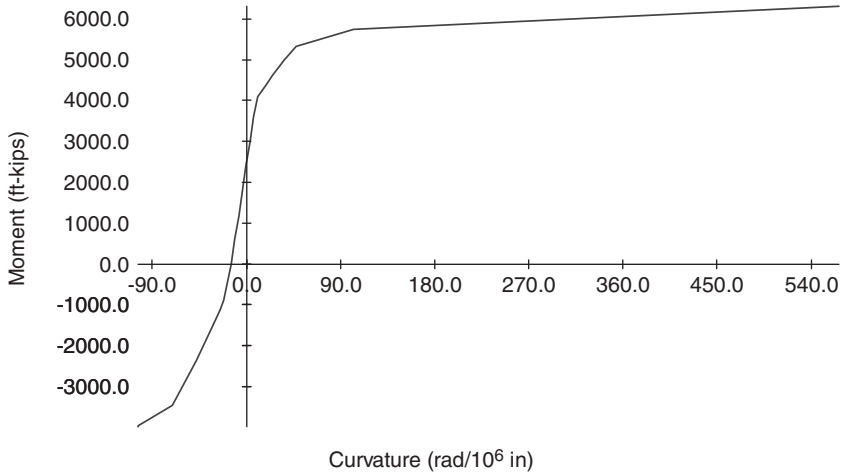

Figure DB.2.2.2-2. Moment curvature analysis plot.

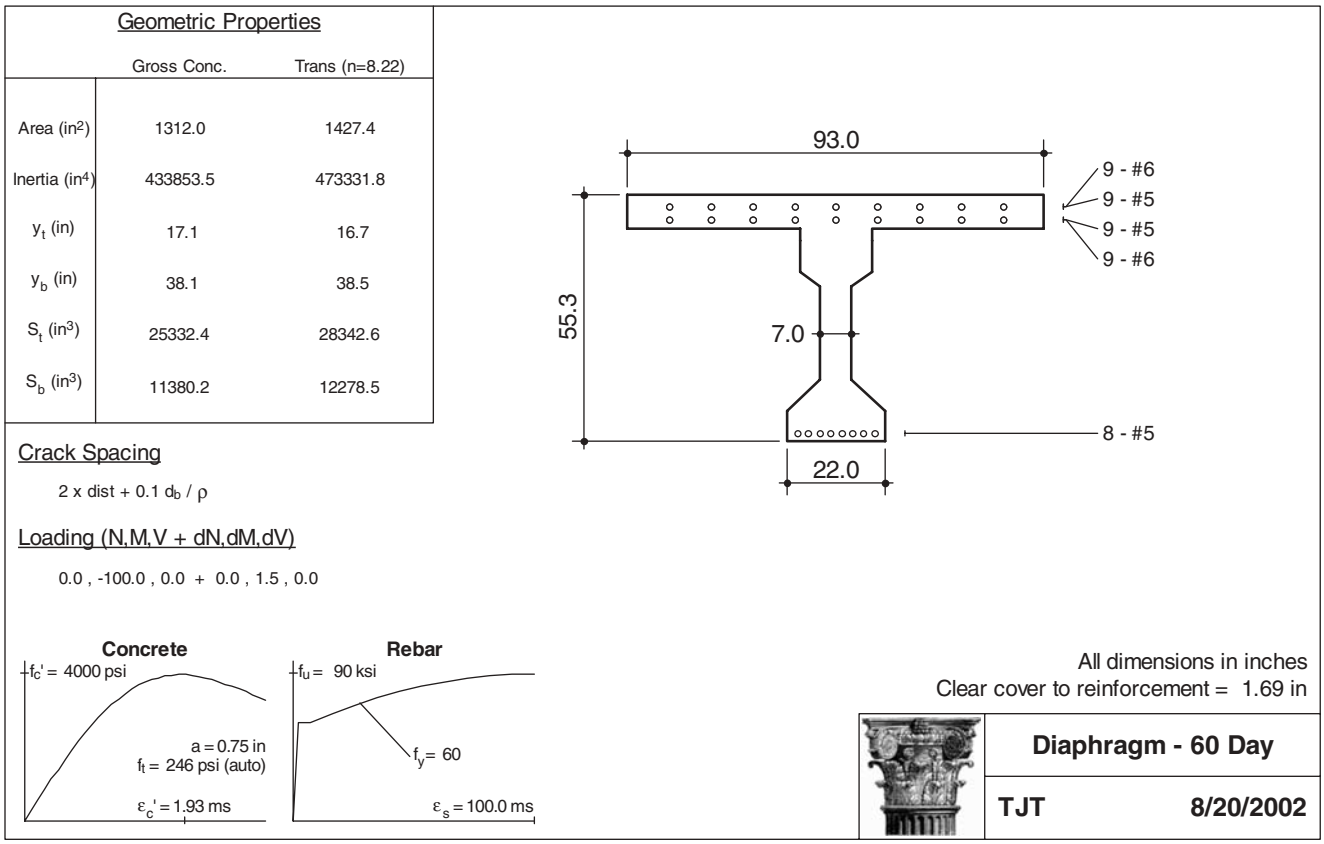

Figure DB.2.2.3-1. Cross section and material information.

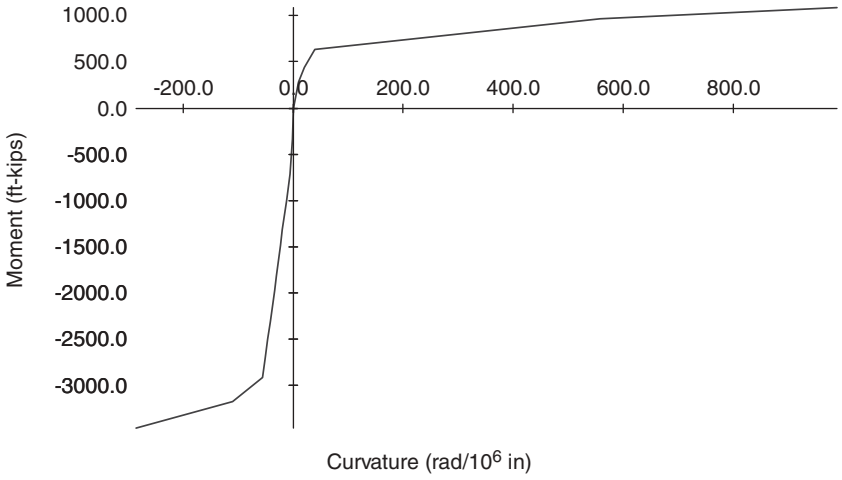

Figure DB.2.2.3-2. Moment curvature analysis plot.

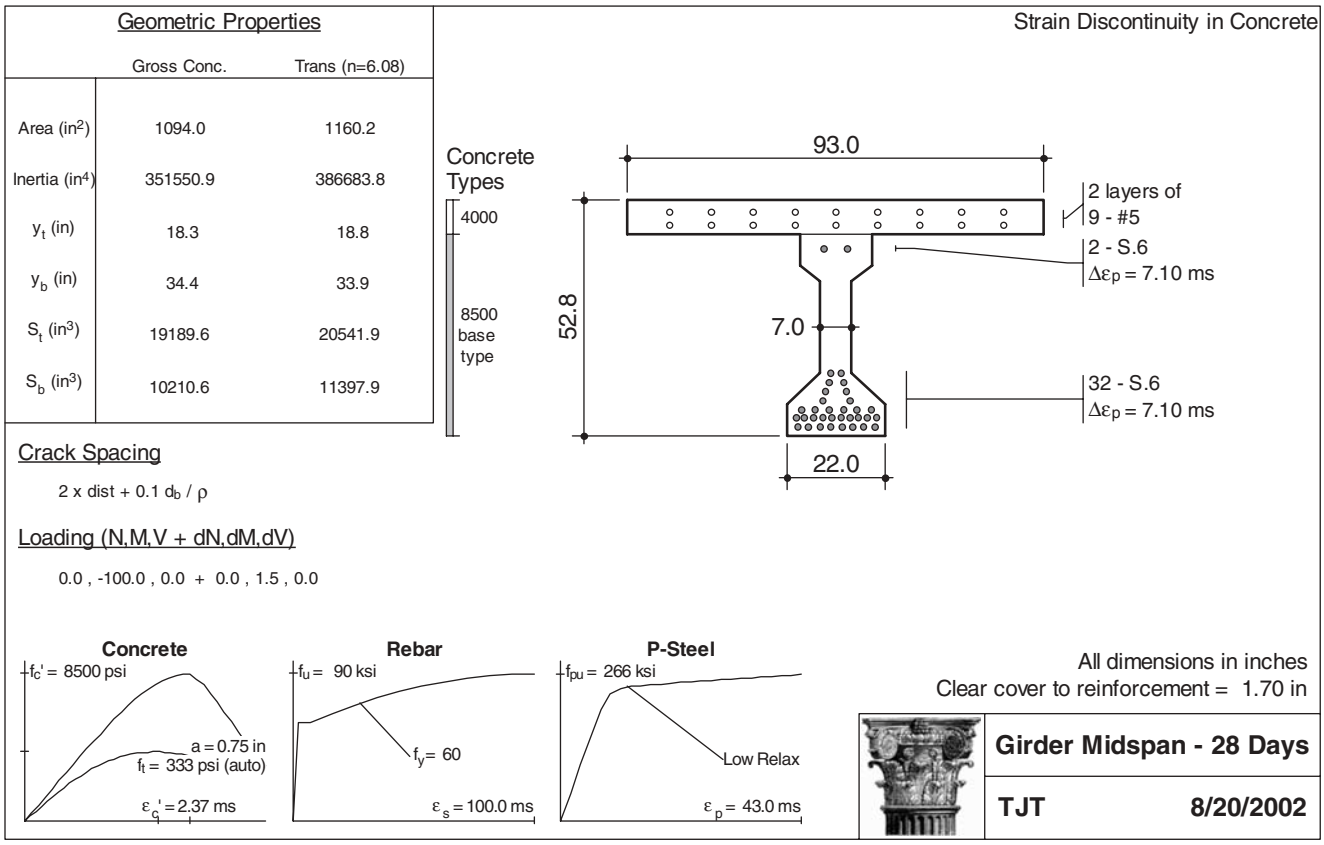

Figure DB.2.3.1-1. Cross section and material information.

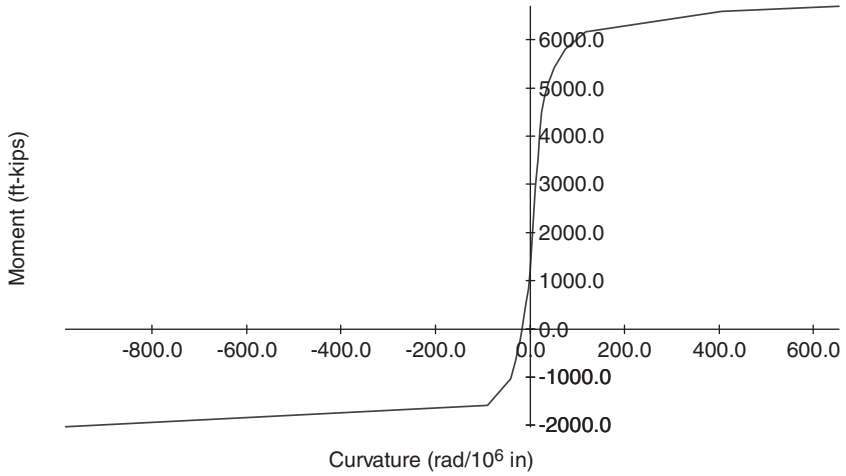

Figure DB.2.3.1-2. Moment curvature analysis plot.

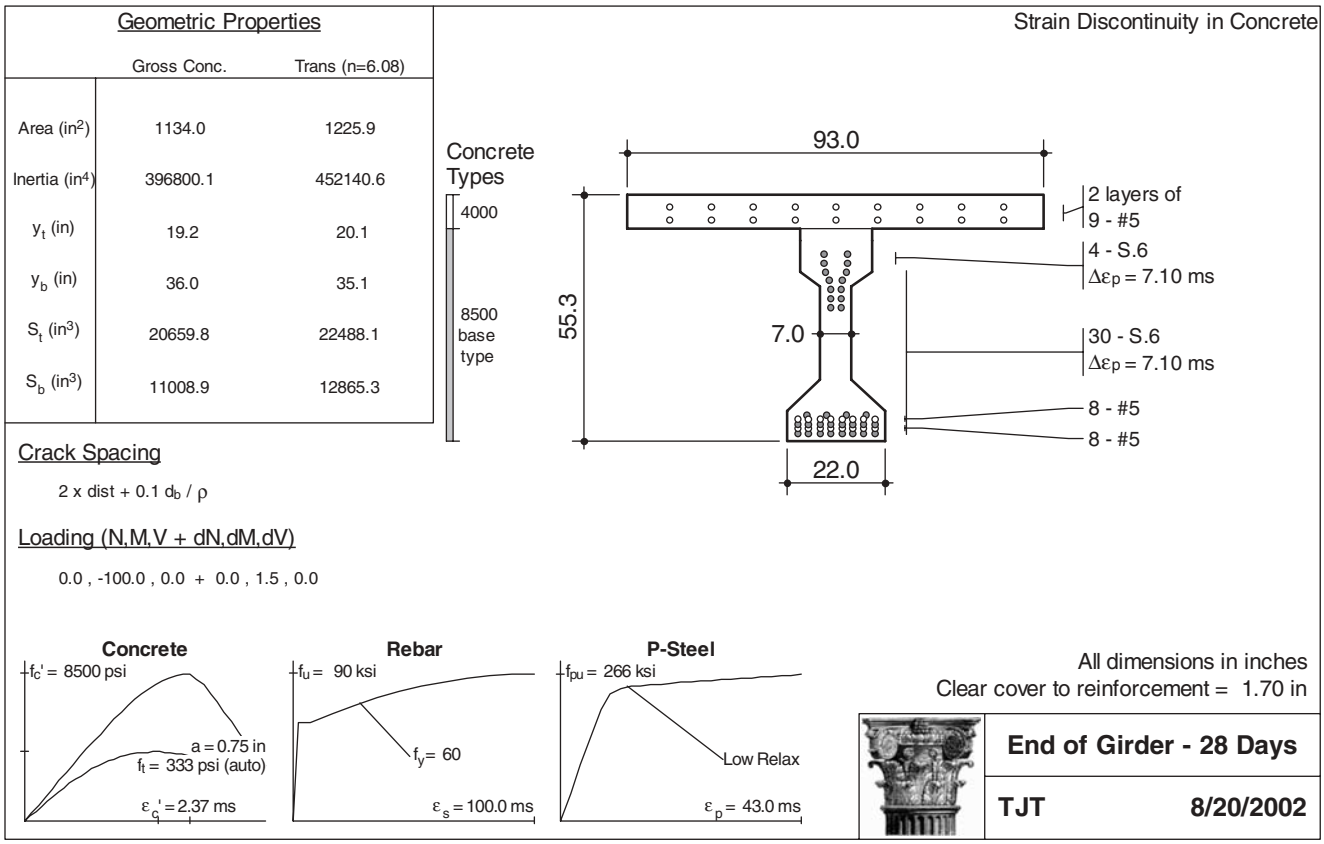

Figure DB.2.3.2-1. Cross section and material information.

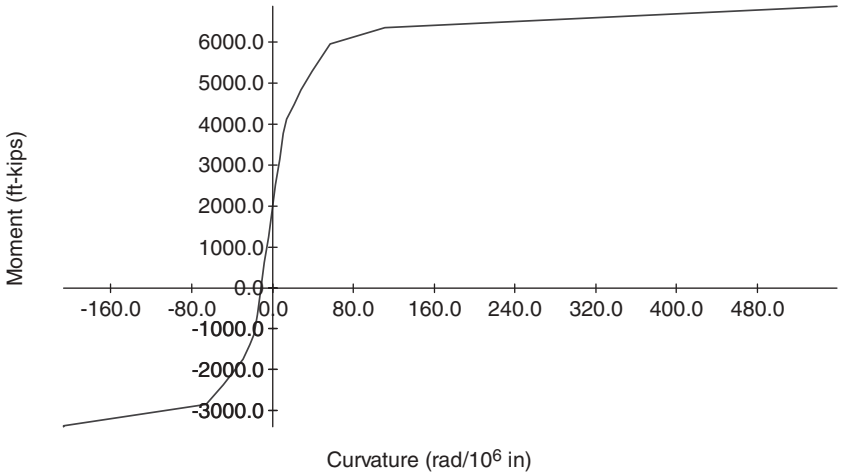

Figure DB.2.3.2-2. Moment curvature analysis plot.

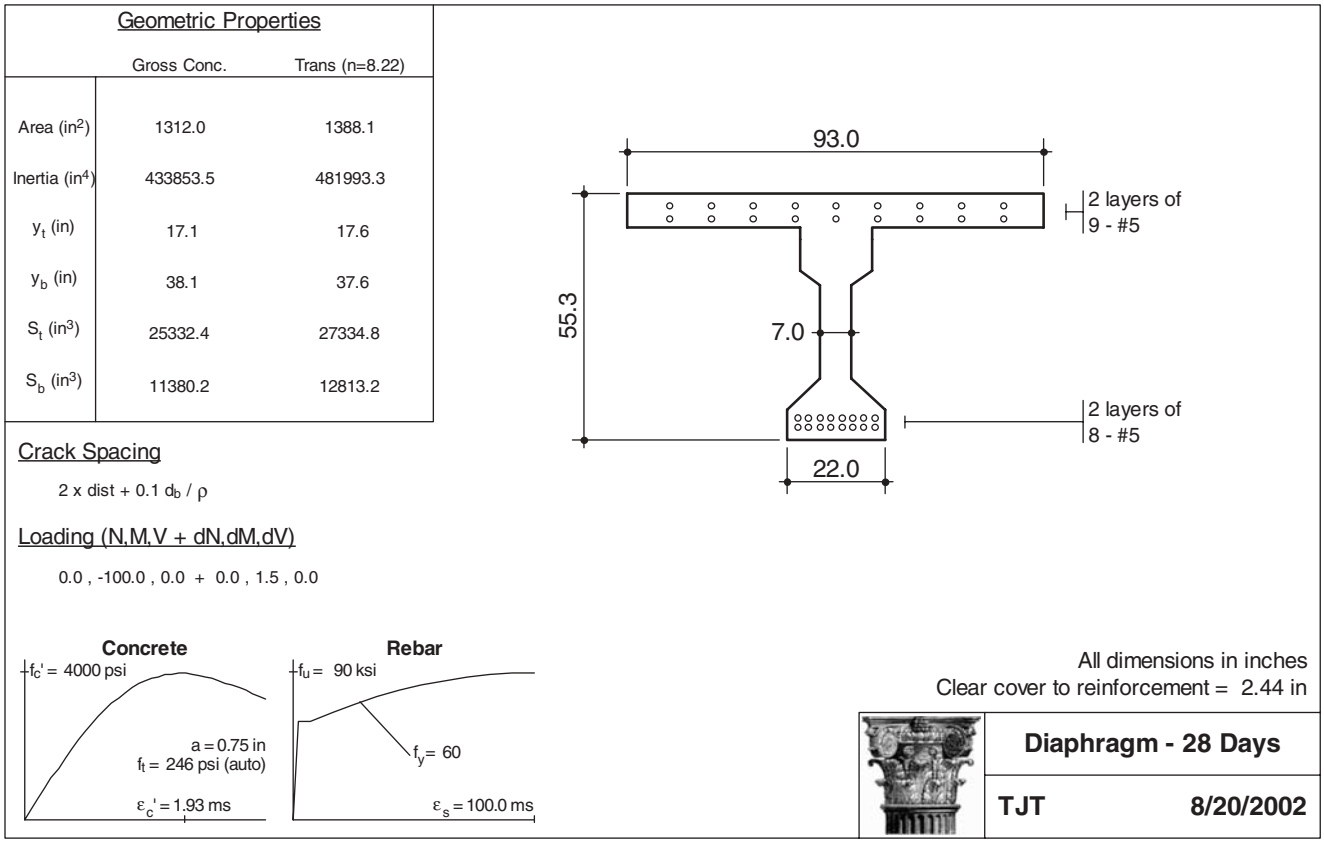

Figure DB.2.3.3-1. Cross section and material information.

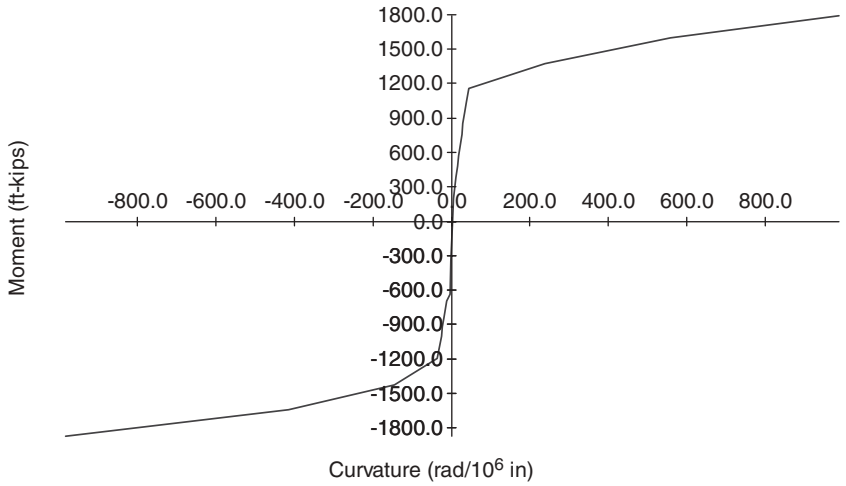

Figure DB.2.3.3-2. Moment curvature analysis plot

SUBAPPENDIX C: INPUT AND OUTPUT FROM QCONBRIDGE

The examples discussed within this subappendix are as follows:

- **Design Example 1: AASHTO Type III Girder Bridge.**
- **Design Example 2: PCI BT-72 Girder Bridge.**
- **Design Example 3: 51-IN.-Deep Spread Box Girder Bridge**—The design spans for the bridge in this example are the same as Design Example 1; therefore, the output from Design Example 1 (see Section DC.1) was used for this example.
- **Design Example 4: AASHTO BIII-48 Adjacent Box Girder Bridge**—The design spans for the bridge in this example are the same as Design Example 1; therefore, the output from Design Example 1 (see Section DC.1) was used for this example.

DC.1 PROGRAM INFORMATION

The program QConBridge was used to compute the fatigue load effects. While QConBridge also reports load effects for other types and combinations of loadings, these were not used in this study because the design for these load effects was performed using another computer program. Therefore, these other results have been deleted from the output that follows.

The program QConBridge was developed by the Washington State DOT and is available free of charge on the department website:

www.wsdot.wa.gov/eesc/bridge/software/index.cfm.

The version of the program used for this study is shown in the figure below taken from the program.

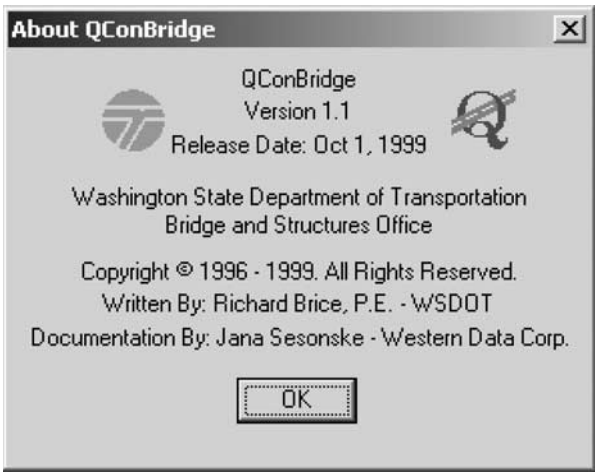

DC.2 DESIGN EXAMPLE 1: AASHTO TYPE III GIRDER BRIDGE

QConBridge Input and Output

```
Washington State Department of Transportation
Bridge and Structures Office
QConBridge Version 1.0


Code: LRFD First Edition 1994

Span Data
---------

Span  1  Length:     86.000 ft

Section Properties
Location      Ax           Iz          Mod. E      Unit Wgt
  (ft)      (in^2)       (in^4)        (psi)       (pcf)
   0.000  1.104e+03    354.081e+03  5.103e+06    149.999e+00

Live Load Distribution Factors
Location  Str/Serv Limit States  Fatigue Limit State
  (ft)         gM        gV          gM        gV
   0.000       1.000     1.000       1.000     1.000

Strength Limit State Factors: Ductility 1.00  Redundancy 1.00  Importance 1.00
Service  Limit State Factors: Ductility 1.00  Redundancy 1.00  Importance 1.00


Span  2  Length:     86.000 ft

Section Properties
Location      Ax           Iz          Mod. E      Unit Wgt
  (ft)      (in^2)       (in^4)        (psi)       (pcf)
   0.000  1.104e+03    354.081e+03  5.103e+06    149.999e+00

Live Load Distribution Factors
Location  Str/Serv Limit States  Fatigue Limit State
  (ft)         gM        gV          gM        gV
   0.000       1.000     1.000       1.000     1.000

Strength Limit State Factors: Ductility 1.00  Redundancy 1.00  Importance 1.00
Service  Limit State Factors: Ductility 1.00  Redundancy 1.00  Importance 1.00


Support Data
------------

Support  1  Roller
Support  2  Pinned
Support  3  Roller


Loading Data
------------
DC Loads
   Self Weight Generation Disabled
   Traffic Barrier Load Disabled

DW Loads
   Utility Load Disabled
   Wearing Surface Load Disabled
Live Load Data
--------------
```

```
Live Load Generation Parameters
   Design Tandem    : Enabled
   Design Truck     : 1 rear axle spacing increments
   Dual Truck Train : Headway Spacing varies from 49.213 ft to 49.213 ft using
1 increments
   Dual Tandem Train: Disabled
   Fatigue Truck    : Enabled

Live Load Impact
   Truck Loads   33.000%
   Lane  Loads    0.000%
   Fatigue Truck 15.000%

   Pedestrian Live Load    0.000e+00 plf

Load Factors
------------
   Strength I   DC min 0.900 DC max 1.250 DW min 0.650 DW max 1.500 LL     1.750
   Service I    DC     1.000 DW     1.000 LL     1.000
   Service II   DC     1.000 DW     1.000 LL     1.300
   Service III  DC     1.000 DW     1.000 LL     0.800
   Fatigue      DC     0.000 DW     0.000 LL     0.750

Analysis Results
----------------
```

Several tables have been deleted. Only tables related to fatigue are shown.

Fatigue Truck Envelopes (Per Lane)

Span	Point	Min Shear(lbs)	Max Shear(lbs)	Min Moment(ft-lbs)	Max Moment(ft-lbs)
1	0	-6.763e+03	62.896e+03	0.000e+00	0.000e+00
1	1	-6.763e+03	53.058e+03	-58.167e+03	456.306e+03
1	2	-9.702e+03	43.607e+03	-116.335e+03	750.048e+03
1	3	-15.334e+03	34.674e+03	-174.503e+03	932.260e+03
1	4	-20.793e+03	26.330e+03	-232.670e+03	982.215e+03
1	5	-29.552e+03	18.877e+03	-290.838e+03	941.287e+03
1	6	-38.987e+03	12.814e+03	-349.006e+03	877.182e+03
1	7	-48.011e+03	8.648e+03	-407.174e+03	691.431e+03
1	8	-56.414e+03	4.984e+03	-465.341e+03	406.489e+03
1	9	-64.072e+03	2.146e+03	-523.509e+03	166.110e+03
1	10	-70.857e+03	0.000e+00	-581.677e+03	0.000e+00
2	0	0.000e+00	67.098e+03	-581.677e+03	0.000e+00
2	1	-2.146e+03	64.072e+03	-523.509e+03	166.110e+03
2	2	-4.984e+03	56.414e+03	-465.341e+03	406.489e+03
2	3	-8.648e+03	48.011e+03	-407.174e+03	691.431e+03
2	4	-12.814e+03	38.987e+03	-349.006e+03	877.182e+03
2	5	-18.877e+03	29.552e+03	-290.838e+03	941.287e+03
2	6	-26.330e+03	20.793e+03	-232.670e+03	982.215e+03
2	7	-34.674e+03	15.334e+03	-174.503e+03	932.260e+03
2	8	-43.607e+03	9.702e+03	-116.335e+03	750.048e+03
2	9	-53.058e+03	6.763e+03	-58.167e+03	456.306e+03
2	10	-62.896e+03	6.763e+03	0.000e+00	0.000e+00

Fatigue Limit State Envelopes

Span	Point	Min Shear(lbs)	Max Shear(lbs)	Min Moment(ft-lbs)	Max Moment(ft-lbs)
1	0	-5.072e+03	47.172e+03	0.000e+00	0.000e+00
1	1	-5.072e+03	39.794e+03	-43.625e+03	342.229e+03
1	2	-7.276e+03	32.705e+03	-87.251e+03	562.536e+03
1	3	-11.500e+03	26.005e+03	-130.877e+03	699.195e+03
1	4	-15.594e+03	19.747e+03	-174.503e+03	736.662e+03
1	5	-22.164e+03	14.158e+03	-218.129e+03	705.965e+03
1	6	-29.240e+03	9.611e+03	-261.754e+03	657.886e+03
1	7	-36.008e+03	6.486e+03	-305.380e+03	518.573e+03
1	8	-42.311e+03	3.738e+03	-349.006e+03	304.867e+03
1	9	-48.054e+03	1.609e+03	-392.632e+03	124.582e+03
1	10	-53.143e+03	0.000e+00	-436.258e+03	0.000e+00
2	0	0.000e+00	50.323e+03	-436.258e+03	0.000e+00
2	1	-1.609e+03	48.054e+03	-392.632e+03	124.582e+03

```
    2     2      -3.738e+03      42.311e+03    -349.006e+03     304.867e+03
    2     3      -6.486e+03      36.008e+03    -305.380e+03     518.573e+03
    2     4      -9.611e+03      29.240e+03    -261.754e+03     657.886e+03
    2     5     -14.158e+03      22.164e+03    -218.129e+03     705.965e+03
    2     6     -19.747e+03      15.594e+03    -174.503e+03     736.662e+03
    2     7     -26.005e+03      11.500e+03    -130.877e+03     699.195e+03
    2     8     -32.705e+03       7.276e+03     -87.251e+03     562.536e+03
    2     9     -39.794e+03       5.072e+03     -43.625e+03     342.229e+03
    2    10     -47.172e+03       5.072e+03       0.000e+00       0.000e+00
```

DC.3 DESIGN EXAMPLE 2: PCI BT-72 GIRDER BRIDGE

QConBridge Input and Output

```
Washington State Department of Transporation
Bridge and Structures Office
QConBridge Version 1.0


Code: LRFD First Edition 1994

Span Data
---------

Span  1  Length:    126.000 ft

Section Properties
Location      Ax           Iz          Mod. E      Unit Wgt
  (ft)      (in^2)       (in^4)        (psi)       (pcf)
   0.000  1.104e+03    354.081e+03  5.103e+06    149.999e+00

Live Load Distribution Factors
Location  Str/Serv Limit States  Fatigue Limit State
  (ft)         gM        gV          gM        gV
   0.000       1.000     1.000       1.000     1.000

Strength Limit State Factors: Ductility 1.00  Redundancy 1.00  Importance 1.00
Service  Limit State Factors: Ductility 1.00  Redundancy 1.00  Importance 1.00


Span  2  Length:    126.000 ft

Section Properties
Location      Ax           Iz          Mod. E      Unit Wgt
  (ft)      (in^2)       (in^4)        (psi)       (pcf)
   0.000  1.104e+03    354.081e+03  5.103e+06    149.999e+00

Live Load Distribution Factors
Location  Str/Serv Limit States  Fatigue Limit State
  (ft)         gM        gV          gM        gV
   0.000       1.000     1.000       1.000     1.000

Strength Limit State Factors: Ductility 1.00  Redundancy 1.00  Importance 1.00
Service  Limit State Factors: Ductility 1.00  Redundancy 1.00  Importance 1.00


Support Data
------------

Support  1  Roller
Support  2  Pinned
Support  3  Roller
```

```
Loading Data
------------
DC Loads
   Self Weight Generation Disabled
   Traffic Barrier Load Disabled

DW Loads
   Utility Load Disabled
   Wearing Surface Load Disabled

Live Load Data
--------------
Live Load Generation Parameters
   Design Tandem    : Enabled
   Design Truck     : 1 rear axle spacing increments
   Dual Truck Train : Headway Spacing varies from 49.213 ft to 49.213 ft using 1
increments
   Dual Tandem Train: Disabled
   Fatigue Truck    : Enabled

Live Load Impact
   Truck Loads   33.000%
   Lane  Loads    0.000%
   Fatigue Truck 15.000%

   Pedestrian Live Load    0.000e+00 plf

Load Factors
------------
   Strength I   DC min 0.900 DC max 1.250 DW min 0.650 DW max 1.500 LL     1.750
   Service I    DC     1.000 DW     1.000 LL     1.000
   Service II   DC     1.000 DW     1.000 LL     1.300
   Service III  DC     1.000 DW     1.000 LL     0.800
   Fatigue      DC     0.000 DW     0.000 LL     0.750

Analysis Results
----------------
```

Several tables have been deleted. Only tables related to fatigue are shown.

Fatigue Truck Envelopes (Per Lane)

Span	Point	Min Shear(lbs)	Max Shear(lbs)	Min Moment(ft-lbs)	Max Moment(ft-lbs)
1	0	-7.428e+03	69.360e+03	0.000e+00	0.000e+00
1	1	-7.428e+03	59.211e+03	-93.600e+03	746.066e+03
1	2	-10.290e+03	49.367e+03	-187.201e+03	1.244e+06
1	3	-16.874e+03	39.954e+03	-280.802e+03	1.555e+06
1	4	-26.459e+03	31.086e+03	-374.403e+03	1.655e+06
1	5	-36.241e+03	22.887e+03	-468.004e+03	1.608e+06
1	6	-45.572e+03	15.561e+03	-561.605e+03	1.466e+06
1	7	-54.325e+03	9.309e+03	-655.206e+03	1.153e+06
1	8	-62.375e+03	5.254e+03	-748.807e+03	704.163e+03
1	9	-69.596e+03	2.146e+03	-842.408e+03	256.896e+03
1	10	-75.894e+03	0.000e+00	-936.009e+03	0.000e+00
2	0	0.000e+00	74.756e+03	-936.009e+03	0.000e+00
2	1	-2.146e+03	69.596e+03	-842.408e+03	256.896e+03
2	2	-5.254e+03	62.375e+03	-748.807e+03	704.163e+03
2	3	-9.309e+03	54.325e+03	-655.206e+03	1.153e+06
2	4	-15.561e+03	45.572e+03	-561.605e+03	1.466e+06
2	5	-22.887e+03	36.241e+03	-468.004e+03	1.608e+06
2	6	-31.086e+03	26.459e+03	-374.403e+03	1.655e+06
2	7	-39.954e+03	16.874e+03	-280.802e+03	1.555e+06
2	8	-49.367e+03	10.290e+03	-187.201e+03	1.244e+06
2	9	-59.211e+03	7.428e+03	-93.600e+03	746.066e+03
2	10	-69.360e+03	7.428e+03	0.000e+00	0.000e+00

Fatigue Limit State Envelopes

Span	Point	Min Shear(lbs)	Max Shear(lbs)	Min Moment(ft-lbs)	Max Moment(ft-lbs)
1	0	-5.571e+03	52.020e+03	0.000e+00	0.000e+00
1	1	-5.571e+03	44.408e+03	-70.200e+03	559.549e+03
1	2	-7.717e+03	37.025e+03	-140.401e+03	933.052e+03
1	3	-12.656e+03	29.966e+03	-210.602e+03	1.166e+06
1	4	-19.844e+03	23.314e+03	-280.802e+03	1.241e+06
1	5	-27.181e+03	17.165e+03	-351.003e+03	1.206e+06
1	6	-34.179e+03	11.671e+03	-421.204e+03	1.100e+06
1	7	-40.744e+03	6.982e+03	-491.405e+03	864.860e+03
1	8	-46.781e+03	3.940e+03	-561.605e+03	528.122e+03
1	9	-52.197e+03	1.609e+03	-631.806e+03	192.672e+03
1	10	-56.920e+03	0.000e+00	-702.007e+03	0.000e+00
2	0	0.000e+00	56.067e+03	-702.007e+03	0.000e+00
2	1	-1.609e+03	52.197e+03	-631.806e+03	192.672e+03
2	2	-3.940e+03	46.781e+03	-561.605e+03	528.122e+03
2	3	-6.982e+03	40.744e+03	-491.405e+03	864.860e+03
2	4	-11.671e+03	34.179e+03	-421.204e+03	1.100e+06
2	5	-17.165e+03	27.181e+03	-351.003e+03	1.206e+06
2	6	-23.314e+03	19.844e+03	-280.802e+03	1.241e+06
2	7	-29.966e+03	12.656e+03	-210.602e+03	1.166e+06
2	8	-37.025e+03	7.717e+03	-140.401e+03	933.052e+03
2	9	-44.408e+03	5.571e+03	-70.200e+03	559.549e+03
2	10	-52.020e+03	5.571e+03	0.000e+00	0.000e+00

APPENDIX E

SUMMARY DATA

A disk containing summary data files for NCHRP Project 12-53 is available upon request to NCHRP, Transportation Research Board; call 202-334-3213. Remit payment to NCHRP, Transportation Research Board, Box 289, Washington, DC, 20055.

Abbreviations used without definitions in TRB publications:

AASHO	American Association of State Highway Officials
AASHTO	American Association of State Highway and Transportation Officials
APTA	American Public Transportation Association
ASCE	American Society of Civil Engineers
ASME	American Society of Mechanical Engineers
ASTM	American Society for Testing and Materials
ATA	American Trucking Associations
CTAA	Community Transportation Association of America
CTBSSP	Commercial Truck and Bus Safety Synthesis Program
FAA	Federal Aviation Administration
FHWA	Federal Highway Administration
FMCSA	Federal Motor Carrier Safety Administration
FRA	Federal Railroad Administration
FTA	Federal Transit Administration
IEEE	Institute of Electrical and Electronics Engineers
ITE	Institute of Transportation Engineers
NCHRP	National Cooperative Highway Research Program
NCTRP	National Cooperative Transit Research and Development Program
NHTSA	National Highway Traffic Safety Administration
NTSB	National Transportation Safety Board
SAE	Society of Automotive Engineers
TCRP	Transit Cooperative Research Program
TRB	Transportation Research Board
U.S.DOT	United States Department of Transportation